Docket 71-9305

AREVA

TRUPACT-III

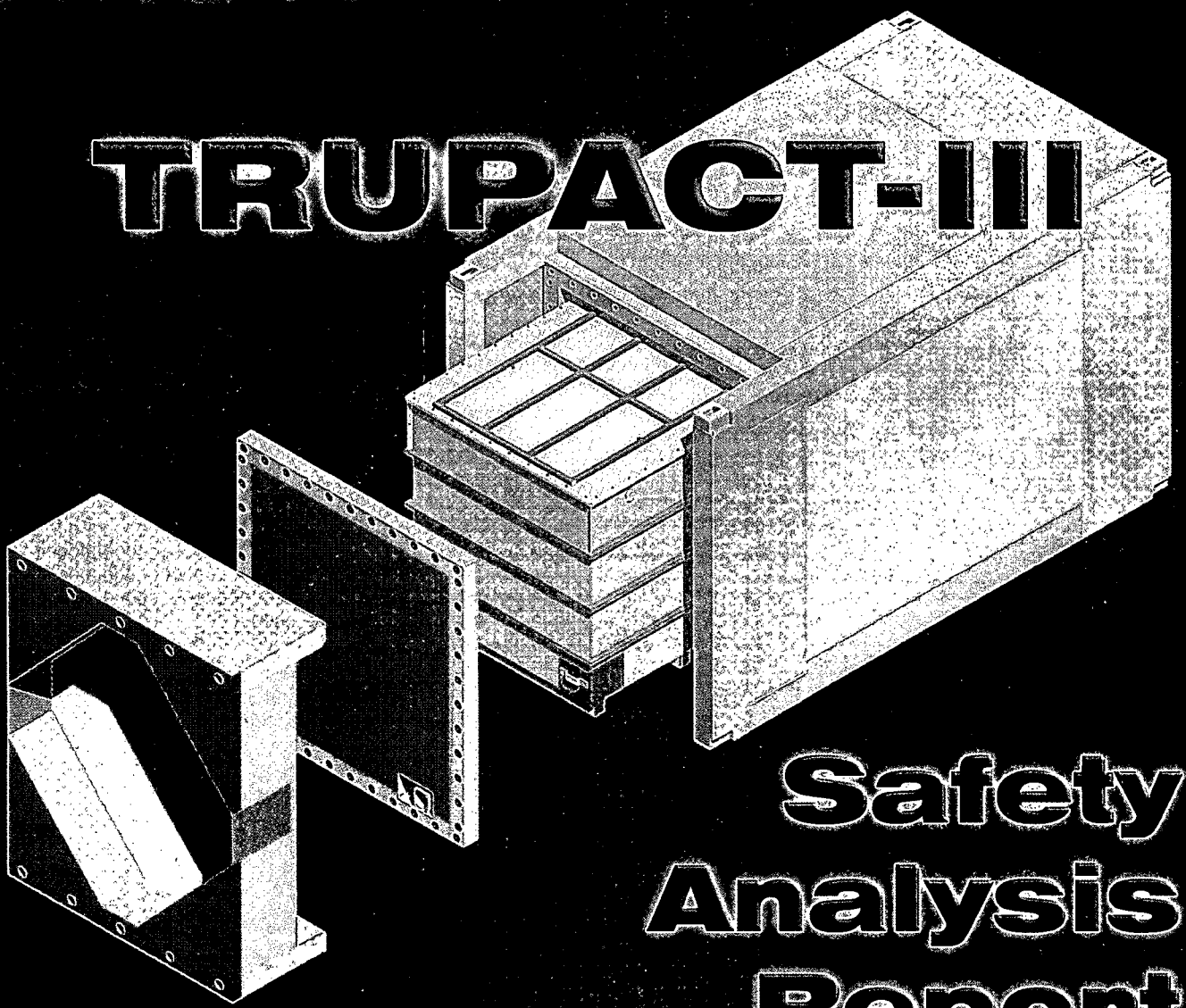

Safety Analysis Report

Revision 1
January 2010

AREVA Federal Services LLC

TABLE OF CONTENTS

This page intentionally left blank.

1.0 GENERAL INFORMATION

This chapter of the Safety Analysis Report (SAR) presents a general introduction and description of the TRUPACT–III contact–handled transuranic (CH–TRU) waste packaging. The major components comprising the TRUPACT–III packaging are presented in Figures 1.1-1 through 1.1-7. Figure 1.1-1 presents an exploded view of all major TRUPACT–III packaging components. Figure 1.1-2 presents a cross–section of the body, with Figure 1.1-3 presenting a cross–section detail of the body wall. Figure 1.1-4 presents the containment structural assembly (CSA). Figure 1.1-5 presents a detailed view of the closure lid and O–ring seal region. Figure 1.1-6 presents a cross–section of the overpack cover. Figure 1.1-7 presents a detailed view of the debris shield. Drawings of the TRUPACT–III packaging design are presented in Appendix 1.3.1, *Packaging General Arrangement Drawings*. All details relating to payloads and payload preparation for shipment in a TRUPACT–III package are presented in the *TRUPACT–III TRU Waste Authorized Methods for Payload Control (TRUPACT–III TRAMPAC)*[1]. Terminology and acronyms used throughout this document are presented as Appendix 1.3.2, *Glossary of Terms and Acronyms*.

1.1 Introduction

The model TRUPACT–III packaging has been developed by AREVA Federal Services LLC (AFS) as a safe method for transportation of CH–TRU waste materials. The TRUPACT–III packaging is intended primarily for truck transport, and may also be transported by rail. In truck transport, a single TRUPACT–III package is transported on a semi–trailer.

The structure of the TRUPACT–III packaging can sustain both normal conditions of transport (NCT) and hypothetical accident condition (HAC) structural and thermal loadings without loss of leaktight capability[2]. Two full–scale TRUPACT–III certification test units (CTU) were subjected to a series of free and puncture drop tests. These tests, together with structural, thermal, and criticality analyses, conclusively demonstrate the containment integrity of the TRUPACT–III package.

The CH–TRU waste material payload within the TRUPACT–III packaging will be confined within a single steel SLB2 container, supported by a payload loading system, such as a pallet and roller floor. Specifications for SLB2 payload containers and loading systems are provided in the TRUPACT–III TRAMPAC.

Based on the shielding and criticality assessments provided in Chapter 5.0, *Shielding Evaluation*, and Chapter 6.0, *Criticality Evaluation*, the Criticality Safety Index (CSI) for the TRUPACT–III package is zero (0.0), and the shielding Transport Index (TI) is determined at the time of shipment. Authorization is sought for shipment of the TRUPACT–III package by truck or railcar as a Type B(U) –96 package per the definition delineated in 10 CFR §71.4[3].

---

[1] U.S. Department of Energy (DOE), *TRUPACT–III TRU Waste Authorized Methods for Payload Control (TRUPACT–III TRAMPAC)*, U.S. Department of Energy, Carlsbad Field Office, Carlsbad, New Mexico.

[2] Leaktight is defined as 1×10^{-8} reference Pascals – cubic meters per second (Pa–m^3/s), or less, air leakage per the definition in ANSI N14.5–1997 (or later), *American National Standard for Radioactive Materials – Leakage Tests on Packages for Shipment,* American National Standards Institute, (ANSI), Inc.

[3] Title 10, Code of Federal Regulations, Part 71 (10 CFR 71), *Packaging and Transportation of Radioactive Material*, 01–01–09 Edition.

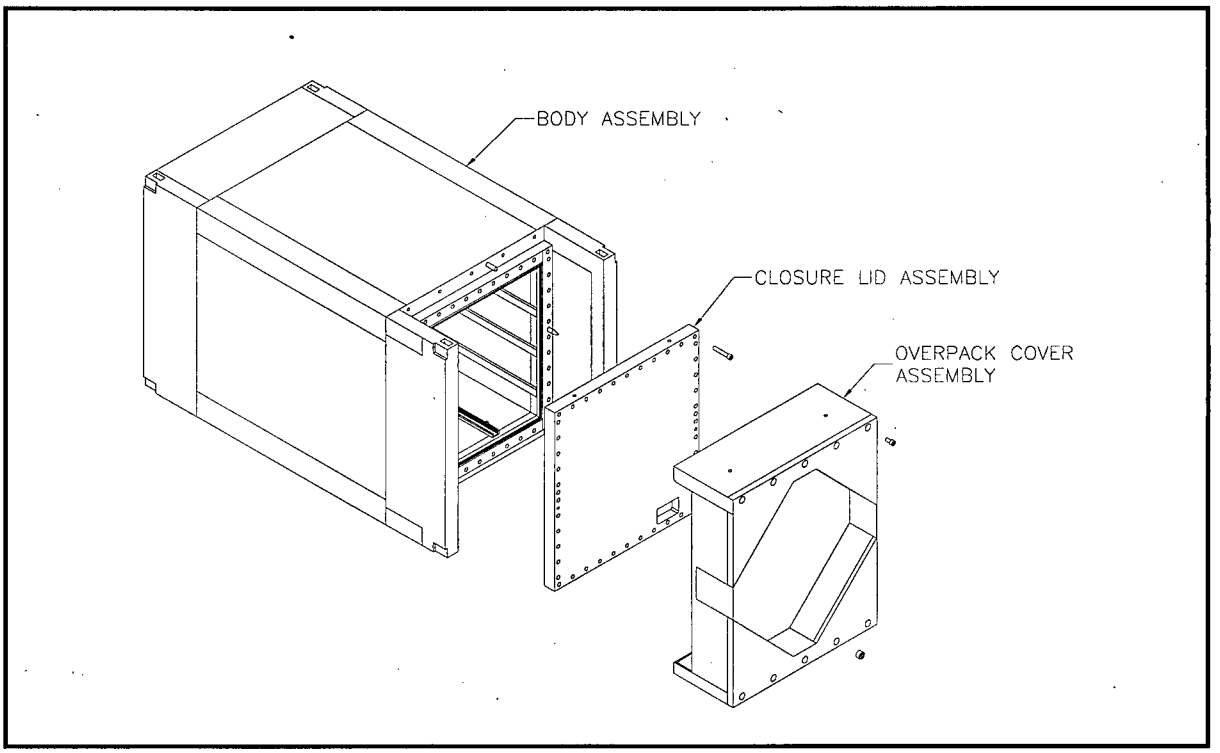

Figure 1.1-1 – TRUPACT–III Packaging Assembly

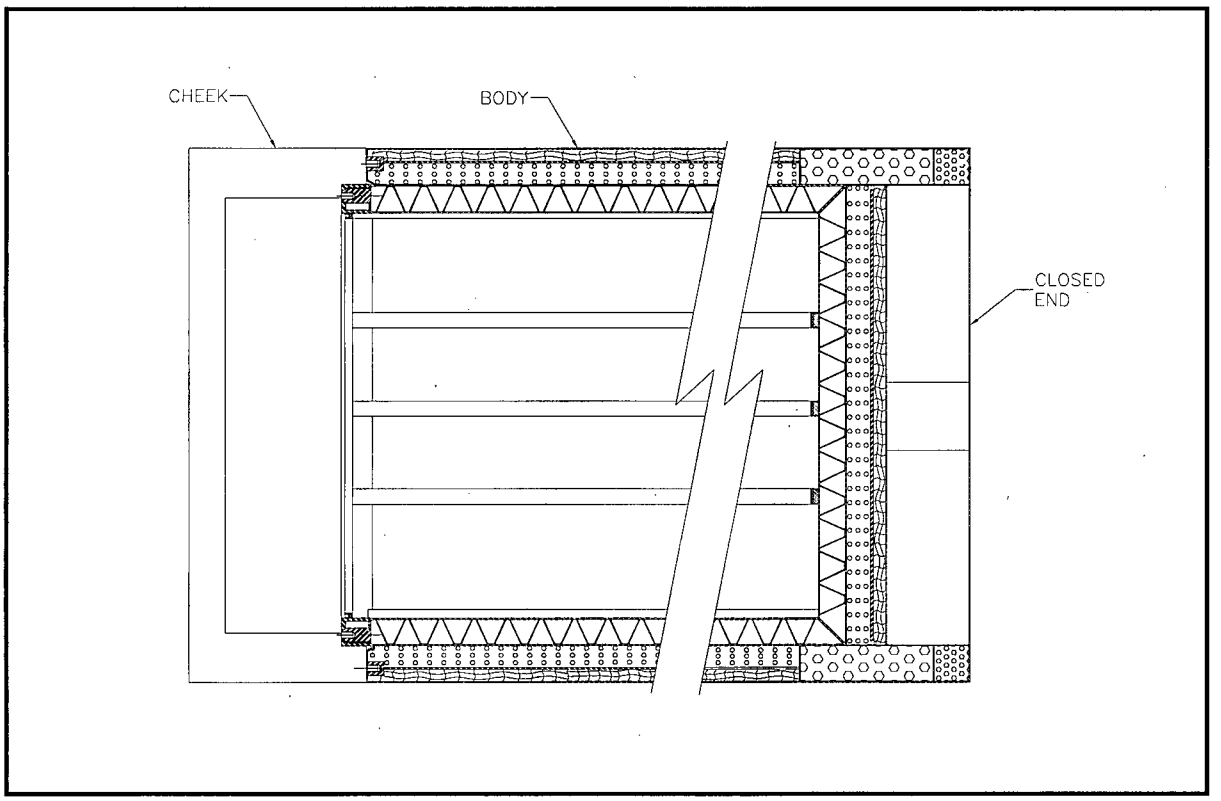

Figure 1.1-2 – TRUPACT–III Packaging Body Cross–Section

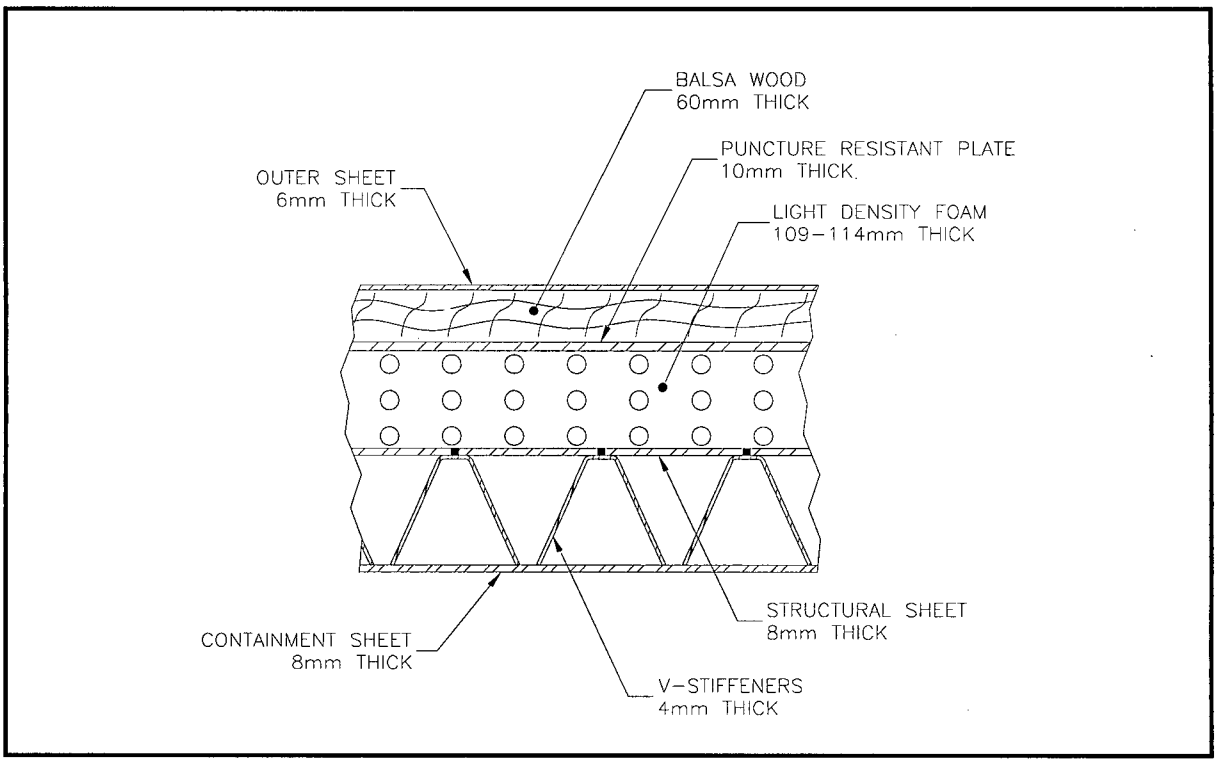

Figure 1.1-3 – TRUPACT–III Packaging Body Side Wall Cross–Section

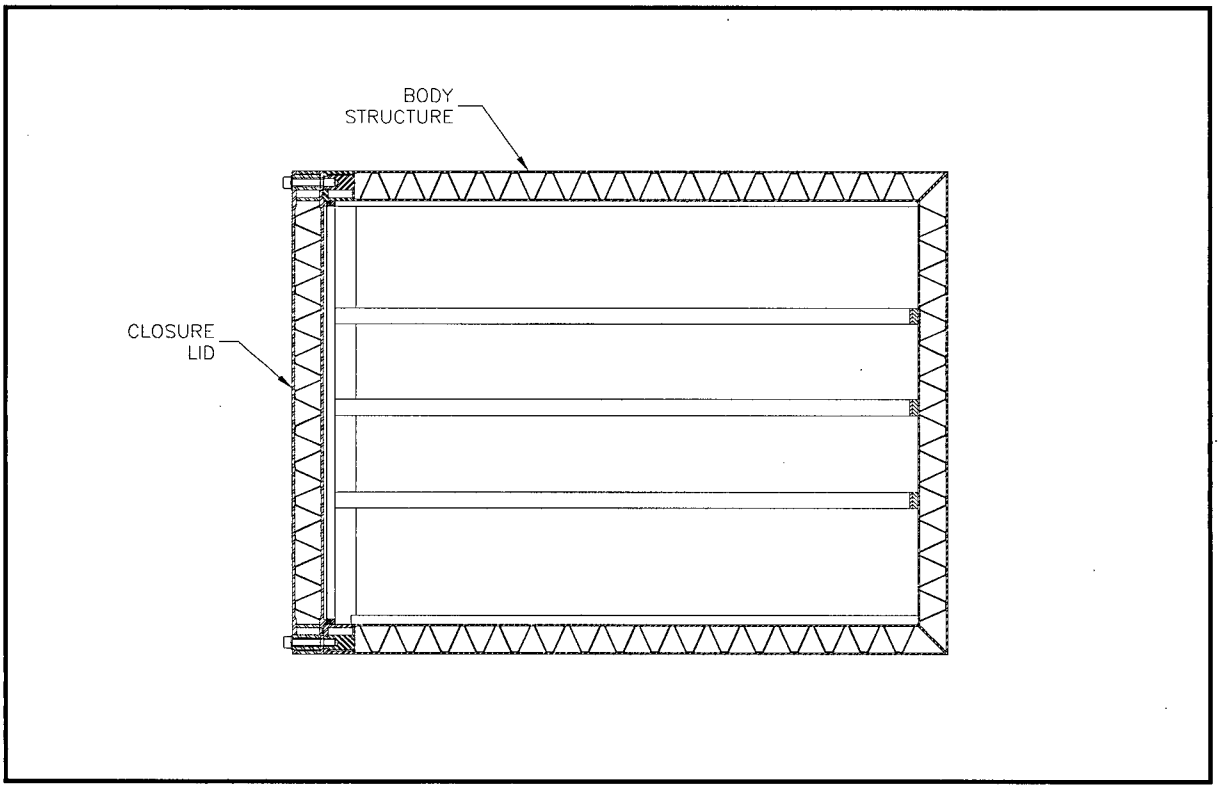

Figure 1.1-4 – TRUPACT–III Packaging Containment Structural Assembly

Security Related Information
Figure Withheld Under 10 CFR 2.390

Figure 1.1-5 – TRUPACT–III Packaging Closure Lid/Seal Flange Details

Security Related Information
Figure Withheld Under 10 CFR 2.390

Figure 1.1-6 – TRUPACT–III Packaging Overpack Cover Cross–Section

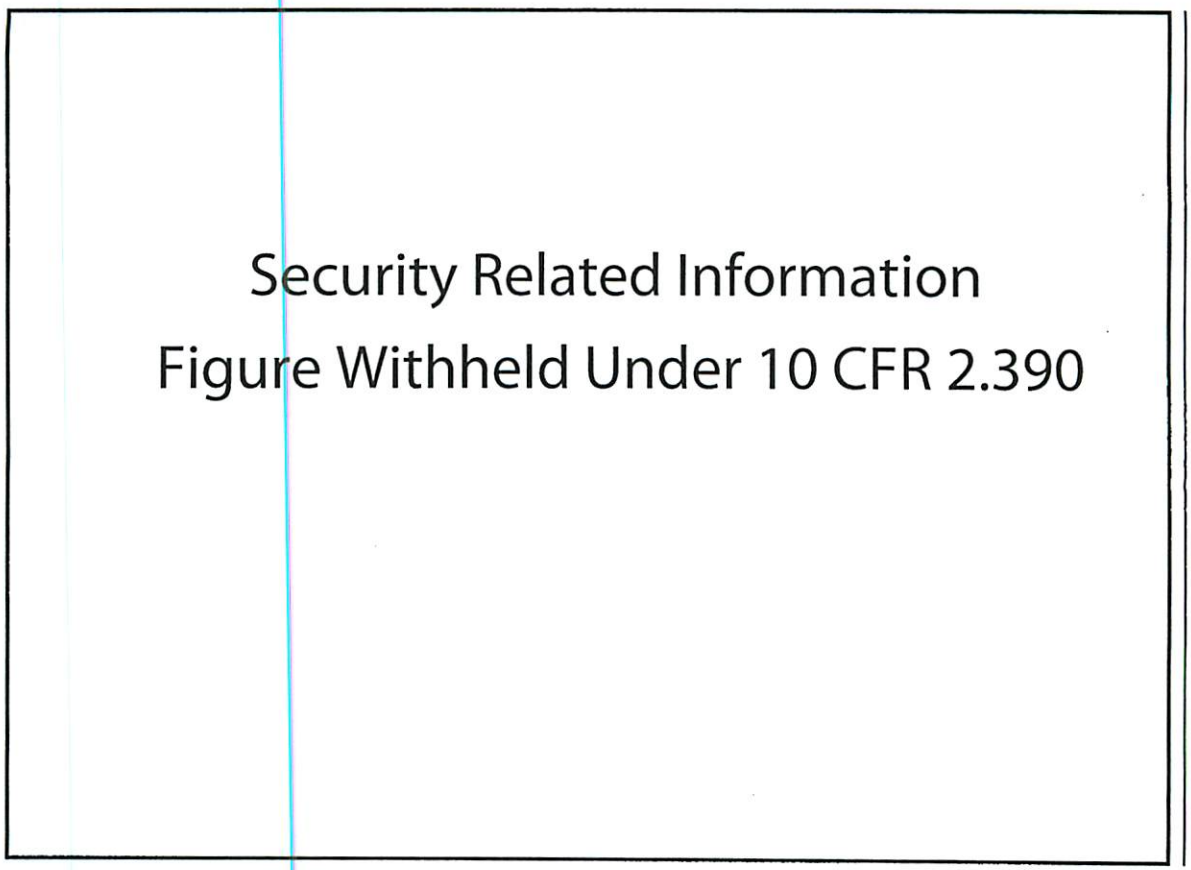

Figure 1.1-7 – TRUPACT–III Debris Shield Cross–Section

This page intentionally left blank.

1.2 Package Description

This section presents a basic description of the TRUPACT–III package. General arrangement drawings of the TRUPACT–III packaging are presented in Appendix 1.3.1, *Packaging General Arrangement Drawings*. Payload assembly details are presented in the TRUPACT–III TRAMPAC[1].

1.2.1 Packaging

The TRUPACT–III packaging is comprised of a body, a closure lid, and an overpack cover, as shown in Figure 1.1-1. The components may be briefly described as follows:

- The body is in the form of a rectangular box. It is comprised of the containment structural assembly (CSA, a rigid rectangular weldment) and an integral energy–absorbing overpack structure.
- The closure lid is a flat, rigid weldment having a construction similar to that of the CSA body, and when bolted in place, completes the CSA.
- The overpack cover is the only separable part of the overpack structure, and allows access to the closure lid and the vent/test ports.

The CSA (body plus bolted closure lid) is the rigid weldment that contains, supports, and reinforces the containment boundary. The containment boundary consists of:

- the inner stainless steel sheets of the CSA body (four sides plus the closed end),
- the closure lid inner sheet,
- the inner O–ring seal located in the flange of the closure lid,
- the vent port insert located in the closure lid,
- the vent port insert inner O–ring seal.

The body, closure lid, and overpack cover are fully described in the following subsections. All detail and sheet references in the following text refer to the drawings presented in Appendix 1.3.1, *Packaging General Arrangement Drawings*. Except for fasteners and some incidental parts as noted, all steel components are made from UNS S31803 duplex stainless steel.

1.2.1.1 Body

The body of the TRUPACT–III packaging is a rectangular box, open on one end. It consists of the body portion of the CSA with an integral overpack structure.

The CSA is a rigid stainless steel weldment consisting of sandwich panels which form the flat walls, as shown in Section BC–BC on Sheet 19. The wall sections are made of inner and outer, 8–mm thick sheets, connected by V–stiffeners of 4–mm thickness. The total wall section thickness of the CSA body is 140 mm. The V–stiffeners are connected to the outside surface of the inner sheets using continuous fillet welds. The outer sheets are connected to the V–stiffeners

[1] U.S. Department of Energy (DOE), *TRUPACT–III TRU Waste Authorized Methods for Payload Control (TRUPACT–III TRAMPAC)*, U.S. Department of Energy, Carlsbad Field Office, Carlsbad, New Mexico.

using either plug welds (on the four sides of the box) or continuous slot welds (on the closed end wall). The walls and V–stiffeners are joined at the edges of the box using diagonal sheets of 10–mm thickness as shown in Detail AX on Sheet 20. The CSA body flange is a rigid box beam structure having 15–mm inner and outer plates and a 25–mm seal face plate thickness, as shown in Detail BE on Sheet 21. The rear plate of the box beam is 10–mm in thickness. The threaded bolting bosses for the closure bolts and closure lid alignment pins pass through the box beam and are welded to both the outer plate and the rear plate. Optionally, alloy steel thread inserts may be used in the bolting bosses. By means of several 10–mm diameter holes in the diagonal corner plates and through other openings, all cavities between the inner (containment) and outer sheets of the CSA are interconnected. When evacuated of air and backfilled with helium, these cavities present a fully enveloping blanket of helium for use during leakage rate testing of the containment boundary. All containment boundary welds are radiograph inspected per Flag Note 15 and liquid penetrant inspected per Flag Note 16 on Sheet 1. All other CSA body welds are liquid penetrant inspected per Flag Note 16 on Sheet 1. The internal cavity dimensions are: 1,840 mm wide, 2,000 mm tall, and 2,790 mm long.

A debris shield receptacle is located on each side of the CSA inner cavity near the opening as shown on Sheet 4. The receptacle is a 26–mm × 38–mm cross section bar made of Type 304L or UNS S31803 duplex stainless steel with a 15–mm wide by approximately 20–mm deep groove cut along its length, as shown on Sheet 19. The groove interfaces with the debris shield insert, described in Section 1.2.1.2, *Closure Lid.* Guide bars are attached to the CSA inner cavity (as shown in Section F–F on Sheet 5 and Section H–H on Sheet 7), having a cross section of 25 mm × 76 mm, and running between the closed end of the CSA and the back edge of the debris shield receptacle. Three guide bars also run across the closed end of the CSA. The guide bars, made of ASTM Type 304/304L stainless steel, are located to correspond to the bumpers of the SLB2 payload container. There are three bars on each side of the cavity and on the closed end, and two on the top. Both the debris shield receptacle and guide bars are attached to the CSA containment sheets using a combination of groove welds and fillet welds.

Two 100–mm × 50–mm × 6–mm austenitic stainless steel channels are installed on the floor of the cavity, and continuously welded to the bottom containment stainless steel sheet. Austenitic stainless steel guide tracks are installed and continuously welded to the channels. Two M24 × 3 threaded bosses made from ASTM Type 304L stainless steel are welded to the channels to provide an anchorage for internal arrangements such as a roller floor, as shown in Detail P on Sheet 21.

The overpack structure fully envelops the CSA body, and is designed to provide energy absorption, puncture resistance, and thermal insulation for the containment seals. Energy absorption is accomplished by the crushing of four different densities of polyurethane foam and by deformation of the outer sheets of the overpack structure, having a thickness of 6– or 8–mm. Puncture resistance is afforded by adjacent layers of balsa wood, stainless steel, and polyurethane foam. Thermal protection is provided by layers of stainless steel, foam, and calcium silicate insulation.

The overpack structure surrounding the CSA body is shown in Section F–F on Sheet 5 and Section G–G on Sheet 6. On the top and bottom walls, the thickness of the structure is 185 mm; on the vertical side walls, 190 mm; and in the octagonal recess on the closed end, the thickness is 201 mm. The overpack structure on the end (outside the octagonal recess) extends 610 mm beyond the CSA weldment, and the total length of the end overpack structure is 838 mm. At the open end of the body, two structures extend beyond the CSA flange face that envelop both sides of the overpack cover.

These structures, known as "cheeks", contain energy absorbing foam and thermal insulation. The cheeks extend 748 mm beyond the CSA flange face, and the total length of the cheek structure is 870 mm. The overall length of the Body assembly, which is equal to the overall length of the assembled packaging, is 4,288 mm. The external width is 2,500 mm, and the external height is 2,650 mm.

The puncture–resistant system of components occupies the central 2,574 mm of the package sides, top, and bottom, and the octagonal recess at the closed end. Starting adjacent to the CSA weldment, the system consists of a 109 – 120–mm thick layer of nominally 0.10 kg/dm^3 polyurethane foam, a puncture resistant plate made from stainless steel, a 60–mm thick layer of nominally 0.12 kg/dm^3 balsa wood, and an outer sheet made from 6–mm thick stainless steel. The puncture–resistant plate is 10–mm thick on the sides, top, and bottom, and 15–mm thick on the closed end. The puncture–resistant plates are fastened to the surrounding structures using pop rivets. As shown in Detail E on Sheet 4, the end faces of the top and bottom overpack structure by the open end each contain five threaded bosses (total of ten) for the attachment of the overpack cover. The threads are M36 × 4 and may optionally feature alloy steel thread inserts. As shown in Section C–C of Sheet 4, a single alignment pin is located between two bolt holes in the top row, used to aid in alignment during installation of the overpack cover.

As shown in Section H–H on Sheet 7, with further detail given in Detail K, the four edges of the overpack in the central 2,574 mm length between the end structures are protected by a chevron–shaped region filled with blocks of 0.29 kg/dm^3 polyurethane foam and enveloped by a 6–mm thick stainless steel sheet.

The end overpack region (228 mm overlapping the end of the CSA weldment and extending 610 mm beyond the end of the CSA for a total length of 838 mm) is composed of nominally 0.48 kg/dm^3 and 0.16 kg/dm^3 polyurethane foam. The heavier density foam is used for protection in corner drops, and is placed as shown in Section J–J on sheet 8. The lighter density foam is used primarily on the end face as shown in Section AU–AU on sheet 8. A puncture–resistant plate of 6–mm thickness separates the two densities of foam. Other views of the end overpack structure are shown in Partial Sections AR–AR and AS–AS on Sheet 9.

At the open end of the body, the cheek structures have a construction similar to the corresponding regions of the closed end overpack. An added feature in the cheeks is a 30–mm thick sheet of calcium silicate thermal insulation placed next to the CSA body flange. The insulation is protected by enveloping stainless steel plates of 16–mm thickness. The cheek is shown in Partial Sections AN–AN and AP–AP on Sheet 9. All welds pertaining to the overpack structure are liquid penetrant inspected per Flag Note 17 on Sheet 1.

A modified International Organization for Standardization (ISO) lifting corner fitting is incorporated into each corner of the body. These ISO fittings provide the handling interface for lifting the TRUPACT–III package from its conveyance and on–site movement for loading/unloading operations. Since these fittings are only designed for lifting and off–road movement of the package, the ISO fittings are disabled during transport to prevent their use as a potential tie–down device.

To limit the axial free space available relative to the SLB2 payload container, plates made of a plastic material such as nylon, polyethylene, or polyurethane are attached to the inner surface of the three guide bars which run transversely across the closed end of the payload cavity. The thickness of the plastic plates is such as to provide a final length of 2,752 ± 3 mm between the plates and the closure lid. The vertical locations of the plates correspond to the bumpers on each

end of the SLB2. For a minimum length SLB2 of 107.38 inches, or 2,727 mm, the maximum axial free space between the package cavity and the SLB2 is 28 mm. A minimum clearance between the SLB2 and the closure lid inner surface of 2 mm will be assured at the time of package closure (see Section 7.1.4, *Loading the Payload into the TRUPACT–III Package*).

To prevent pressurization of the overpack structure in the event of the HAC fire, the outer sheets feature a total of (36) 1–inch NPT fusible plastic plugs. All external surfaces of the body assembly except the external bottom surface, surfaces covered by the overpack cover, and the ISO corner fittings, are coated with a low–halogen white paint. The external bottom surface may be painted as an option.

1.2.1.2 Closure Lid

The closure lid, shown on Sheets 13 and 14, is a rigid stainless steel weldment that completes the CSA. It consists of inner and outer, 12–mm thick sheets, connected by V–stiffeners of 4–mm thickness. The total thickness of the weldment is 148 mm (not including the shear lip), the width is 2,108 mm, and the height is 2,280 mm. The V–stiffeners are attached to the outside of the inner (containment) sheet using continuous fillet welds. The outer sheets are connected to the V–stiffeners using continuous slot welds (similar in kind to the corresponding welds on the closed end).

Around the outside of the lid is located a rigid box beam flange which mates with the flange on the CSA body. As shown in Detail Y on Sheet 14, the inner (seal side) plate of the flange is 20–mm thick. The opposite side of the flange is also 20–mm in thickness. The remaining two plates of the flange are of 16–mm thickness. Bolt tubes of 10–mm radial thickness are welded at each end to the inner and outer flange plates, and which carry the closure bolt loads through the thickness of the lid. A shear lip runs on all four sides of the lid and engages the opening of the CSA body. It has a shear thickness of 20 mm and a bearing width of 10 mm. All containment boundary welds are radiograph inspected per Flag Note 15 and liquid penetrant inspected per Flag Note 16 on Sheet 1. All other closure lid welds are liquid penetrant inspected per Flag Note 16 on Sheet 1. As with the CSA body, all cavities within the closure lid are interconnected. When evacuated of air and backfilled with helium, these cavities present a fully enveloping blanket of helium for use during leakage rate testing of the containment boundary. Access to these cavities (including those between the inner and outer sheets of the CSA body) is provided by small ports in the lower right–hand corner of the lid and CSA body flanges, as shown in Section Z–Z on Sheet 15.

Extending inward from the shear lip inner surface (as shown in Figure 1.1-7) is the debris shield holder, made of the same material as the lid. It is 4 mm thick and 15 mm long, and is integral with the shear lip. The debris shield insert, shown on Sheet 4, has a U–shaped cross–section and is made of silicone foam rubber. It is attached to both sides of the holder using double–sided tape. The insert mates with the receptacle described in Section 1.2.1.1, *Body,* to form the completed debris shield, as shown on Sheet 4. Each of the four shear lips features two, 5/16–inch (7.9 mm) diameter filters made from porous polyethylene. These filtered passages prevent a pressure differential across the debris shield and permit helium to reach the containment O–ring seal during leakage rate testing.

In the lower right–hand corner on the exterior surface, a 200–mm × 320–mm recess is located, which contains the vent port and the seal test port, as shown in Section Z–Z on Sheet 15. The seal test port communicates with the cavity between the containment and test O–ring seals in the closure lid and is used during leakage rate or pressure rise testing. The vent port (a containment boundary

penetration) is 50–mm in diameter. It is closed by an aluminum bronze insert and sealed by a butyl O–ring seal. A test O–ring seal is also located in the vent port insert. The insert is retained in position using an aluminum bronze, M120 × 6 threaded retaining ring, which in turn is locked in place using an aluminum bronze locking ring. In the region of the 200 mm × 320 mm recess, the closure lid inner plate is 40–mm in thickness (20–mm elsewhere).

The closure lid is attached to the body by (44) M36 × 205 mm bolts that are tightened to 1,600 N–m (lubricated) torque. The bolts are made from ASTM A320, L43 alloy steel and are cadmium plated. Washers are used with the closure bolts, made of ASTM A564, Grade 630, Condition H1025 (17–4 PH) material. The sealing flange of the closure lid contains two dovetail grooves to retain the butyl rubber containment and test O–rings, each of which is nominally of 12–mm cross–sectional diameter. At each corner of the closure lid, the containment seal groove changes direction using a 50–mm radius, while the test O–ring groove utilizes a 74–mm radius. Both containment O–ring seals (i.e., the inner seal on the vent port and the inner seal of the closure lid) are made from Rainier Rubber R–0405–70 material, meeting the requirements of Section 8.1.5.3, *Butyl Rubber O–rings.*

Lifting of the closure lid is performed using two standard lifting eyes that are threaded into M36 threaded bosses installed on the top surface. During transport, these lifting points are covered by the overpack cover, making them inoperable.

One M36 threaded hole is located near the middle of each side of the lid (total of four holes). These holes are used if needed to separate the closure lid from the body. Two holes for the closure lid guide pins (attached to the CSA body flange) are located immediately above the horizontal centerline. As an option, thread inserts may be installed in all internal threads of the closure lid.

1.2.1.3 Overpack Cover

The overpack cover has a design very similar to that of the overpack structure on the closed end. When installed, the overpack cover fits between the cheeks on the body and completely envelops the closure lid and CSA body flange. It is designed to provide energy absorption, puncture resistance for the closure lid, and thermal insulation for the containment seals, and is depicted on Sheets 16 through 18.

The overpack cover of the TRUPACT–III packaging consists of a rectangular stainless steel sheet structure encasing an impact–absorbing and thermal insulation materials structure. Similar to the body closed end overpack structure, the central area of the overpack cover consists of a nominally 393–mm deep octagonal recess. The recess consists of a 6–mm cover sheet, a 60–mm thick balsa wood sheet, a 15–mm thick puncture–resistant stainless steel sheet, and a 120–mm thickness of 0.10 kg/dm^3 polyurethane foam, adjacent to a 6–mm thick inner cover sheet. Outside the recess, the overpack cover features 272 mm long, upper and lower flanges which envelop the CSA body flange. The remainder of the 870–mm total thickness is taken up by a 42–mm thick layer of calcium silicate insulation, a 16–mm thick stainless steel protective plate, a 382–mm thickness of 0.48 kg/dm^3 polyurethane foam, a 6–mm thick puncture–resistant plate, a 140–mm thickness of 0.16 kg/dm^3 polyurethane foam, and an outer 8–mm thick steel sheet. The calcium silicate thermal insulation and the 16–mm thick protective stainless steel sheet include a region that covers the vent test ports as shown in Section AF–AF on Sheet 17. The upper and lower flanges feature 30–mm thick thermal insulation (corresponding to the thermal insulation in the body cheeks), protected by 16–mm thick stainless steel plates.

The overpack cover is attached to the body by ten, M36 × 60 mm bolts that are tightened to 1,600 N–m (lubricated) torque. The bolts are made from ASTM A320, Type L43 alloy steel and are cadmium plated. The bolts (five each along the top and bottom edges) are installed through thin–wall, ASTM Type 304L stainless steel access tubes that are located on the top and bottom edges. The bolts thread into 70–mm diameter stainless steel threaded bosses that are welded in the exterior stainless steel sheet of the body. Two of the access tubes (lower left and lower right) are configured to accept a tamper–indicating seal. On the inside surface, short, 3½–inch diameter cylindrical depressions are located around the perimeter to provide receptacles for the heads of the closure lid bolts. A 44–mm wide and 84–mm tall opening located on the top flange of the overpack cover interfaces with the guide pin installed in the mating flange of the body assembly.

Lifting of the overpack cover is performed using two standard lifting eyes that are threaded into M36 threaded bosses installed on the top surface. These threaded bosses are made inoperable during transport to prevent their use as a tie–down device and to prevent the collection of water. As an option, a thread insert may be installed in these internal threads. On one side of the overpack cover (protected by a side cheek), is located a recess in which a pressure relief valve is installed, and which will prevent an excessive pressure differential from developing inside the overpack cover shell. To prevent pressurization of the overpack cover in the event of the HAC fire, the outer face sheet features a total of (8) 1–inch NPT fusible plastic plugs.

The overpack cover has nominal external dimensions of 2,108–mm wide, 2,650–mm high, and 870–mm thick. All overpack cover welds are liquid penetrant inspected per Flag Note 17 on Sheet 1. All surfaces of the overpack cover that form the outside surface when installed on the TRUPACT–III, except the external bottom surface, are coated with a low–halogen white paint. The external bottom surface may be painted as an option.

1.2.1.4 Gross Weight

The gross shipping weight of a TRUPACT–III package is 25,000 kg (55,116 lbs) maximum. A summary of overall component weights is shown in Table 2.1-2 and discussed in Section 2.1.3, *Weights and Centers of Gravity.*

1.2.1.5 Neutron Moderation and Absorption

The TRUPACT–III package does not require specific design features to provide neutron moderation and absorption for criticality control. Fissile materials in the payload are limited to amounts that ensure safely subcritical packages for both NCT and HAC. The fissile material limits for a single TRUPACT–III package are based on an optimally moderated and reflected fissile material. The structural materials in the TRUPACT–III packaging are sufficient to maintain reactivity between the fissile materials in an infinite array of damaged TRUPACT–III packages at an acceptable level. Further discussion of neutron moderation and absorption is provided in Chapter 6.0, *Criticality Evaluation.*

1.2.1.6 Receptacles, Valves, Testing, and Sampling Ports

There are no receptacles used on the TRUPACT–III packaging. However, a vent port, a seal test port, and a body helium fill port access port are located in the closure lid as described in Section 1.2.1.2, *Closure Lid.* The vent port provides access to the payload cavity for sampling or venting

the payload cavity during unloading operations. The vent port, in conjunction with the seal test port, is also used to perform leakage rate testing of the inner containment O–ring seal to verify proper assembly of the TRUPACT–III package prior to shipment. The vent port and the seal test port are accessed through a recess located in the lower right corner of the closure lid. The body helium fill port access port is accessible on the surface of the closure lid, near the recess. All ports are inaccessible when the overpack cover is installed.

1.2.1.7 Heat Dissipation

The TRUPACT–III package design capacity is 80 thermal watts maximum. The TRUPACT–III package dissipates this low internal heat load entirely by passive heat transfer for both NCT and HAC. The TRUPACT–III packaging does not utilize any coolants. To improve the insolation resistance for NCT, the external surfaces of the packaging are painted with a low–halogen white paint. No other features or special devices are needed or utilized to enhance the dissipation of heat. Features are included in the design to enhance thermal performance in the HAC thermal event. These features include the use of a high temperature insulating material (calcium silicate insulating board) and polyurethane foam in the body and overpack cover. A more detailed discussion of the package thermal characteristics is provided in Chapter 3.0, *Thermal Evaluation.*

1.2.1.8 Lifting and Tie–down Devices

Lifting of the TRUPACT–III package is via the ISO fittings at each upper corner. Under excessive load, the ISO corner fittings are designed to fail in shear prior to compromising the structure of the packaging. The ISO corner fittings are covered during transport and rendered inoperable to preclude their use as a tie–down device.

The closure lid and the overpack cover are lifted via two M36 lifting eyes. These lifting points are designed for lifting only their respective component, and therefore, are covered during transport and rendered inoperable to preclude their use as a tie–down device.

There are no tie–down devices on the TRUPACT–III package. The TRUPACT–III package is secured to the transport vehicle (semi–trailer or rail car) by straps or a tie–down frame that is positioned over the top of the package.

A detailed discussion of lifting and tie–down designs, with corresponding structural analyses, is provided in Section 2.5, *Lifting and Tie–down Standards for All Packages.*

1.2.1.9 Pressure Relief System

There are no pressure relief systems included in the TRUPACT–III package design to relieve pressure from within the containment boundary. A pressure relief valve is utilized in the overpack cover to prevent a significant gage pressure from occurring within the overpack cover outer shell. In addition, fire–consumable, plastic vent plugs are employed on the exterior surface of the body and overpack cover.

1.2.1.10 Shielding

Due to the nature of the contact–handled transuranic (CH–TRU) payloads, no biological shielding is necessary or provided by the TRUPACT–III packaging.

1.2.2 Contents

The TRUPACT–III packaging is designed to transport contact–handled transuranic (CH–TRU) waste and other authorized payloads that do not exceed 10^5 A_2 quantities, as defined in the TRUPACT–III TRAMPAC. All users of the TRUPACT–III package shall comply with all payload requirements outlined in the TRUPACT–III TRAMPAC, using one or more of the methods described in that document.

1.2.3 Special Requirements for Plutonium

The TRUPACT–III package may contain plutonium in excess of 0.74 Tbq (20 Ci), which is in solid or solidified form.

1.2.4 Operational Features

The TRUPACT–III package is not operationally complex. All operational features are readily apparent from an inspection of the drawings provided in Appendix 1.3.1, *Packaging General Arrangement Drawings*, and the previous discussions presented in Section 1.2.1, *Packaging*. Operational procedures and instructions for loading, unloading, and preparing an empty TRUPACT–III package for transport are provided in Chapter 7.0, *Operating Procedures*.

1.3 Appendices

1.3.1 Packaging General Arrangement Drawings

1.3.2 Glossary of Terms and Acronyms

This page intentionally left blank.

1.3.1 Packaging General Arrangement Drawings

This section presents the TRUPACT–III packaging general arrangement drawing[1], consisting of 21 sheets entitled, *TRUPACT–III Packaging SAR Drawing*, Drawing Number 51199–SAR, Rev. 1.

Within the packaging general arrangement drawing, dimensions important to the packaging's safety are dimensioned and toleranced (e.g., sealing regions on the seal flanges). All other dimensions are provided as a reference dimension, and are toleranced in accordance with the general tolerance block.

[1] The TRUPACT–III packaging general arrangement drawing utilizes the uniform standard practices of ASME Y14.5M–1994, *Dimensioning and Tolerancing*, American National Standards Institute, Inc. (ANSI).

This page intentionally left blank.

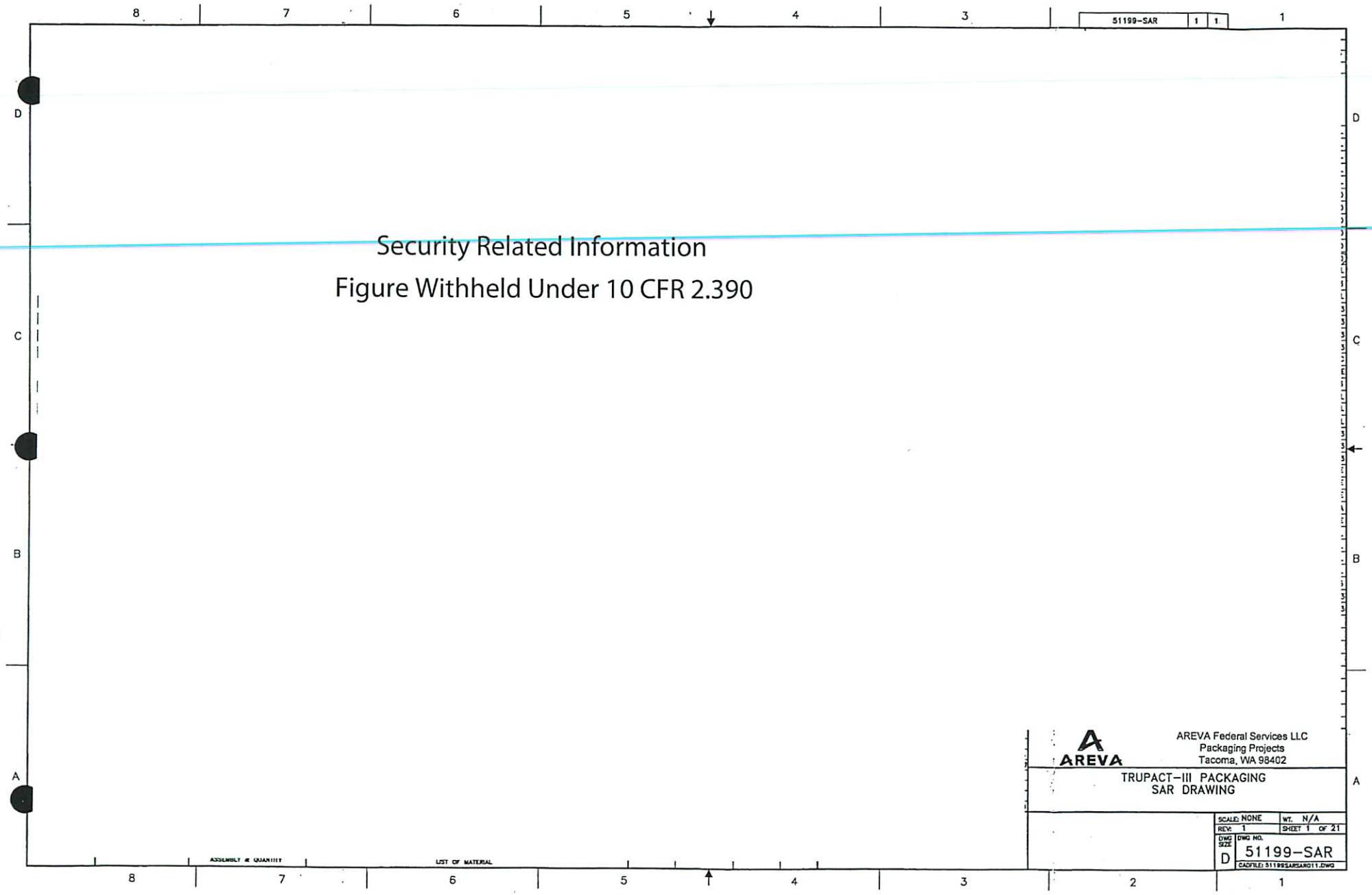
51199-SAR
1
1
Security Related Information
Figure Withheld Under 10 CFR 2.390
AREVA
AREVA Federal Services LLC
Packaging Projects
Tacoma, WA 98402
TRUPACT-III PACKAGING
SAR DRAWING
SCALE: NONE
WT. N/A
REV: 1
SHEET 1 OF 21
DWG SIZE D
DWG NO. 51199-SAR
CADFILE: 51199SARSAR011.DWG
ASSEMBLY # QUANTITY
LIST OF MATERIAL

Security Related Information

Figure Withheld Under 10 CFR 2.390

Security Related Information

Figure Withheld Under 10 CFR 2.390

Security Related Information

Figure Withheld Under 10 CFR 2.390

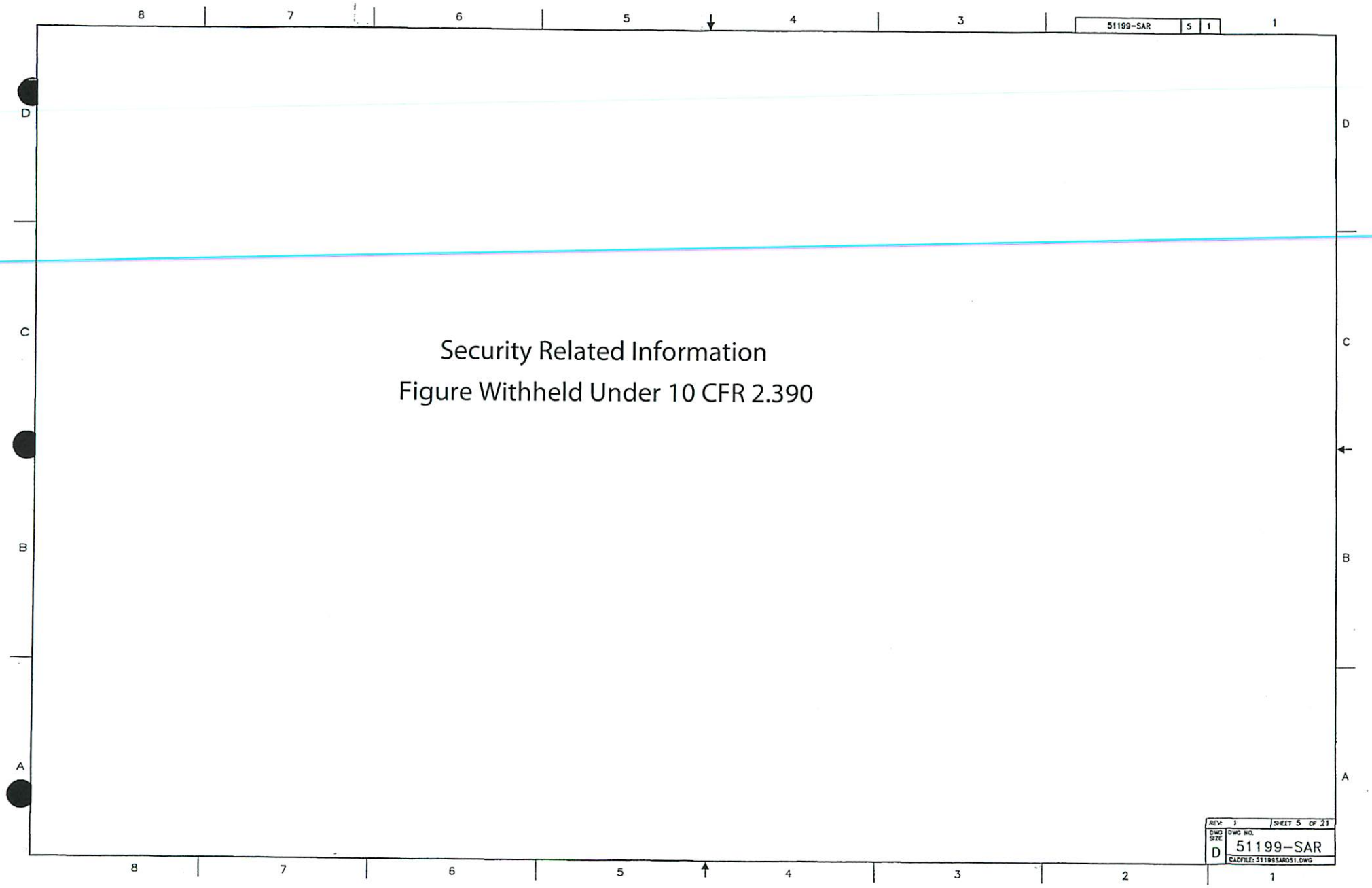
51199-SAR 5 1
Security Related Information
Figure Withheld Under 10 CFR 2.390
REV: J
SHEET 5 OF 21
DWG SIZE D
DWG NO. 51199-SAR
CADFILE: 51199SAR051.DWG

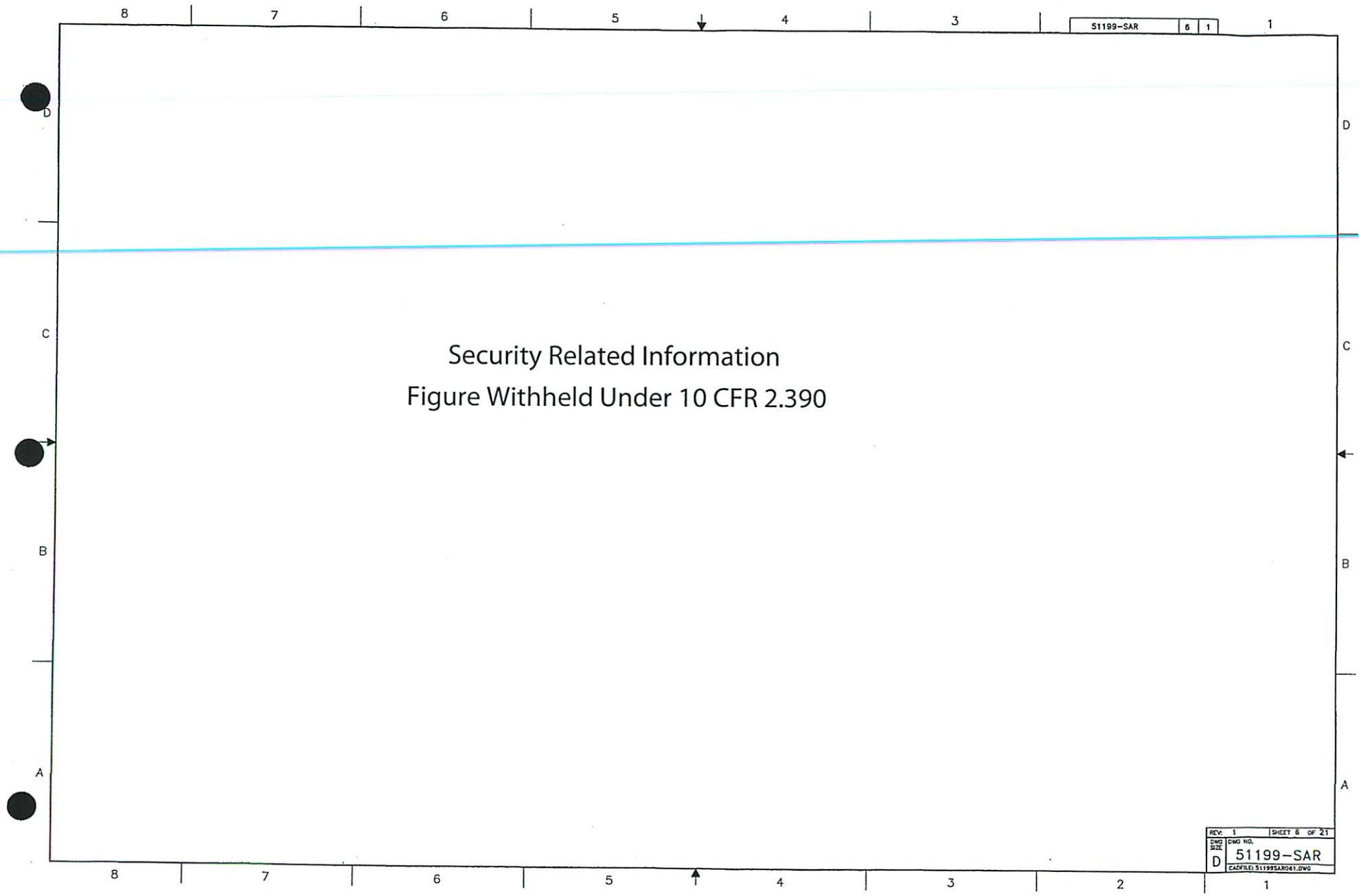
51199-SAR 6 1
Security Related Information
Figure Withheld Under 10 CFR 2.390
REV: 1
SHEET 6 OF 21
DWG SIZE D
DWG NO. 51199-SAR
CADFILE: 51199SAR061.DWG

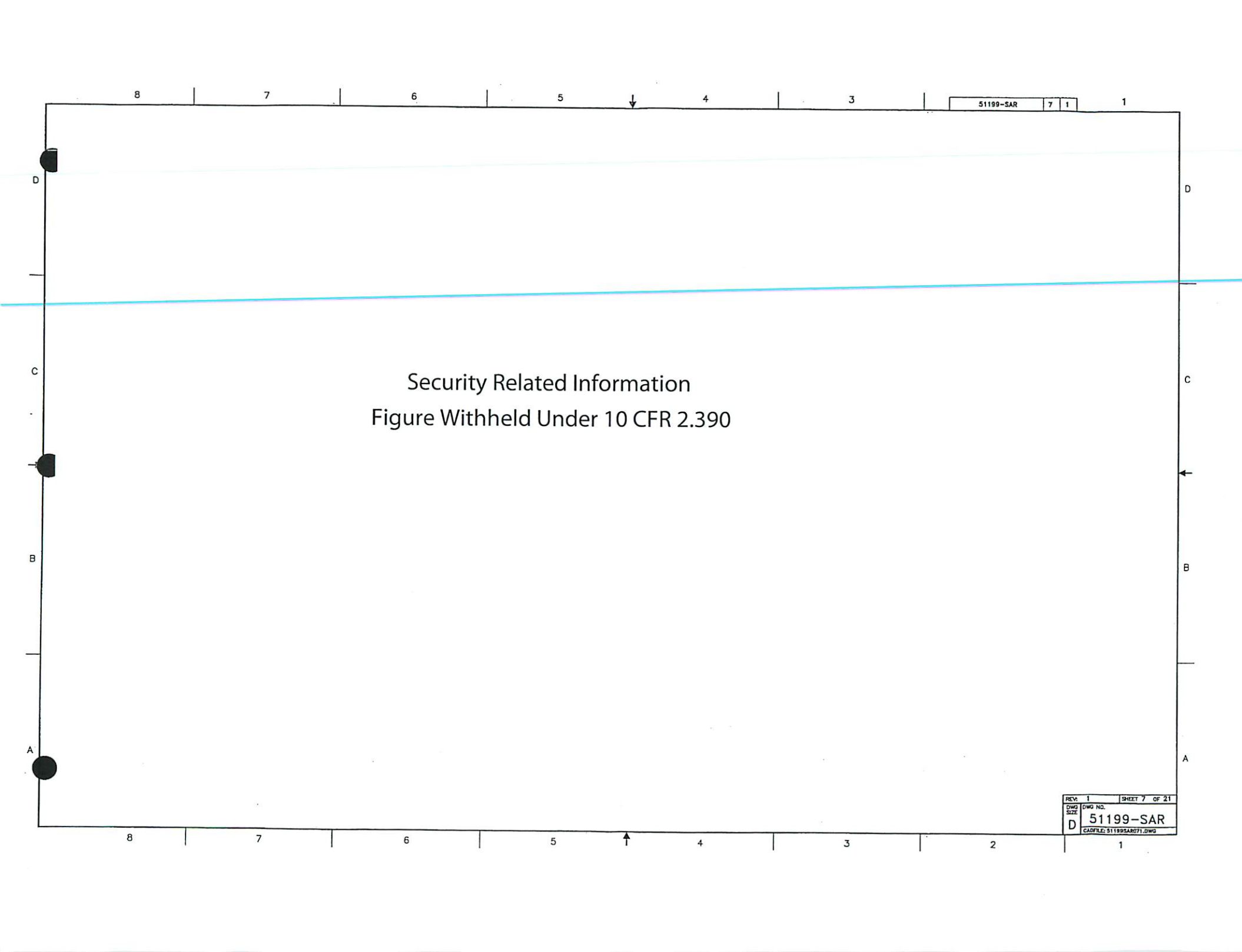
8
7
6
5
4
3
2
1
51199-SAR
7
1
D
C
B
A
Security Related Information
Figure Withheld Under 10 CFR 2.390
REV. 1
SHEET 7 OF 21
DWG SIZE
D
DWG NO.
51199-SAR
CADFILE: 51199SAR071.DWG

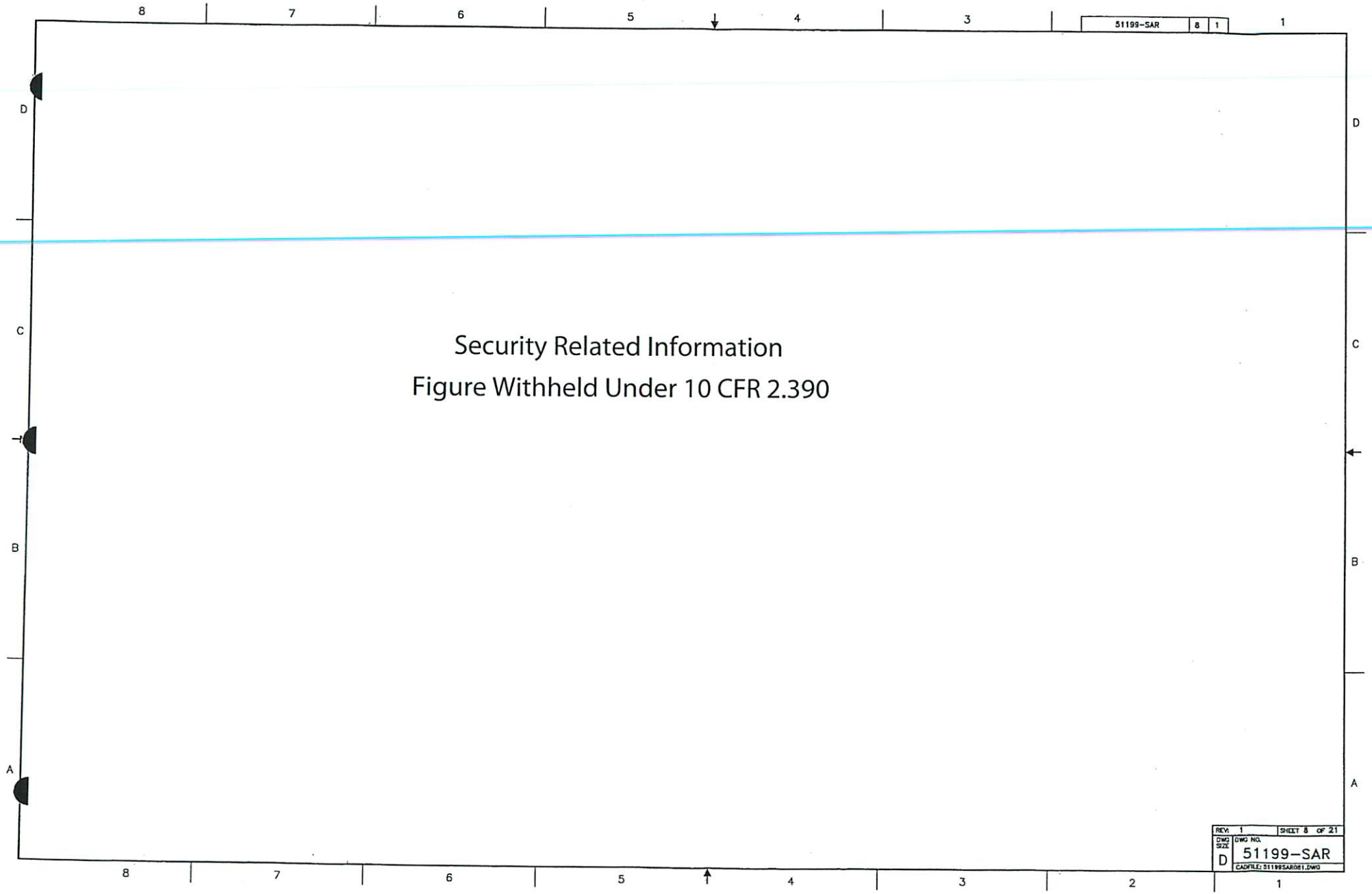

Security Related Information

Figure Withheld Under 10 CFR 2.390

Security Related Information

Figure Withheld Under 10 CFR 2.390

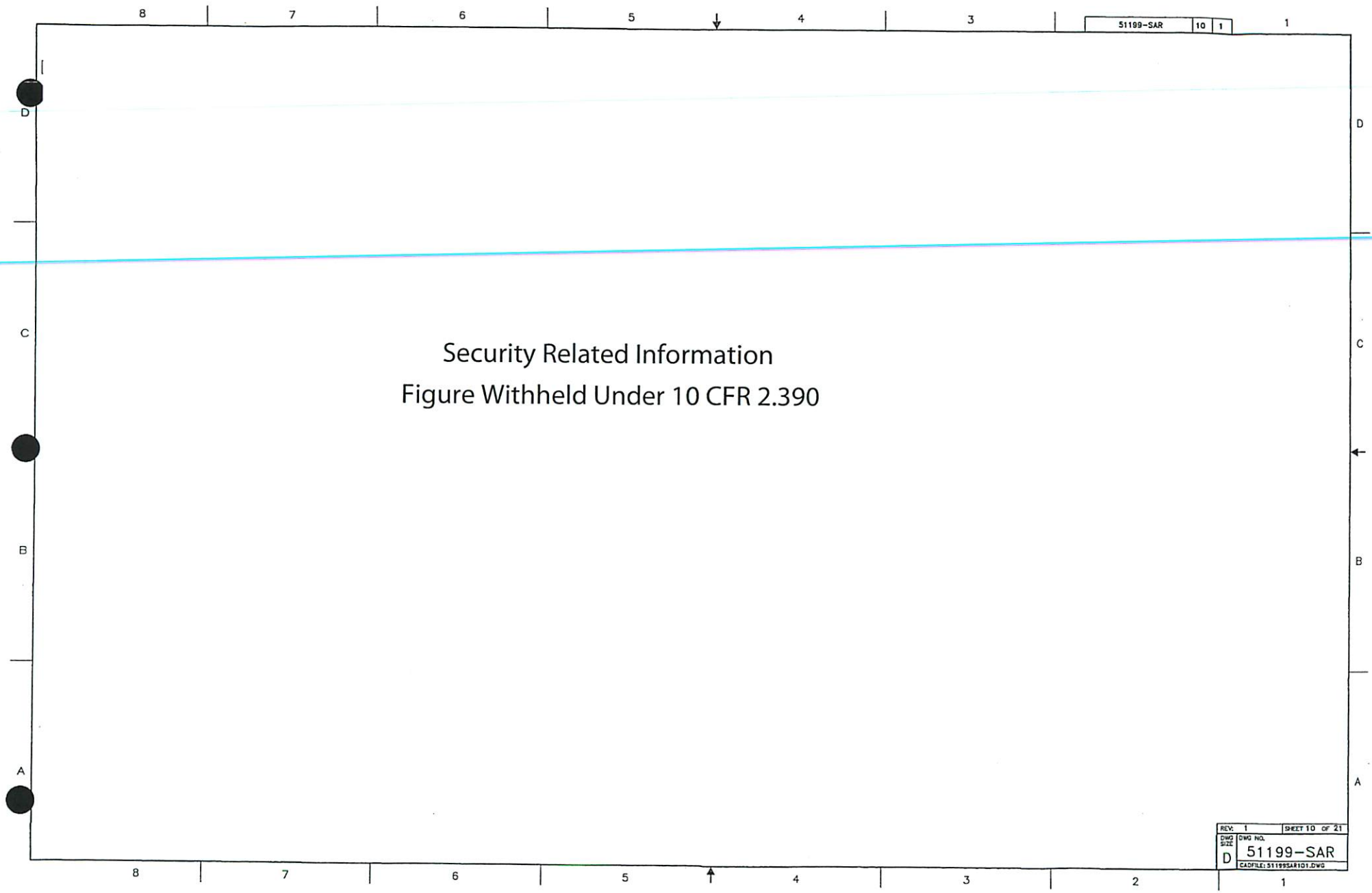

Security Related Information

Figure Withheld Under 10 CFR 2.390

Security Related Information

Figure Withheld Under 10 CFR 2.390

Security Related Information

Figure Withheld Under 10 CFR 2.390

Security Related Information

Figure Withheld Under 10 CFR 2.390

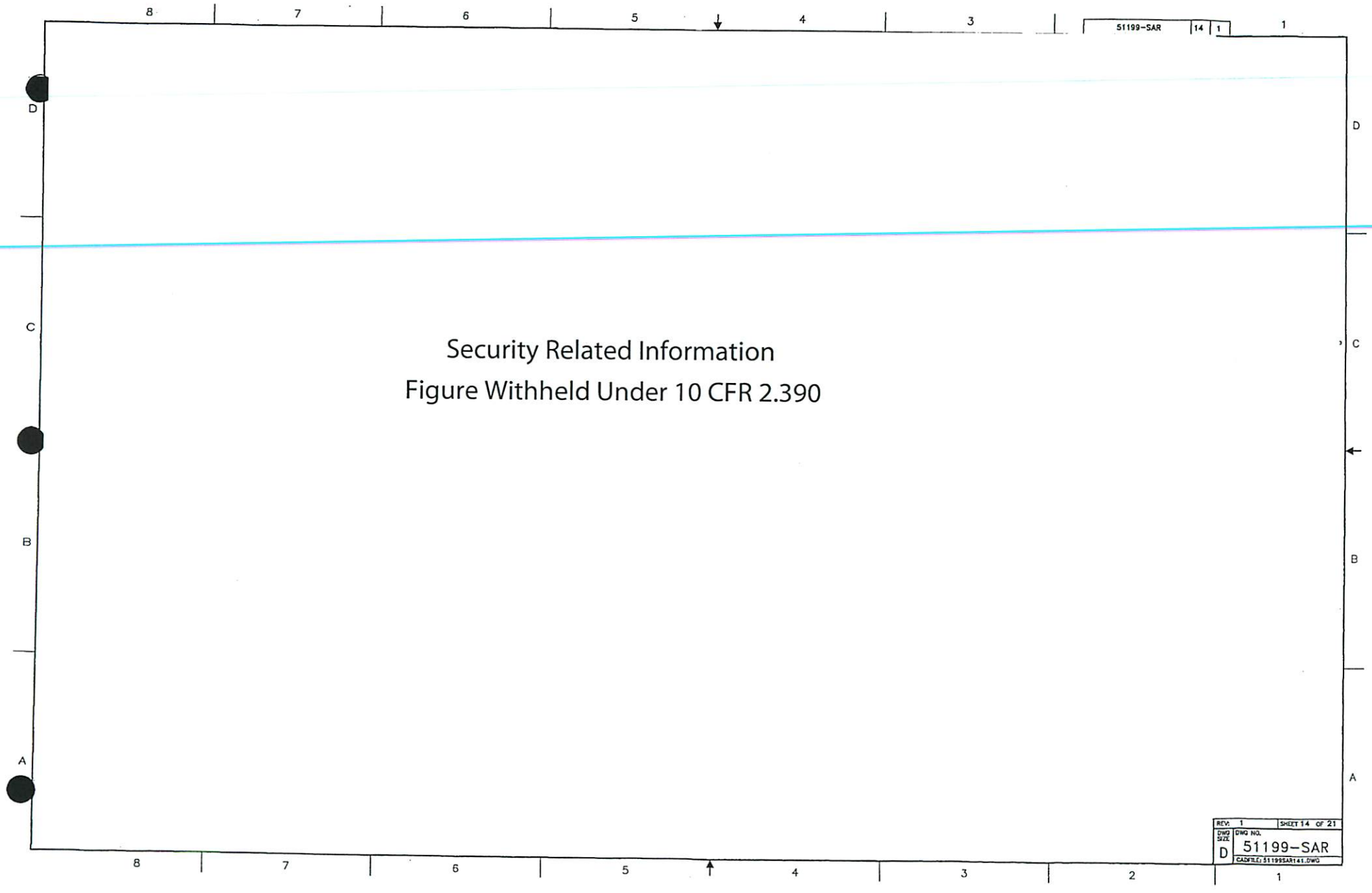
51199-SAR 14 1
Security Related Information
Figure Withheld Under 10 CFR 2.390
REV: 1
SHEET 14 OF 21
DWG SIZE D
DWG NO. 51199-SAR
CADFILE: 51199SAR141.DWG

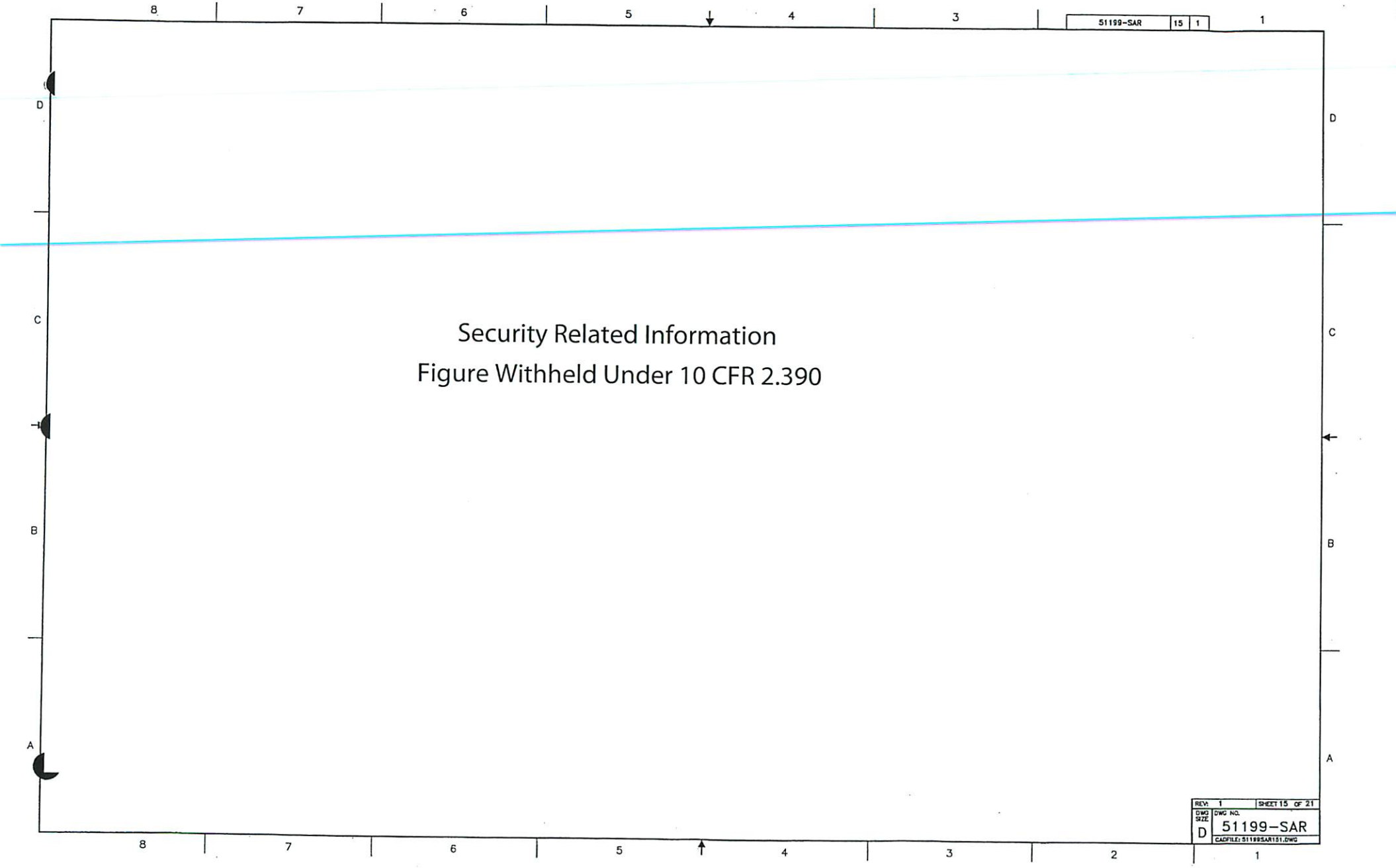
8
7
6
5
4
3
2
1
51199-SAR
15
1
D
C
B
A
Security Related Information
Figure Withheld Under 10 CFR 2.390
REV: 1
SHEET 15 OF 21
DWG SIZE
D
DWG NO.
51199-SAR
CADFILE: 51199SAR151.DWG

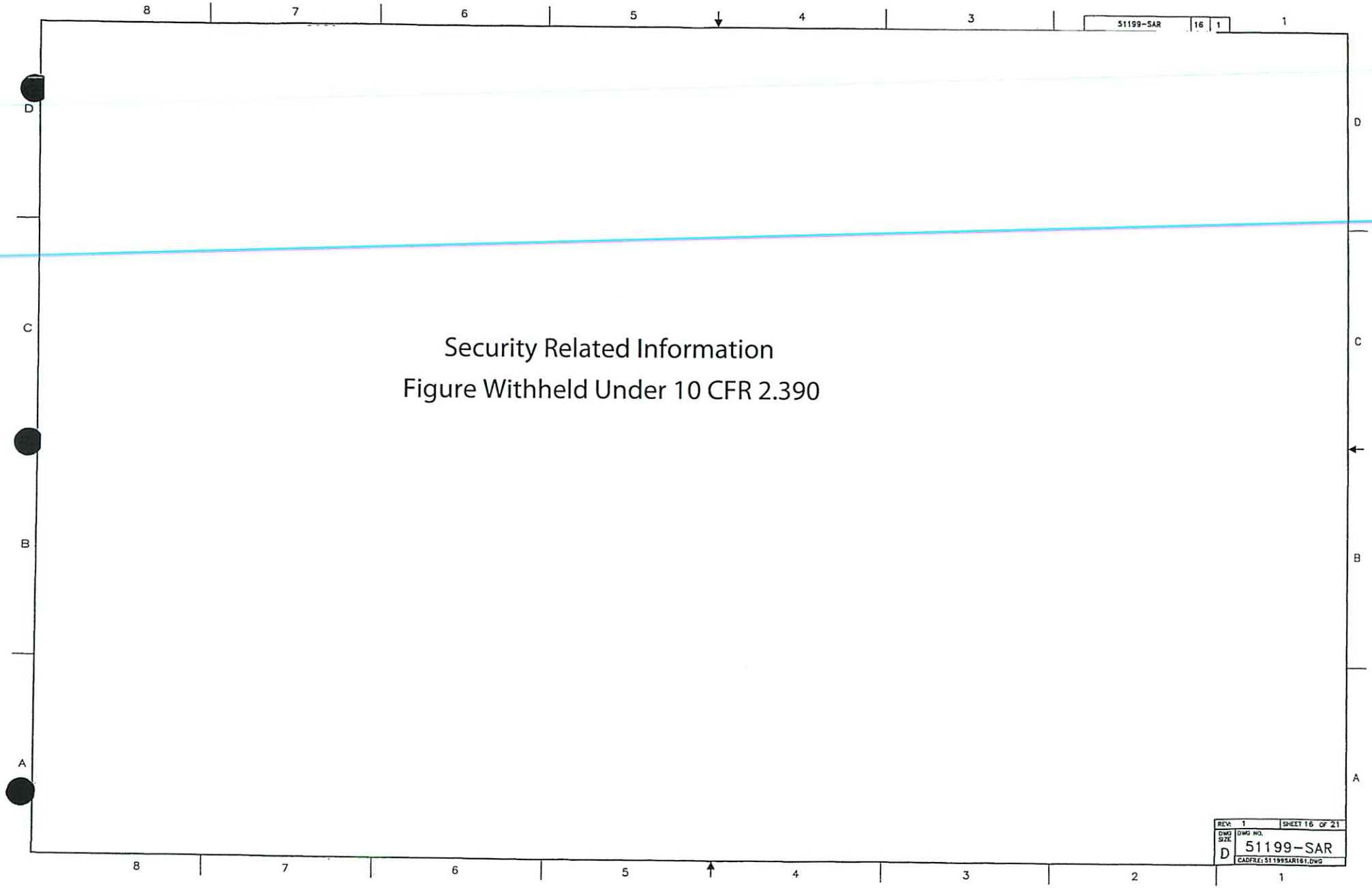
8
7
6
5
4
3
2
1
D
C
B
A
51199-SAR
16
1
Security Related Information
Figure Withheld Under 10 CFR 2.390
REV: 1
SHEET 16 OF 21
DWG SIZE
D
DWG NO.
51199-SAR
CADFILE: 51199SAR161.DWG

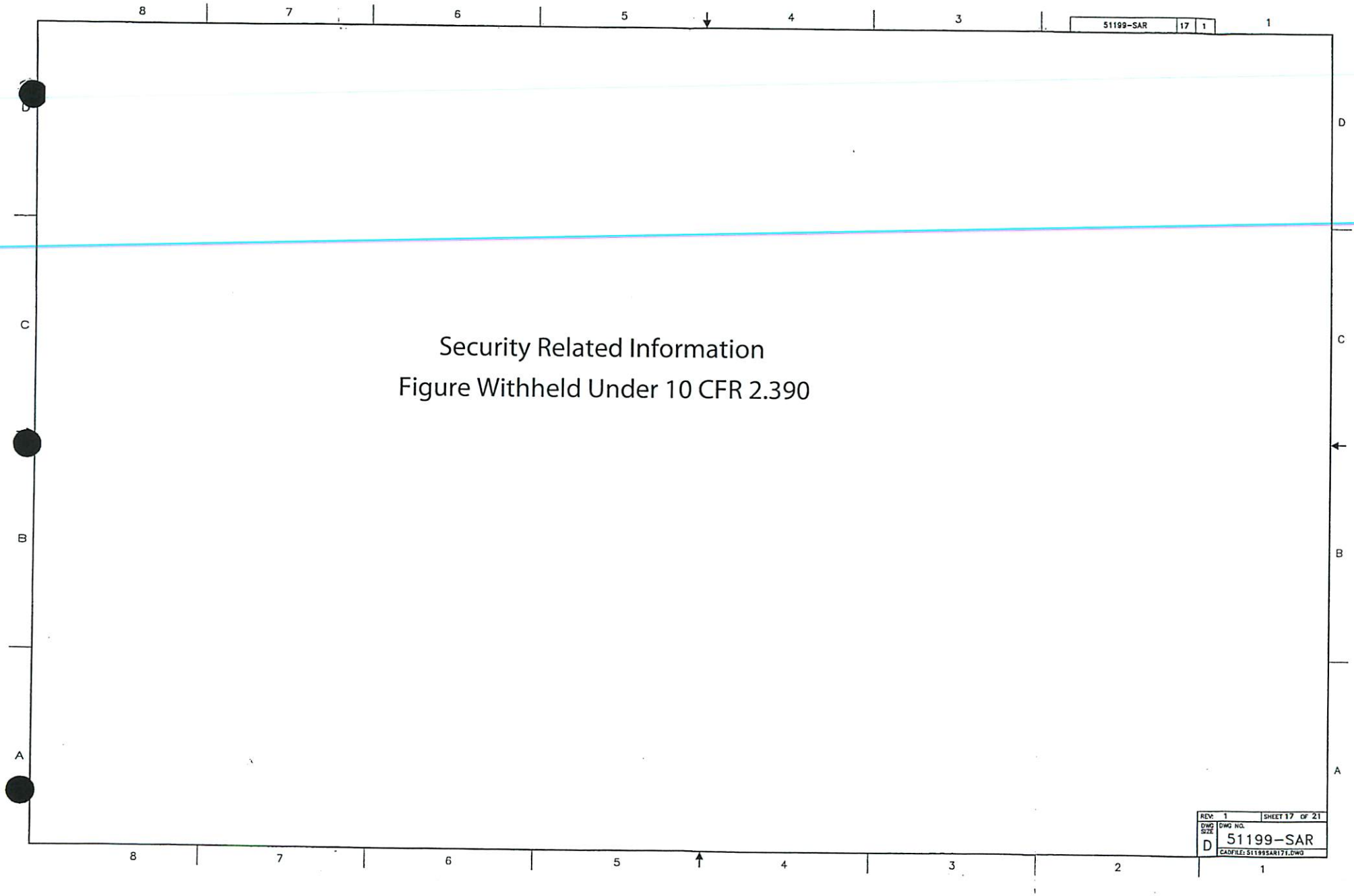
8
7
6
5
4
3
2
1
51199-SAR
17
1
A
B
C
D
Security Related Information
Figure Withheld Under 10 CFR 2.390
REV: 1
SHEET 17 OF 21
DWG SIZE
D
DWG NO.
51199-SAR
CADFILE: 51199SAR17I.DWG

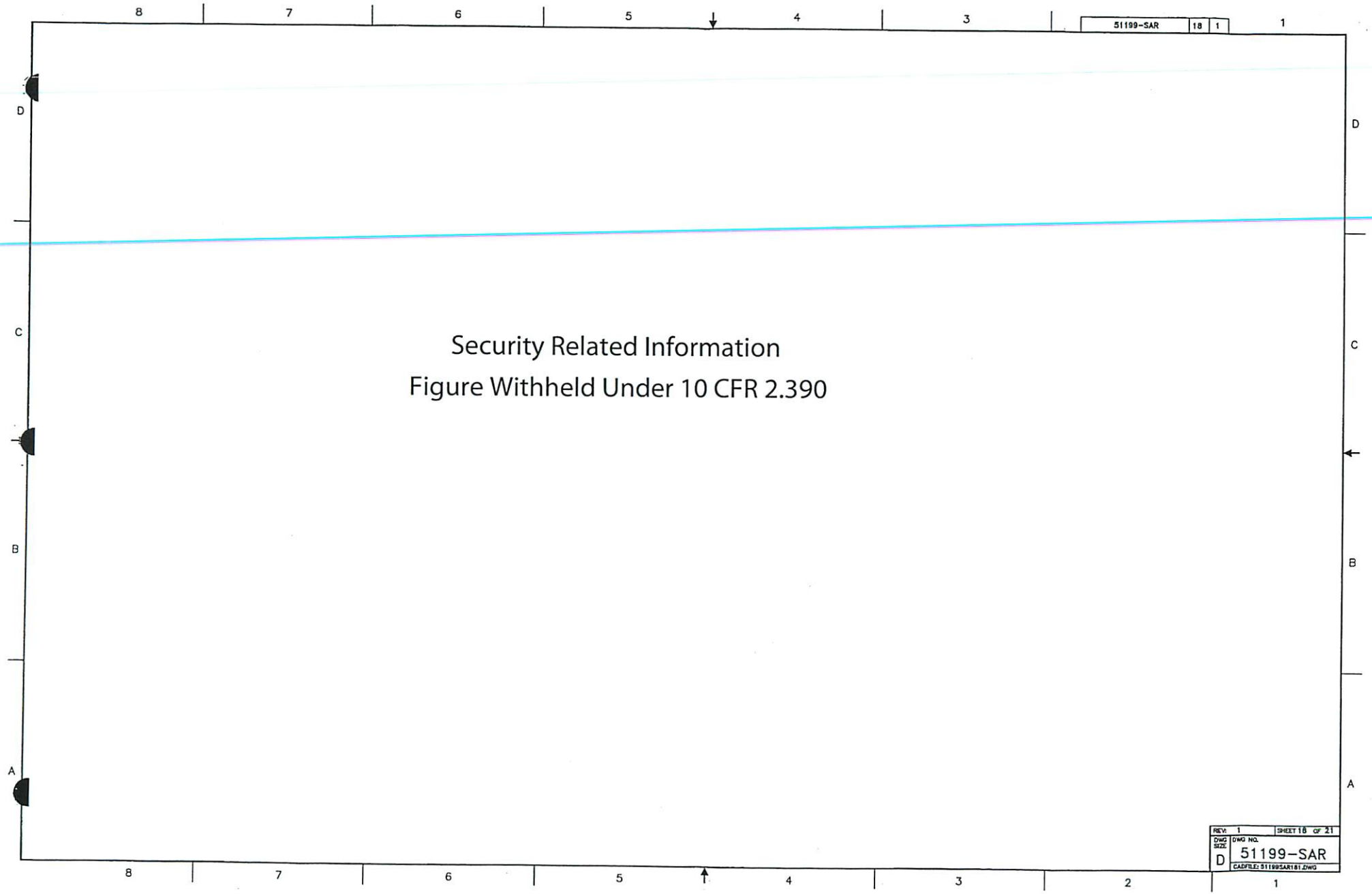
8
7
6
5
4
3
2
1
51199-SAR
18
1
D
C
B
A
Security Related Information
Figure Withheld Under 10 CFR 2.390
REV: 1
SHEET 18 OF 21
DWG SIZE
D
DWG NO.
51199-SAR
CADFILE: 51199SAR181.DWG

Security Related Information

Figure Withheld Under 10 CFR 2.390

Security Related Information

Figure Withheld Under 10 CFR 2.390

Security Related Information

Figure Withheld Under 10 CFR 2.390

REV: 1 SHEET 21 OF 21

DWG SIZE D DWG NO. 51199-SAR

CADFILE: 51199SAR211.DWG

1.3.2 Glossary of Terms and Acronyms

ANSI – American National Standards Institute.

ASME – American Society of Mechanical Engineers.

ASME B&PVC – ASME Boiler and Pressure Vessel Code.

ASTM – American Society for Testing and Materials.

AWS – American Welding Society.

Body Assembly – The rectangular box, which together with the closure lid and overpack cover, constitutes the TRUPACT–III packaging.

Body Helium Fill Access Plugs – The threaded aluminum bronze plugs that seal the helium fill ports in the closure lid and body seal flange; consists of a plug on both sides of the closure lid.

Body Helium Fill Access Ports – The penetrations in the closure lid sealing flange to permit access to the body helium fill port; consists of a port on both sides of the closure lid.

Body Helium Fill Port – The penetration into the V–stiffener cavity of the sealing/bolting flange of the body that permits the introduction of helium for helium leakage rate testing of the containment boundary.

Body Helium Fill Port Plug – The threaded aluminum bronze plug that seals the body helium fill port.

Cheeks – The extensions of the body assembly which protect the sides of the overpack cover.

Closure Lid – The packaging component that closes and seals the payload cavity. The closure lid is part of the CSA.

Containment O–ring Seal – The inner O–ring seal located in the closure lid; forms part of the containment boundary.

Containment Structural Assembly – The rigid weldment that contains, supports, and reinforces the containment boundary. Consists of two vertical walls, the top and bottom walls, the closed end wall, the closure lid, and closure bolts.

CSA – Containment Structural Assembly.

CTU – Certification Test Unit.

CH–TRU Waste – Contact–Handled Transuranic Waste.

Debris Shield Receptacle, Holder, and Insert – The receptacle is attached to the body and receives the insert. The holder is attached to the closure lid, and supports the insert. The insert is the silicone rubber extrusion that provides the shield when interfacing with the receptacle.

Guide Bar – Steel component attached to the CSA inner cavity to guide the payload container and protect the debris shield from damage.

HAC – Hypothetical accident conditions.

Lifting Arms – Reinforced steel structures at each end of the package that carry the lifting loads from the ISO lift fittings into the CSA. The front lifting arms are identical with the cheeks.

NCT – Normal conditions of transport.

Overpack Cover – The protective cover that is installed over the closure lid, and which completes the packaging overpack.

Overpack Structure – The structures and materials attached to the outside of the CSA.

Packaging – The assembly of components necessary to ensure compliance with packaging requirements as defined in 10 CFR §71.4.

Package – The packaging with its radioactive contents, or payload, as presented for transportation as defined in 10 CFR §71.4.

Payload – Contact–handled transuranic (CH–TRU) waste or other authorized contents contained within the approved payload container. In this SAR, the payload includes a loaded SLB2 payload container and a payload loading system, such as a pallet and roller floor. Payload requirements are defined by the TRUPACT–III TRAMPAC.

Payload Container – The payload container is the SLB2.

Payload Loading Pallet – A lightweight pallet used for handling the payload containers.

Roller Floor – A structure supported by the floor of the TRUPACT–III interior cavity. It may be equipped with retractable rollers or equivalent means to facilitate insertion and removal of the payload loading pallet.

SAR – Safety Analysis Report (this document).

Seal Test Port – The penetration in the closure lid to evacuate for helium leakage rate testing or pressure rise testing of the main containment O–ring seal.

Seal Test Port Plug – The threaded aluminum bronze plug that seals the seal test port.

SLB2 – Standard Large Box, a payload container for use within the TRUPACT–III packaging.

Test O–ring Seal – The outer O–ring seal in the closure lid; forms the vacuum boundary for leakage rate testing.

TRUPACT–III Package – The package consisting of a TRUPACT–III packaging and payload.

TRUPACT–III Packaging – The packaging consisting of a body, closure lid, and an overpack cover.

TRUPACT–III TRAMPAC – TRUPACT–III TRU Waste Authorized Methods for Payload Control.

UNS – Unified National Standard.

Vent Port – The penetration into the cavity that is located in the closure lid; used to obtain an air sample, vent, and introduce helium into the payload cavity.

Vent Port Dust Plug – The threaded aluminum bronze plug that seals the vent port insert.

Vent Port Insert – The aluminum bronze solid plug that contains a containment and test O–ring seals; forms part of the containment boundary.

Vent Port Locking Ring – The threaded aluminum bronze ring that locks the vent port retaining ring into the closure lid.

Vent Port Retaining Ring – The threaded aluminum bronze ring that secures the vent port insert into the closure lid.

2.0 STRUCTURAL EVALUATION

This section presents evaluations demonstrating that the TRUPACT–III package meets all applicable structural criteria. The TRUPACT–III packaging, consisting of a body, a closure lid, and an overpack cover, is evaluated and shown to provide adequate protection for the payload. Normal conditions of transport (NCT) and hypothetical accident condition (HAC) evaluations, using analytic and empirical techniques, are performed to address 10 CFR 71[1] performance requirements. Analytic demonstration techniques, which apply to most NCT and some HAC evaluations, comply with the methodology presented in NRC Regulatory Guides 7.6[2] and 7.8[3]. Empirical demonstration techniques, which apply to free drop and puncture drop evaluations, consist of certification testing, utilizing two full-scale certification test units (CTU-1 and CTU-2). In all, the CTUs were subjected to a total of one 0.3-m NCT free drop, five 9-m HAC free drops, and six 1-m puncture drop tests. Results of the certification tests are provided in Appendix 2.12.3, *Certification Tests on CTU-1* and Appendix 2.12.6, *Certification Tests on CTU-2*. The design of the TRUPACT–III and the scope of the certification testing were guided by prior engineering tests on a half-scale test unit, as detailed in Appendix 2.12.1, *Engineering Tests*.

2.1 Description of Structural Design

2.1.1 Discussion

A comprehensive discussion of the TRUPACT–III packaging design and configuration is provided in Section 1.2, *Package Description*. A summary of that information follows.

From a structural viewpoint, the TRUPACT–III packaging consists of a rigid containment structural assembly (CSA) which is surrounded by energy-absorbing and thermally-protective overpack structure, shown in Section B-B on Sheet 4 of drawing 51199-SAR.

From an operational viewpoint, the TRUPACT–III packaging consists of a body assembly, a closure lid assembly, and an overpack cover assembly, as shown on Sheet 2 of drawing 51199-SAR. A detailed description of the TRUPACT–III body assembly is given in Section 1.2.1.1, *Body*; that of the closure lid assembly in Section 1.2.1.2, *Closure Lid*, and that of the overpack cover assembly in Section 1.2.1.3, *Overpack Cover*.

2.1.2 Design Criteria

Proof of performance for the TRUPACT–III packaging is achieved by a combination of analytic and empirical evaluations. The acceptance criteria for analytic assessments are in accordance with Regulatory Guide 7.6. The acceptance criterion for empirical assessments is a demonstration that the

[1] Title 10, Code of Federal Regulations, Part 71 (10 CFR 71), *Packaging and Transportation of Radioactive Material*, 01–01–09 Edition.

[2] U. S. Nuclear Regulatory Commission, Regulatory Guide 7.6, *Design Criteria for the Structural Analysis of Shipping Cask Containment Vessels*, Revision 1, March 1978.

[3] U. S. Nuclear Regulatory Commission, Regulatory Guide 7.8, *Load Combinations for the Structural Analysis of Shipping Casks for Radioactive Material*, Revision 1, March 1989.

containment boundary remains leaktight[4] following the imposed loading conditions. Additionally, package deformations obtained from certification testing must be such that deformed geometry assumptions used in subsequent thermal and criticality evaluations are validated.

The remainder of this section presents the detailed acceptance criteria used for analytic structural assessments of the TRUPACT–III packaging.

2.1.2.1 Analytic Design Criteria (Allowable Stresses)

This section defines the allowable stresses for primary membrane, primary bending, secondary, shear, peak, and buckling stresses for containment and non-containment structures. These allowable stresses are used for all analytic assessments of TRUPACT–III packaging structural performance.

2.1.2.1.1 Containment Structures

A summary of allowable stresses used for containment structures, which includes the CSA body, closure lid, and closure bolts, is presented in Table 2.1-1. These data are consistent with Regulatory Guide 7.6, and the ASME Boiler and Pressure Vessel Code, Section III, Subsection NB-3000 and Appendix F[5].

2.1.2.1.2 Non-Containment Structures

Overpack structures (both body and overpack cover) are expected to deform and absorb energy in the NCT and HAC free drop events and the HAC puncture drop event. Thus, specific design criteria are not applicable to overpack structures. The performance of the overpack structures is discussed in Sections 2.7.1, *Free Drop*, and 2.7.3, *Puncture*.

The allowable stress applicable to package lifting is limited to one-third of the material yield strength, consistent with the requirements of 10 CFR §71.45(a). Since there are no tie-down devices in the TRUPACT–III packaging design, allowable stress applicable to tie-down loading is not required.

2.1.2.2 Miscellaneous Structural Failure Modes

2.1.2.2.1 Brittle Fracture

By avoiding the use of ferritic steels in the TRUPACT–III packaging, brittle fracture concerns are precluded. Specifically, the primary structural components are fabricated of Alloy UNS S31803 duplex stainless steel. This material satisfies the brittle fracture requirements of

---

[4] Leaktight is defined as leakage of 1×10^{-8} Pascals - cubic meters per second (Pa-m^3/s), air, or less per ANSI N14.5–1997, *American National Standard for Radioactive Materials – Leakage Tests on Packages for Shipment,* American National Standards Institute, Inc. (ANSI).

[5] American Society of Mechanical Engineers (ASME) Boiler and Pressure Vessel Code, Section III, *Rules for Construction of Nuclear Facility Components*, Division 1 - Subsection NB, *Class 1 Components*, and Appendix F, *Rules for Evaluation of Service Loadings with Level D Service Limits,* 2004 Edition, 2005 and 2006 Addenda.

Regulatory Guide 7.11[6] and ASTM E604[7] at the minimum service temperature of -29 °C required by 10 CFR §71.73(b). Therefore, the material is safe from brittle fracture.

The closure lid and overpack cover attachment bolts are socket head cap screws fabricated from ASTM A320, L43 material, ensuring that brittle fracture is not of concern. Other fasteners used in the TRUPACT–III packaging assembly, such as the vent port retaining ring, are made from copper alloy material, again eliminating brittle fracture concerns..

2.1.2.2.2 Fatigue Assessment

2.1.2.2.2.1 Normal Operating Cycles

Normal operating cycles do not present a fatigue concern for the TRUPACT–III components over a 35 year service life. The basis for this conclusion is reached using the six criteria of Article NB-3222.4(d) of the ASME Boiler and Pressure Vessel Code. A summary of the six criteria and their application are discussed below.

(1) Atmospheric to Service Pressure Cycle: The total number of atmospheric-to-operating pressure cycles during normal operations does not exceed the number of cycles on the fatigue curve corresponding to a value of $S_a = 3S_m$ for Alloy UNS S31803 stainless steel. From Section 2.2.1, *Material Properties and Specifications* at a bounding temperature of 71 °C per Section 2.6.1.1, *Summary of Pressures and Temperatures*, the S_m value for UNS S31803 stainless steel is 207 MPa, which corresponds to an alternating stress value of $S_a = 3S_m = 621$ MPa. The corresponding number of cycles for a value of $S_a = 621$ MPa is approximately 2,000 from Figure I-9.2.1 and Table I-9.1M of the ASME Code.[8] The package has a design life of 35 years, with the expected maximum number of shipments to be 50 per year. The package undergoes one atmospheric-to-operating pressure cycle per shipment, therefore the package will experience $35 \times 50 = 1{,}750$ atmospheric-to-operating pressure cycles in its life. Since the allowable number of cycles is greater than the maximum expected number of cycles, the first criterion is satisfied.

(2) Normal Service Pressure Fluctuation: The specified full range of pressure fluctuations during normal service does not exceed the quantity 1/3(Design Pressure)(S_a / S_m), where the design pressure is 172 kPa, S_a is the value obtained from the Alloy UNS S31803 stainless steel design fatigue curve for the total specified number of significant pressure fluctuations, and S_m is the allowable stress intensity for the material at the service temperature. The total number of service cycles is less than 10^6 cycles. From Table I-9.1M for Figure I-9.2.1 of the ASME Code, $S_a = 195$ MPa for 10^6 cycles as a lower bound. When adjusted for temperature to 71 °C using the ratio of the modulus of elasticity from Section 2.2.1, *Material Properties and Specifications*, S_a becomes (19.2(10^4)/

---

[6] U.S. Nuclear Regulatory Commission, Regulatory Guide 7.11, *Fracture Toughness Criteria of Base Material for Ferritic Steel Shipping Cask Containment Vessels with Maximum Wall Thickness of 4 Inches (0.1 m)*, June 1991.

[7] ASTM E604–83 (2002), *Standard Test Method for Dynamic Tear Testing of Metallic Materials*, American National Standards Institute (ANSI), Inc.

[8] American Society of Mechanical Engineers (ASME) Boiler and Pressure Vessel Code, Section III, *Rules for Construction of Nuclear Facility Components*, Appendix I, *Design Stress Intensity Values, Allowable Stresses, Material Properties, and Design Fatigue Curves*, 2004 Edition, 2005 and 2006 Addenda.

$19.5(10^4)) \times 195 = 192$ MPa. The value of S_m was defined above as 207 MPa at service temperature. The significant pressure fluctuation (SPF) becomes:

$$SPF = 1/3(\text{Design Pressure})(S_a/S_m)$$

$$SPF = 1/3(172)(192/207) = 53 \text{ kPa}$$

Next, the maximum pressure fluctuations in the package will be determined. If the package temperature in storage varies between the extremes of $T_1 = -40$ °C to $T_2 = 71$ °C, the increase in internal pressure from atmospheric, $P_1 = 101$ kPa, is:

$$\frac{P_2}{P_1} = \frac{T_2}{T_1} \Rightarrow P_2 = P_1\left(\frac{T_2}{T_1}\right) = 101\left(\frac{71+273}{-40+273}\right) = 149 \text{ kPa}$$

The resulting pressure fluctuation is 149 - 101 = 48 kPa, which is less than 53 kPa presented above. Therefore, the second criterion is satisfied.

(3) Temperature Difference — Startup and Shutdown: The temperature between adjacent points of a package component during normal service does not exceed $1/2(S_a/E\alpha)$, where S_a is the design fatigue curve value taken from Table I-9.1M for Figure I-9.2.1 of the ASME Code for Alloy UNS S31803 stainless steel for the total specified number of temperature difference fluctuations, E is the modulus of elasticity, and α is the mean coefficient of thermal expansion, all evaluated at temperature. The total number of temperature fluctuations will not exceed the number of uses of the package, which is 1,750 as calculated above. It will be conservative to use the value of S_a from Table I-9.1M of the ASME Code for 2,000 cycles, which is 669 MPa. From Section 2.2.1, *Material Properties and Specifications* at a bounding temperature of 71 °C, the value of the mean thermal expansion coefficient is $13.0(10^{-6})$. Therefore, the value of $1/2(S_a/E\alpha) = 1/2(669/[19.2(10^4)13.0(10^{-6})] = 134$ °C, which corresponds to 2,000 cycles. Since the package design temperature is 71 °C under ambient conditions of 38 °C, the temperature difference between any two adjacent points cannot approach the 134 °C value. Thus, the third criterion is satisfied.

(4) Temperature Difference — Normal Service: The temperature difference between any two adjacent points does not change during normal service by more than the quantity $1/2(S_a/E\alpha)$, where S_a, E, and α are as defined above. However, normal operating temperatures of the CSA are largely decoupled from the fluctuations of the outer sheets, and any changes in temperature will be relatively slow and even due to the large thermal mass of the package. Therefore, the fourth criterion is satisfied.

(5) Temperature Difference — Dissimilar Materials: Except for the closure bolts (see below), there are only two other dissimilar materials used: UNS S31803 and Type 304L stainless steel. The total algebraic temperature range does not exceed the quantity $S_a/[2(E_1\alpha_1 - E_2\alpha_2)]$, where S_a is the design fatigue curve value taken from Table I-9.1M for Figure I-9.2.1 of the ASME Code at 10^6 cycles. The subscripts 1 and 2 refer to Type 304L and UNS S31803 material properties, respectively. The quantity defined above is the significant temperature fluctuation, or STF. The total temperature range is between the NCT cold temperature of -40 °C and the design temperature of 71 °C, or 111 °C. The mean temperature, used for the evaluation of properties, is 55.5 °C. At this temperature, from Section 2.2.1, *Material Properties and Specifications*, the modulus of elasticity $E_1 = E_2 = 19.27(10^4)$ MPa. From ASME Code, Section II, Part D, Table TE-1, the instantaneous value of α_1 (Material Group 3) is

equal to $15.84(10^{-6})$ per °C, and the instantaneous value of α_2 (Material Group 2) is equal to $12.96(10^{-6})$ per °C. From paragraph (2) above, the design fatigue strength for 10^6 cycles (conservatively adjusted for the maximum temperature of 71 °C) is 192 MPa. The STF therefore is:

$$STF = \frac{S_a}{2(E_1\alpha_1 - E_2\alpha_2)} = \frac{192}{2\left[19.27(10^4)\times 15.84(10^{-6}) - 19.27(10^4)\times 12.96(10^{-6})\right]} = 173\ °C$$

Since the maximum temperature fluctuation range of 111 °C is less than the STF of 173 °C, the fifth criterion is not a concern.

(6) Mechanical Loads: The specified full range of mechanical loads does not result in load stresses whose range exceeds the S_a design fatigue curve taken from Table I-9.1M for Figure I-9.2.1 of the ASME Code for Alloy UNS S31803 stainless steel for the total specified number of load fluctuations. The only repeating mechanical loads will be those associated with lifting and handling. Since the package is handled twice for each transport cycle (load and unload), the maximum number of cycles is 2 × 1,750 = 3,500. From Table I-9.1M, S_a = 576 MPa for 3,500 cycles. The maximum temperature of the lifting arms (cheeks) is bounded by 83 °C. When adjusted for a temperature of 83 °C using the ratio of the modulus of elasticity, S_a becomes $(19.1(10^4)/19.5(10^4)) \times 576 = 564$ MPa. Lifting stress is limited by 10 CFR §71.45(a) to a value of one-third of the material's minimum yield strength. For a lifting temperature of 83 °C, the minimum yield strength of UNS S31803 stainless steel is 408 MPa. Thus, one-third of the minimum yield strength is 1/3(408) = 136 MPa. Since the adjusted S_a is greater than this value, the sixth criterion is satisfied.

Summary: The previous discussion verifies that fatigue failure of the package body due to normal operating cycles is not a concern, per Section III, Subsection NB, Article NB-3222.4(d) of the ASME Code. Therefore the TRUPACT–III packaging's resistance to fatigue is adequate to ensure a minimum 35 year service life (assuming 50 shipments per year).

Closure Bolt Fatigue Evaluation: The maximum stress intensity developed in the closure bolts during normal operations, given in Section 2.6.1.6, *Closure Bolts*, is S_{max} = 446 MPa. This stress includes preload stress, thermal stress, and a conservative inclusion of 50% of the applied preload torque as a residual torsion stress. From Table 2.2-4, the ASME allowable stress, S_m, at 71 °C is 233 MPa. From Table I-9.1M of the ASME B&PV Code, the Maximum Nominal Stress (MNS) of 446 MPa is less than $2.7S_m$ (2.7(233) = 629 MPa). Therefore, from Table I-9.1M for Figure I-9.4 for ASTM A320 L43 bolting material, the allowable number of cycles for a corresponding alternating stress above that of one-half the value of S_{max} (i.e., 1/2(446) = 223 MPa) is over 10,000 cycles. Per NB-3232.3, a stress concentration factor of four shall be applied to one-half the value of S_{max}, i.e., $4(1/2S_{max}) = 4 \times 223 = 892$ MPa. Per NB-3232.3(d), the alternating stress must be adjusted for the elastic modulus used in the fatigue curves. The modulus used for the fatigue curve, per Table I-9.1M is $207(10^3)$ MPa. Conservatively using the lower modulus for 93 °C from Table 2.2-4 of $18.7(10^4)$ MPa, the adjusted alternating stress is:

$$S_{ALT} = \frac{20.7}{18.7}892 = 987\ \text{MPa}$$

The corresponding cycles allowed per Table I-9.1M for Figure I-9.4 is interpolated per Note 2 of the table:

$$N = N_i\left(\frac{N_j}{N_i}\right)^{[\log(S_i/S)]/\log(S_i/S_j)} = 500\left(\frac{1000}{500}\right)^{[\log(986/987)]/\log(986/690)} = 499 \text{ cycles}$$

Since closure bolts are tightened twice per package service cycle, the allowable number of package service cycles is half of this value. Therefore, the closure bolts should be replaced approximately every 499/2 = 250 service cycles for the package.

2.1.2.2.2.2 Normal Vibration Over the Road

Fatigue associated with normal vibration over the road is addressed in Section 2.6.5, *Vibration.*

2.1.2.2.2.3 Extreme Total Stress Intensity Range

Per paragraph C.7 of Regulatory Guide 7.6:

> The extreme total stress intensity range (including stress concentrations) between the initial state, the fabrication state, the normal operating conditions, and the accident conditions should be less than twice the adjusted value (adjusted to account for modulus of elasticity at the highest temperature) of S_a at 10 cycles given by the appropriate design fatigue curves.

Since the response of the TRUPACT–III packaging to accident conditions is evaluated empirically rather than analytically, the extreme total stress intensity range for all conditions has not been quantified. However, both full-scale certification test units were tested at minimum ambient temperatures during free drop testing. Both CTUs were also fabricated in accordance with the drawings in Appendix 1.3.1, *Packaging General Arrangement Drawings*, thus incurring prototypic fabrication induced stresses, stresses consistent with an increased internal pressure equal to 150% of MNOP applied during fabrication pressure testing, and stresses from reduced internal pressure (i.e., a full vacuum during leak testing), applied as part of initial acceptance. Exposure to these extreme conditions including stresses resulting from certification testing, while consistently demonstrating the leak tightness of the containment boundary, satisfies the intent of paragraph C.7 of Regulatory Guide 7.6.

2.1.2.2.3 Buckling Assessment

Buckling, per Regulatory Guide 7.6, is an unacceptable failure mode for the containment vessel. The intent of this provision is to preclude large deformations that would compromise the validity of linear analysis assumptions and quasi-linear stress allowable limits, as given in Paragraph C.6 of Regulatory Guide 7.6.

The methodology of corrugated-core sandwich sheets is applied to the containment structural assembly (CSA). Buckling from pressure loading is governed by the HAC immersion case. Analysis results are provided in Section 2.7.6, *Immersion – All Packages*, and details provided in Appendix 2.12.4, *HAC Immersion Buckling Evaluation.*

Consistent with Regulatory Guide 7.6 philosophy, factors of safety corresponding to ASME Boiler and Pressure Vessel Code, Level A and Level D service conditions are employed. For NCT (Service Level A), the factor of safety is 2.0, and for HAC (Service Level D), the factor of safety is 1.34.

It is noted that 9-m drop tests performed on the full-scale certification test unit with the package in various orientations produced no evidence of buckling of any part of the CSA structure (refer to Appendix 2.12.3, *Certification Tests*). Although certification testing does not provide a specific determination of the margin of safety against buckling, it is considered evidence that buckling will not occur.

2.1.3 Weights and Centers of Gravity

The maximum gross weight of the TRUPACT–III package, including a maximum payload weight of 5,210 kg (11,486 lbs), is 25,000 kg (55,116 lbs). The empty packaging therefore weighs 25,000 - 5,210 = 19,790 kg (43,630 lb). With reference to Figure 2.1-1, a detailed breakdown of the TRUPACT–III package component weights are summarized in Table 2.1-2.

Due to symmetry of design, the center of gravity (CG) of the empty package is located at the geometric center of the package cross-section: 1,325 mm (52.2 in) above the bottom outside surface of the package and 1,250 mm (49.2 in) from either outer side of the package on the longitudinal axis. The longitudinal CG of the empty package is located 2,356 mm (93 in) from the outer closed-end surface of the package. Since the thickness of the end material between the datum plane and the rear inside of the payload cavity is 750 mm, and given the length of the payload cavity as 2,790 mm, the location of the center of gravity of a uniformly loaded package relative to the datum plane is:

$$x = \frac{19{,}790(2{,}356) + 5{,}210\left(750 + \frac{2{,}790}{2}\right)}{25{,}000} = 2{,}312 \text{ mm}$$

The center of gravity is located 168 mm (6.6 in) towards the closure end from the longitudinal geometric center, based on an overall package length of 4,288 mm. The TRUPACT–III package will be so loaded that the center of gravity of the loaded package will not deviate more than ±150 mm (5.9 in) laterally or vertically, or ±200 mm (7.9 in) longitudinally from this location.

2.1.4 Identification of Codes and Standards for Package Design

The TRUPACT–III package contents potentially exceed an amount of $3{,}000A_2$, and according to Table 1 of Regulatory Guide 7.11, the TRUPACT–III is therefore a Category 1 package. Per the guidance of NUREG/CR-3854[9], the appropriate design criteria is Section III, Subsection NB of the ASME B&PV Code. Consequently, the design of the containment boundary is based on the methodology of Regulatory Guide 7.6, and load cases are applied and combined according to Regulatory Guide 7.8.

All welds in the containment boundary shell (see Section 1.2.1.1, *Body*, and Section 1.2.1.2, *Closure Lid*) are full penetration welds inspected by visual, dye penetrant, and radiographic methods. The fillet welds connecting the V-stiffeners to the outer surface of the containment sheets are classified as fillet welded attachments per ASME B&PV Code, Section III, Subsection NB, paragraph NB-3123.2. Welds outboard of these fillet welds (e.g., the plug welds connecting the V-stiffeners to the CSA outer sheets, and all overpack welds) do not qualify as Subsection

[9] L. E. Fischer, W. Lai, *Fabrication Criteria for Shipping Containers,* NUREG/CR–3854, UCRL–53544, U.S. Nuclear Regulatory Commission, March 1985.

NB weld types. These welds are evaluated using other codes, such as AWS D1.6, and inspected using visual and dye penetrant techniques as described in Section 2.3.2, *Examination.*

To fully ensure adequate package performance, a certification test unit was subjected to a series of free drop and puncture events as described in Section 2.7.1, *Free Drop*, and Section 2.7.3, *Puncture*. Additionally, during fabrication each package is subjected to an internal pressure equal to 150% of the design pressure, and a full vacuum. This combination of the use of codes, standards, and verification testing ensures satisfactory package performance.

Table 2.1-1 – Containment Structure Allowable Stress Limits

Stress Category	NCT	HAC
General Primary Membrane Stress Intensity	S_m	Lesser of: $2.4S_m$, $0.7S_u$
Local Primary Membrane Stress Intensity	$1.5S_m$	Lesser of: $3.6S_m$, S_u
Primary Membrane + Bending Stress Intensity	$1.5S_m$	Lesser of: $3.6S_m$, S_u
Range of Primary + Secondary Stress Intensity	$3.0S_m$	Not Applicable
Pure Shear Stress	$0.6S_m$	$0.42S_u$
Bearing	S_y	S_y
Peak	Per Section 2.1.2.2.2, *Fatigue Assessment*	
Buckling	Per Section 2.1.2.2.3, *Buckling Assessment*	
*Containment Fasteners:*①		
Average Tensile Stress Intensity	S_m②	Lesser of: $1.0S_y$, $0.7S_u$
Average Tensile + Average Shear + Bending + Residual Torsion Stress Intensity	$1.35S_m$②	Not Applicable
For Non-Linear Analysis:		
General Primary Membrane Stress Intensity	Not Applicable	Greater of: $0.7S_u$, $S_y + (1/3)(S_u - S_y)$
Maximum Primary Stress Intensity	Not Applicable	$0.9S_u$

Notes: ① Containment fastener stress limits are in accordance with NUREG/CR-6007.
② S_m is defined as $(2/3)S_y$ as recommended by NUREG/CR-6007.

Table 2.1-2 – TRUPACT–III Component Weights

Item	Weight, kg (lb)	
	Component	Assembly
Total Empty Package		19,790 (43,630)
Body	15,100 (33,290)	
Closure Lid	1,840 (4,057)	
Overpack Cover	2,850 (6,283)	
Payload and Payload Components		5,210 (11,486)
Loaded SLB2	4,763 (10,500)	
Payload Loading System (e.g., pallet and roller floor)	447 (986)	
Total Loaded Package (Maximum)		25,000 (55,116)

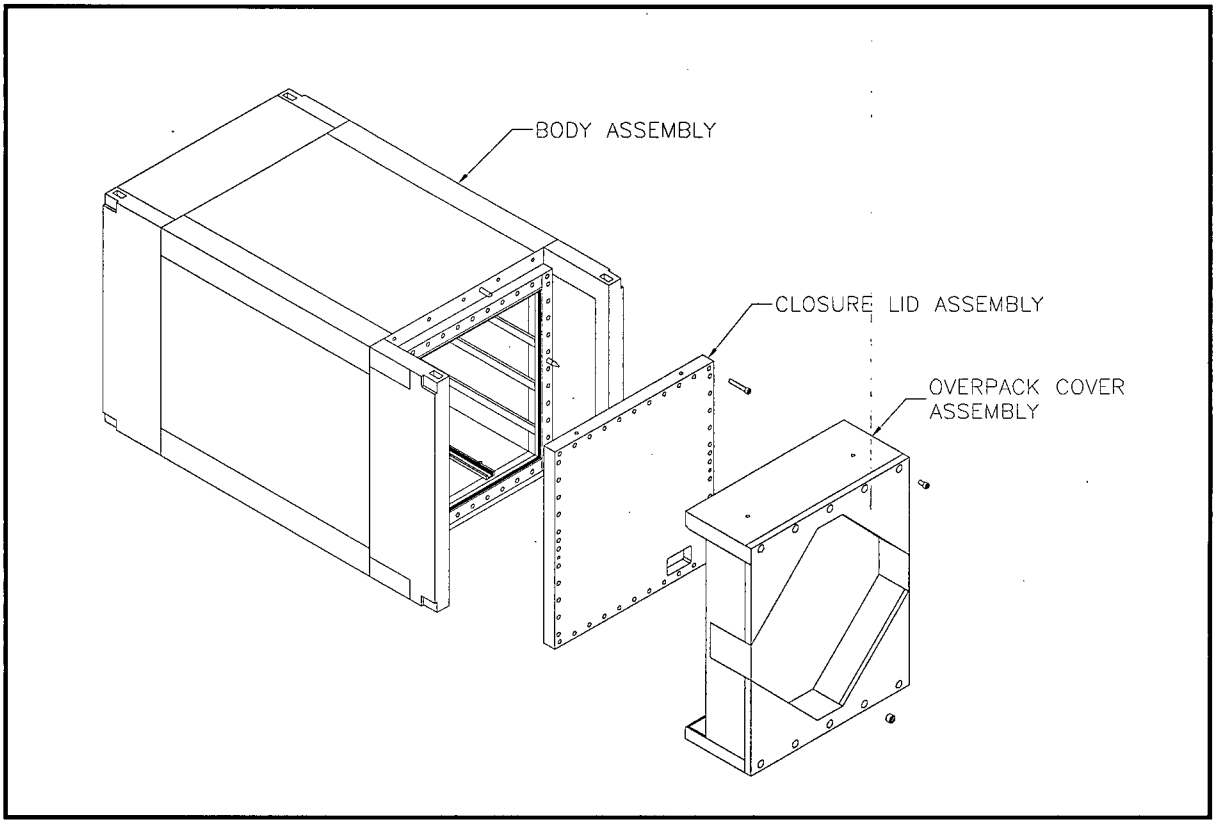

Figure 2.1-1 – TRUPACT–III Packaging Components

2.2 Materials

The TRUPACT–III CSA and overpack steel components are fabricated primarily from Alloy UNS S31803 duplex stainless steel. Polyurethane foam and balsa wood are used for impact resistance. Other materials performing a structural function are copper alloy UNS C63200 (for the vent port plug, retaining ring, and locking ring), and ASTM A320, L43, carbon steel (for the closure lid bolts and overpack cover attachment bolts). Type 304/304L stainless steel is utilized for a limited number of parts not having an important structural function, such as the lid guide pin, the overpack cover guide pin, the guide bars in the payload cavity, debris shield receptacle, and the bolt access tubes on the overpack cover. Several varieties of non-structural materials are also utilized. Representative non-structural materials include butyl rubber O-ring seals, calcium silicate insulation, and plastic fire consumable vent plugs used in the foam cavities. The drawings presented in Appendix 1.3.1, *Packaging General Arrangement Drawings*, delineate the specific materials used for each TRUPACT–III packaging component.

The remainder of this section presents the pertinent mechanical properties for the materials that perform a structural function.

2.2.1 Material Properties and Specifications

Tables 2.2-1 through 2.2-8 present the mechanical properties for the structural materials used in the TRUPACT–III packaging. Each of the mechanical properties of Alloy UNS S31803 stainless steel is taken from Code Case N-635-1 or Section II of the ASME Boiler and Pressure Vessel Code[1]. Any analyses of the CSA utilize the properties presented for Alloy UNS S31803, ASTM A240/A479 stainless steel. The density of stainless steel is taken as 7.89 kg/dm^3, and Poisson's Ratio is 0.3. Data is interpolated or extrapolated from the available data, as necessary, as noted in the tables.

Where required, non-linear material properties are utilized in the form of true stress-strain curves, developed in the following paragraphs. The material models for Alloy UNS S31803 and ASTM Type 304L are evaluated at the minimum temperature of -29 °C for consistency with the maximum HAC cold free drop impact magnitudes. Alloy UNS S31803 is also evaluated at the maximum NCT temperature of 71 °C.

For the Alloy UNS S31803 material, the non-linear properties are based on tensile tests of as-received specimens at temperature. The data set is then adjusted for the minimum yield strength given in Code Case N-635-1. The stress-strain curves thus obtained conservatively represent the minimum strength allowed for the material. Utilizing a standard Ramberg-Osgood[2] curve, the engineering stress-strain curve is developed up to the yield strength for each temperature using the following equations:

$$\varepsilon = \frac{\sigma}{E_0} + 0.002\left(\frac{\sigma}{S_y}\right)^n \qquad n = \frac{\ln(20)}{\ln\left(\frac{S_y}{\sigma_{0.01}}\right)}$$

[1] American Society of Mechanical Engineers (ASME) Boiler and Pressure Vessel Code, Section III, *Code Case N–635–1*.

[2] National Advisory Committee for Aeronautics – Technical Note No. 902, *Description of Stress–Strain Curves by Three Parameters*, Walter Ramberg and William R. Osgood, July 1943.

where: ε = strain, mm/mm

σ = stress, MPa

E_o= average elastic modulus of test samples, MPa

$\sigma_{0.01}$ = stress at 0.01% strain, MPa

S_y = yield strength, MPa

To develop the engineering stress-strain curve between the yield and ultimate strengths, a linear progression is used as follows:

$$\sigma'_{eng} = \sigma_{eng} - \left[\frac{\Delta S_u - \Delta S_y}{\varepsilon_2 - \varepsilon_1}\left(\varepsilon_{eng} - \varepsilon_1\right) + \Delta S_y\right]$$

where: σ'_{eng} = resultant engineering stress, MPa

σ_{eng} = stress at a given strain ε, MPa

ΔS_u = difference between ASME and test sample ultimate strengths, MPa

ΔS_y = difference between ASME and test sample yield strengths, MPa

ε_{eng} = engineering strain at a given stress σ_{eng}, mm/mm

ε_1 = strain at average yield strength of test samples, mm/mm

ε_2 = strain at average ultimate strength of test samples, mm/mm

The engineering stress-strain values are converted into true stress-strain using the following equations:

$$\varepsilon_{true} = \ln\left(\varepsilon_{eng} + 1\right) \qquad \sigma_{true} = \sigma_{eng}\left(\varepsilon_{eng} + 1\right)$$

The resulting true stress-strain curves for UNS S31803 at temperatures of -29 °C and 71 °C are given in Table 2.2-2 and shown graphically in Figure 2.2-1.

For Type 304L material, nonlinear properties are based on the following material model taken from the literature:[3]

$$\sigma = \sigma_p + A\left(\varepsilon_p - \varepsilon_L\right)^n$$

where: σ_p = 193.06 MPa [28,000 psi]

A = 1,329 MPa [192,746 psi]

n = 0.74819

ε_p = true plastic strain

ε_L = Luder's strain (equal to zero for stainless steel)

This model applies at room temperature. To adjust it to the properties at the minimum temperature of -29 °C, the model is multiplied by the ratio:

$$\frac{\sigma_{true-y}}{\sigma_p} = \frac{201.2}{193.06} = 1.04$$

[3] Sandia National Laboratories, *Reexamination of Spent Fuel Shipment Risk Estimates*, NUREG/CR–6672, Vol. 1, U.S. Nuclear Regulatory Commission, March 2000, p. 5-7.

where σ_p is defined above and the true yield stress at temperature, $\sigma_{true\text{-}y}$, is found from:

$$\sigma_{true-y} = \sigma_{eng-y}\left(1 + \frac{\sigma_{eng-y}}{E}\right) = 201.2 \text{ MPa}$$

where the engineering yield strength and Young's modulus at a temperature of -29 °C from Table 2.2-3 are:

$\sigma_{eng\text{-}y}$ = 201 MPa (extrapolated from 38 °C and 93 °C)[4]

E = $19.8(10^4)$ MPa

Further, since the model reports only plastic strain, the total strain used in analysis is obtained from:

$$\varepsilon_{tot} = \varepsilon_p + \frac{\sigma_{eng-y}}{E}$$

in which the last term is equal to the elastic strain, or 0.001. The resulting true stress-strain curve for Type 304L material at -29 °C is given in Table 2.2-2 and shown graphically in Figure 2.2-1.

The performance of the TRUPACT–III in free drop and puncture events is dependent on polyurethane foam and balsa wood. The foam and wood are prepared for installation within the overpack as prefabricated blocks or panels. A total of four nominal foam densities and one balsa wood density are used. The drawings presented in Appendix 1.3.1, *Packaging General Arrangement Drawings*, show the placement of the various densities of foam and wood and the direction of the foam rise (or wood grain). Section 8.1.5.1, *Polyurethane Foam* and Section 8.1.5.2, *Balsa Wood* present the details of acceptance tests for these materials. The nominal, room-temperature crush properties of the polyurethane foam components are given in Table 2.2-5, and for balsa wood in Table 2.2-6. Bronze material properties are given in Table 2.2-7.

2.2.2 Chemical, Galvanic, or Other Reactions

The major materials of construction of the TRUPACT–III packaging (i.e., stainless steel, alloy steel, copper alloy, polyurethane foam, balsa wood, calcium silicate insulation board, and butyl rubber O-ring seals) will not have significant chemical, galvanic or other reactions in air, inert gas or water environments. These materials have been previously used, without incident, in radioactive material (RAM) packages for transport of similar payload materials. With the exception of butyl rubber and polyurethane foam, these materials of construction have been used in the TN–Gemini package[5] for several years without incident, carrying essentially identical payload materials as will be carried in the TRUPACT–III package. Polyurethane foam and butyl rubber have been used in many other RAM packagings, such as the TRUPACT–II.[6] A successful RAM packaging history combined with successful use of these fabrication materials in similar industrial environments ensures that the integrity

[4] According to MIL–HDBK–5F, Figure 2.7.1.1.1(a), the yield strength of Type 304L stainless steel varies essentially linearly between -29 °C and 93 °C.

[5] AREVA Cogema Logistics (ACL), *Safety Analysis Report for the TN–Gemini Package*, French Certificate of Approval F/343/B(U)F–85 Bg, AREVA Cogema Logistics, Paris, France.

[6] U. S. Department of Energy (DOE), *Safety Analysis Report for the TRUPACT–II Shipping Package*, USNRC Certificate of Compliance 71–9218, U.S Department of Energy, Carlsbad Field Office, Carlsbad, New Mexico.

of the TRUPACT–III package will not be compromised by any chemical, galvanic or other reactions. The materials of construction and the payload are further evaluated below for potential reactions.

2.2.2.1 Packaging Materials of Construction

The TRUPACT–III packaging is primarily constructed of UNS S31803 stainless steel. This material is highly corrosion resistant to most environments. The metallic structure of the TRUPACT–III packaging is composed entirely of this material and compatible weld material. The weld material and processes have been selected in accordance with the ASME Boiler and Pressure Vessel Code[7] to provide as good or better material properties, including corrosion resistance, as the base material. Since both the base and weld materials are essentially the same, they have nearly identical electrochemical potential thereby minimizing any galvanic corrosion that could occur.

The polyurethane foam and balsa wood that is used in the TRUPACT–III packaging is essentially identical to many previously licensed transportation packagings. All of these packagings have had a long and successful record of performance demonstrating that the polyurethane foam and/or wood does not cause any adverse conditions with the packaging. The polyurethane foam in the packaging is a rigid, closed-cell (non-water absorbent) foam that is free of halogens and chlorides, as discussed in Section 8.1.5.1, *Polyurethane Foam*. The balsa wood used in the outer overpack layer does not react with the stainless steel or foam. The foam and wood material cavities are sealed with plastic threaded plugs to exclude moisture.

The various copper alloy fittings used in the TRUPACT–III packaging are very corrosion resistant. Any damage that could occur to the material is easily detectable since the fittings are all handled and/or visible each time the TRUPACT–III package is loaded and unloaded.

The butyl rubber elastomer that is used for the O-ring seals and the silicone that is used for the debris seal foam insert contain no corrosives that would react with or adversely affect the TRUPACT–III packaging. These materials are organic in nature and non-corrosive to the stainless steel containment boundary of the TRUPACT–III packaging. The silicone foam debris shield is closed-cell, and will not retain corrosive fluids. Silicone rubber is an inert material with wide use in many industrial environments. Should any corrosion occur, it will not affect containment, and will be easily detectable since the debris shield is inspected for wear or damage (see Section 7.1.5, *Closure Lid Installation*, Step 4). Similarly, the polyethylene filters associated with the debris shield are made of an inert material which will not contribute to corrosion. The hard plastic plates used with the rear-wall guide bars are also inert and will not contribute to corrosion.

2.2.2.2 Payload Interaction with Packaging Materials of Construction

The materials of construction of the TRUPACT–III packaging are checked for compatibility with the various payload chemistries when the payloads are evaluated for chemical compatibility. All

[7] American Society of Mechanical Engineers (ASME) Boiler and Pressure Vessel Code, Section III, *Rules for Construction of Nuclear Facility Components*, 2004 Edition, 2005 and 2006 Addenda.

payload materials are in approved SLB2 payload containers meeting the specifications for payload containers delineated in the TRUPACT–III TRAMPAC.[8]

The payload configuration within payload containers ensures that the payload material has an insignificant level of contact with the TRUPACT–III packaging materials of construction. However, the evaluation of compatibility is based on complete interaction of payload materials with the packaging.

The design of the TRUPACT–III package is for transport of CH–TRU materials and other authorized payloads that are limited in form to solid or solidified material. Corrosive materials, pressurized containers, explosives, non-radioactive pyrophorics, and liquid volumes greater than 1% are prohibited. These restrictions ensure that the waste in the payload is in a non-reactive form for safe transport in the TRUPACT–III package. For a comprehensive discussion defining acceptable payload properties, refer to the TRUPACT–III TRAMPAC.

2.2.3 Effects of Radiation on Materials

Since the payload of the TRUPACT–III is contact handled transuranic waste material, the level of radiation inside the package is negligible. Furthermore, the materials of construction, including the butyl rubber containment seal, have been used for many years in RAM transport packagings without any incident relating to radiation exposure. For these reasons, there will be no radiation effects on the packaging, and the requirements of 10 CFR §71.43(d) are met.

[8] U.S. Department of Energy (DOE), *TRUPACT–III TRU Waste Authorized Methods for Payload Control (TRUPACT–III TRAMPAC)*, U.S. Department of Energy, Carlsbad Field Office, Carlsbad, New Mexico.

This page intentionally left blank.

Table 2.2-1 – Mechanical Properties① of Alloy UNS S31803 Stainless Steel Components

Material Specification	Temperature (°C)	Yield Strength, S_y (MPa)	② Ultimate Strength, S_u (MPa)	Allowable Strength, S_m (MPa)	③ Elastic Modulus, E ($\times 10^4$ MPa)	④ Thermal Expansion Coefficient, α ($\times 10^{-6}$ mm/mm/°C)
Alloy UNS S31803 ASTM A240 ASTM A479	-40	-----	-----	-----	19.9	11.9
	-29	-----	-----	-----	19.8	12.0
	21	-----	-----	-----	19.5	12.6
	38	448	621	207	19.4	12.8
	93	399	621	207	19.0	13.1
	149	370	598	199	18.6	13.3
	204	353	576	192	18.3	13.7
	260	342	563	188	17.8	13.9
	316	330	556	185	17.4	14.0

Notes: ① Data from ASME Code Case N-635-1, unless otherwise noted. Table data converted from English units.

② ASME Code, Section II, Part D, Table U.

③ Modulus not given in ASME Code, Section II, Part D, Table TM-1; data is for Group G (selected based on chromium content.) Values for -40 °C and -29 °C interpolated from 21 °C and -73 °C.

④ ASME Code, Section II, Part D, Table TE-1, Material Group 2, Mean Coefficient. Values for -40 °C and -29 °C extrapolated from 21 °C and 38 °C.

Table 2.2-2 – True Stress-Strain Values for Alloy UNS S31803 and Type 304L Stainless Steel Components

Alloy UNS S31803 at -29 °C		**Alloy UNS S31803 at 71 °C**		**Type 304L at -29 °C**	
Strain (%)	Stress (MPa)	Strain (%)	Stress (MPa)	Strain (%)	Stress (MPa)
0.00	0.0	0.00	0.0	0	0.0
0.16	317.9	0.08	151.7	0.10	200.8
0.22	414.4	0.16	276.5	0.20	208.7
0.32	484.0	0.23	345.4	0.30	214.0
0.47	528.8	0.42	420.6	0.50	223.0
0.70	568.8	1.92	497.1	1.10	244.9
4.31	681.9	4.66	572.3	4.10	325.1
10.89	779.8	10.89	654.3	10.10	447.6
22.31	888.8	26.24	806.7	25.10	690.7

Table 2.2-3 – Mechanical Properties① of Type 304L Stainless Steel

Material Specification	Temperature (°C)	② Yield Strength, S_y (MPa)	③ Ultimate Strength, S_u (MPa)	④ Allowable Strength, S_m (MPa)	⑤ Elastic Modulus, E ($\times 10^4$ MPa)	⑥ Thermal Expansion Coefficient, α ($\times 10^{-6}$ mm/mm/°C)
ASTM A240 ASTM A249 ASTM A269 ASTM A479 Type 304L	-40	-----	-----	-----	19.9	-----
	-29	-----	-----	-----	19.8	-----
	21	-----	-----	-----	19.5	15.3
	38	172	483	115	19.4	15.5
	93	148	456	115	19.0	16.0
	149	132	422	115	18.6	16.6
	204	121	405	109	18.3	17.1
	260	113	396	102	17.8	17.5

Notes: ① Table data converted from English units.

② ASME Code, Section II, Part D, Table Y-1.

③ ASME Code, Section II, Part D, Table U.

④ ASME Code, Section II, Part D, Table 2A.

⑤ ASME Code, Section II, Part D, Table TM-1, Material Group G. Values for -40 °C and -29 °C interpolated from 21 °C and -73 °C.

⑥ ASME Code, Section II, Part D, Table TE-1, Material Group 3, Mean.

Table 2.2-4 – Mechanical Properties① of ASTM A320, Grade L43 Alloy Bolting Material

Material Specification	Temperature (°C)	② Yield Strength, S_y (MPa)	③ Ultimate Strength, S_u (MPa)	④ Allowable Strength, S_m (MPa)	⑤ ASME Allowable Strength, S_m (MPa)	⑥ Elastic Modulus, E ($\times 10^4$ MPa)	⑦ Thermal Expansion Coefficient, α ($\times 10^{-6}$ mm/mm/°C)
ASTM A320 Grade L43	-40	-----	-----	-----	-----	19.5	10.8
	-29	-----	-----	-----	241	19.4	10.9
	21	-----	-----	-----	241	19.2	11.5
	38	724	862	483	241	19.1	11.7
	93	683	-----	455	228	18.7	12.1
	149	660	-----	440	220	18.4	12.4
	204	633	-----	422	211	18.0	12.8
	260	610	-----	407	203	17.7	13.1

Notes: ① Table data converted from English units.
② ASME Code, Section II, Part D, Table Y-3.
③ ASME Code, Section II, Part D, Table Y-3.
④ Computed as 2/3Sy per NUREG/CR-6007.
⑤ ASME Code, Section II, Part D, Table 4.
⑥ ASME Code, Section II, Part D, Table TM-1, Material Group B. Values for -40 °C and -29 °C interpolated from 21 °C and -73 °C.
⑦ ASME Code, Section II, Part D, Table TE-1, Material Group 1, Mean Coefficient. Values for -40 °C and -29 °C extrapolated from 21 °C and 38 °C.

Table 2.2-5 – Crush Strength of Polyurethane Foam

	Foam Nominal Density, kg/dm^3			
	0.10	0.16	0.29	0.48
Strain, %	**Crush Strength, MPa**			
Parallel to Rise				
10	0.98	2.30	6.88	18.0
40	1.05	2.53	8.42	24.3
60				44.9
70	2.15	6.58	24.8	
Perpendicular to Rise				
10	0.96	2.30	6.83	18.0
40	1.01	2.53	8.35	24.4
60				45.2
70	2.15	6.69	24.7	

Table 2.2-6 – Mechanical Properties of Balsa Wood

Property	Direction	Nominal Value
Compressive Strength, S	Parallel-to-Grain	8.0 MPa
Density, ρ	-----	0.11 kg/dm^3

Table 2.2-7 – Mechanical Properties of Bronze Material

Material	Minimum Mechanical Properties
ASTM B150, UNS C63200 Copper Alloy (Aluminum Bronze)	σ_y = 275 MPa σ_u = 620 MPa

Table 2.2-8 – Mechanical Properties① of Closure Bolt Washer Material

Material Specification	Temperature (°C)	② Yield Strength, S_y (MPa)	③ Ultimate Strength, S_u (MPa)	④ Elastic Modulus, E ($\times 10^4$ MPa)
ASTM A564 Grade 630 H1025	21	1,000	1,069	19.7
	93	925	1,069	19.2

Notes: ① Table data converted from English units.
② ASME Code, Section II, Part D, Table Y-1.
③ ASME Code, Section II, Part D, Table U.
④ ASME Code, Section II, Part D, Table TM-1, for S17400.

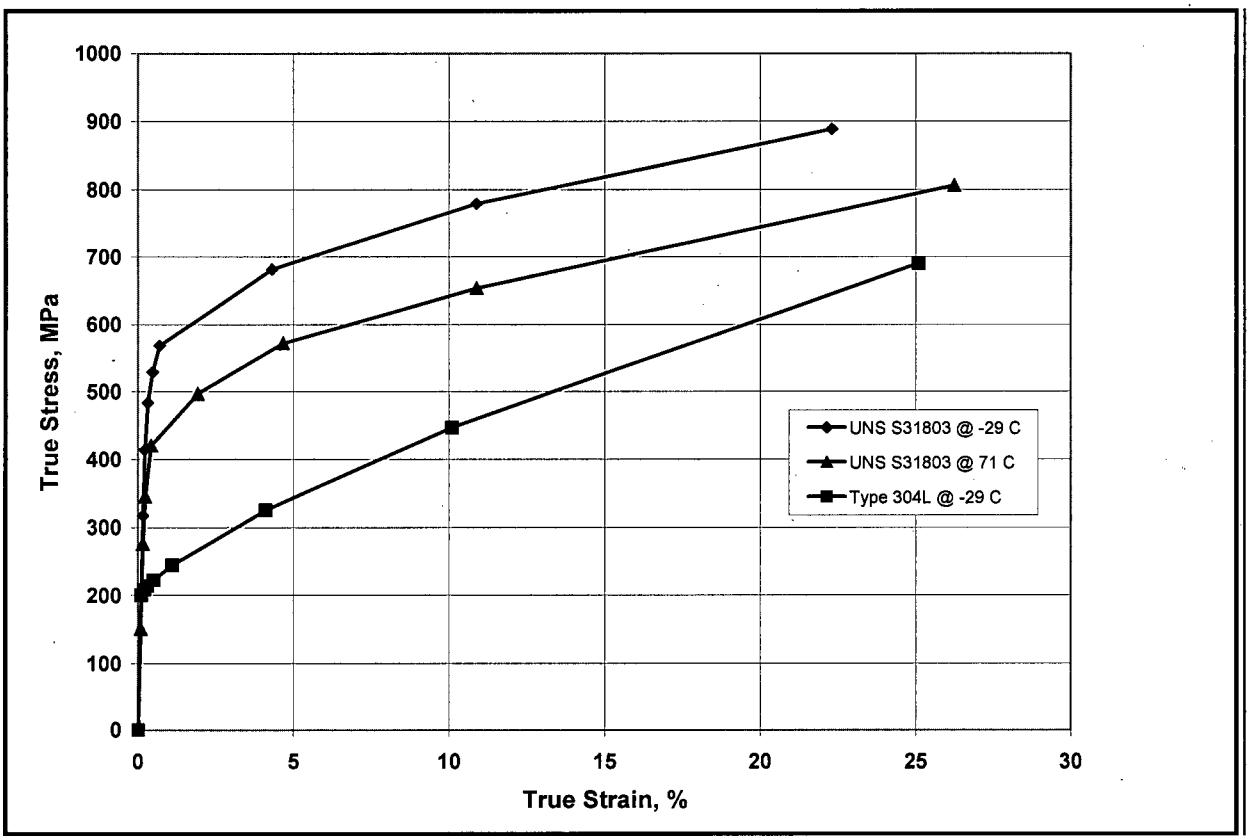

Figure 2.2-1 – True Stress-Strain Curves for Alloy UNS S31803 and Type 304 Stainless Steel

2.3 Fabrication and Examination

2.3.1 Fabrication

The TRUPACT–III packaging is fabricated using conventional metal forming and joining techniques. All welding procedures and welding personnel must be qualified in accordance with Section IX of the ASME Boiler and Pressure Vessel Code.[1] Where possible, containment boundary weld joints are made in flat sections and are full penetration butt joints. Where a corner joint is necessary, such as at the closed end of the containment boundary or at the body flange inner corner joints, the joint is a full penetration corner joint. Threaded parts are fabricated according to ASME B1.13M.[2] All non-containment joints, such as those connecting the CSA outer sheets, are fabricated in accordance with the requirements delineated on the drawings in Appendix 1.3.1, *Packaging General Arrangement Drawings*.

The polyurethane foam, calcium silicate insulation, balsa wood, and butyl rubber O-rings are procured using written procedures. See Section 8.1.5, *Component Tests*, for details of the fabrication and performance requirements of these components.

2.3.2 Examination

Each of the materials performing a significant safety function must meet the ASTM specifications delineated on the drawings in Appendix 1.3.1, *Packaging General Arrangement Drawings*. Safety-significant materials not having an ASTM designation are controlled by means of written procedures whose requirements are summarized in Section 8.1.5, *Component Tests*.

All welds are subject to visual examination per AWS D1.6.[3] Welds of the containment boundary plates and flanges are examined additionally by radiographic inspection in accordance with the ASME Boiler and Pressure Vessel Code, Section III, Division 1, Subsection NB, Article NB-5000, and Section V, Article 2,[4] and by liquid penetrant inspection on the final pass in accordance with the ASME Boiler and Pressure Vessel Code, Section III, Division 1, Subsection NB, Article NB-5000, and Section V, Article 6.[5] Fillet welds attaching the V-stiffeners to the containment sheets, and all other welds of the CSA outboard of that location, are inspected in the same way, omitting the radiographic inspection. Welds between components of the overpack structures (including welds to the outside of the CSA) are inspected visually as noted above, and additionally using liquid

---

[1] American Society of Mechanical Engineers (ASME) Boiler and Pressure Vessel Code, Section IX, *Qualification Standard for Welding and Brazing Procedures, Welders, Brazers, and Welding and Brazing Operators*, 2004 Edition, 2005 and 2006 Addenda.

[2] American Society of Mechanical Engineers (ASME) B1.13M, *Metric Screw Threads – M Profile*.

[3] ANSI/AWS D1.6:1999, *Structural Welding Code--Stainless Steel*, American Welding Society (AWS).

[4] American Society of Mechanical Engineers (ASME) Boiler and Pressure Vessel Code, Section III, *Rules for Construction of Nuclear Facility Components*, Division 1 - Subsection NB, *Class 1 Components*, and Section V, *Nondestructive Examination*, Article 2, *Radiographic Examination*, 2004 Edition, 2005 and 2006 Addenda.

[5] American Society of Mechanical Engineers (ASME) Boiler and Pressure Vessel Code, Section V, *Nondestructive Examination*, Article 6, *Liquid Penetrant Examination*, 2004 Edition, 2005 and 2006 Addenda.

penetrant inspection on the final pass in accordance with the ASME Boiler and Pressure Vessel Code, Section III, Division 1, Subsection NF, Article NF-5000, and Section V, Article 6.[6]

Each TRUPACT–III packaging will also be subjected to the following three tests:

- CSA internal pressure test, in which the containment boundary is pressurized to at least 150% of the MNOP. The pressure test requirements are described in Section 8.1.3.2, *Containment Vessel Pressure Testing.*
- Containment boundary leakage rate test, which includes helium leakage rate tests of the structural containment boundary, the containment O-ring seal, and the vent port containment O-ring seal. The requirements are described in Section 8.1.4, *Fabrication Leakage Rate Tests.*
- Load test of the upper ISO lift fittings, in which each fitting is tested to 150% of its maximum working load. The load test requirements are described in Section 8.1.3.1, *Lifting Device Load Testing.*

[6] American Society of Mechanical Engineers (ASME) Boiler and Pressure Vessel Code, Section III, *Rules for Construction of Nuclear Facility Components*, Division 1 - Subsection NF, *Supports*, 2004 Edition, 2005 and 2006 Addenda.

2.4 General Requirements for All Packages

This section defines the general standards for all packages. The TRUPACT–III package meets all requirements delineated for this section.

2.4.1 Minimum Package Size

The minimum dimension of the TRUPACT–III package is 2,500 mm (the package width). Thus, the 10–cm minimum requirement of 10 CFR §71.43(a)[1] is satisfied.

2.4.2 Tamper-Indicating Feature

Tamper-indicating seals are installed through two of the access tubes for the overpack cover, as delineated on the drawings in Appendix 1.3.1, *Packaging General Arrangement Drawings*. A lock wire device is used between two tie-points. Failure of the tamper-indicating devices provides evidence of possible unauthorized access. Thus, the requirement of 10 CFR §71.43(b) is satisfied.

2.4.3 Positive Closure

The TRUPACT–III package cannot be opened unintentionally. The overpack cover, which is secured with ten (10) M36 socket head cap screws, fully conceals the closure lid and the vent port. The closure lid is secured with (44) M36 closure bolts (socket head cap screws). Thus, the requirements of 10 CFR §71.43(c) are satisfied.

2.4.4 Valves

The containment boundary of the TRUPACT–III packaging does not contain any valves. The overpack cover features one pressure relief valve to relieve any large internal pressure differential which could occur within the overpack cover shells due to atmospheric or temperature conditions. Besides the closure lid, the TRUPACT–III packaging has a vent port penetration into the containment cavity. This vent port penetration is closed using an aluminum bronze insert that is held in place by a threaded retaining ring, and sealed using a butyl rubber O–ring seal. In addition to the retaining ring, access to the vent port penetration is prevented by the overpack cover, as discussed in Section 2.4.3, *Positive Closure*. Thus, the requirements of 10 CFR §71.43(e) are satisfied.

2.4.5 Package Design

As shown in Chapter 2.0, *Structural Evaluation*, Chapter 3.0, *Thermal Evaluation*, Chapter 5.0, *Shielding Evaluation*, and Chapter 6.0, *Criticality Evaluation*, the structural, thermal, shielding, and criticality requirements, respectively, of 10 CFR §71.43(f) are satisfied for the TRUPACT–III package.

[1] Title 10, Code of Federal Regulations, Part 71 (10 CFR 71), *Packaging and Transportation of Radioactive Material*, 01–01–09 Edition.

2.4.6 External Temperatures

As shown in Table 3.3-2 from Section 3.3.1, *Heat and Cold*, the maximum accessible surface temperature with maximum internal decay heat load and no insolation is 42 °C. Since the maximum external temperature does not exceed 50 °C, the requirements of 10 CFR §71.43(g) are satisfied for non–exclusive use shipments.

2.4.7 Venting

The TRUPACT–III package does not include any features intended to allow continuous venting of the containment boundary during transport. Thus, the requirements of 10 CFR §71.43(h) are satisfied.

2.5 Lifting and Tie-down Standards for All Packages

For analysis of the lifting and tie-down components of the TRUPACT–III packaging, material properties from Section 2.2.1, *Material Properties and Specifications*, are taken at a temperature of 86 °C. This temperature is essentially identical to the overpack outer skin maximum temperature of 86.6 °C given in Section 2.6.1.1, *Summaries of Pressures and Temperatures*. The primary structural material for lifting is Alloy UNS S31803 stainless steel.

A loaded TRUPACT–III package is only lifted by the four upper ISO fittings, located at each corner of the body. Properties of Alloy UNS S31803 stainless steel are summarized below.

Material Property	Value	Reference
Alloy UNS S31803 Stainless Steel at 86 °C		
Elastic Modulus, E	19.1×10^4 MPa	Table 2.2-1
Yield Strength, σ_y	405 MPa	
Shear Stress, equal to $(0.6)\sigma_y$	243 MPa	

2.5.1 Lifting Devices

This section demonstrates that the ISO corner fittings, the only attachments designed to lift the TRUPACT–III package, are designed with a minimum safety factor of three against yielding, per the requirements of 10 CFR §71.45(a)[1]. Figure 2.5-1 illustrates the lifting device configuration for the TRUPACT–III package.

2.5.1.1 Lifting Forces

When lifting the entire TRUPACT–III package, the applied lift force without yielding is simply three times the total package weight of 25,000 kg, as given in Section 2.1.3, *Weights and Centers of Gravity*.

$$F_L = (3)(25{,}000) = 75{,}000 \text{ kg}$$

The entire package is lifted via four ISO fittings located at each corner of the body. For the purposes of this analysis, it is conservatively assumed that only two, diagonally opposed ISO fittings support the applied load. An additional conservatism is applied by offsetting the center of gravity (CG) by the maximum offset. According to Section 2.1.3, *Weights and Centers of Gravity*, the CG of a uniformly loaded package is located 2,312 mm from the outer surface of the closed-end of the package. In this analysis, the essentially identical value of 2,313 mm will be used. In addition, the package will be loaded so that the CG will translate no more than ±200 mm from that location. Therefore, the most biased position is 2,313 + 200 = 2,513 mm from the outside closed-end wall, with the maximum lifting load on the ISO fitting occurring at the closure lid end of the package. The extreme ends of the package are utilized as essentially equivalent to the lift locations of the ISO fittings. This assumption is also conservative for the bending analysis performed below. The maximum load is:

[1] Title 10, Code of Federal Regulations, Part 71 (10 CFR 71), *Packaging and Transportation of Radioactive Material*, 01–01–09 Edition.

$$F_{ISO} = \left(\frac{2{,}513}{4{,}288}\right)(75{,}000) = 43{,}954\,\text{kg} = 431{,}189\,\text{N}$$

where 4,288 mm is the overall length of the package.

2.5.1.2 Lifting Failure Modes

Several failure modes are considered for the ISO corner fitting due to the lifting force. The failure modes that are considered are:

(a) Shear tearout of the ISO twistlock in top ISO fitting plate,

(b) Shear failure of the welds attaching the top ISO fitting plate,

(c) Bending failure in the lifting arm structures.

2.5.1.2.1 Shear Tearout of Twistlock Top Plate

Figure 2.5-2 presents the dimensional details of the twistlock top plate for evaluation of shear tearout due to lifting forces. The top plate shear area is the length of the twistlock cam multiplied by the top plate thickness. The length of the twistlock cam outline is determined from the following expression:

$$l = 2\left[\frac{2r\alpha\pi}{180} + (w_1 - w_2)\right] = 2\left[\frac{2(50)\left[\sin^{-1}\frac{28.5}{50}\right]\pi}{180} + (82 - 63.5)\right] = 158\,\text{mm}$$

The top plate thickness, t, is 28.5 mm. Thus, the total shear area, A_s, is:

$$A_s = l \times t = 158 \times 28.5 = 4{,}503\ \text{mm}^2$$

The maximum shearing force, V, is the maximum lifting force on the ISO fitting, F_{ISO} = 431,189 N from Section 2.5.1.1, *Lifting Forces*, resulting in a corresponding shear stress of:

$$\tau_V = \frac{F_{ISO}}{A_s} = \frac{431{,}189}{4{,}503} = 95.8\,\text{MPa}$$

The allowable shear stress for UNS S31803 material is 243 MPa. Therefore, the margin of safety is:

$$MS = \frac{243.0}{95.8} - 1.0 = +1.54$$

2.5.1.2.2 Shear Failure of Twistlock Top Plate Attachment Welds

Figure 2.5-3 presents the dimensional details for the top plate attachment welds. The total length of the weld is 2(149 + 178 + 28.5) = 711 mm. The effective weld thickness for the attachment welds is equal to the thickness of the lifting arm, i.e., 8 mm. Thus, the total shear area for the attachment weld is:

$$A_{weld} = (711)(8) = 5{,}688\ \text{mm}^2$$

The maximum shearing force, V, is the maximum lifting force on the ISO fitting, F_{ISO} = 431,189 N from Section 2.5.1.1, *Lifting Forces*, resulting in a corresponding shear stress of:

$$\tau_{weld} = \frac{F_{ISO}}{A_{weld}} = \frac{431,189}{5,688} = 75.8\,MPa$$

The allowable shear stress for UNS S31803 material is 243 MPa. Therefore, the margin of safety is:

$$MS = \frac{243.0}{75.8} - 1.0 = +2.21$$

2.5.1.2.3 Bending Stress in Lifting Arm Structures

Figure 2.5-4 presents the configuration of the lifting arm structures that react the lifting loads. A breakdown of the material thicknesses for the lifting arm structure is presented in Figure 2.5-5. The lifting arm structures are fabricated entirely from Alloy UNS S31803 stainless steel.

The front and rear lifting arms are constructed differently. The front lifting arm design utilizes a longer length sheet than the rear lifting arm design. In addition, the rear lifting arm design utilizes thinner sheet materials than the front lifting arm design. For conservatism, the thinner sheet material of the rear lifting arm design and the longer length sheet of the front lifting arm design will be utilized in the analysis. The lifting arm structure is approximated by a varying cross-section and will be analyzed as a fixed cantilever beam, as illustrated in Figure 2.5-6. For simplicity, the "open" end of the cantilever (located 532 mm from the fixed end as shown in Figure 2.5-6) will be used to calculate the section properties. The open section has less material than the fixed end, and when combined with the larger bending moment of the fixed end, the resulting bending stress will be conservative.

Because of symmetry, the centroid of the cantilever beam, relative to the base, is located at a height of:

$$\bar{x} = \frac{2,500}{2} = 1,250\,mm$$

The moment of inertia at the open end is:

$$I = \frac{188(2,500)^3}{12} - \frac{174(2,488)^3}{12} - \frac{6(2,000)^3}{12} = 1.75\times10^{10}\ mm^4$$

The cross-sectional area at the open end is:

$$A = 2,500(188) - 2,488(174) - 6(2000) = 25,088\ mm^2$$

The maximum bending moment, M, is the maximum lifting force at the base, F_{ISO}, with a moment arm of 870 – 102 = 768 mm, resulting in a corresponding bending stress of:

$$\sigma_{closed} = \frac{M\bar{x}}{I} = \frac{431,189(768)1,250}{1.75\times10^{10}} = 23.7\ MPa$$

The maximum shearing force, V, is the maximum lifting force at the base, F_{ISO}, resulting in a corresponding shear stress of:

$$\tau_{closed} = \frac{F_{ISO}}{A} = \frac{431,189}{25,088} = 17.2 \text{ MPa}$$

The yield stress for Alloy UNS S31803 stainless steel is 405 MPa and the shear yield stress is 243 MPa. The margin of safety on bending stress at the extreme fiber is:

$$MS = \frac{405.0}{23.7} - 1.0 = +16.1$$

The margin of safety on maximum shear at the neutral axis is:

$$MS = \frac{243.0}{17.2} - 1.0 = +13.1$$

The weld of the lifting arm to the fixed end is a complex structure consisting of a combination of complete-joint-penetration and full-thickness-leg fillet welds. However, its configuration is bounded by a hypothetical, 6 mm fillet weld having the same dimensions as used above to calculate the full section properties. The weld may therefore be conservatively modeled as a rectangle 2,500 mm tall, 188 mm wide, with 2,000 mm removed from one long side (see Figure 2.5-6), and a width of 6 × 0.707 = 4.24 mm. The moment of inertia of the weld is:

$$I_w = \frac{188(2,500)^3}{12} - \frac{(188-2\times4.24)(2,500-2\times4.24)^3}{12} - \frac{4.24(2,000)^3}{12} = 1.06\times10^{10} \text{ mm}^4$$

The cross-sectional area of the weld is:

$$A_w = 2,500(188) - (2,500-2\times4.24)(188-2\times4.24) - 4.24(2,000) = 14,296 \text{ mm}^2$$

Using the same fixed-end moment as calculated above, the bending stress in the weld is:

$$\sigma_w = \frac{M\bar{x}}{I_w} = \frac{431,189(768)1,250}{1.06\times10^{10}} = 39.1 \text{ MPa}$$

The shear stress in the weld is:

$$\tau_w = \frac{F_{ISO}}{A_w} = \frac{431,189}{14,296} = 30.2 \text{ MPa}$$

The maximum combined shear stress in the weld is:

$$\tau_T = \sqrt{\sigma_w^2 + \tau_w^2} = \sqrt{39.1^2 + 30.2^2} = 49.4 \text{ MPa}$$

Using the shear yield stress for the weld, the margin of safety is:

$$MS = \frac{243.0}{49.4} - 1.0 = +3.92$$

2.5.1.3 Summary

All margins of safety for the lifting devices are positive relative to a minimum factor of safety of three against yielding, per 10 CFR §71.45(a). The smallest tensile or shear margin of safety, i.e., MS = +1.54, is for shear tearout failure of the top plate on the ISO fitting, indicating that this item will be the mode of failure for lifting devices under excessive load condition. In accordance with

10 CFR §71.45(a), this failure mode does not compromise the performance capabilities of the TRUPACT–III package since no main structural part of the package is affected.

2.5.2 Tie–down Devices

During transport, the TRUPACT–III package is secured to its conveyance by tie-rods (or equivalent) which connect to a frame installed over the top of the package. Horizontal restraint is provided by structural pockets on the conveyance in the vicinity of the four lower ISO fittings. However, no attachment is made to any (upper or lower) ISO fittings during transport. As such, the TRUPACT-III has no integral tie-down devices that are part of the package. Therefore, per 10 CFR §71.45(b)(1), no analysis of tie–down devices is required.

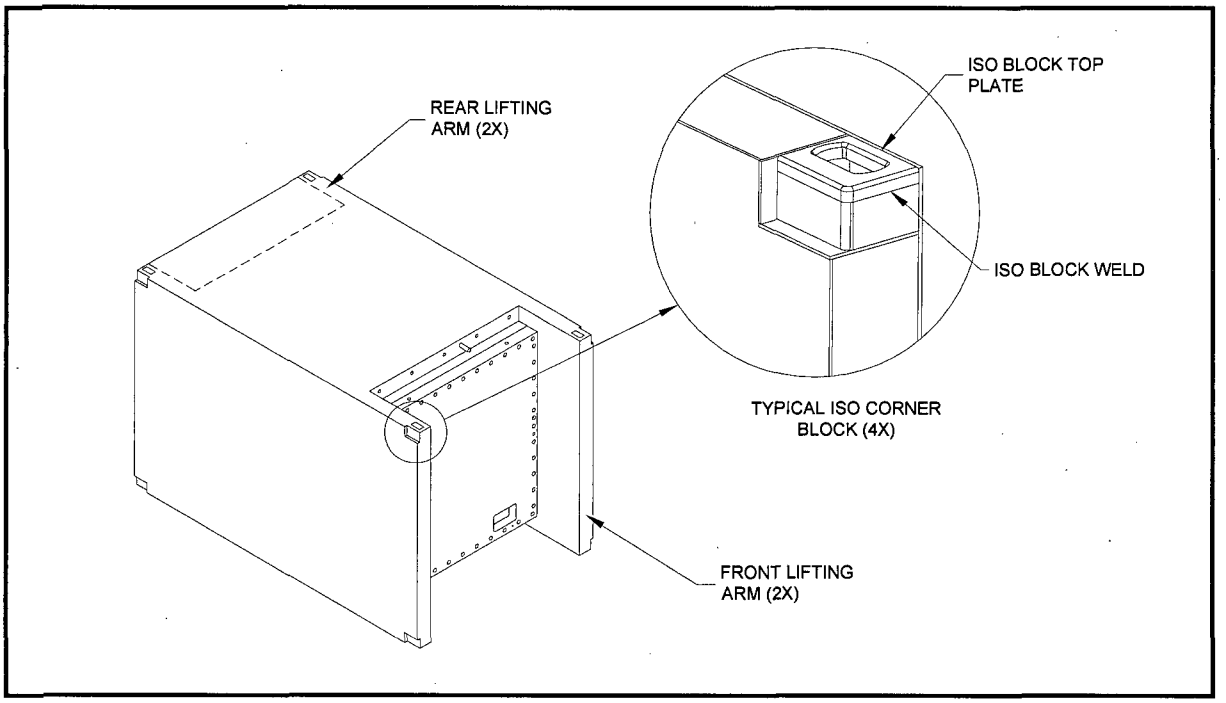

Figure 2.5-1 – Lifting Device Configuration

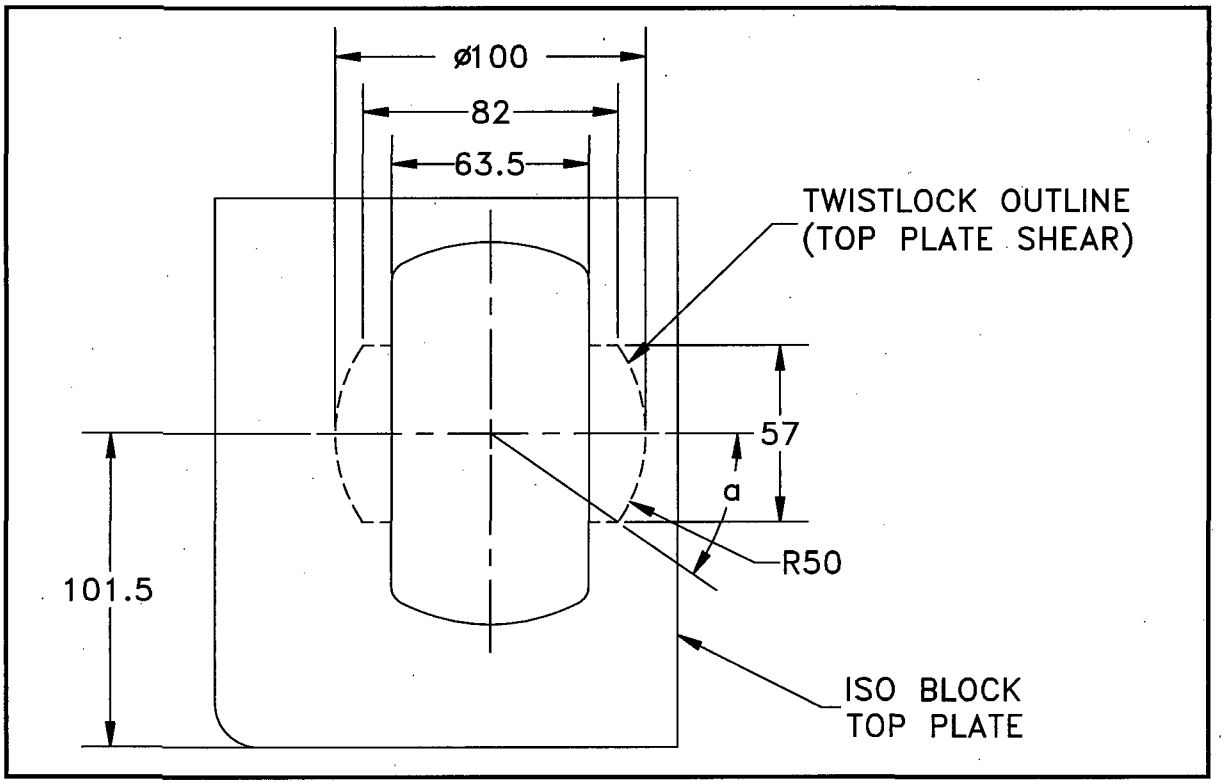

Figure 2.5-2 – Shear Tearout of Twistlock Top Plate

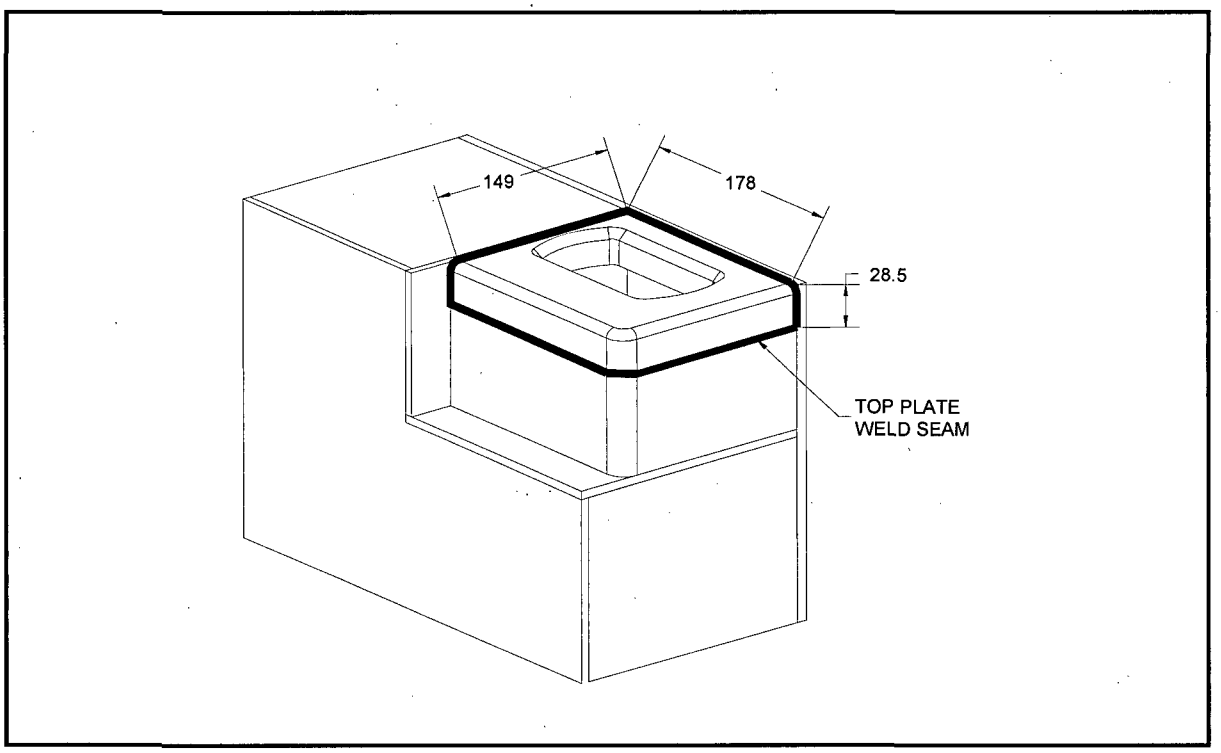

Figure 2.5-3 – Shear Failure of Twistlock Top Plate Attachment Welds

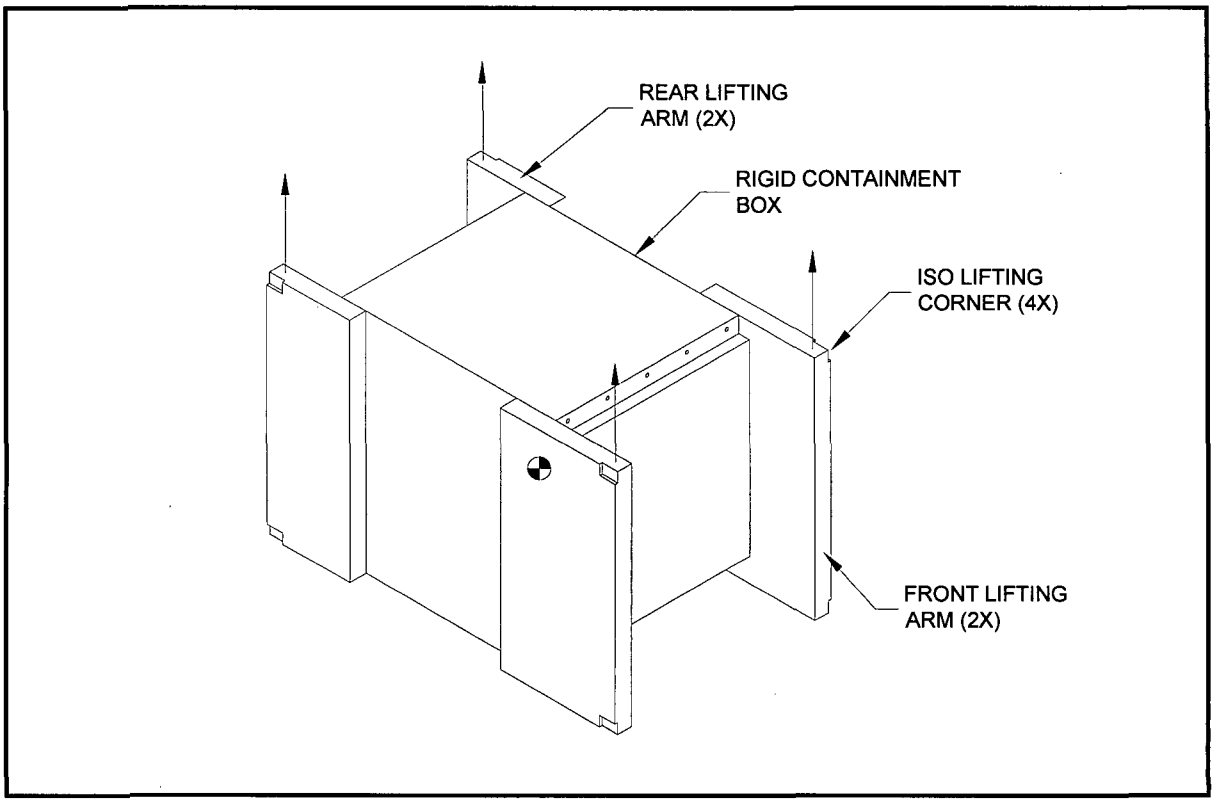

Figure 2.5-4 – Lifting Arm Structure Bending

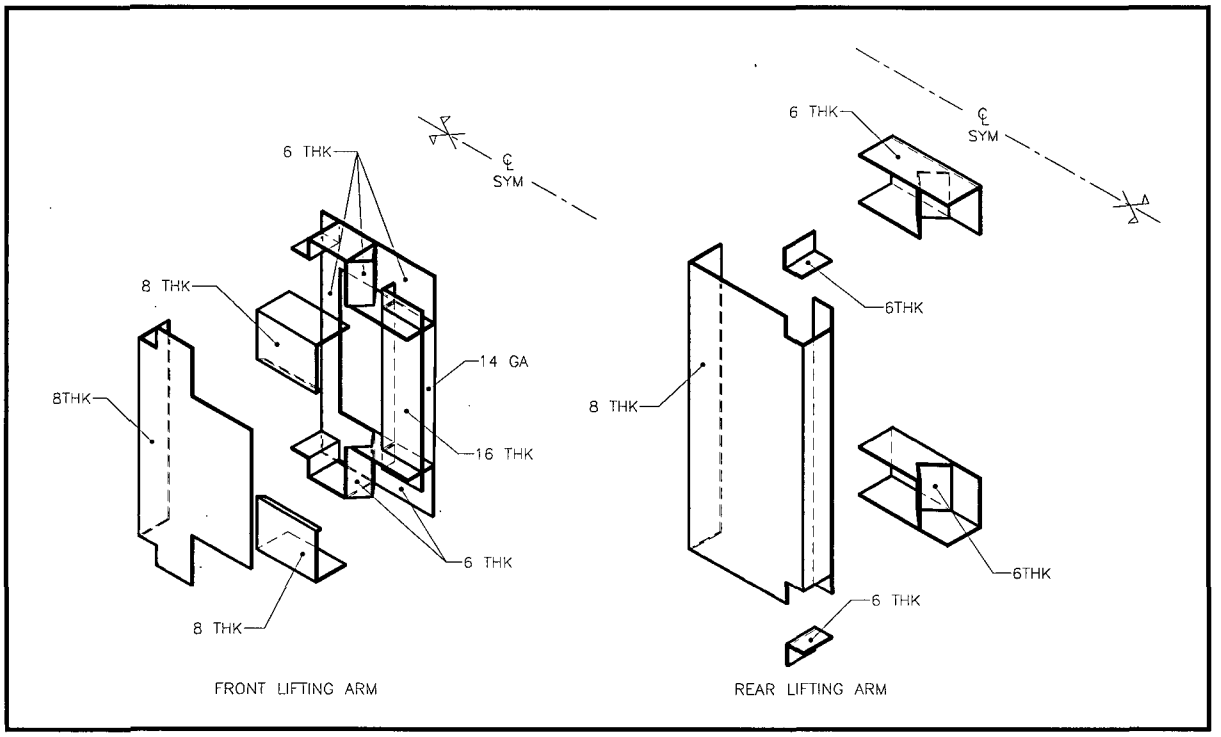

Figure 2.5-5 – Lifting Arm Material Thicknesses

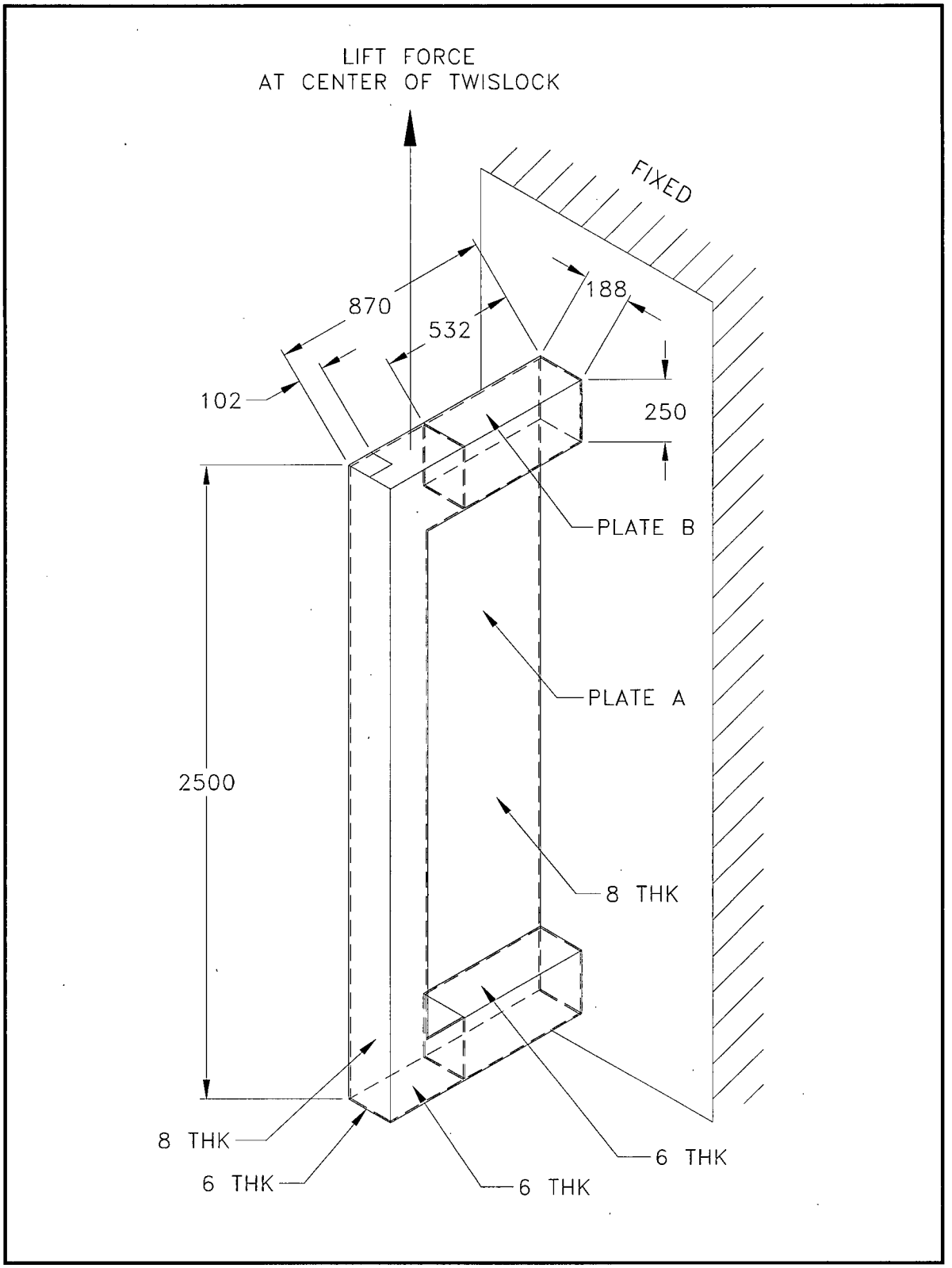

Figure 2.5-6 – Lifting Arm Analysis Model

2.6 Normal Conditions of Transport

The TRUPACT–III package, when subjected to the normal conditions of transport (NCT) specified in 10 CFR §71.71[1], is shown to meet the performance requirements specified in Subpart E of 10 CFR 71. As discussed in the introduction to this chapter, the primary proof of NCT performance is via analytic methods. Regulatory Guide 7.6[2] criteria are demonstrated as acceptable for all NCT analytic evaluations presented in this section. Specific discussions regarding brittle fracture and fatigue are presented in Section 2.1.2.2, *Miscellaneous Structural Failure Modes*, and are shown not to be limiting cases for the TRUPACT–III packaging design. The performance capabilities of the butyl containment O-ring seals are documented in Appendix 2.12.2, *Elastomer O-ring Seal Performance Tests*.

NCT analyses for heat, cold, reduced external pressure, increased external pressure, and vibration are performed in this section. The NCT free drop demonstration is by test as discussed in Section 2.6.7, *Free Drop*. Dimensions are taken from the drawings in Appendix 1.3.1, *Packaging General Arrangement Drawings*. Allowable stress limits are consistent with Table 2.1-1 in Section 2.1.2.1, *Analytic Design Criteria (Allowable Stresses)*, using temperature-adjusted material properties taken from the tables in Section 2.2.1, *Material Properties and Specifications*. Properties at selected temperatures are summarized below.

Table 2.6-1 – NCT Material Properties

Material Property	Material Property Value (MPa)			Reference
	-29 °C	21 °C	71 °C	
ASTM A240 & ASTM A479, UNS S31803 Stainless Steel				
Elastic Modulus, E	19.8×10^4	19.5×10^4	19.2×10^4	Table 2.2-1
Design Stress Intensity, S_m	207	207	207	
Yield Strength, S_y	448	448	419	
ASTM A320 Grade L43 Bolting Material				
Elastic Modulus, E	19.4×10^4	19.2×10^4	18.9×10^4	Table 2.2-4
Yield Strength, S_y	724	724	699	

2.6.1 Heat

The NCT thermal analyses presented in Section 3.3, *Thermal Evaluation for Normal Conditions of Transport*, consist of exposing the TRUPACT–III package to direct sunlight and 38 °C still air per the requirements of 10 CFR §71.71(b). Although the actual internal heat load depends on the particular payload being transported, this section utilizes the maximum internal heat allowed within a TRUPACT–III package of 80 thermal watts, and which results in the maximum temperature gradients throughout the TRUPACT–III package.

---

[1] Title 10, Code of Federal Regulations, Part 71 (10 CFR 71), *Packaging and Transportation of Radioactive Material*, 01–01–09 Edition.

[2] U. S. Nuclear Regulatory Commission, Regulatory Guide 7.6, *Design Criteria for the Structural Analysis of Shipping Cask Containment Vessels*, Revision 1, March 1978.

2.6.1.1 Summary of Pressures and Temperatures

The maximum normal operating pressure (MNOP) is 172 kPa gauge (273 kPa absolute), as determined in Section 3.3.2, *Maximum Normal Operating Pressure*. The pressure stress analyses within this section combine the internal pressure of 172 kPa gauge due to MNOP with a reduced external pressure, per 10 CFR §71.71(c)(3), of 25 kPa absolute. Therefore, the net resulting internal pressure utilized in all NCT structural analyses considering internal pressure is 273 - 25 = 248 kPa.

The NCT heat input results in modest temperatures and temperature gradients throughout the TRUPACT–III package. Maximum temperatures for the major packaging components are summarized in Table 3.1-1 from Section 3.1.4, *Summary Tables of Temperatures*. As shown in the table, the maximum temperature of the containment structural assembly (CSA) is 57.6 °C (for the outer structural sheet). The maximum temperature of the CSA containment sheet is 55.6 °C. Due to the relatively small temperature gradients between CSA components, temperature gradients are of no concern. For conservatism, structural analyses of the package for NCT utilize a bounding uniform temperature of 71 °C. The maximum temperature of overpack outer skin is 86.6 °C.

2.6.1.2 Differential Thermal Expansion

In the absence of significant temperature gradients, concern with differential expansions is limited to regions of the TRUPACT–III packaging that employ adjacent materials with sufficiently different coefficients of thermal expansion. The CSA is a double-wall, composite construction of inner and outer stainless steel sheets that are joined by a stainless steel V-stiffener interior structure. The CSA double-wall construction is composed entirely of the same material and subsequently does not exhibit differential expansions. The guide bars attached to the inside of the containment sheets are made of ASTM Type 304/304L material. Any fatigue concerns with this construction are evaluated and dismissed in Section 2.1.2.2.2.1, *Normal Operating Cycles*. The only potential for meaningful differential expansion is between the closure lid bolts, composed of ASTM A320, Grade L43, alloy steel, and the material clamped by the bolts, composed of UNS S31803 stainless steel. The effect of varying temperature on the closure lid bolt stress and clamping force is evaluated in Section 2.6.1.6, *Closure Bolts*.

2.6.1.3 Stress Calculations

The internal pressure considers the effects of a maximum normal operating pressure (MNOP) of 172 kPa gauge (273 kPa absolute) internal, coupled with a reduced external pressure of 25 kPa absolute. The net result is an internal pressure of 273 – 25 = 248 kPa. This evaluation will use classical methods to find the stresses in the CSA walls. Bending and membrane stresses will conservatively be directly added. The margins of safety will be conservatively evaluated using mechanical properties at 71°C.

The side longitudinal and rear walls of the CSA will be evaluated for maximum membrane-plus-bending stresses. The TRUPACT–III longitudinal walls support global bending along their span and local bending between the V-stiffeners from pressure loading. The walls also support axial and lateral loads from the pressure loads acting on the adjacent walls. The contribution of the V-stiffeners to the bending moment of inertia is conservatively neglected. Figure 2.6-1(f) shows the typical wall section used for the global bending and membrane evaluations. Figure 2.6-1(g) and Figure 2.6-1(h) show the cross sections used for the local bending evaluations. The axial and lateral loads are translated by

neighboring walls as membrane stresses through the combined thickness of the adjoining inner and outer sheets of each wall. The side longitudinal walls have a greater span, which makes them the more vulnerable to bending stresses than the top and bottom containment walls.

Assumptions

1. The edge loads (resulting from pressure loads on the adjacent walls) will be evaluated with the areas shown in Figure 2.6-1(a) through Figure 2.6-1(e).
2. The height of the side wall extends from the center of the bottom wall cross section to the center of the top wall cross section. Similarly, the width of the top/bottom wall extends from the center of one side wall cross section to the center of the other side wall cross section. The length of any wall extends from the center of the end wall to the bolted seal flange. These dimensions are:

   H = height of side wall = 2,140 mm

   W = width of top/bottom sheets = 1,980 mm

   L = length of any wall = 2,860 mm
3. Referring to Figure 2.6-1(a), the pressure load acting on Area 1 of the rear wall applies forces to the end edges of the side wall.
4. From the same figure, the pressure load on Area 2 of the top wall loads the top and bottom edges of the side wall.
5. Referring to Figure 2.6-1(b), the pressure load acting on Area 3 of the top wall loads the top and bottom edges of the rear wall.
6. From the same figure, the pressure load on Area 4 of the side wall loads the side edges of the rear wall.
7. All edges are conservatively assumed to be simply supported. Since the closure lid has sheets which are 50% thicker than the body walls, the assumption of simply supported edges means that the closure lid does not need to be considered.

Calculation Input Parameters

Internal design pressure differential: P = 248 kPa =248,000 Pa

Thickness of inner and outer sheets: t = 8 mm = 0.008 m

Distance between inner & outer sheet neutral axes: d = 132 mm = 0.132 m

Area of one face sheet per unit width, b: $A = b(t) = 8\ mm^2 = 8.0 \times 10^{-6}\ m^2$

Membrane and maximum fiber distances from central axis:

$$c_m = \frac{d}{2} = 0.066\,m \qquad c_o = \frac{d+t}{2} = 0.070\,m$$

Second moment of area (about central axis):

$$I_1 = 2A\left(\frac{d}{2}\right)^2 = 2(8\times10^{-6}\ m^2)\left(\frac{0.132\,m}{2}\right)^2 = 6.97\times10^{-8}\ m^4$$

Stress Analysis of the Governing CSA Wall

Due to local bending stress, the inner containment sheet is governing. Coordinate directions are shown on Figure 2.6-1(b). The x-direction is parallel to the V-stiffeners and y is perpendicular to the V-stiffeners. The following stresses are evaluated and combined:

- Membrane stress on the neutral axis, and membrane-plus-bending stress on the inner surface of the inner sheet due to global bending of the side wall (x-direction)
- Local bending stress generated by pressure acting over the span of the inner sheet between V-stiffener supports (y-direction)
- Axial membrane stress (parallel to V-stiffeners) generated by pressure on Area 2 (x-direction)
- Lateral membrane stress (perpendicular to V-stiffeners) generated by pressure on Area 1 (y-direction)

Stresses due to global bending:

Maximum moment, conservatively assuming the walls are pinned at the edge:

$$M_{side} = \frac{PbH^2}{8} = \frac{(248{,}000\,\text{Pa})(0.001\,\text{m})(2.140\,\text{m})^2}{8} = 141.97\,\text{N-m}$$

Membrane stress, σ_{mbx}:

$$\sigma_{mbx} = \frac{M_{side}c_m}{I_1} = \frac{(141.97\,\text{N-m})(0.066\,\text{m})}{(6.97\times10^{-8}\,\text{m}^4)}\times10^{-6}\,\frac{\text{MPa}}{\text{Pa}} = 134.4\,\text{MPa}$$

Maximum global bending stress, σ_{gbx}:

$$\sigma_{gbx} = \frac{M_{side}c_o}{I_1} = \frac{(141.97\,\text{N-m})(0.070\,\text{m})}{(6.97\times10^{-8}\,\text{m}^4)}\times10^{-6}\,\frac{\text{MPa}}{\text{Pa}} = 142.6\,\text{MPa}$$

Local bending stress:

Unsupported span of inner sheet between V-stiffeners: S = 145 mm = 0.145 m

Area moment of inertia for inner sheet:

$$I_2 = \frac{bt^3}{12} = \frac{(0.001\,\text{m})(0.008\,\text{m})^3}{12} = 4.27\times10^{-11}\,\text{m}^4$$

Maximum moment, conservatively assuming the sheet has pinned edges at the locations supported by V-stiffeners:

$$M_{side\text{-}local} = \frac{P\,b\,S^2}{8} = \frac{(248{,}000\,\text{Pa})(0.001\,\text{m})(0.145\,\text{m})^2}{8} = 0.652\,\text{N-m}$$

Maximum local bending stress:

$$\sigma_{lby} = \frac{(t/2)M_{side\text{-}local}}{I_2} = \frac{(0.008\,\text{m}/2)(0.652\,\text{N-m})}{(4.27\times10^{-11})}\times10^{-6}\,\frac{\text{MPa}}{\text{Pa}} = 61.1\,\text{MPa}$$

Axial membrane stress:

Load supplied by area A_2 (see Figure 2.6-1(d)): $A_2 = 2(0.5)0.990^2 + 0.880 \times 0.990 = 1.851\ m^2$

Edge load per unit length in the x-direction (parallel to the core longitudinal axis):

$$N_x = \frac{PA_2}{L} = \frac{(248{,}000\ Pa)\,(1.851\ m^2)}{(2.860\ m)} \times 10^{-3}\ \frac{kN}{N} = 160.5\ kN/m$$

Axial stress in the x-direction (parallel to the core longitudinal axis):

$$\sigma_x = \frac{N_x}{2t} = \frac{160.5\ kN/m}{2(0.008\ m)} \times 10^{-3}\ \frac{MPa}{kPa} = 10.0\ MPa$$

Lateral membrane stress:

Load supplied by area A_1 (see Figure 2.6-1(c)): $A_1 = 2(0.5)0.990^2 + 0.160 \times 0.990 = 1.139\ m^2$

Edge load per unit length in the y-direction (perpendicular to the core longitudinal axis):

$$N_y = \frac{PA_1}{H} = \frac{(248{,}000\ Pa)\,(1.139\ m^2)}{(2.140\ m)} \times 10^{-3}\ \frac{kN}{N} = 132.0\ kN/m$$

Lateral stress in the y-direction (perpendicular to the core longitudinal axis):

$$\sigma_y = \frac{N_y}{2t} = \frac{132.0\ kN/m}{2(0.008\ m)} \times 10^{-3}\ \frac{MPa}{kPa} = 8.3\ MPa$$

Conservatively combining all membrane stresses arithmetically, regardless of direction:

$$SI_{pm} = \sigma_{mbx} + \sigma_x + \sigma_y = 134.4 + 10.0 + 8.3 = 152.7\ MPa$$

The allowable stress for this case is S_m, or 207 MPa for Alloy UNS S31803 stainless steel at 71°C. Therefore, the margin of safety (MS) is:

$$MS = \frac{207}{SI_{pm}} - 1.0 = +0.36$$

Conservatively combining all membrane-plus-bending stresses arithmetically, regardless of direction,

$$SI_{pmb} = \sigma_{gbx} + \sigma_{lby} + \sigma_x + \sigma_y = 142.6 + 61.1 + 10.0 + 8.3 = 222.0\ MPa$$

The allowable stress this case is $1.5S_m$. Therefore, the margin of safety is:

$$MS = \frac{1.5\,(207)}{SI_{pmb}} - 1.0 = +0.40$$

Wall stiffener weld evaluation

As previously described, the CSA walls have a sandwich construction. V-stiffeners are welded to the inner and outer sheets of each wall. The V-stiffeners are attached to the inner containment sheet by continuous skewed fillet welds, which have an equivalent throat thickness of at least 4 mm. The V-stiffeners are attached to the outer structural sheet by equally spaced 20-mm diameter plug welds. As shown below, the equivalent shear width of the plug welds is 5.5 mm, and

therefore, this shear width is bounding compared to the inner sheet welds that have a combined effective throat of 2 × 4 = 8 mm. The calculation parameters are:

Number of plug welds per V-stiffener: N = 40

Diameter of plug welds, D: D = 20 mm = 0.020 m

Conservative V-stiffener length, L: L = 2,280 mm = 2.280 m

Distance between plug weld rows, d_p: d_p = 164 mm = 0.164 m

Equivalent plug weld shear width, t_e, per V-stiffener:

$$t_e = \frac{(\pi/4)\, D^2\, N}{L} = \frac{(\pi/4)\,(0.020\,\text{m})^2\,(40)}{(2.280\,\text{m})} = 0.0055\,\text{m}$$

Equivalent plug weld shear width, t_{eb}, per unit width b:

$$t_{eb} = \frac{t_e b}{164\,\text{mm}} = \frac{(0.0055\,\text{m})\,(0.001\,\text{m})}{(0.164\,\text{m})} = 3.354\times10^{-5}\,\text{m}$$

Shear Force, V: V = ½P(b)(H) = ½(248,000 Pa)(0.001 m)(2.140 m) = 265.4 N

Plug Weld Shear Stress, $\tau_{\text{plug weld}}$:

$$\tau_{\text{plug weld}} = \frac{VQ}{I_1 t_{eb}} = \frac{(265.4\,\text{N})\,(5.28\times10^{-7}\,\text{m}^3)}{(6.97\times10^{-8}\,\text{m}^4)\,(3.354\times10^{-5}\,\text{m})}\times10^{-6}\,\frac{\text{MPa}}{\text{Pa}} = 59.9\,\text{MPa}$$

where: Q = (cm)(t)(b) = (0.066 m)(0.008 m)(0.001 m) = 5.28 × 10^{-7} m^3

The allowable shear stress for this case is $0.6S_m$ = 124.2 MPa for Alloy UNS S31803 stainless steel at 71 °C. Therefore, the margin of safety is:

$$MS = \frac{124.2}{\tau_{\text{plug weld}}} - 1.0 = +1.07$$

Of note, the rear wall has the same fillet welds to the containment sheet, but has continuous welds to the structural sheet, and is therefore bounded by the analysis of the side wall shown here.

The fillet welds attaching the V-stiffeners to the containment sheets are classified as fillet welded attachments per ASME Code, paragraph NB-3123.2. For this application, a fatigue analysis of the welds must be performed. The applied loading range is for the full internal pressure differential of P = 248 kPa to the full internal vacuum and normal ambient external pressure differential of 101 kPa.

The fillet weld shear width per unit width b, t_{fb}, is:

$$t_{fb} = \frac{(\text{combined fillet throat})b}{164} = \frac{(0.008\,\text{m})(0.001\,\text{m})}{0.164\,\text{m}} = 4.878\times10^{-5}\,\text{m}$$

The fillet weld shear stress due to the internal pressure differential is:

$$\tau_{\text{fw-ip}} = \frac{VQ}{I_1 t_{fb}} = \frac{(265.4\,\text{N})\,(5.28\times10^{-7}\,\text{m}^3)}{(6.97\times10^{-8}\,\text{m}^4)\,(4.878\times10^{-5}\,\text{m})}\times10^{-6}\,\frac{\text{MPa}}{\text{Pa}} = 41.2\,\text{MPa}$$

For the internal vacuum case, the differential pressure arises from the normal atmospheric external absolute pressure of 101 kPa and an internal pressure of zero. The corresponding fillet weld stress may be determined by scaling to be:

$$\tau_{fw-ep} = \tau_{fw-ip}\frac{101}{248} = 16.8\,\text{MPa}$$

The range of stress between these two states is 41.2 + 16.8 = 58 MPa. Since this stress is a shear stress in a fillet weld, the stress intensity is twice this value, or 116 MPa. The maximum stress is increased by a stress concentration factor of 4 in accordance with ASME B&PV Code, paragraph NB-3232.3. The alternating stress intensity is equal to half of this result, or:

$$S_{alt} = 0.5(116)(4) = 232\ \text{MPa}$$

This value must be adjusted for the modulus of elasticity at temperature. The modulus of elasticity at a temperature of 71 °C is 19.2(10^4) MPa from Table 2.6-1. The modulus at a temperature of 21 °C, for which the fatigue curve is prepared, is 19.5(10^4) MPa. The temperature-adjusted value of S_{alt} is:

$$S_{alt-adj} = S_{alt}\frac{19.5}{19.2} = 235.6\,\text{MPa}$$

The allowable cycles are taken from Table I-9.1M (for Figure I-9.2.1M) of the ASME Code. Conservatively assuming that the stress $S_{alt-adj}$ is equal to a value of 248 MPa, the allowable fatigue cycles are 2(10^5). This value is well above the requirement calculated in Section 2.1.2.2.2.1, *Normal Operating Cycles*, of 1,750 cycles. Thus, the fatigue of the V-stiffener fillet welds is not of concern.

Stress Analysis of the Rear Wall

As for the side wall, the inner containment sheet is governing. Coordinate directions are shown on Figure 2.6-1(b). The x-direction is perpendicular to the end V-stiffeners and z is parallel to the end V-stiffeners. The following stresses are evaluated and combined:

- Membrane stress on the neutral axis, and membrane-plus-bending stress on the inner surface of the inner sheet due to global bending of the side wall (z-direction)
- Local bending stress generated by pressure acting over the span of the inner sheet between V-stiffener supports (x-direction)
- Axial membrane stress (parallel to V-stiffeners) generated by pressure on Area 4 (z-direction)
- Lateral membrane stress (perpendicular to V-stiffeners) generated by pressure on Area 3 (x-direction)

Stresses due to global bending:

Maximum moment, M_{end}, conservatively assuming the walls are pinned at the edge:

$$M_{end} = \frac{P\,(b)W^2}{8} = \frac{(248{,}000\,\text{Pa})\,(0.001)\,(1.980\,\text{m})^2}{8} = 121.5\,\text{N-m}$$

Membrane Stress, σ_{mbx}:

$$\sigma_{mbz} = \frac{M_{end}c_m}{I_1} = \frac{(121.5\,\text{N-m})\,(0.066\,\text{m})}{(6.97\times10^{-8}\,\text{m}^4)}\times10^{-6}\,\frac{\text{MPa}}{\text{Pa}} = 115.1\,\text{MPa}$$

Maximum Global Bending Stress, σ_{gbx}:

$$\sigma_{gbz} = \frac{M_{end} c_o}{I_1} = \frac{(121.5\,\text{N-m})(0.070\,\text{m})}{(6.97\times10^{-8}\,\text{m}^4)}\times10^{-6}\,\frac{\text{MPa}}{\text{Pa}} = 122.0\,\text{MPa}$$

Local bending stress:

Unsupported span of inner sheet between V-stiffeners: S = 151 mm = 0.151 m

Area moment of inertia for inner containment sheet:

$$I_2 = \frac{bt^3}{12} = \frac{(0.001\,\text{m})(0.008\,\text{m})^3}{12} = 4.27\times10^{-11}\,\text{m}^4$$

Maximum moment, $M_{end\text{-}local}$, conservatively assuming sheet has pinned edges at locations supported by V-stiffeners:

$$M_{end\text{-}local} = \frac{bPS^2}{8} = \frac{(0.001\,\text{m})(248{,}000)(0.151\,\text{m})^2}{8} = 0.707\,\text{N-m}$$

Maximum Local Bending Stress, σ_{lbz}:

$$\sigma_{lbx} = \frac{t/2(M_{end-local})}{I_2} = \frac{(0.008\,\text{m}/2)(0.707\,\text{N-m})}{(4.27\times10^{-11}\,\text{m}^4)}\times10^{-6} = 66.2\,\text{MPa}$$

Axial membrane stress:

Loading is supplied by area A_4 (see Figure 2.6-1(e)): $A_4 = ½(1.070)(2.140) = 1.14\ \text{m}^2$

Edge load per unit length in the z-direction, N_z, (parallel to the V-stiffener):

$$N_z = \frac{PA_4}{H} = \frac{(248{,}000\,\text{Pa})(1.14\,\text{m}^2)}{(2.140\,\text{m})}\times10^{-3}\,\frac{\text{kN}}{\text{N}} = 132.1\,\text{kN/m}$$

Axial stress in the z-direction, σ_z, (parallel to the core longitudinal axis):

$$\sigma_z = \frac{N_z}{2t} = \frac{132.1\,\text{kN/m}}{2(0.008\,\text{m})}\times10^{-3}\,\frac{\text{MPa}}{\text{kPa}} = 8.3\,\text{MPa}$$

Lateral membrane stress

Loading is supplied by area A_3 (see Figure 2.6-1(d)): $A_3 = ½(0.990)1.980 = 0.98\ \text{m}^2$

Edge load per unit length in the x-direction, N_x, (perpendicular to the core longitudinal axis):

$$N_x = \frac{PA_3}{W} = \frac{(248{,}000\,\text{Pa})(0.980\,\text{m}^2)}{(1.980\,\text{m})}\times10^{-3}\,\frac{\text{kN}}{\text{N}} = 122.7\,\text{kN/m}$$

Lateral stress in the x-direction, σ_x, (perpendicular to the core longitudinal axis):

$$\sigma_x = \frac{N_x}{2t} = \frac{122.7\,\text{kN/m}}{2(0.008\,\text{m})}\times10^{-3}\,\frac{\text{MPa}}{\text{kPa}} = 7.7\,\text{MPa}$$

Conservatively combining all membrane stresses arithmetically, regardless of direction,

$$SI_{pm} = \sigma_{mbx} + \sigma_x + \sigma_z = 115.1 + 7.7 + 8.3 = 131.1\ \text{MPa}$$

The allowable stress for this case is S_m, or 207 MPa, for Alloy UNS S31803 stainless steel at 71°C. Therefore, the margin of safety is:

$$MS = \frac{207}{SI_{pm}} - 1.0 = +0.58$$

Conservatively, combining all membrane-plus-bending stresses arithmetically, regardless of direction:

$$SI_{pmb} = \sigma_{gbx} + \sigma_{lbz} + \sigma_x + \sigma_z = 122.0 + 66.2 + 7.7 + 8.3 = 204.2 \text{ MPa}$$

The allowable stress for this case is $1.5S_m$ for Alloy UNS S31803 stainless steel at 71 °C. Therefore, the margin of safety is:

$$MS = \frac{1.5\,(207)}{SI_{pmb}} - 1.0 = +0.52$$

2.6.1.4 Comparison with Allowable Stresses

Section 2.1.2, *Design Criteria*, presents the design criteria for structural evaluation of the TRUPACT–III packaging. The containment vessel design criteria for NCT analyses are in accordance with Regulatory Guide 7.6, which uses as a basis the criteria defined for Level A service limits in Section III of the ASME Boiler and Pressure Vessel Code.[3] Load combinations follow the guidelines of Regulatory Guide 7.8.[4]

From Table 2.6-1, the design stress intensity for Alloy UNS S31803 stainless steel is S_m = 207 MPa at 71°C. From Table 2.1-1, the allowable stress intensities for the NCT hot condition are S_m for general primary membrane stress intensity (P_m), $1.5S_m$ for local primary membrane stress intensity (P_L), $1.5S_m$ for primary membrane (general or local)-plus-primary bending stress intensity ($P_m + P_b$ or $P_L + P_b$).

Maximum stress intensity, allowable stress intensity, and minimum margins of safety for each stress category and each load case are summarized in Table 2.6-2. Since all margins of safety are positive, the design criteria are satisfied.

[3] American Society of Mechanical Engineers (ASME) Boiler and Pressure Vessel Code, Section III, *Rules for Construction of Nuclear Power Plant Components*, 2004 Edition, 2005 and 2006 Addenda.

[4] U. S. Nuclear Regulatory Commission, Regulatory Guide 7.8, *Load Combinations for the Structural Analysis of Shipping Casks for Radioactive Material*, Revision 1, March 1989.

Table 2.6-2 – Margins of Safety for NCT Hot Case

Stress Type	Stress, MPa	Location	Allowable, MPa	Margin of Safety
Membrane	152.7	Side wall inner and outer sheets	207.0	+0.36
Membrane + Bending	222.0	Side wall inner containment sheet	310.5	+0.40
Weld Shear	59.9	Outer sheet plug welds	124.2	+1.07
Membrane	131.1	Rear wall inner and outer sheets	207.0	+0.58
Membrane + Bending	204.2	Rear wall inner containment sheet	310.5	+0.52

2.6.1.5 Range of Primary-Plus-Secondary Stress Intensities

Per Paragraph C.4 of Regulatory Guide 7.6, the maximum range of primary-plus-secondary stress intensity for NCT must be less than $3.0S_m$. This limitation on stress intensity range applies to the entire history of NCT loadings and not only to the stresses from each individual load transient. To conservatively encompass the maximum stress intensity range, the maximum stress condition in the CSA was doubled to account for the worst possible stress reversal. From the table above, the maximum CSA stress is 222 MPa in the side wall containment sheet, for the maximum internal pressure with reduced external pressure. Doubling this value results in a maximum stress intensity range of 444 MPa. The allowable stress, at NCT temperatures, is $3.0S_m$, or 3(207) = 621 MPa. The margin of safety is then:

$$MS = \frac{621}{444} - 1.0 = +0.40$$

Therefore, the criterion of Paragraph C.4 of Regulatory Guide 7.6 is met.

2.6.1.6 Closure Bolts

The closure lid bolt stresses are determined using the recommendations of NUREG/CR 6007[5] and Shigley, *Mechanical Engineering Design*[6]. Allowable stresses are defined in Table 2.1-1 and obtained from Table 2.2-4 for the ASTM A320, Grade L43 bolting material. The maximum bolt stress occurs during the NCT hot operating condition. The resulting tensile stress is 327.9 MPa, which includes the preload and effects of differential thermal expansion. When compared to the allowable tensile stress of S_m, where S_m is $2/3S_y$ (or 466 MPa), the corresponding margin of safety is +0.42. Due to the magnitude of the closure lid bolt preload compared to the internal pressure load, there is no significant prying stress on the bolts. The portion of the internal pressure load taken by the closure lid bolts is 6.3

[5] G. C. Mok, L. E. Fischer, S. T. Hsu, *Stress Analysis of Closure Bolts for Shipping Casks*, NUREG/CR-6007, U.S. Nuclear Regulatory Commission, Washington, DC 20555, January 1993.

[6] Shigley, J. E., Mischke, C. R., *Mechanical Engineering Design*, Fifth Edition, McGraw-Hill, 1989, New York, NY.

kN, which is less than 3% of the 222.2 kN preload. Adding the residual torsion to the tensile stress, the total stress intensity is 445.6 MPa. The corresponding margin of safety on the allowable of $1.35S_m$ (or 629.1 MPa) is +0.41. Details of this analysis are provided below. A depiction of the various bolting parameters is provided in Figure 2.6-2.

Calculation Input Parameters

Nominal bolt diameter:	$d = 36$ mm
Nominal shank diameter:	$d_s = 30$ mm
Thread pitch:	$p = 4$ mm
Pitch diameter:	$d_m = d - 0.649519(p) = 33.0$ mm $= 0.033$ m
Minor diameter:	$d_r = d - 1.226869(p) = 31.0$ mm $= 0.031$ m
Mean of pitch and minor diameters, d_{rm}:	$d_{rm} = \frac{d_m + d_r}{2} = 0.032$ m
Threaded tensile area, A_t, of fastener:	$A_t = \pi/4 (d_{rm}^2) = 8.042 \times 10^{-4}$ m^2
Length of threaded portion of grip:	$L_t = 0$ mm
Shank tensile area, A_d, of fastener:	$A_d = \pi/4 (d_s^2) = 7.069 \times 10^{-4}$ m^2
Length of unthreaded portion of grip:	$L_d = 155$ mm $= 0.155$ m
Total grip length:	$L = L_d + L_t = 0.155$ m
Elastic modulus of bolt:	E_b at 21 °C $= 19.2 \times 10^4$ MPa (ASTM A320 L43)
Elastic modulus of clamped material:	E_m at 21 °C $= 19.5 \times 10^4$ MPa (UNS S31803)
Installation torque :	$T = 1{,}600$ N-m
Installation torque factor :	$K = 0.20$

Bolt Calculations at 21 °C

The bolt stiffness, k_b, is:

$$k_b = \frac{A_d E_b}{L_d} = \frac{(7.069 \times 10^{-4}\ \text{m}^2)(19.2 \times 10^4\ \text{MPa})}{(0.155\ \text{m})} = 875.6\ \text{MN/m}$$

The cross-sectional area of the closure lid boss, A_m (i.e., the tube forming the bolt hole in the lid, having an outer diameter of 64 mm and an inner diameter of 44 mm) is:

$$A_m = \pi/4 (D_o^2 - D_i^2) = \pi/4 (64^2 - 44^2) \times 10^{-6} = 1.696 \times 10^{-3}\ \text{m}^2$$

The member stiffness, k_m, is:

$$k_m = \frac{A_m E_m}{L} = \frac{(1.696 \times 10^{-3}\ \text{m}^2)(19.5 \times 10^4\ \text{MPa})}{(0.155\ \text{m})} = 2133.7\ \text{MN/m}$$

The preload, F_i, is:

$$F_i = \frac{T}{Kd} = \frac{1600\ \text{N-m}}{(0.20)(0.036\ \text{m})} \times 10^{-3}\ \frac{\text{kN}}{\text{N}} = 222.2\ \text{kN}$$

The external tensile load per bolt, P, is found using the MNOP (248 kPa), the square dimensions of the containment O-ring seal (1.888 m by 2.048 m), and the quantity of closure bolts (44):

$$P = \frac{\text{Pressure (Area)}}{\text{Number of Bolts}} = \frac{(248\ \text{kPa})(1.888\ \text{m})(2.048\ \text{m})}{44} = 21.8\ \text{kN}$$

The portion of P reacted by bolt, P_b, is:

$$P_b = \frac{k_b P}{k_b + k_m} = \frac{(875.6\ \text{MN/m})\ (21.8\ \text{kN})}{(875.6\ \text{MN/m} + 2133.7\ \text{MN/m})} = 6.3\ \text{kN}$$

And the portion of P reacted by members, P_m, is:

$$P_m = \frac{k_m P}{k_b + k_m} = \frac{(2133.7\ \text{MN/m})\ (21.8\ \text{kN})}{(875.6\ \text{MN/m} + 2133.7\ \text{MN/m})} = 15.5\ \text{kN}$$

As shown, the bolt preload is significantly greater than the applied pressure load per bolt, and is the dominant factor in determining the bolt stress.

The resultant bolt load is: $F_b = P_b + F_i = 6.3 + 222.2 = 228.5$ kN

The resultant load on members is: $F_m = P_m - F_i = 15.5 - 222.2 = -206.7$ kN

The maximum bolt tensile stress, $\sigma_{tensile}$, is:

$$\sigma_{tensile} = \frac{F_b}{A_d} = \frac{228.5\ \text{kN}}{7.069 \times 10^{-4}\ \text{m}^2} \times 10^{-3}\ \frac{\text{MPa}}{\text{kPa}} = 323.2\ \text{MPa}$$

The residual bolt torque is: $T_r = 0.5(T) = 800$ N-m

The residual bolt torsion stress, τ_r, is:

$$\tau_r = \frac{T_r d_s}{\pi(d_s/2)^4} = \frac{(800\ \text{N-m})\ (0.030\ \text{m})}{\pi(0.030\ \text{m}/2)^4} \times 10^{-6}\ \frac{\text{MPa}}{\text{Pa}} = 150.9\ \text{MPa}$$

The stress intensity, SI, is:

$$SI = \sqrt{\sigma_{tensile}^2 + 4\tau_r^2} = \sqrt{(323.2\ \text{MPa})^2 + 4(150.9\ \text{MPa})^2} = 442.2\ \text{MPa}$$

The margin of safety for tensile stress using the allowable of $(2/3)S_y$ at 21°C is:

$$MS = \frac{(2/3)S_y}{\sigma_{tensile}} - 1.0 = \frac{2/3\,(724)}{323.2} - 1.0 = +0.49$$

The margin of safety for tensile-plus-residual torsion using the allowable of $1.35*(2/3)S_y$ at 21°C is:

$$MS = \frac{1.35(2/3)S_y}{SI} - 1.0 = \frac{652}{442.2} - 1.0 = +0.47$$

Bolt Calculations at -40 °C

Assuming that the bolts are installed and pretensioned at a temperature of 21 °C, the remaining preload under cold (-40 °C) conditions is evaluated as follows. The required mechanical and physical properties are given in the table below.

Elastic modulus of bolt, $E_{b\text{-}40}$, at -40 °C	19.5×10^4 MPa
Coefficient of thermal expansion of bolt, $\alpha_{b\text{-}40}$, at -40 °C	10.8×10^{-6} mm/mm/°C
Coefficient of thermal expansion of clamped material (UNS S31803), $\alpha_{ss\text{-}40}$, at -40 °C	11.9×10^{-6} mm/mm/°C

The initial preload bolt displacement, δ_I, is:

$$\delta_1 = \frac{F_i L}{A_d E_b} = \frac{(222.2\times10^3\ \text{N})(0.155\ \text{m})}{(7.069\times10^{-4}\ \text{m}^2)(19.2\times10^{10}\ \text{Pa})} = 2.54\times10^{-4}\ \text{m}$$

The change in bolt length due to the temperature change is:

$$\delta_{t1} = \alpha_{b\text{-}40} L\ (-40 - 21) = (10.8 \times 10^{-6}\ \text{m/m/°C})\ (0.155\ \text{m})\ (-40\ °\text{C} - 21\ °\text{C}) = -1.02 \times 10^{-4}\ \text{m}$$

The change in closure lid height due to the temperature change is:

$$\delta_{t2} = \alpha_{ss\text{-}40} L\ (-40 - 21) = (11.9 \times 10^{-6}\ \text{m/m/°C})\ (0.155\ \text{m})\ (-40\ °\text{C} - 21\ °\text{C}) = -1.13 \times 10^{-4}\ \text{m}$$

The net change in displacement between the bolt and the closure lid is:

$$\delta_{net} = \delta_{t2} - \delta_{t1} = (-1.13 \times 10^{-4}\ \text{m}) - (-1.02 \times 10^{-4}\ \text{m}) = -1.10 \times 10^{-5}\ \text{m}$$

The decrease in initial preload bolt displacement from the temperature change is:

$$\delta_2 = \delta_1 + \delta_{net} = (2.54 \times 10^{-4}\ \text{m}) + (-1.10 \times 10^{-5}\ \text{m}) = 2.43 \times 10^{-4}\ \text{m}$$

The remaining bolt preload at -40 °C is:

$$F_{ri} = \frac{\delta_2 A_d E_{b\text{-}40}}{L} = \frac{(2.43\times10^{-4}\ \text{m})(7.069\times10^{-4}\ \text{m}^2)(19.5\times10^{10}\ \text{Pa})}{(0.155\ \text{m})} \times 10^{-3}\ \frac{\text{kN}}{\text{N}} = 216.1\ \text{kN}$$

$$\text{Percent Reduction} = \frac{F_{ri} - F_i}{F_i} \times 100 = \frac{(216.1\ \text{kN}) - (222.2\ \text{kN})}{(222.2\ \text{kN})} \times 100 = -2.7\%$$

This small reduction in preload force at -40 °C may be neglected.

Bolt Calculations at 71 °C

Assuming that the bolts are installed and pretensioned at a temperature of 21 °C, the effects of NCT hot (71 °C) conditions are evaluated as follows. The required mechanical and physical properties are given in the table below.

Elastic modulus of bolt, E_{b71}, at 71 °C	18.8×10^4 MPa
Coefficient of thermal expansion of bolt, α_{b71}, at 71 °C	11.9×10^{-6} mm/mm/°C
Coefficient of thermal expansion of clamped material (UNS S31803), α_{ss71}, at 71 °C	13.0×10^{-6} mm/mm/°C

The change in bolt length due to the temperature change is:

$$\delta_{t1} = \alpha_{b71} L (71 - 21) = (11.9 \times 10^{-6} \text{ m/m/°C}) (0.155 \text{ m}) (71 \text{ °C} - 21 \text{ °C}) = 9.22 \times 10^{-5} \text{ m}$$

The change in closure lid height due to the temperature change is:

$$\delta_{t2} = \alpha_{ss71} L (71 - 21) = (13.0 \times 10^{-6} \text{ m/m/°C}) (0.155 \text{ m}) (71 \text{ °C} - 21 \text{ °C}) = 1.01 \times 10^{-4} \text{ m}$$

The net change in displacement between the bolt and the closure lid boss is:

$$\delta_{net} = \delta_{t2} - \delta_{t1} = (1.01 \times 10^{-4} \text{ m}) - (9.22 \times 10^{-5} \text{ m}) = 8.80 \times 10^{-6} \text{ m}$$

The increase in initial preload bolt displacement from the temperature change is:

$$\delta_2 = \delta_1 + \delta_{net} = (2.54 \times 10^{-4} \text{ m}) + (8.80 \times 10^{-6} \text{ m}) = 2.63 \times 10^{-4} \text{ m}$$

The increased bolt preload at 71 °C is:

$$F_{ii} = \frac{\delta_2 A_d E_{b71}}{L} = \frac{(2.63\times10^{-4}\text{ m})(7.069\times10^{-4}\text{ m}^2)(18.8\times10^{10}\text{ Pa})}{(0.155\text{ m})}\times10^{-3}\frac{\text{kN}}{\text{N}} = 225.5\text{ kN}$$

$$\text{Percent Increase} = \frac{F_{ii} - F_i}{F_i}\times100 = \frac{(225.5\text{ kN}) - (222.2\text{ kN})}{(222.2\text{ kN})}\times100 = 1.5\%$$

The resultant bolt load is: $F_{b71} = P_b + F_{ii} = 6.3 + 225.5 = 231.8$ kN

(Note: the slight change in P_b due to changes in bolt and joint stiffness which result from the temperature difference between 21 °C and 71 °C is negligible.) The maximum bolt tensile stress, $\sigma_{tensile}$, is:

$$\sigma_{tensile} = \frac{F_{b71}}{A_d} = \frac{231.8\text{ kN}}{7.069\times10^{-4}\text{ m}^2}\times10^{-3}\frac{\text{MPa}}{\text{kPa}} = 327.9\text{ MPa}$$

From above, the residual bolt torsion stress, $\tau_r = 150.9$ MPa. The stress intensity, SI, is:

$$SI = \sqrt{\sigma_{tensile}^2 + 4\tau_r^2} = \sqrt{(327.9\text{ MPa})^2 + 4(150.9\text{ MPa})^2} = 445.6\text{ MPa}$$

The margin of safety for tensile stress using the allowable of $(2/3)S_y$ at 71°C is:

$$MS = \frac{(2/3)S_y}{\sigma_{tensile}} - 1.0 = \frac{2/3(699)}{327.9} - 1.0 = +0.42$$

The margin of safety for tensile-plus-residual torsion using the allowable of $1.35*(2/3)S_y$ at 71°C is:

$$MS = \frac{1.35(2/3)S_y}{SI} - 1.0 = \frac{1.35(2/3)(699)}{445.6} - 1.0 = +0.41$$

Internal Thread Evaluation

The internal thread stripping area,[7] A_{in}, per engagement length of the M36 × 4 threads is 84.1 mm²/mm. With a thread engagement length, L_t, of 50 mm, the shear stress of the internal closure bolt threads, $\tau_{int\ threads}$, is then:

[7] Industrial Fasteners Institute, *Manufacturer's Capability Guide*, Table 2, 1986, Cleveland, Ohio.

$$\tau_{\text{int threads}} = \frac{F_{b71}}{A_{in}L_t} = \frac{(231.8\text{ kN})}{(0.0841\text{ m}^2/\text{m})(0.050\text{ m})} \times 10^{-3}\ \frac{\text{MPa}}{\text{kPa}} = 55.1\text{ MPa}$$

The allowable stress for the Alloy UNS S31803 boss material is $0.6S_m$. Therefore, the margin of safety for the internal threaded material is:

$$MS_{\text{shear}} = \frac{0.6S_m}{\tau_{\text{int threads}}} - 1.0 = \frac{0.6(207)}{55.1} - 1.0 = +1.25$$

The optional alloy steel thread insert has material strength properties equal to or greater than the Alloy UNS S31803 material. Therefore, the shear stress for thread insert is bounded by the base material.

The maximum stresses and minimum margins of safety for each closure bolt load case are summarized in Table 2.6-3. Since all margins of safety are positive, the design criteria are satisfied.

Table 2.6-3 – Summary of Closure Lid Bolt and Thread Analysis

Condition	Stress, MPa	Allowable Stress	Margin of Safety
Tensile stress at 21 °C	323.2	$(2/3)S_y = 482.7$	+0.49
Tensile plus residual torsion stress at 21 °C	442.2	$1.35(2/3)S_y = 651.6$	+0.47
Tensile stress at 71 °C	327.9	$(2/3)S_y = 466$	+0.42
Tensile plus residual torsion stress at 71 °C	445.6	$1.35(2/3)S_y = 629.1$	+0.41
Internal Thread Shear Stress (UNS S31803)	55.1	$0.6S_m = 124.2$	+1.25

2.6.2 Cold

For the NCT cold condition, a -40 °C steady state ambient temperature is utilized per 10 CFR §71.71(c)(2), with zero insulation and zero decay heat. This results in a uniform temperature of -40 °C throughout the package. With no internal heat load (i.e., no contents to produce heat and, therefore, pressure), the net pressure differential is assumed to be zero (101 kPa absolute internal, 101 kPa absolute external). The materials of construction for the TRUPACT–III packaging are not adversely affected by the -40 °C condition.

Brittle fracture at -40 °C is addressed in Section 2.1.2.2.1, *Brittle Fracture*. Performance of the O-ring seals at -40 °C is discussed in Appendix 2.12.2, *Elastomer O-ring Seal Performance Tests*.

The closure bolts are fabricated of ASTM A320, Grade L43 having a coefficient of thermal expansion which is lower than that of the cask body and closure lid bosses, as presented in Section 2.2.1, *Material Properties and Specifications*. Therefore, under cold conditions, the initial bolt preload force is reduced below the value at room temperature. However, a significant positive preload force remains, and bolt stresses developed are well within allowable limits, as described above in Section 2.6.1.6, *Closure Bolts*. The minimum bolt preload force under cold conditions is 216.1 kN per bolt. This force is only 2.7% less than the installation preload and is more than adequate to compress the elastomer O-ring seals.

2.6.3 Reduced External Pressure

The effect of a reduced external pressure of 25 kPa absolute, per 10 CFR §71.71(c)(3), is negligible for the TRUPACT–III packaging. This conclusion is based on the analyses presented in Section 2.6.1, *Heat*, addressing the ability of the CSA to independently withstand a maximum normal operating pressure (MNOP) of 172 kPa gauge internal pressure at the same reduced external pressure, equivalent to a 248 kPa gauge internal pressure.

2.6.4 Increased External Pressure

The effect of an increased external pressure of 140 kPa absolute (39 kPa gauge external pressure), per 10 CFR §71.71(c)(4), is negligible for the TRUPACT–III packaging. The external pressure induces small compressive stresses in the containment boundary that are limited by stability (buckling) requirements. The bounding buckling case is in fact the HAC load case of immersion under 15 meters head of water, which corresponds to an external gauge pressure of 150 kPa. From Appendix 2.12.4, *HAC Immersion Buckling Evaluation*, using the greater HAC external gauge pressure, the combined stress in the critical sidewall is 88.7 MPa, and the allowable inelastic buckling load is 391 MPa. The factor of safety against buckling is:

$$FS = \frac{(\sigma_{cr})_x}{\sigma} = \frac{391}{88.7} = 4.41$$

This is considerably in excess of the minimum factor of safety of 2.0 for NCT per ASME Code Case N-284-1, corresponding to ASME Code, Service Level A conditions. Note that the factor of safety requirement for NCT is easily met using the HAC pressure, which is 150/39 = 3.8 times larger than the required pressure. Therefore, the NCT external pressure of 39 kPa gauge is not of concern. Details of the analysis are given in Appendix 2.12.4, *HAC Immersion Buckling Evaluation*. Of note, the containment vessel is designed to withstand a full vacuum equivalent to 101 kPa external pressure during acceptance leakage rate testing of the TRUPACT–III package, as described in Section 8.1.4, *Fabrication Leakage Rate Tests*.

2.6.5 Vibration

By comparing the alternating stresses arising during NCT with the established endurance limits of the TRUPACT–III packaging materials of construction, the effects of vibration normally incident to transport are shown to be acceptable. By conservatively comparing NCT stresses with endurance stress limits for an infinite service life, the development of accurate vibratory loading cycles is not required.

ANSI N14.23[8] provides a basis for estimating peak truck trailer vibration inputs. A summary of peak vibratory accelerations for a truck semi-trailer bed with light loads (less than 15 tons) is provided in Table 2 of ANSI N14.23. The component accelerations are given in Table 2 as 1.3*g* longitudinally, 0.5*g* laterally, and 2.0*g* vertically. A fully loaded TRUPACT–III package on a single trailer will exceed the light load limit, but acceleration magnitudes associated with light loads are conservative for heavy loads per Table 2 of ANSI N14.23. The commentary provided within Section 4.2, *Package*

[8] ANSI N14.23, *Design Basis for Resistance to Shock and Vibration of Radioactive Material Packages Greater than One Ton in Truck Transport* (Draft), 1980, American National Standards Institute, Inc, (ANSI).

Response, of ANSI N14.23 states that recent "*...tests conducted by Sandia National Laboratories have shown that the truck bed accelerations provide an upper bound on cask (response) accelerations.*" Based upon these data, conservatively assume the peak acceleration values from Table 2 are applied to the TRUPACT–III package in a continuously cycling fashion.

As described in Section 2.5.2, *Tie-down Devices*, the TRUPACT-III is supported during transport by structural pockets on the conveyance in the vicinity of the four lower ISO fittings. Lifting the package by the upper ISO fittings is structurally equivalent to supporting the package by the bottom ISO fittings. Only the magnitude of loading is different. As shown in Section 2.5.1, *Lifting Devices*, the shear stress in the lifting arm (i.e., cheek) attachment welds, for a lifting load of 3g, is 49.4 MPa. Scaling the stress for a 2g vertical acceleration gives a shear stress of (2/3) × 49.4 = 32.9 MPa. In calculating this stress, a conservative assumption was made that only two of the four lifting arms actually support any load. Since the package weight during transport is supported by a relatively lightweight and therefore structurally compliant trailer, a uniform load distribution on all four ISO fittings may be reasonably assumed. Therefore the stress in the attachment weld will be half as much as calculated above, so that the stress in transport is 32.9/2 = 16.5 MPa. Including a stress concentration factor of 4 as described in ASME B&PV Code, Subsection NB-3232.3, gives an adjusted shear stress of 16.5 × 4 = 66 MPa. As calculated below in this section, the temperature-adjusted fatigue value for 10^6 cycles in shear is $\tau_{fatigue}$ = 115.2 MPa. The margin of safety is:

$$MS = \frac{115.2}{66} - 1 = +0.75$$

Therefore, the TRUPACT-III lifting arms do not exhibit any fatigue limitations resulting from normal transportation vibration.

The bottom wall of the CSA supports the payload in normal transport and may be subject to vibration. The vibration analysis is performed by calculating the stress in the wall (i.e., the CSA floor) assuming an upper bound mass for the wall and including the mass of the payload, under the action of a 2g inertia force. The total inertia load on the wall is then analyzed as an applied pressure. For conservatism, the wall is assumed to be simply supported on all four edges. The length of the wall, which is conservatively assumed to extend from the center of the rear wall to the bolted seal flange, is L = 2,860 mm. The width, which extends to the centers of the side walls, is W = 1,980 mm. The wall self-mass is very conservatively assumed to be equal to one quarter of *total* empty packaging mass.

Calculation Input Parameters

Bottom containment wall self-mass: $M_1 = 19{,}825/4 = 4{,}956$ kg

Payload mass: $M_2 = 5{,}175$ kg

The total pressure distributed over the wall (including 2g factor):

$$P = 2g\left[\frac{M_1 + M_2}{LW}\right] = 2 \times (9.81\ m/s^2)\left[\frac{(4{,}956\ kg) + (5{,}175\ kg)}{(2.860\ m) \times (1.980\ m)}\right] \times 10^{-3}\ \frac{kPa}{Pa} = 35\ kPa$$

Thickness of inner and outer sheets: $t = 8$ mm $= 0.008$ m

Distance between inner & outer sheet centroids: $d = 132$ mm $= 0.132$ m

Area of one face sheet per unit width: $A = 1 \times 10^{-6}\ (t) = 8 \times 10^{-6}$ m

Outer fiber distance: $c_o = \frac{d+t}{2} = 70\text{ mm} = 0.070\text{ m}$

Area moment of inertia (see Section 2.6.1.3): $I_1 = 6.97 \times 10^{-8}\text{ m}^4$

Bottom Containment Wall Fatigue Evaluation

The maximum moment in the wall, assuming pinned edges, is:

$$M_{max_1} = \frac{PbW^2}{8} = \frac{(35\text{ kPa})(0.001\text{ m})(1.98\text{ m})^2}{8} \times 10^3 \frac{\text{Pa}}{\text{kPa}} = 17.15\text{ N-m}$$

The maximum global bending stress, σ_{gbx}, is:

$$\sigma_{gbx} = \frac{M_{max_1} c_o}{I_1} = \frac{(17.15\text{ N-m})(0.070\text{ m})}{(6.97\times10^{-8}\text{ m}^4)} \times 10^{-6} \frac{\text{MPa}}{\text{Pa}} = 17.2\text{ MPa}$$

The local bending stress in the region between the V-stiffeners will next be considered. The unsupported span of the wall between V-stiffeners is S = 145 mm. The area moment of inertia for the wall inner sheet is:

$$I_2 = \frac{bt^3}{12} = \frac{(0.001\text{ m})(0.008\text{ m})^3}{12} = 4.267\times10^{-11}\text{ m}^4$$

The maximum local moment, again assuming pinned edges at the V-stiffeners, is:

$$M_{max_2} = \frac{PbS^2}{8} = \frac{(35\text{ kPa})(0.001\text{ m})(0.145\text{ m})^2}{8} \times 10^3 \frac{\text{Pa}}{\text{kPa}} = 0.092\text{ N-m}$$

The maximum local bending stress is:

$$\sigma_{lby} = \frac{(0.008\text{ m}/2)(0.092\text{ N}-\text{m})}{(4.267\times10^{-11}\text{ m}^4)} \times 10^{-6} \frac{\text{MPa}}{\text{Pa}} = 8.6\text{ MPa}$$

The maximum primary membrane-plus-bending stress intensity is:

$$SI_{pmb} = \sigma_{gbx} + \sigma_{lby} = 17.2 + 8.6 = 25.8\text{ MPa}$$

The fatigue allowable stress for Alloy UNS S31803 stainless steel corresponding to 1.0×10^6 cycles is 195 MPa, per Table I-9.1M for Figure I-9.2.1 of the ASME Code. The fatigue allowable is then factored by the ratio of the modulus of elasticity at 21 °C and 71 °C to adjust for service at temperature, where $E_{21} = 19.5 \times 10^4$ MPa is the modulus at 21 °C and $E_{71} = 19.2 \times 10^4$ MPa is the modulus at 71 °C:

$$\sigma_{fatigue} = \frac{E_{71}}{E_{21}}(195) = \frac{19.2\times10^4}{19.5\times10^4}(195) = 192\text{ MPa}$$

The maximum stress intensity is increased by a stress concentration factor of 4 in accordance with ASME B&PV Code, Subsection NB 3232.3.

$$\sigma_{factored} = 4SI_{pmb} = 4 \times 25.8\text{ MPa} = 103.2\text{ MPa}$$

The maximum factored stress of 103.2 MPa is less than the fatigue allowable of 192 MPa at a service temperature of 71 °C. The margin of safety is:

$$MS = \frac{\sigma_{fatigue}}{\sigma_{factored}} - 1.0 = \frac{192}{103.2} - 1.0 = +0.86$$

Therefore, the bottom containment wall does not exhibit any fatigue limitations resulting from normal transportation vibration.

Bottom Containment Wall Weld Fatigue Evaluation

The V-stiffeners are attached to the inner containment sheet by continuous skewed fillet welds, which have an equivalent throat thickness of 4 mm. The V-stiffeners are attached to the outer structural sheet by a series of 20-mm diameter plug welds. As shown below, the equivalent shear width of the plug welds is 5.9 mm, and therefore, this shear width is bounding compared to the inner sheet welds that have a combined effective throat of 2 × 4 = 8 mm. The calculation parameters are:

Number of plug welds per V-stiffener: N = 40

Diameter of plug welds, D: D = 20 mm = 0.020 m

V-stiffener length, L: L = 2,120 mm = 2.120 m
(conservatively equal to the full width of the CSA)

Distance between plug weld rows, d_p: d_p = 164 mm = 0.164 m

The equivalent plug weld shear width, t_e, per V-stiffener is:

$$t_e = \frac{(\pi/4)\, D^2\, N}{L} = \frac{(\pi/4)\,(0.020\ \text{m})^2\,(40)}{(2.120\ \text{m})} = 0.0059\ \text{m}$$

The equivalent plug weld shear width, t_{eb}, per unit width is:

$$t_{eb} = \frac{t_e b}{164\ \text{mm}} = \frac{(0.0059\ \text{m})\,(0.001\ \text{m})}{(0.164\ \text{m})} = 3.60 \times 10^{-5}\ \text{m}$$

The weld shear force, V, is:

$$V = \tfrac{1}{2}P(b)(W) = \tfrac{1}{2}(35\ \text{kPa})(0.001\ \text{m})(1.980\ \text{m}) = 34.7\ \text{N}$$

The plug weld shear stress, $\tau_{plug\ weld}$, is:

$$\tau_{plug\ weld} = \frac{VQ}{I_1 t_{eb}} = \frac{(34.7\ \text{N})(5.28\times10^{-7}\ \text{m}^3)}{(6.97\times10^{-8}\ \text{m}^4)(3.60\times10^{-5}\ \text{m})} \times 10^{-6}\ \frac{\text{MPa}}{\text{Pa}} = 7.30\ \text{MPa}$$

where: d = 132 mm t = 8 mm b = 1 mm

$I_1 = 6.97 \times 10^{-8}\ \text{m}^4$ $Q = (\tfrac{1}{2}d)(t)(b) = 5.28 \times 10^{-7}\ \text{m}^3$

As determined above, the fatigue allowable stress for Alloy UNS S31803 stainless steel at 71°C is 192 MPa. Factoring this value for 0.6 for shear loading, the shear fatigue allowable is:

$$\tau_{fatigue} = 0.6(192) = 115.2\ \text{MPa}$$

The maximum stress is increased by a stress concentration factor of 4 in accordance with ASME B&PV Code, Subsection NB 3232.3.

$$\tau_{factored} = 4\tau_{plug\ weld} = 4(7.30\ \text{MPa}) = 29.2\ \text{MPa}$$

The maximum factored stress of 29.2 MPa is less than the fatigue allowable of 115.2 MPa at a service temperature of 71 °C. The margin of safety is:

$$MS = \frac{\tau_{fatigue}}{\tau_{factored}} - 1.0 = \frac{115.2}{29.2} - 1.0 = +2.95$$

Therefore, the bottom containment wall plug welds do not exhibit any fatigue limitations resulting from transportation vibration.

2.6.6 Water Spray

The materials of construction utilized for the TRUPACT–III package are such that the water spray test identified in 10 CFR §71.71(c)(6) will have a negligible effect on the package.

2.6.7 Free Drop

10 CFR §71.71(c)(7) requires a NCT free drop from a height of 0.3 m for packages weighing more than 15,000 kg. The TRUPACT–III is designed to withstand the effects of a 9-m free drop while maintaining leaktight containment. The NCT free drop height of 0.3-m represents a potential energy at impact of only 3.3% of the HAC, 9-m free drop. A 0.3-m free drop was performed during full-scale certification testing of CTU-1, resulting in negligible visible damage to the test unit. This test was followed by four HAC, 9-m free drops. The structural performance of the TRUPACT–III was demonstrated to be acceptable as described in Section 2.7, *Hypothetical Accident Conditions*. Therefore, the requirements of 10 CFR §71.71(c)(7) are met.

2.6.8 Corner Drop

This test does not apply, since the package weight is in excess of 100 kg, as delineated in 10 CFR §71.71(c)(8).

2.6.9 Compression

This test does not apply, since the package weight is in excess of 5,000 kg, as delineated in 10 CFR §71.71(c)(9).

2.6.10 Penetration

The one meter drop of a 6 kilogram, hemispherically-headed, 3.2-cm diameter steel cylinder, as delineated in 10 CFR §71.71(c)(10), is of negligible consequence to the TRUPACT–III package. This conclusion is due to the fact that the TRUPACT–III package is designed to minimize the consequences associated with the much more limiting case of a one meter drop of the entire package onto a puncture bar as discussed in Section 2.7.3, *Puncture*. The 6-mm minimum thickness outer sheet is not damaged by the penetration event.

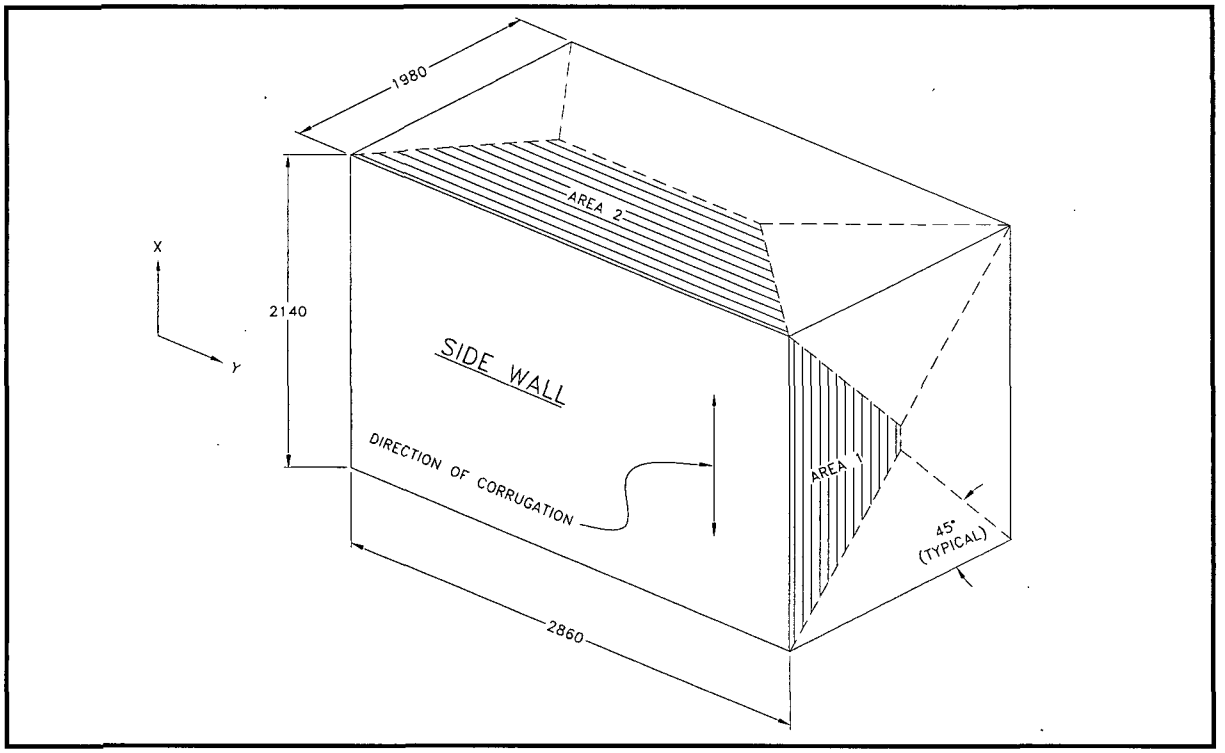

Figure 2.6-1(a) – View of Side Walls and Adjacent Walls, Showing Areas Used to Calculate Edge Loads for Side Walls

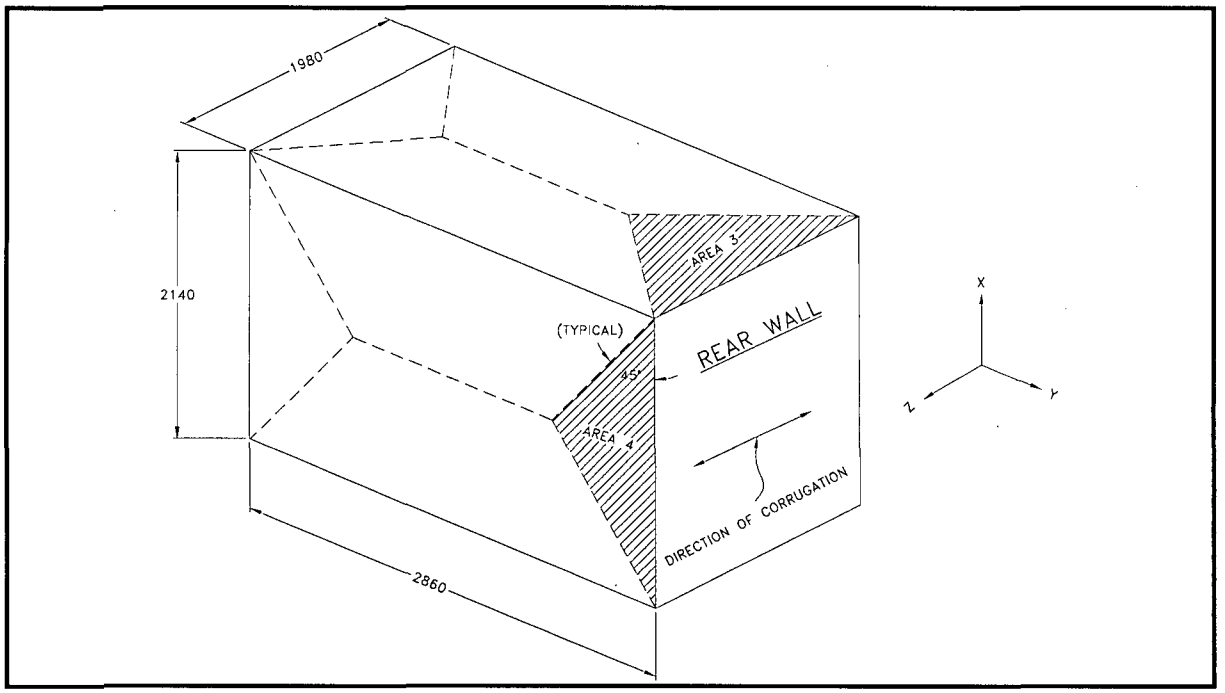

Figure 2.6-1(b) – View of Rear Wall and Adjacent Walls, Showing Areas Used to Calculate Edge Loads for the Rear Wall

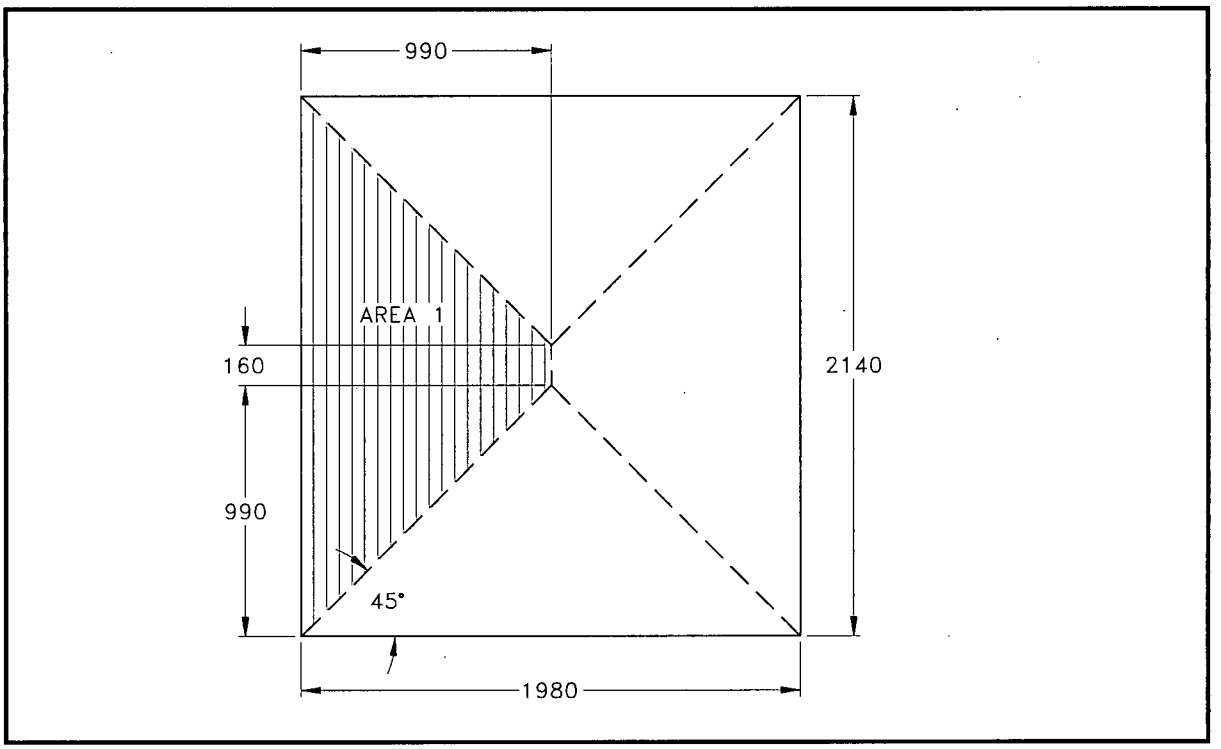

Figure 2.6-1(c) – View of Area 1 on End Wall Used to Calculate End Edge Load on Side Wall

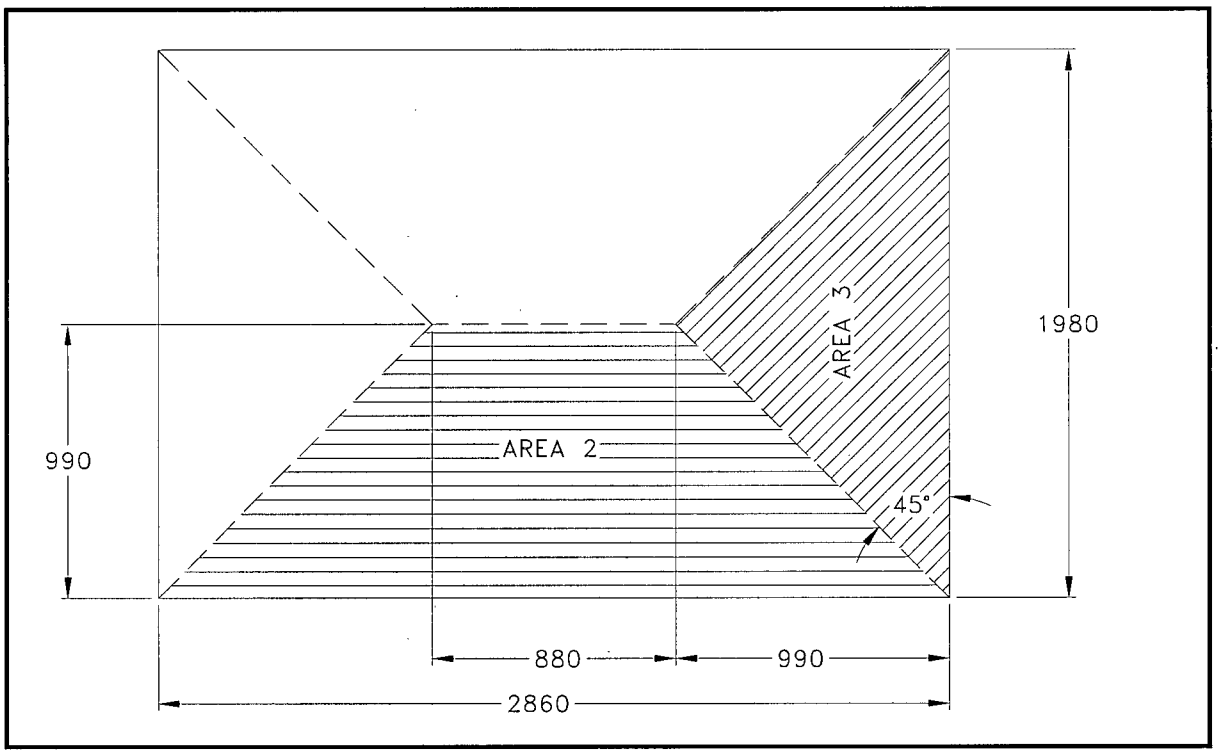

Figure 2.6-1(d) – View of Areas 2 & 3 on Top Wall Used to Calculate Edge Loads on Side & Rear Walls

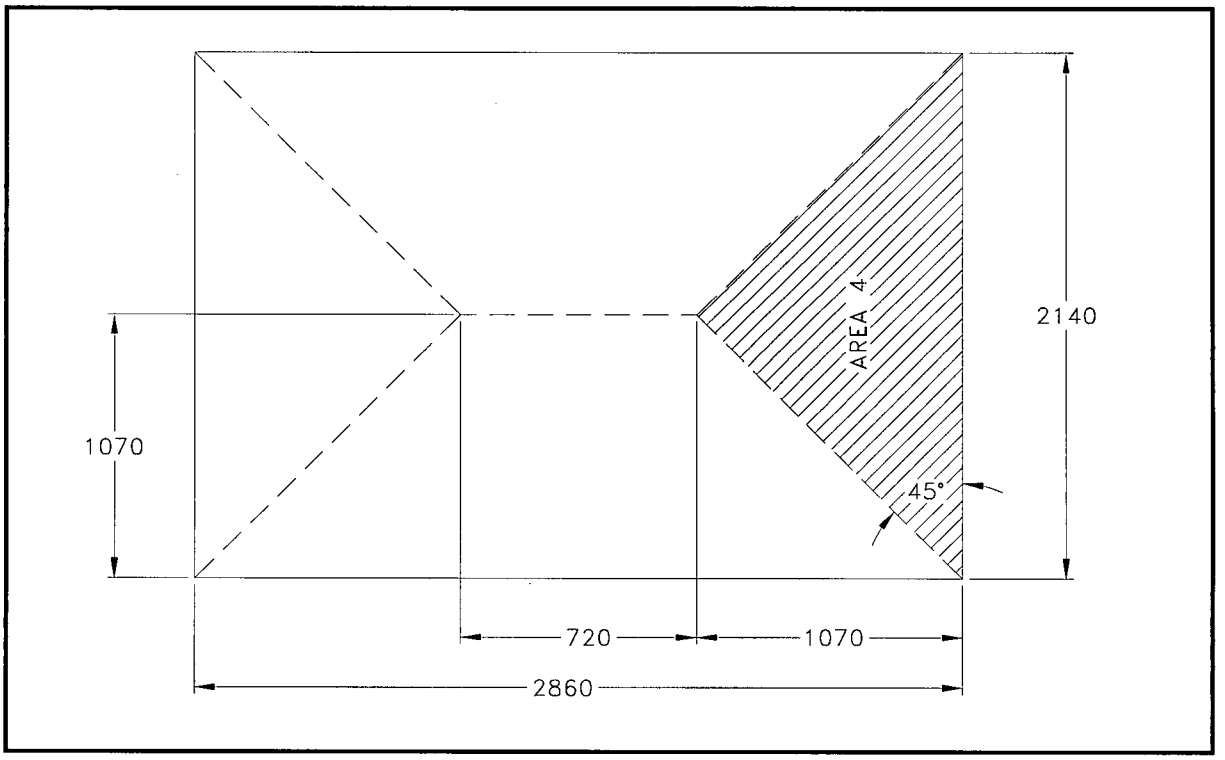

Figure 2.6-1(e) – View of Area 4 on Side Wall Used to Calculate Edge Load on Rear Wall

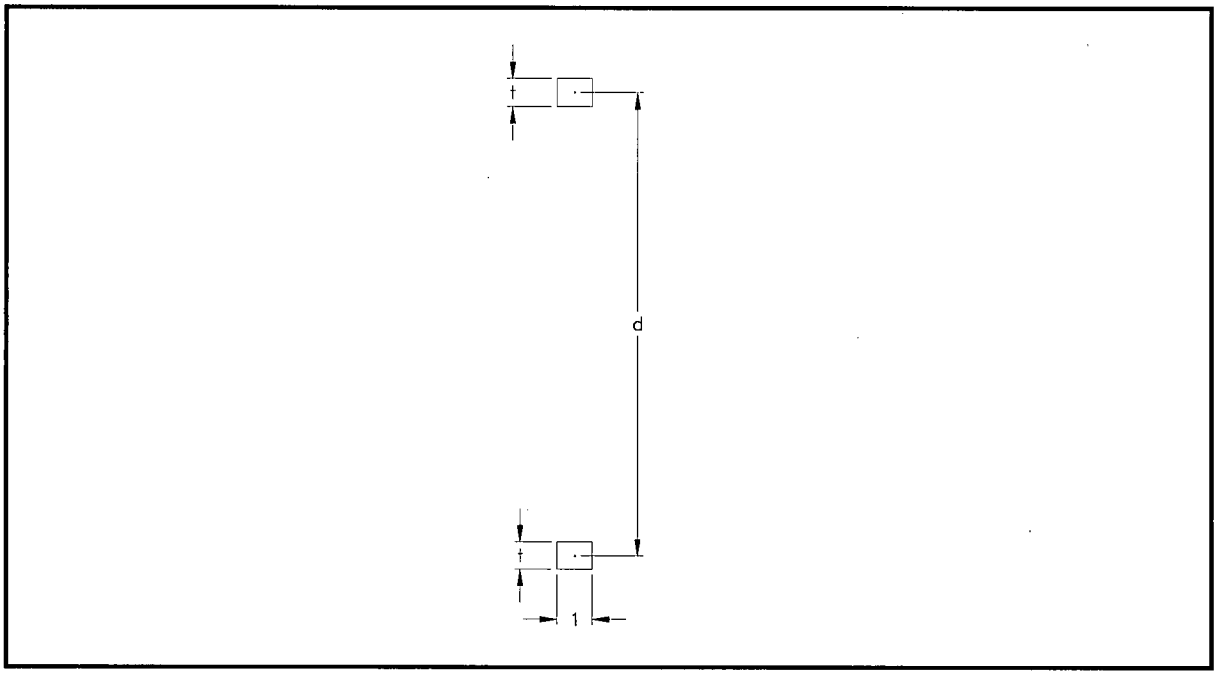

Figure 2.6-1(f) – Typical Wall Section for Global Bending and Membrane Analysis

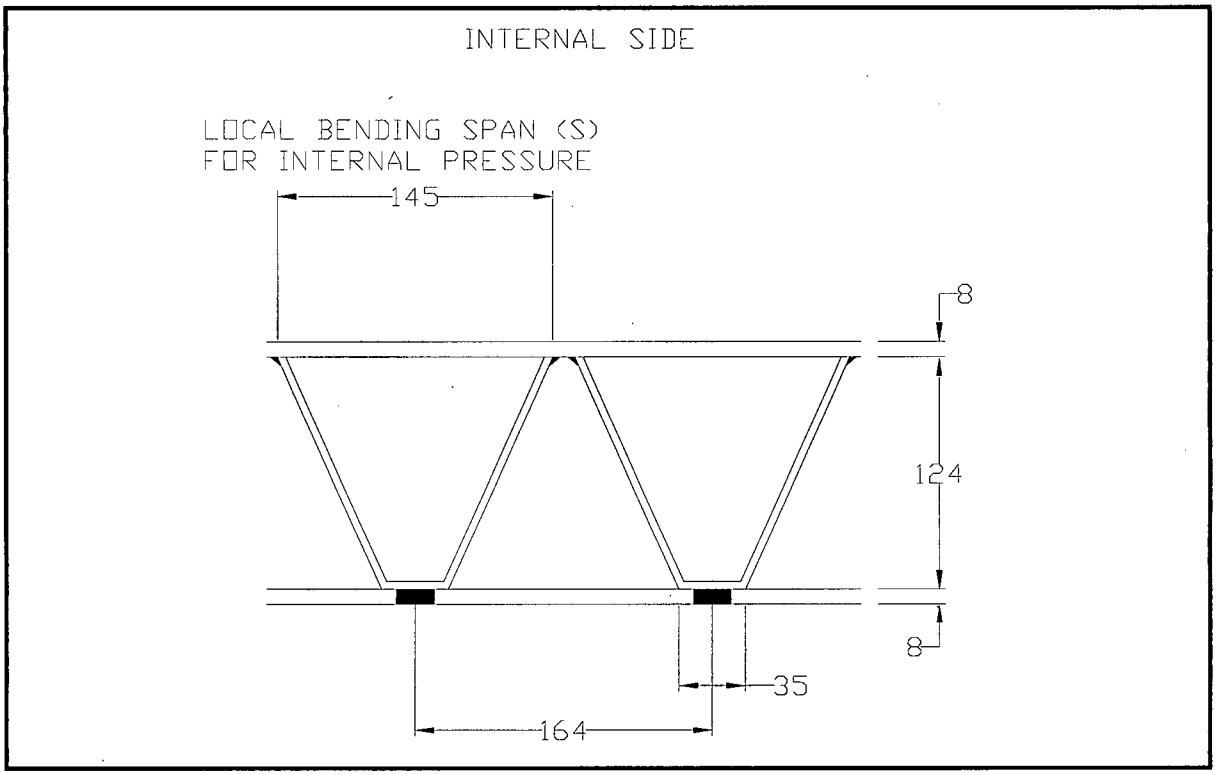

Figure 2.6-1(g) – Local Bending Spans for Side Wall

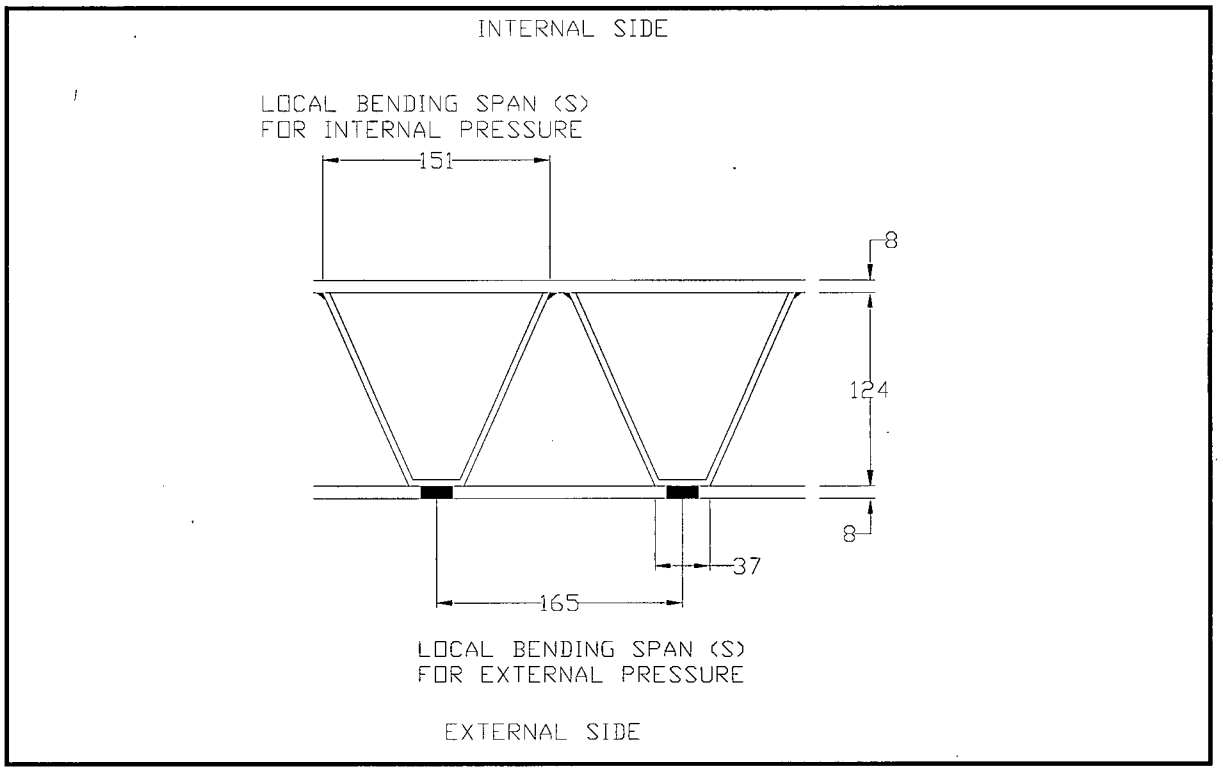

Figure 2.6-1(h) – Local Bending Spans for Rear Wall

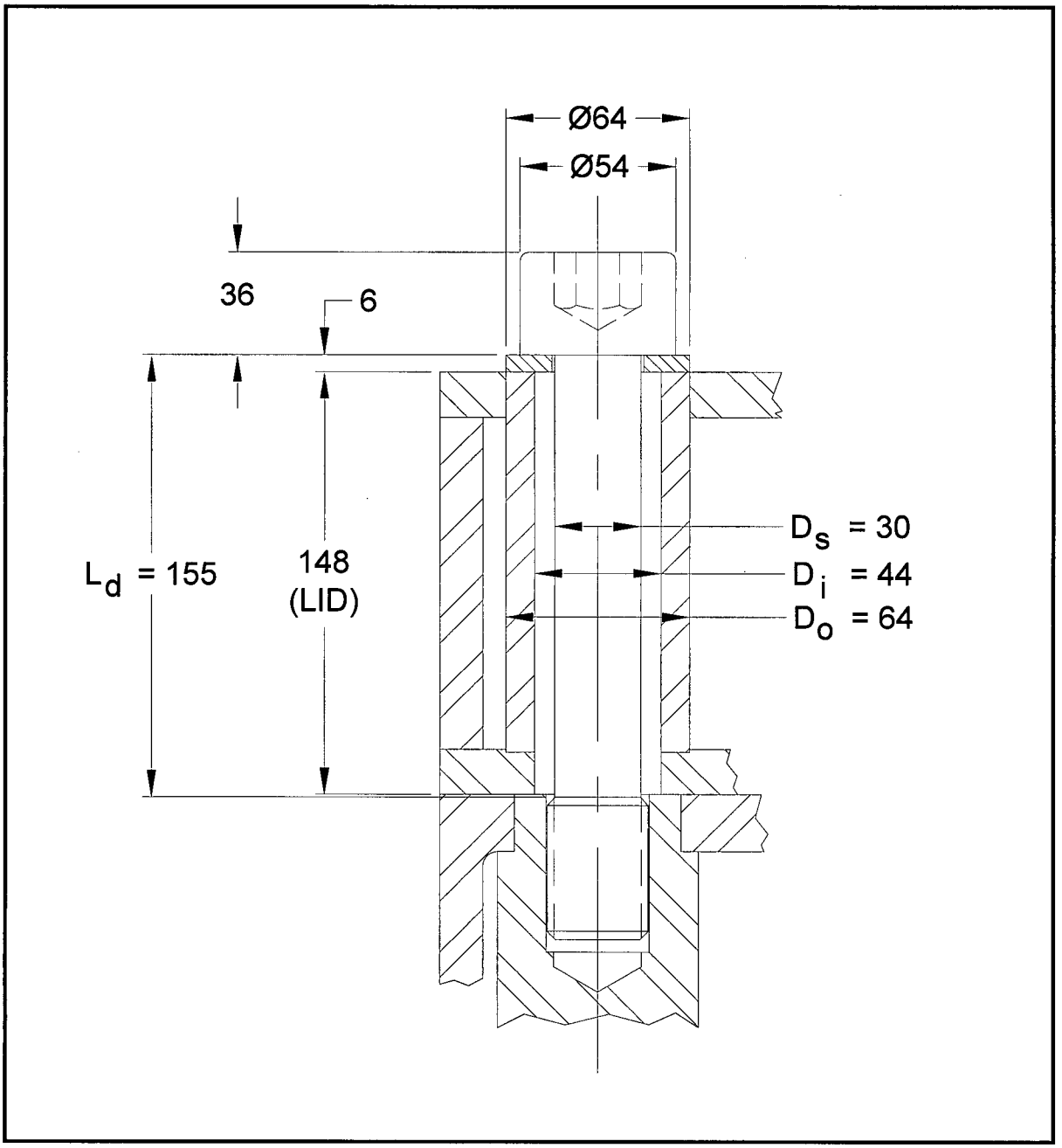

Figure 2.6-2 – Closure Bolt Analysis Parameters

This page intentionally left blank.

2.7 Hypothetical Accident Conditions

The TRUPACT–III package, when subjected to the sequence of hypothetical accident condition (HAC) tests specified in 10 CFR §71.73, subsequent to the sequence of normal conditions of transport (NCT) tests specified in 10 CFR §71.71, is shown to meet the performance requirements specified in Subpart E of 10 CFR 71[1]. Demonstration of compliance with the requirements is by a combination of test and analysis. Analysis is used for all NCT events except the free drop, and for the HAC thermal and immersion cases. Testing is used for the NCT & HAC free drop events, and for the HAC puncture drop event. Two full-scale certification test units (CTU-1 and CTU-2) were used for all test demonstrations. Test results are summarized in Section 2.7.8, *Summary of Damage*, with details provided in Appendix 2.12.3, *Certification Tests on CTU-1* and Appendix 2.12.6, *Certification Tests on CTU-2*. An analytical evaluation of the debris shield, which was included in CTU-2, is provided in Section 2.12.5, *Closure Lid Debris Shield*. A significant number of engineering tests using a half-scale prototype test unit were performed, as documented in Section 2.12.1, *Engineering Tests*.

2.7.1 Free Drop

Subpart F of 10 CFR 71 requires performing a free drop test in accordance with the requirements of 10 CFR §71.73(c)(1). The free drop test involves performing a 9-m free drop onto a flat, essentially unyielding, horizontal surface, with the package striking the surface in an orientation for which maximum damage is expected. The ability of the TRUPACT–III package to adequately withstand this specified free drop is demonstrated by testing of a full-scale CTU. A total of four, 9-m HAC free drops were performed on CTU-1, preceded by one, 0.3-m NCT free drop. One, 9-m HAC free drop was performed on CTU-2.

2.7.1.1 Technical Basis for the Free Drop Tests

In order to determine the worst-case free drop orientation, an exhaustive consideration of all uniquely different free drop orientations was made. Each was evaluated to determine if bounding forces, stresses, strains, or damage to the containment sealing area would occur. The criteria used to evaluate each free drop were based on the following considerations:

- Rupture of containment boundary
- Buckling of the CSA
- Excessive deformation in the containment sealing area (body and closure lid flanges)
- Separation of the closure lid from the body
- Separation of the overpack cover from the package
- Excessive compression, damage, or exposure of the overpack structures (e.g., foam or calcium silicate insulation).

[1] Title 10, Code of Federal Regulations, Part 71 (10 CFR 71), *Packaging and Transportation of Radioactive Material*, 01–01–09 Edition.

Of note, shielding integrity is not of concern since the payload is contact-handled transuranic waste. For the criticality analysis, deformations are conservatively bounded as shown in Section 6.0, *Criticality Evaluation.* All of the free drops considered are individually evaluated below.

Note: In the following, an *edge* is defined as a line where two sides meet at a right angle. A *corner* is defined as a point where three sides meet.

Drops on the Ends (Total of 12)

A. Flat end (package vertical). Total of two drops. Although the overpack construction is essentially the same at each end, the CSA construction is somewhat different.

B. Near vertical on each edge. Total of four drops, since each end has only two unique edges.

C. C.g.-over-end edges. Total of four drops, since each end has only two unique edges.

D. C.g.-over-each corner. Total of two drops, since there is one unique corner per end.

Drops on the Sides (Total of 9)

A. Flat side (package horizontal). Total of two drops, since there are only two unique sides.

B. On side edges (package horizontal). Total of one drop, since all four side-edges are identical.

C. Slapdown on flat side, lid primary. Total of two drops, since there are two unique sides.

D. Slapdown on flat side, lid secondary. Total of two drops, since there are two unique sides.

E. Slapdown on side-edge, lid primary. Total of one drop, since all side-edges are identical.

F. Slapdown on side-edge, lid secondary. Total of one drop, since all side-edges are identical.

Each drop orientation is evaluated to determine whether it is unique and whether it places bounding loads on the package, or represents bounding damage to the containment sealing area that could affect thermal performance. The result of all of these evaluations is summarized in Table 2.7-1 and illustrated in Figure 2.7-1. As documented in Section 2.12.1, *Engineering Tests*, many orientations have been tested in prior testing programs using a half-scale test article. The results of these tests provided a database of information which was used to guide the choice of bounding tests to be performed on the full-scale CTU. Tables 2.12.1-2 through 2.12.1-4 show the extent of previous testing using the half-scale article. The following detailed discussions justify the orientations chosen for certification testing. In the following small figures, a number in parentheses (e.g., *LD1*), indicates that the orientation has been specifically evaluated by full-scale certification testing as summarized in Table 2.7-1. All references in the following paragraphs to prior testing are discussed in more detail in Section 2.12.1, *Engineering Tests.* The test performed on CTU-2 is discussed in Section 2.7.1.1.3, *Free Drop Test on CTU-2.*

2.7.1.1.1 Drops on the Ends

A. Flat End Free Drops (Package Vertical). The overpack construction at each end is essentially identical, and therefore the impacts are considered identical at each end. However, the CSA structure is different at each end: the closed end has 8 mm plates and is continuously connected to the sides, whereas the lid has 12 mm plates and is connected to the sides by closure bolts.

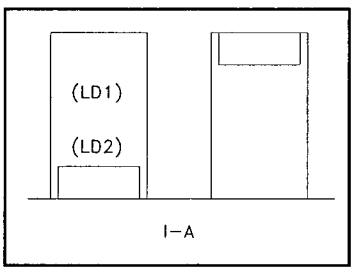

Consequently, the closed end structure is a plate with essentially fixed edges and the lid is a plate which is essentially simply supported. Under a distributed load (such as the payload in a vertical drop), the bending stress at the edges of the closed end is about 50% greater than at the center of the lid. However, the lid flange may rotate and affect the ability of the containment seal to remain leaktight. From these considerations, it is not obvious whether the lid down or closed end down drops would present a bounding case. The lid end down orientation places the greatest loads on the lid structure and on the closure, potentially deforming the sealing area; the closed end down potentially creates bounding stresses in the containment boundary.

During the certification testing of the TN–Gemini in France in 1994, the half-scale test article was dropped 9 m on the closed end with an equivalent full scale impact of 179g. No damage or deformation was noted in the closed end region of the CSA after this, and several subsequent tests. Since the construction of the CSA of the TRUPACT–III package is essentially identical to that of the TN-Gemini, and since the maximum end drop impact of the TRUPACT–III package was of a similar magnitude at 204g, it was not necessary to test the closed end down orientation. The robust nature of the TRUPACT–III package closed end has been adequately demonstrated in the half-scale test. But since the lid end down orientation places the greatest loads on the lid structure and closure, the TRUPACT–III package was tested in a lid-down orientation under maximum-impact (cold) conditions in both the NCT (0.3-m) and HAC (9-m) free drop configurations.

B. Near-Vertical End Free Drops. The impact magnitude drops off rapidly with the off-vertical angle of impact, and consequently the near-vertical impact will be much less than the vertical impact. This was demonstrated in the half-scale tests described in Section 2.12.1.7.2.1, *Free Drop Test No. FD1* and Section 2.12.1.7.2.3, *Free Drop Test No. FD3*. In the bottom-down end drop, the impact occurred at an angle of approximately 6° - 7° from the vertical, with an equivalent full scale impact of 109g. An equivalent impact under the same conditions on the opposite end of the article, in which the orientation was essentially perfectly vertical, and where the impact absorbing structures were essentially identical, was 327g, or three times higher. Therefore, near-vertical impacts have a significantly lower magnitude compared to vertical. Also, since the lid is supported by the overpack cover only in the vicinity of its four corners, it will still be left unsupported near the middle of its four sides, even in a pure vertical drop. Finite element analyses show that the deflections of the lid will be greatest at the middle of the sides. In other words, whether the package orientation is vertical or near vertical, the most vulnerable areas of the closure and sealing structures are unsupported by impact absorbing structures. Therefore, since the forces driving seal area deformation fall off rapidly, even for small off-vertical angles, but the vulnerability of the closure structures are essentially unchanged, the near-vertical end free drops are not bounding and do not need to be performed.

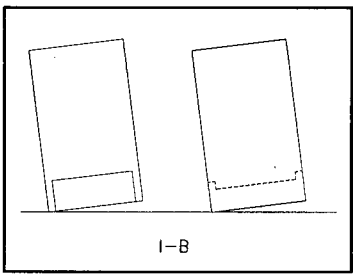
I–B

C. C.g.-Over-End Edges. These orientations provide neither maximum component loading nor maximum seal area stress, as discussed in the section above. Further, the thermally-relevant crush in the seal area is less than the softer corner case discussed below.

If dropped on one edge of the cover, an "overturning moment" might be applied to the cover attachments. However, since the

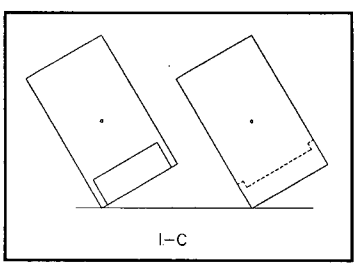
I–C

cover is relatively soft, allowing the crush to be localized, there is no risk of sufficient load transfer to the opposite side so as to fail the cover attachment bolts. This condition was demonstrated in the certification testing described in Section 2.12.1.7.1.4, *Free Drop Test No. A4*, in which a 9-m, c.g.-over-lid-end edge test was performed, without any apparent challenge to the cover attachment. Therefore, this free drop is not bounding and does not need to be performed.

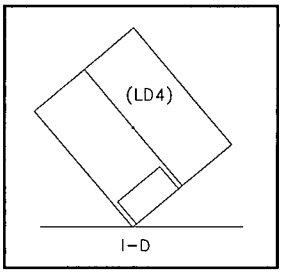

D. C.g.-Over-Corner. This orientation produces the greatest total deformation, since the crushed area is relatively small compared to other orientations. The impact-absorbing structures are essentially identical on each end. However, due to the presence of the thermal shield and associated protective structures on the lid end, the TRUPACT–III package was tested in the lid-down, c.g.-over-corner orientation. This was one of the two orientations producing the greatest thermally-relevant free drop damage (the other is discussed in Section 2.7.1.1.2(B), *Side-Edge Free Drop*). The test was performed at ambient temperature. More deformation would have occurred at maximum NCT temperature, but as shown in Section 2.7.1.5, *Crush Deformation Extrapolations*, the additional deformation caused by the accumulation of damage of this drop with the vertical end drop (see paragraph 2.7.1.1.1(A), *Flat End Free Drops, Package Vertical*) is essentially the same. In other words, the crush damage as measured after the test, including damage accumulation from the two free drops, was essentially the same as if the c.g.-over-corner drop had occurred at maximum NCT temperature without damage accumulation. This test was repeated at the cold, -29 °C temperature as discussed in Section 2.7.1.1.3, *Free Drop Test on CTU-2*.

2.7.1.1.2 Drops on the Sides

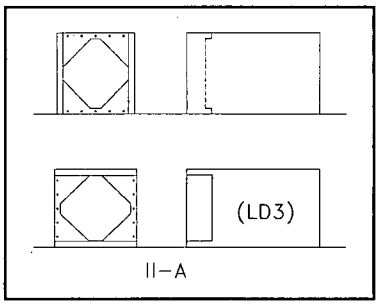

A. Flat Side Free Drops. In these orientations (upper side/bottom side or left side/right side), the wall towards the ground is squeezed by the payload, and the upper flat wall is in bending under its own weight. Impact loads in the left side/right side orientation are bounding due to their slightly larger size. Slapdown is not governing as discussed below. The TRUPACT–III package was dropped on the side opposite the special test ports, with the impact surface horizontal, under maximum-impact (cold) conditions.

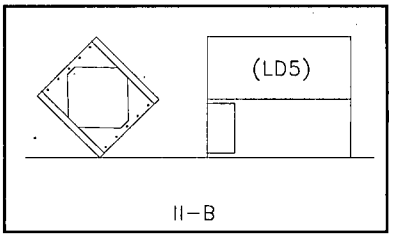

B. Side-Edge Free Drop. In this orientation, the package is horizontal, with one side edge down and the opposite side edge directly above (c.g.-over-edge). This is a single orientation since all four edges are alike. A side-edge drop was performed as described in Section 2.12.1.7.1.9, *Free Drop Test No. A6*. The greatest risk in this orientation is to the thermal insulation shield, since excessive deformation along the crush axis could damage the shield or the thermal insulation behind it. Therefore, the TRUPACT–III package was tested in the side-edge orientation. The test was performed at ambient temperature. To obtain the maximum deformation, the test results were extrapolated to maximum temperatures by analysis as discussed in

Section 2.7.1.5, *Crush Deformation Extrapolations*. This test is discussed further in Section 2.7.1.1.3, *Free Drop Test on CTU-2*.

C. Slapdown on Flat Sides, Lid Primary. There are two orientations, one with the cheeks vertical (normal transport orientation), and one with the cheeks horizontal. The cheeks vertical case would presumably put greater loads on dislodging the cover, but the cheeks horizontal case would be overall a larger load since it represents a slightly larger impact area. Since the difference in side length is less than 6%, the distinction between sides can be ignored, and the orientation of interest is the short side down, with the cover vertical. In this orientation, the apparent loads on cover attachments would be greatest.

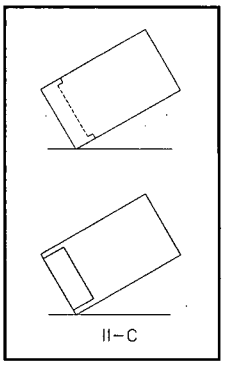

However, the loads on the cover attachments are not significant. Based on the fact that the impact limiting cover is "soft" (see I-C above), the primary impact of the cover will not place any important "moment" loads on the cover. The initial impact is in a direction to drive the cover on, but there will be little moment transfer to the top row of attachment bolts. The loads on the lid itself are bounded in the axial direction by the vertical drop (Section 2.7.1.1.1(B), *Near-Vertical End Free Drops*) and in the lateral direction by the flat side drop (Section 2.7.1.1.2(A), *Flat Side Free Drops*). Therefore, this drop is not bounding and does not need to be performed.

D. Slapdown on Flat Sides, Lid Secondary. Again, there are two orientations, one with the cheeks vertical, and one with the cheeks horizontal. However, since the secondary impact angle is nearly horizontal, very little crush damage is experienced either way, as described in Section 2.12.1.7.2.4, *Free Drop Test No. FD4*. In that test, the crush deformation at the secondary end of the package was only about 50 mm (in equivalent full scale), or less than 2% of the total height of the package. The secondary impact of the package, perpendicular to the ground, was 325g, and decreased rapidly going toward the package center. As a result of changes to the overpack energy absorbing materials, and to the fact that the package is shorter than the one tested previously, the slapdown secondary impact will fall well below 325g, and is instead bounded by the flat side drop discussed in Section 2.7.1.1.2(A), *Flat Side Free Drops*. Since the flat side drop impact will bound the slapdown secondary impact, and since the flat side orientation is essentially the same as the slapdown secondary orientation (i.e., essentially horizontal), the flat side drop bounds the impact conditions of the slapdown drop, particularly at the closure lid, and the slapdown free drop test does not need to be performed.

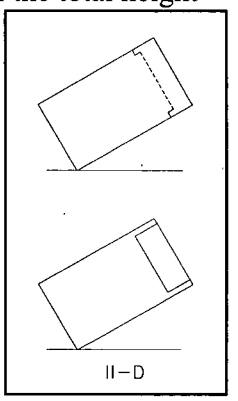

E. Slapdown on Side Edge, Lid Primary. Since the side edge drop is softer in impact than the flat side drop, the impact in this case is not governing. Further, since the c.g.-over-corner end drop puts all of the package energy into a single corner, but the diagonal slapdown divides the energy between corners, the damage to the corner will be governed by the c.g.-over-corner drop (Section 2.7.1.1.1(D), *C.G.-over-Corner*). Therefore, this free drop is not bounding and does not need to be performed.

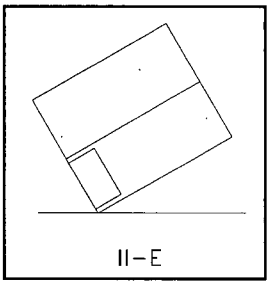

F. Slapdown on Side Edge, Lid Secondary. For the same reasons stated above, neither the crush deformations nor the impacts will be governing, and consequently, this free drop does not need to be performed.

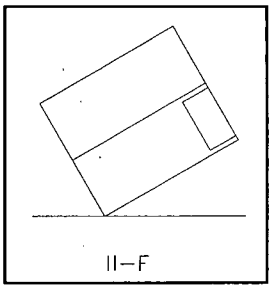

Summarizing the above discussions, the free drop tests performed on CTU-1 were (9-m, HAC unless stated otherwise):

- Vertical, Lid Down (0.3-m, NCT) (Section 2.7.1.1.1(A))
- Vertical, Lid Down (Section 2.7.1.1.1(A))
- C.G.-over-Corner (Section 2.7.1.1.1(D))
- Flat Side (Section 2.7.1.1.2(A))
- Side-Edge (Section 2.7.1.1.2(B))

This information is summarized in greater detail in Table 2.7-1 and depicted in Figure 2.7-1.

2.7.1.1.3 Free Drop Test on CTU-2

As discussed in Section 2.7.8, *Summary of Damage*, the closure lid containment seal of CTU-1 was not leaktight subsequent to the full series of tests. The cause was judged to be the intrusion of internal debris on the sealing surface, but some closure bolts had become bent as well, involving some loss of preload. Therefore the cause could not be ascertained with absolute certainty. A debris shield was added to the design subsequent to the tests on CTU-1. To test the performance of the debris shield and to obtain positive confirmation of the leaktight ability of the package, additional certification testing was required.

During the testing of CTU–1, intermediate vacuum tests of the containment seal were used to track the performance of the package as testing progressed. The vacuum test was successful after the first three free drops (0.3 m NCT free drop LD1, the 9 m end drop LD2, and the 9 m side drop LD3), but not after the last two (the 9 m side–edge drop LD5 and the 9 m c.g.–over–corner drop LD4). Therefore, the one worst–case free drop must be one of those two free drops. All other orientations have been either justified as not requiring test, or successfully tested in either a prior engineering or certification test.

As stated above, the items of concern relative to the leaktight condition of the containment seal are a) the bending of bolts, and b) the function of the debris shield. Therefore, the c.g.–over–corner and the side–edge orientations will be evaluated relative to these considerations. The following discussion relies on the evaluations of CTU-1 presented in Section 2.7.8, *Summary of Damage*.

The bending of the bolts was caused by contact with the overpack cover recess cups. This result was made possible by the sliding motion of the overpack cover during impact deformation. The direction of bolt bending correlated to the 11 o'clock direction, facing the closure lid. The overpack cover would have slid in a direction approximately halfway between 10 and 11 o'clock in the c.g.–over–corner orientation, and in a direction approximately halfway between 7 and 8 o'clock in the side–edge orientation. In both cases, the direction of motion is taken to be in a direction opposite to

the ground, driven by the crush deformation of the overpack structures. Therefore, it is concluded that the c.g.–over–corner orientation was responsible for the bending of the closure bolts.

It is further noted that the driving force for overpack cover motion may be greater in the c.g.–over–corner case. As observed from testing, the deformation of the cover at the corner nearest to the ground in the c.g.–over–corner case (see Figure 2.12.3-19) is significantly larger than for the side–edge case (see Figure 2.12.3-16). The deformation of the cover correlates to the force applied to the cover. Even though the cover is nominally located between fixed bounds (e.g., the limits of the side cheeks and the top and bottom lips of the cover), a larger force has a larger potential for deforming the bounds, and thus moving the cover further, than a smaller force would.

The function of the debris shield is to prevent internal debris from reaching the closure lid containment seal during the impact event. The debris shield is designed to function in the presence of both axial and lateral relative motions of the lid. However, from the design of the debris shield, it is clear that lateral motions in either direction only serve to compress the foam rubber component on one side or the other and improve its function, as shown in Figure 2.12.5-2. Only axial motions could possibly compromise the shield, if the motion exceeds the insertion length of the foam rubber component into the receptacle. Therefore, of the two candidate orientations, the one with the greatest potential for axial motion is clearly the worst case. The side–edge orientation has no component of impact force which is axial to the package; the closure lid is loaded by only its own inertia, in its own plane, against the lid lips. During testing of CTU–1, it was demonstrated that the lid lips and the interfacing body flange were adequate to support the closure lid in the lateral direction against the impact forces of the side–edge free drop. Any lateral motion of the body flange due to outward deformation of the body walls would only compress the debris shield foam rubber as stated above, with no effect on its performance. In the c.g.–over–corner orientation, although the total impact is smaller than the side–edge case, an axial component exists which applies the inertia loading of both the payload as well as the closure lid against the closure joint, creating the potential for some axial relative motion across the debris shield. Therefore, although the axial motion is not expected to come anywhere near the design capacity of the debris shield, the c.g.–over–corner orientation is again judged to be the worst case.

The appropriate temperature of the c.g.–over–corner drop is evident from the preceding considerations. The force applied to the overpack cover, and thus its potential to move far enough to contact the bolt heads and possibly bend the bolts, is greatest for the largest impact load. Likewise, for the greatest axial motion at the debris shield, the greatest deflection of the closure lid will occur with the greatest impact force, which corresponds to the cold case. Therefore the worst–case free drop is the c.g.–over–corner orientation, performed at the cold, -29 °C condition.

Of the four corners available for the c.g.–over–corner free drop, the bottom left corner should be used. The left side is remote from the side containing the CTU test ports, lowering the likelihood of damage to this important area, needed for leakage rate testing. The bottom side should be used since the possible sliding of the overpack cover is important, and the vertical gap between the overpack cover and the body is present only on the bottom. Since the cover can only slide upward, the impact must therefore be on the bottom corner.

In summary, the worst-case test on CTU-2 was a 9 m, c.g.–over–corner orientation, striking the lower left corner (viewed from the closure end), with the region of deformation at cold temperature (-29 °C). Two puncture drop tests were also performed on CTU-2 as described in Section 2.7.3, *Puncture*.

2.7.1.2 Certification Test Unit and Test Conditions

CTU-1

CTU-1 was an essentially prototypic representation, in full-scale, of the TRUPACT–III packaging. Any differences between it and the drawings of Appendix 1.3.1, *Packaging General Arrangement Drawings*, were insignificant, and are discussed and justified in Section 2.12.3.3, *Test Unit Configuration.* Since internal pressure has the effect of increasing containment boundary stress, for the free drops the CSA was pressurized at ambient temperature to an internal pressure of 172 kPa, equal to the design pressure. The simulated payload used inside the CTU consisted primarily of a quantity of aluminum bars. Since the structures normally present within the packaging (the payload container(s), the pallet, and the roller floor) may contribute some beneficial energy absorption under impact, these structures were conservatively omitted. However, their weight was included in the simulated payload. The total weight of the test payload was 6,746 kg, which is 29.5% more than the maximum TRUPACT–III payload of 5,210 kg. This condition is particularly conservative for impact loads on the closure lid. The gross weight of the CTU was 25,052 kg, essentially equal to the maximum allowed weight of 25,000 kg.

CTU-2

CTU-2 was an essentially prototypic representation, in full-scale, of the TRUPACT–III packaging. Any differences between it and the drawings of Appendix 1.3.1, *Packaging General Arrangement Drawings*, were insignificant, and are discussed and justified in Section 2.12.6.3, *Test Unit Configuration.* An internal pressure of 172 kPa (ambient basis) was again used. The simulated payload consisted of a prototypic roller floor, pallet, and SLB2 container. The SLB2 was loaded with aluminum bars and weighed 5,543 kg, which is conservatively 16% more than the maximum loaded SLB2 weight of 4,763 kg. The sum of the weight of the contents was 5,974 kg, which is significantly more than the maximum contents weight of 5,210 kg. The total weight of CTU-2 was 25,154 kg, which is essentially equal to the maximum allowed weight of 25,000 kg. To test the performance of the debris shield, approximately one quart of fine, granular debris was dumped into the payload cavity (external to the SLB2) prior to installing the closure lid.

The significance of temperature, and the choice of temperature for each free drop test, is discussed in Section 2.7.1.1, *Technical Basis for the Free Drop Tests.* For cold temperature tests, the temperature of the polyurethane foam energy absorbing material which was crushed in each case was at a temperature of -29 °C or less. Foam material which was outside the region of crushing deformation in a given impact orientation was not required to be at this temperature. For ambient temperature tests, the foam material experiencing crush was required to be at least +7 °C at impact.

The certification testing took place at the Sandia National Laboratories. For CTU-1, the tests occurred between November 1 and November 10, 2006. For CTU-2 the tests occurred on November 20, 2009. A discussion of the test facilities and CTU instrumentation is provided in Section 2.12.3.2, *Test Facilities.*

2.7.1.3 Test Criteria

The following are the acceptance criteria for both the free drop and puncture drop testing of the TRUPACT–III package:

1. When combined with damage due to the puncture test (see Section 2.7.3, *Puncture*), the worst-case sequence of free drop and puncture damage must not affect the ability of the containment boundary to remain leaktight per ANSI N14.5[2], as demonstrated by post-test leakage rate testing. Since several free drop and puncture tests were performed on CTU-1 and CTU-2, the containment boundary must be leaktight at the conclusion of all free and puncture drop testing.
2. The worst-case combination of free drop and puncture damage must not be of such a magnitude that the maximum temperature limit of the containment seals or of the CSA material would be exceeded in a subsequent HAC fire.

2.7.1.4 Summary of Results of the Free Drop Analyses and Tests

The results of each of the free drops evaluated are described below indicating the reference number as listed in Table 2.7-1. Under each heading, the results of the free drop test are described. A detailed test description, test results, and photographs are given in Appendix 2.12.3, *Certification Tests on CTU-1* and in Appendix 2.12.6, *Certification Tests on CTU-2*. The discussion below begins with test LD2, since the results of the NCT free drop, test LD1, are discussed in Section 2.6.7, *Free Drop*. Post-test leakage rate testing demonstrated that the containment metallic boundary and vent port insert O-ring seal remained leaktight per ANSI N14.5 after the conclusion of all certification testing for both CTU-1 and CTU-2, and the closure lid O-ring seal remained leaktight per ANSI N14.5 for CTU-2. The closure lid O-ring seal of CTU-1 did not meet the leakage rate criteria of ANSI N14.5, most likely due to the presence of debris in the sealing nip[3]. The debris shield, which was not present in CTU-1, is analytically evaluated in Section 2.12.5, *Closure Lid Debris Shield*. The debris shield was present in CTU-2, and was evaluated in free drop test LD91.

The closure bolt washers used on CTU-1 were made from Type 304 stainless steel. The material used for CTU-2 and subsequent production units is ASTM A564 Grade 630 H1025 (17-4 PH) precipitation hardened stainless steel. A finite element evaluation of the function of the closure bolt washer under high loads is given in Appendix 2.12.7, *Closure Lid, Bolt, and Washer Interaction*. This analysis shows that, if the closure joint were to be loaded up to the yield load of the bolt shank, the washer made of 17-4PH material would not experience any permanent deformation.

2.7.1.4.1 Vertical, Lid Down Free Drop Results (CTU-1, Ref. No. LD2)

The TRUPACT–III CTU was dropped at a foam material temperature of approximately -34 °C and with an internal pressure of 172 kPa. The CTU struck the ground on the end face of the overpack cover and cheeks. The resulting impact was 204g. The axial crush from test LD2 was 29 mm. This combined with the crush from test LD1 of 7 mm for a total of 36 mm of axial crush from the two

[2] ANSI N14.5–1997 (or later), *American National Standard for Radioactive Materials – Leakage Tests on Packages for Shipment,* American National Standards Institute, Inc. (ANSI).

[3] After removal of the debris, the closure lid containment O-ring seal did pass the ANSI N14.5 criteria in two separate tests: one using a torque of only 149 N-m on all 44 bolts (9.3% of the nominal preload torque of 1,600 N-m) and a second test, using a torque of 149 N-m on only the four corner bolts. Of note, all leakage rate tests performed subsequent to the removal of the debris passed the criteria. These leakage rate tests are discussed fully in Section 2.7.8.2, *Closure Bolts*.

tests. Some cracks occurred in the welds of the overpack cover near the corners of the octagonal opening in the cover, ranging from approximately 51 mm to 152 mm in length. Small cracks and deformations occurred close to the ISO fittings due to the translation of the stiff fittings relative to the cheeks. In addition, the impact load was carried into the overpack cover attachment flange on the body, and caused some deformation and outward bending of the body top and bottom outer shell sheets. Overall, however, deformation of the CTU was modest from the test. As shown from measurements of the payload cavity before and after all testing, there was no indication of any buckling behavior in the CSA structure (see Section 2.12.3.8.2, *CTU Measurements*).

2.7.1.4.2 Flat Side Free Drop Results (CTU-1, Ref. No. LD3)

The TRUPACT–III CTU was dropped at a material temperature of approximately -39 °C and with internal pressure of 172 kPa. The resulting impact was 407g. As expected given the large impact surface, the impact magnitude was relatively high, and the deformations correspondingly small. Other than a few more weld cracks around the ISO corners, there was essentially no externally identifiable damage. By means of four small drilled holes, it was determined that the CSA moved toward the impact surface by approximately 7 mm, by inside-out action. This movement could be accommodated by relatively small deformations of internal structures. There was no indication of contact of the lid shear lip with the body flange in this test.

2.7.1.4.3 CG-Over-Corner Free Drop Results (CTU-1, Ref. No. LD4)

For convenience in rigging the package during the free drops, test LD4 was performed after test LD5. The TRUPACT–III CTU was dropped at a material temperature of approximately +12 °C and with internal pressure of 172 kPa. The resulting impact and deformation, perpendicular to the ground, was 53g and 323 mm, respectively. The deformation was calculated from the measurements of the triangular crushed surface, as follows. The three sides of the triangle (i.e., the plane of contact with the ground) were: a = 800 mm, b = 838 mm, and c = 1,054 mm. The area of the triangle was (noting that angle A is opposite side a, B opposite side b, and C opposite side c, and A1 is the area of the crush plane):

$$A = \cos^{-1}\frac{b^2 + c^2 - a^2}{2bc} = 48.386°$$

$$B = \sin^{-1}\frac{b}{a}\sin A = 51.550°$$

$$C = 180 - A - B = 80.064°$$

$$A1 = \frac{ab}{2}\sin C = 330{,}172\ \text{mm}^2$$

From Section 2.7.1.5.1, *CG-Over-Corner Free Drop Extrapolation*, the crush distance and the area of the crush plane are related by:

$$A1 = \frac{d^2}{2\sin^2\theta\cos\theta}\left[\frac{H}{W} + \frac{W}{H}\right]$$

from which the crush distance, d, is:

$$d = \left(A1 \sin^2\theta \cos\theta\right)^{1/2} = 323 \text{ mm}$$

where, since the package height, H = 2,650 mm and width, W = 2,500 mm, the term in brackets cancels the numeral 2 in the denominator, and the angle of impact of the end face to the ground is θ = 90 – 50 = 40°.

The combined damage from all of the free drops caused a slight bowing of the right cheek, and a gap of up to 76 mm at the center between the cheek and the overpack cover right edge. The gap was however blocked with buckled material starting about 89 mm deep into the gap, and the gap reduced to zero width at the top and bottom of the cheek-to-cover joint. No significant weld seam failures were noted from this test, and no significant exposure of foam was found.

The free crush distance (i.e., the length of crushable material in the direction of impact) is calculated between the struck corner and the corner of the 16-mm thick box which surrounds the calcium silicate insulation (i.e., the thermal shield). In calculating this distance, only polyurethane foam is considered. Any intervening steel sheets and the entire lift point structure (even though hollow and not rigid) are conservatively excluded. First, the distance along the three primary coordinate axes (axial = T_X; lateral = T_Y; and vertical = T_Z) are calculated.

T_X: From the SAR drawings given in Section 1.3.1, *Packaging General Arrangement Drawings*, Sheet 9, Section AN-AN, the length of the cheek is 870 mm. After subtracting the thermal shield length of 334 mm, the lift point length of 178 mm, the rear sheet of the lift point of 6 mm, and the thickness of the chevron shaped piece of 6 mm, the remaining axial crushable distance is $T_X = 870 - 334 - 178 - 6 - 6 = 346$ mm.

T_Y: From the SAR drawing Sheet 6, Section G-G (lower left corner of view), the full thickness of the overpack side region is equal to 190 mm. After subtracting the inner and outer side sheet thickness of 6 mm and 8 mm, respectively, the thermal shield of 16 mm, and the insulation board of 30 mm, the remaining crushable distance on the side is $T_Y = 190 - 6 - 8 - 16 - 30 = 130$ mm.

T_Z: The overall height of the package is 2,650 mm. After subtracting the height of the thermal shield of 2,436 mm (from SAR drawing Sheet 5, Section F-F), dividing by two, and subtracting the outer sheet thickness of 8 mm, the remaining crushable distance vertically is:

$$T_Z = \frac{2{,}650 - 2{,}436}{2} - 8 = 99 \text{ mm}$$

The diagonal distance from the outer corner of the thermal shield to the inner corner of the overpack (i.e., in a plane perpendicular to the package axis) is:

$$T_{YZ} = \left(T_Y^2 + T_Z^2\right)^{1/2} = 163 \text{ mm}$$

The shortest crushable distance from the inner surface at the c.g. over corner impact point to the thermal shield corner is:

$$T = \left(T_X^2 + T_{YZ}^2\right)^{1/2} = 382 \text{ mm}$$

The angle between the end face of the package and hypotenuse T is:

$$\lambda = \tan^{-1}\left(\frac{T_X}{T_{YZ}}\right) = 64.8°$$

In the c.g.-over-corner orientation, the angle between the end face and the ground is $\theta = 40°$, as stated above. Therefore, during impact, the angle between the distance T and the vertical is equal to $\delta = \theta + \lambda - 90 = 14.8°$. The total crushable distance along the line of impact is equal to:

$$D = T\cos(\delta) = 369 \text{ mm}$$

The distance of crush in test LD4 was equal to 323 mm, and as shown in Section 2.7.1.5.1, *CG-Over-Corner Free Drop Extrapolation*, does not require correction for maximum NCT temperature. The remaining crush distance is equal to 369 – 323 = 46 mm. The amount of available crush used in the worst case is:

$$\frac{323}{369} \times 100 = 87.5\%$$

This amount of crush is acceptable since it represents only the minimum at the corner point, and is much larger elsewhere.

2.7.1.4.4 Side-Edge Free Drop Results (CTU-1, Ref. No. LD5)

For convenience in rigging the package during the free drops, test LD5 was performed before test LD4. The TRUPACT–III CTU was dropped at a material temperature of approximately +7 °C and with internal pressure of 172 kPa. The resulting impact, perpendicular to the ground, was 142g. The deformation is found from:

- The initial clear distance between the inside of the edge and the near corner of the calcium silicate protection box (i.e., thermal shield), found above as $T_{YZ} = 163$ mm
- The measured distance between the inside of the crush surface and the near corner of the thermal shield after test, $T_{Remaining} = 95$ mm

The crush deformation distance was therefore $T_{YZ} - T_{Remaining} = 68$ mm.

During the impact, a length of the weld at the front edge of the large outer side sheet on the right side of the CTU opened up for a distance of approximately 914 mm. The fissure started in the folded region associated with the side-edge deformation. The maximum opening distance was approximately 51 mm. The opening exposed the forward edge of the outer layer of balsa wood. The puncture-resistant plate, the underlying 0.10 kg/dm^3 foam, and the CSA were not affected. The weld was specified to be 6-mm full penetration, but examination of the failed edges of the fissure revealed that penetration was typically only half of this value. The inadequate weld penetration was traced to the process and technique used. For production units, the weld process and technique will be changed to ensure full penetration occurs on all TRUPACT-III welds. As discussed in Section 3.5.2.6, *Description of Thermal Model for HAC Conditions*, the thermal fire analysis conservatively assumes that the worst case puncture damage occurred directly on this weld fissure.

As stated above, the remaining free distance between the inside of the crushed surface and the nearest corner of the thermal shield, which is taken as a "hard corner", was measured to be 95 mm. As shown in Section 2.7.1.5.2, *Side-Edge Free Drop Extrapolation*, the crush distance must be increased by 30 mm to account for the effect of maximum NCT temperature. The crush deformation distance calculated above is 68 mm. Under NCT maximum temperature conditions the distance is 68 + 30 = 98 mm. The amount of available crush used in the worst case is:

$$\frac{98}{163} \times 100 = 60\%$$

This amount of crush is well within the capability of the foam to provide a margin of safety on crush distance as well as thermal protection in the HAC fire.

2.7.1.4.5 CG-Over-Corner Free Drop Results (CTU-2, Ref. No. LD91)

CTU-2 was dropped at a material temperature of -33.6 °C and with internal pressure of 172 kPa (at ambient). The resulting impact, perpendicular to the ground, was 80.8g. As in the case of the c.g.-over-corner drop on CTU-1, the deformation surface was a triangle with lengths 737 mm along the overpack cover, 864 mm along the bottom, and 787 mm along the left side of the CTU. Since these values are less than those for the CTU-1 test (as expected, since the CTU-1 test was performed at a temperature of approximately +12 °C), the crush deformation is less than that of the prior test and not bounding. Consequently the crush extrapolation performed in Section 2.7.1.5.1, *CG-Over-Corner Free Drop Extrapolation*, remains bounding. No significant weld seam failures or exposed foam was noted.

After the test, a vacuum was applied to the annulus between the two O-rings in the closure lid. The lowest vacuum achieved was below 200 millitorr, indicating a good seal. After the two subsequent puncture tests, a helium leakage rate test was performed, and the leakage rate of the containment boundary, the closure lid containment seal, and the vent port seal met the leaktight criteria of ANSI N14.5. Detailed test results are given in Appendix 2.12.6, *Certification Tests on CTU-2*.

2.7.1.5 Crush Deformation Extrapolations

Since two of the free drops on CTU-1 (the c.g.-over-corner free drop, ref. no. LD4, and the side-edge free drop, ref. no. LD5) were performed in order to obtain the worst-case deformation damage, the damage actually incurred at the test temperature must be extrapolated to the damage that would occur at maximum NCT temperatures.

2.7.1.5.1 CG-Over-Corner Free Drop Extrapolation

The damage present after the c.g.-over-corner free drop (LD4) includes the damage incurred during the two vertical, lid down free drops (ref. nos. LD1, NCT and LD2, HAC). The following analysis shows that the combination of damage from the c.g.-over-corner free drop (performed at ambient temperature) and the vertical, lid down free drops (performed at cold temperature) is essentially the same as would occur from the c.g.-over-corner free drop alone, if performed at the maximum NCT temperature. In other words, the damage observed in the certification testing is equivalent to the maximum damage which could occur if the c.g.-over-corner free drop were performed alone at NCT temperature.

Energy is absorbed in the c.g.-over-corner orientation by the deformation of the outer steel shell, by the crush of the forward slab (140-mm thick) of low density, 0.16 kg/dm^3 foam, and by the crush of the internal block of high density, 0.48 kg/dm^3 foam. Each of these quantities can be calculated by knowing the geometry of the package, the crush strength of the crushable media,

and the deformation force of the steel. The latter quantity is calculated using the test results from the engineering testing of the half-scale test unit.

Since the increment of shell deformation energy is equal to the crush area perimeter times the deformation force per unit length times the crush increment, the total energy absorbed by the deformation of the shell is equal to the crush area times the deformation force per unit length, or:

$$E_s = AF$$

where A is the crush area and F is the force to deform the steel shell per unit length. Similarly, since the increment of foam crush energy is equal to the crush area times the crush stress times the crush increment, the total energy absorbed by crush of the foam is equal to the total crushed volume times the crush stress, or:

$$E_c = V\sigma$$

where V is the total volume of the crushed region, and σ is equal to the foam crush strength.

Next, the relation between the crush area, A, the crushed volume, V, and the crush depth, d, will be determined. From the left side of Figure 2.7-2, which is a depiction of a diagonal section of the package during impact, the crush distance perpendicular to the ground is d. The measurement of the crushed region parallel to the package side-edge is h. It may be seen that:

$$h = \frac{d}{\cos\theta}$$

where θ is the orientation of the package, defined as the angle between the ground and the end face. From the right side of the figure, which depicts the crush area projected onto the undeformed package end face, the two areas A_1 and A_2 are:

$$A_1 = \frac{1}{2}a^2 \tan\alpha$$

$$A_2 = \frac{1}{2}a^2 \tan\beta$$

where:

$$a = \frac{d}{\sin\theta}, \qquad \tan\alpha = \frac{H}{W}, \qquad \tan\beta = \frac{W}{H}$$

On the plane of the package end face, the total area affected by impact is:

$$A_B = A_1 + A_2 = \frac{d^2}{2\sin^2\theta}\left[\frac{H}{W} + \frac{W}{H}\right]$$

The crushed volume is a wedge-shaped pyramid. One large face of the pyramid (on the ground) is area A_B, and which is associated with a height of h. The other large face (on the package) is the crush area, A, associated with height d. Since the volume of any pyramid is equal to (1/3) × baseplane area × height, then:

$$V = \frac{1}{3}A_B h = \frac{1}{3}Ad$$

This may be rearranged to give:

$$A = \frac{A_B h}{d}$$

Substituting for h and d:

$$A = \frac{d^2}{2\sin^2\theta\cos\theta}\left[\frac{H}{W} + \frac{W}{H}\right]$$

Since the package height, H = 2,650 mm and the width, W = 2,500 mm, it can be seen that the term in brackets cancels the numeral 2 in the denominator, and the area can be simplified to:

$$A = \frac{d^2}{\sin^2\theta\cos\theta} = C_A d^2$$

By integration, the volume is:

$$V = \frac{Ad}{3} = \frac{d^3}{3\sin^2\theta\cos\theta} = C_V d^3$$

In a HAC free drop, the low density material local to the impact is fully crushed, and a maximum stroke of 80% of its thickness may be assumed. Therefore the usable crush distance (parallel to dimension d) in the low density material is:

$$T = 0.8T_B\cos\theta$$

where T_B is the axial thickness of the low density material, or 140 mm.

It is now possible to state the energy relationships in the c.g.-over-corner impact as follows:

$$W(9.81)(9+d) = C_V\sigma_{LD}\left[d^3 + (d-T)^3\right] + C_V\sigma_{HD}(d-T)^3 + C_A F d^2$$

where the term on the left is the total impact energy of the package, and the terms on the right are the energy absorbed by the low density foam, the energy absorbed by the high density foam, and the energy absorbed by the steel shell, respectively. Notations not previously defined are:

W = package mass, kg

σ_{LD} = crush strength of low density material, N/m^2

σ_{HD} = crush strength of high density material, N/m^2

F = deformation force of the steel shell, N/m

The c.g.-over-corner angle defined above is readily calculated by noting that it is equal to the angle between the package diagonal and the vertical. The end face diagonal is:

$$x_d = \sqrt{H^2 + W^2} = 3{,}643\text{ mm}$$

The c.g.-over-corner angle is:

$$\theta = \tan^{-1}\left(\frac{x_d}{L}\right)$$

where L is the package length. For the TN Gemini, L = 6,058 mm, and $\theta_G = 31°$. For the TRUPACT–III, L = 4,288 mm, and $\theta_{TP3} = 40.4°$.[4]

In order to evaluate the above equation, the crush strengths of the crushable materials and the deformation strength of the steel shell need to be evaluated. As stated above, the deformation strength of the steel shell is found using the above equation with known parameters, including total crush distance, from a prior engineering test. The crushable media strengths are evaluated as follows. Since the engineering test in question used redwood and balsa, an evaluation of these materials is needed, as well as an evaluation of the foams used in the TRUPACT–III.

All of the crushable materials have orthotropic properties (axes of orthotropy being parallel or perpendicular, respectively, to the grain or rise of the material.) The crush strength at a given intermediate angle is found using the well-known Hankinson formula[5]:

$$\sigma_\theta = \frac{\sigma_{par}\sigma_{per}}{\sigma_{per}\sin^2\theta + \sigma_{par}\cos^2\theta}$$

where σ_{par} is the strength parallel to the grain or rise, σ_{per} is the strength perpendicular to the grain or rise, and θ is the orientation angle.

The engineering test is described in Section 2.12.1.7.1.6, *Free Drop No. C7*. In that test, a half-scale test unit was dropped 9-m in the c.g.-over-corner orientation at ambient temperature. The configuration of the steel in the cheeks and overpack cover were essentially identical to that of the TRUPACT–III. For this reason, the results of this test can be used to obtain the average steel deformation force. The unit was fabricated with materials having crush strengths shown in the table below. The aggregate crush strengths in the drop orientation are calculated using the Hankinson formula with an orientation angle of 31°. To account for the dynamic effect, the static strengths were multiplied by a factor of 1.5[3].

Material	Crush strength parallel to grain, MPa	Crush strength perpendicular to grain, MPa	Crush strength, Hankinson, 31°, MPa	Including dynamic factor of 1.5, MPa
Balsa	8	1	2.80	$\sigma_{LD} = 4.20$
Redwood	46	10	23.5	$\sigma_{HD} = 35.3$

Using an angle of $\theta_G = 31°$ and the formulas above, the area coefficient, $C_A = 4.40$, and the volume coefficient, $C_V = 1.47$. In full scale, the mass of the test unit would have been 30,000 kg, and the front slab thickness, $T_B = 0.14$ m. The crush distance in the direction of the drop, in full scale, was d = 0.36 m. Using these parameters, the energy equation can then be solved for a steel deformation force of $F = 2.85(10^6)$ N/m.

It now remains to compare the deformation under certification test conditions with the deformation under NCT maximum temperature conditions using TRUPACT–III-specific parameters. The

[4] This result assumes the c.g. is at the geometric center of the package. As shown in Section 2.1.3, *Weights and Centers of Gravity*, it is actually shifted slightly towards the overpack cover end. However, since the effect of this shift on the c.g.-over-corner angle is only about 2°, it may be neglected for the purposes of this analysis.

[5] Cramer, Steven M., Hermanson, John C., and McMurtry, Wayne M., *Characterizing Large Strain Crush Response of Redwood*, SAND96-2966, Sandia National Laboratories, December 1996.

polyurethane foam crush strengths are found under dynamic conditions from the foam manufacturer's data, and are listed in the table below. Each value represents the average of crush strengths at 20, 30, and 40% strain. The average foam temperature during the c.g.-over-corner certification test (LD4) was 12 °C, and for the NCT maximum temperature, 60 °C is used, which is conservatively higher than the bulk average temperature of the foam in the cheek of 49.7 °C recorded in Chapter 3, Table 3.1-1. The angle used in the Hankinson formula for the TRUPACT–III is 41°, which is sufficiently close to the angle of $\theta_{TP3} = 40.4°$ found above. Finally, the maximum temperature foam crush strength is further conservatively modified by a factor of 0.9, which reflects the minimum crush strength tolerance allowed on the foam, while the foam strength at test temperature is based on the actual density of the foam taken from the fabrication records of the CTU.

Foam, kg/dm^3	Crush strength parallel to rise, σ_{par}, MPa	Crush strength perp. to rise, σ_{per}, MPa	Crush strength, used, σ_θ, MPa (Hankinson @ 41°)
Test foam at 12 °C, dynamic, actual density basis			
0.16	3.77	3.63	$\sigma_{LD} = 3.71$
0.47	30.1	32.7	$\sigma_{HD} = 31.2$
NCT max temp (60 °C), dynamic, min strength basis (90% of nominal)			
0.16	2.74	2.55	$\sigma_{LD} = 2.65$
0.48	18.2	20.1	$\sigma_{HD} = 18.9$

Using an angle of $\theta_{TP3} = 40.4°$ and the formulas above, the area coefficient, $C_A = 3.13$, and the volume coefficient, $C_V = 1.04$. The mass of the TRUPACT–III CTU was 25,052 kg, and the front slab thickness, $T_B = 0.14$ m. For the maximum temperature case, the steel force F is reduced by 5% based on the difference between the steel flow stress (that is, the average of yield and ultimate strength) at temperatures of 38 °C and 93 °C, using data from Table 2.2-1. The value of the steel deformation force, F, at maximum NCT temperature is then:

$$F_{HOT} = F(0.95) = 2.71(10^6)\,N/m$$

Using these parameters, the crush distance in the ambient, actual strength case is d = 386 mm, and in the maximum NCT temperature, minimum strength case, d = 420 mm. Note that these values are not certification test predictions, but analytical results which can be compared with each other on the same basis. The difference between these results is the additional crush distance which would be expected to occur if the CTU had been tested using minimum strength foam at maximum NCT temperature, and is equal to 420 – 386 = 34 mm.

However, as shown in Section 2.7.1.4.1, *Vertical, Lid Down Free Drop Results*, the measured deformation (along the package axis) from the sum of end drop tests LD1 and LD2 was 36 mm. Along the line of action of the c.g.-over-corner free drop, the value is:

$$d = 36\cos(\theta_3) = 27.4 \text{ mm}$$

That is, the c.g.-over-corner free drop damage as actually measured on the CTU is 27.4 mm greater than if the c.g.-over-corner free drop had been performed on a "virgin" corner. Since difference between the additional damage due to maximum NCT temperature (34 mm) and the additional damage due to the prior free drop (27.4 mm) is only 6.6 mm, it may be neglected.

Thus, the actual measured crush of the CTU subsequent to the c.g.-over-corner free drop (LD4) does not require further adjustment.

2.7.1.5.2 Side-Edge Free Drop Extrapolation

The damage present after the side-edge free drop includes some damage incurred during the two vertical, lid-down drops, but since the damage is relatively small and since the end drop damage is at right angles to the side-edge damage, its effect is negligible and may be conservatively neglected. The procedure in this case is similar to the c.g.-over-corner case. First, the effect of the steel is found using engineering test results. Then, crush results at ambient, actual-strength conditions are calculated and compared to crush results at maximum NCT temperature, minimum-strength conditions. The difference between these two results is the added crush which would be expected to occur under worst case conditions.

In the side-edge orientation, one long edge is down, and the diagonally opposite edge is at the top. Since the height and width of the package are nearly the same, an angle of 45° is assumed for analysis purposes. Energy is absorbed by the deformation of the outer steel shell, and by the crush of the following foam components:

- The two end slabs of 0.16 kg/dm^3 foam, each 140 mm long, perpendicular to rise. (Low density balsa was used in the engineering test.)
- Two sections of 0.48 kg/dm^3 foam, 722 mm (front) and 682 mm (rear) long, 45° to rise. (Redwood was used in the engineering test, perpendicular to grain.)
- One section of 0.29 kg/dm^3 foam, 2,574 mm long, parallel to rise (High density balsa, 4,344 mm long, equivalent full-scale, was used in the engineering test.)

The side-edge orientation free drop test was performed on the half-scale test unit at ambient temperature as described in Section 2.12.1.7.1.9, *Free Drop No. A6*. The equivalent full-scale deformation was 138 mm and the impact was 112g. The crush strengths of the various wood components are shown in the table below. (Since crush takes place either parallel or perpendicular to the grain, strengths are given only in the relevant directions.) As for the c.g.-over-corner analysis, a dynamic increase factor of 1.5 is applied to the static strengths.

Material	Crush strength parallel to grain, MPa	Crush strength perpendicular to grain, MPa	Including dynamic factor of 1.5, MPa	Length, mm
LD balsa	N/A	1	$\sigma_1 = 1.50$	$L_1 = (2 \times 140) = 280$
Redwood	N/A	10	$\sigma_2 = 15.0$	$L_2 = (722 + 682) = 1{,}404$
HD balsa	12	N/A	$\sigma_3 = 18.0$	$L_3 = 4{,}344$

As shown in Section 2.7.1.5.1, *CG-Over-Corner Free Drop Extrapolation*, the total energy absorbed by the deformation of the shell is:

$$E_s = AF$$

and the total energy absorbed by the crush of foam (or wood) is:

$$E_c = V\sigma$$

As shown in Figure 2.7-3, the area of crush is equal to 2dL, where L is the total length of the package. By integration, the volume is equal to d^2L, or for a particular crush component, equal to d^2L_x, where L_x represents the length of the component. For example, the energy absorbed by a single wood component having a length L_x and a crush strength σ_x would be:

$$E_x = d^2 L_x \sigma_x$$

The energy relationships in the side-edge impact are therefore as follows:

$$W(9.81)(9+d) = d^2(L_1\sigma_1 + L_2\sigma_2 + L_3\sigma_3) + 2d(L_1 + L_2 + L_3)F$$

where the term on the left is the total impact energy, the first term on the right is the crush energy for the three components, and the second term on the right is the steel deformation energy. W is again the package mass of 30,000 kg, and F is the steel deformation force per unit length.

Using these parameters and a deformation distance of 138 mm, the energy equation can be solved for a steel deformation force of $4.70(10^5)$ N/m. (This value is less than the corresponding c.g.-over-corner case since the majority of the steel deformation strain in the side-edge case is much less severe.) As a check, the impact force can be found from:

$$I = [2d(L_1\sigma_1 + L_2\sigma_2 + L_3\sigma_3) + 2(L_1 + L_2 + L_3 + 2d)F]/W = 114g$$

which compares well with the equivalent full-scale engineering test average impact of 112g.

It now remains to compare the deformation under certification test conditions with the deformation under NCT maximum temperature conditions using TRUPACT–III-specific parameters. The polyurethane foam crush strengths are found under dynamic conditions from the foam manufacturer's data[6], and are listed in the table below. Each value represents the average of crush strengths at 20, 30, and 40% strain. The foam temperature during the side-edge certification test (LD5) was 7 °C, and for the NCT maximum temperature, 60 °C is used, which is conservatively higher than the bulk average temperature of the foam of 50 °C for the package body recorded in Chapter 3, Table 3.1-1. The maximum temperature foam crush strength is further conservatively modified by a factor of 0.9, which reflects the minimum crush strength tolerance allowed on the foam, while the foam strength at test temperature is based on the actual density of the foam taken from the fabrication records of the CTU.

[6] *General Plastics Last-a-Foam® FR-3700 for Crash and Fire Protection of Nuclear Material Shipping Containers*, General Plastics Manufacturing Company.

Foam, kg/dm^3	Crush strength parallel to rise, MPa	Crush strength perpendicular to rise, MPa	Crush strength, used, MPa	Basis
Test foam at 7 °C, dynamic, actual density basis				
0.16	3.96	3.78	$\sigma_1 = 3.78$	Perpendicular to rise
0.47	30.6	33.5	$\sigma_2 = 32.0$	Hankinson formula at 45°
0.27	11.1	11.2	$\sigma_3 = 11.1$	Parallel to rise
NCT max temp (60 °C), dynamic, min strength basis (90% of nominal)				
0.16	2.74	2.55	$\sigma_1 = 2.55$	Perpendicular to rise
0.48	18.2	20.1	$\sigma_2 = 19.1$	Hankinson formula at 45°
0.29	8.36	8.54	$\sigma_3 = 8.36$	Parallel to rise

Similar to Section 2.7.1.5.1, *CG-Over-Corner Free Drop Extrapolation*, the steel force, F, in the maximum temperature case is reduced by 5% as follows:

$$F_{HOT} = F(0.95) = 4.465(10^5)\,N/m$$

Component lengths L_1 and L_2 are the same as in the engineering test, but L_3 = 2,574 mm in the TRUPACT–III case. Using these parameters, the crush distance in the ambient, actual strength case is d = 149 mm, and in the maximum NCT temperature case, d = 179 mm. Note that these values are not certification test predictions, but analytical results which can be compared with each other on the same basis. The difference between these results is the additional crush distance which would be expected to occur if the CTU had been tested using minimum strength foam at maximum NCT temperature, and is equal to 179 – 149 = 30 mm.

Table 2.7-1 – Summary of Free Drops Performed on the TRUPACT–III

Test Description①	Discussion Paragraph	Test Ref. No.②	Test Temperature③	Purpose
Vertical, Lid Down, (NCT 0.3-m, CTU-1)	Section 2.7.1.1.1(A)	LD1	Cold	Test closure lid attachments & O-ring seal area under maximum NCT impact conditions.
Vertical, Lid Down, HAC (CTU-1)	Section 2.7.1.1.1(A)	LD2	Cold	Test closure lid attachments & O-ring seal area under maximum impact conditions.
Flat Side (CTU-1)	Section 2.7.1.1.2(A)	LD3	Cold	Test closure lid attachments, O-ring seal area, lid lateral support, and unsupported wall under maximum impact conditions.
C.G.-over-Corner (CTU-1)	Section 2.7.1.1.1(D)	LD4	Ambient	Quantifies maximum crush for use in thermal analysis
Side-Edge (CTU-1)	Section 2.7.1.1.2(B)	LD5	Ambient	Quantifies maximum crush for use in thermal analysis
C.G.-over-Corner (CTU-2)	Section 2.7.1.1.3	LD91	Cold	Test debris shield and confirm ability to remain leaktight in worst-case free drop

Notes:

① The free drop distance was equal to 9-m, except when stated otherwise.

② The test sequence on CTU-1 was: LD1, LD2, LD3, LD5, LD4.

③ In this column, *cold* means -29 °C or less. The conversion of ambient temperature results to maximum NCT temperature results is discussed in Section 2.7.1.5.1, *Crush Deformation Extrapolation.*

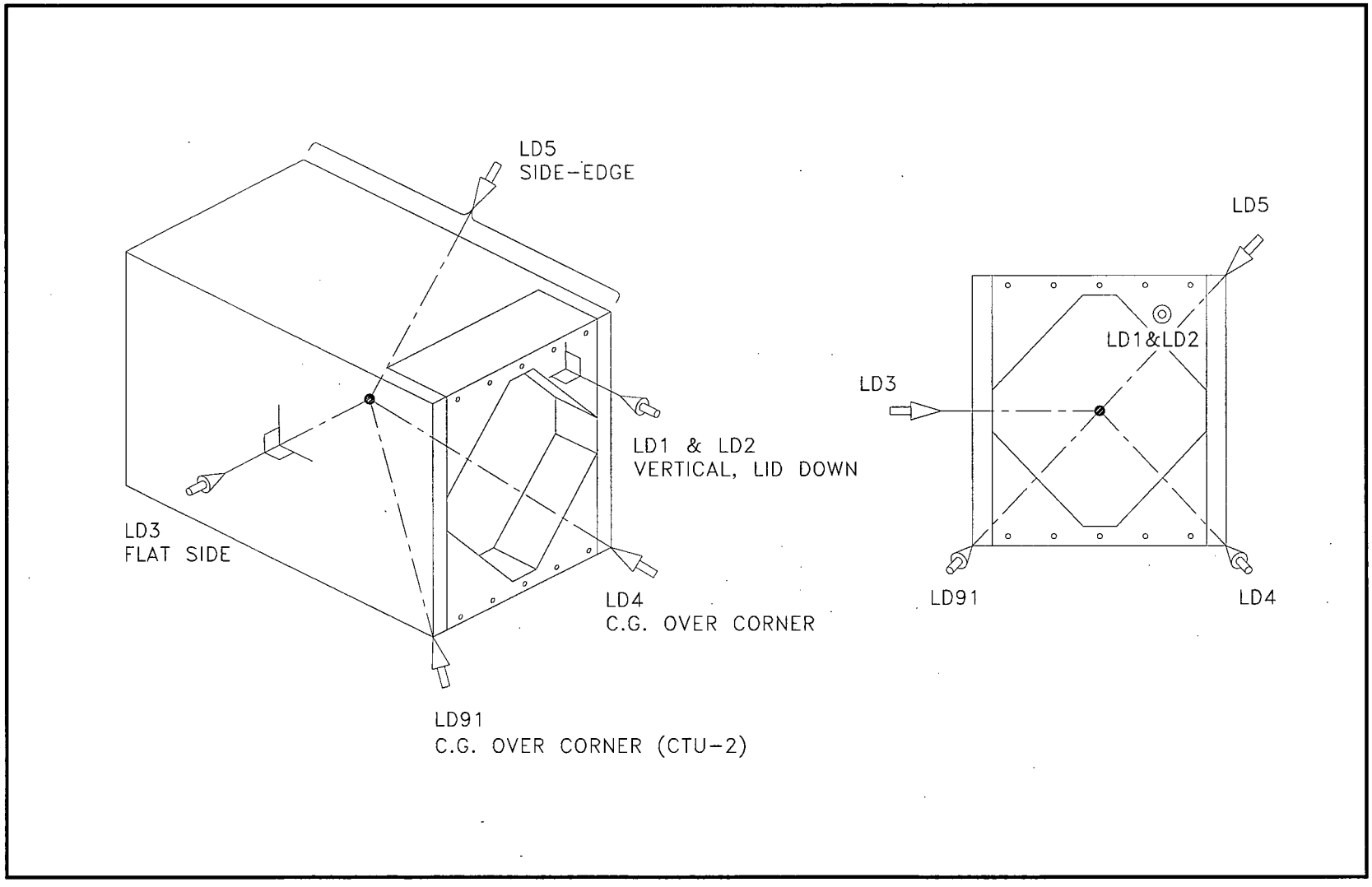

Figure 2.7-1 – Schematic of TRUPACT–III Free Drop Orientations

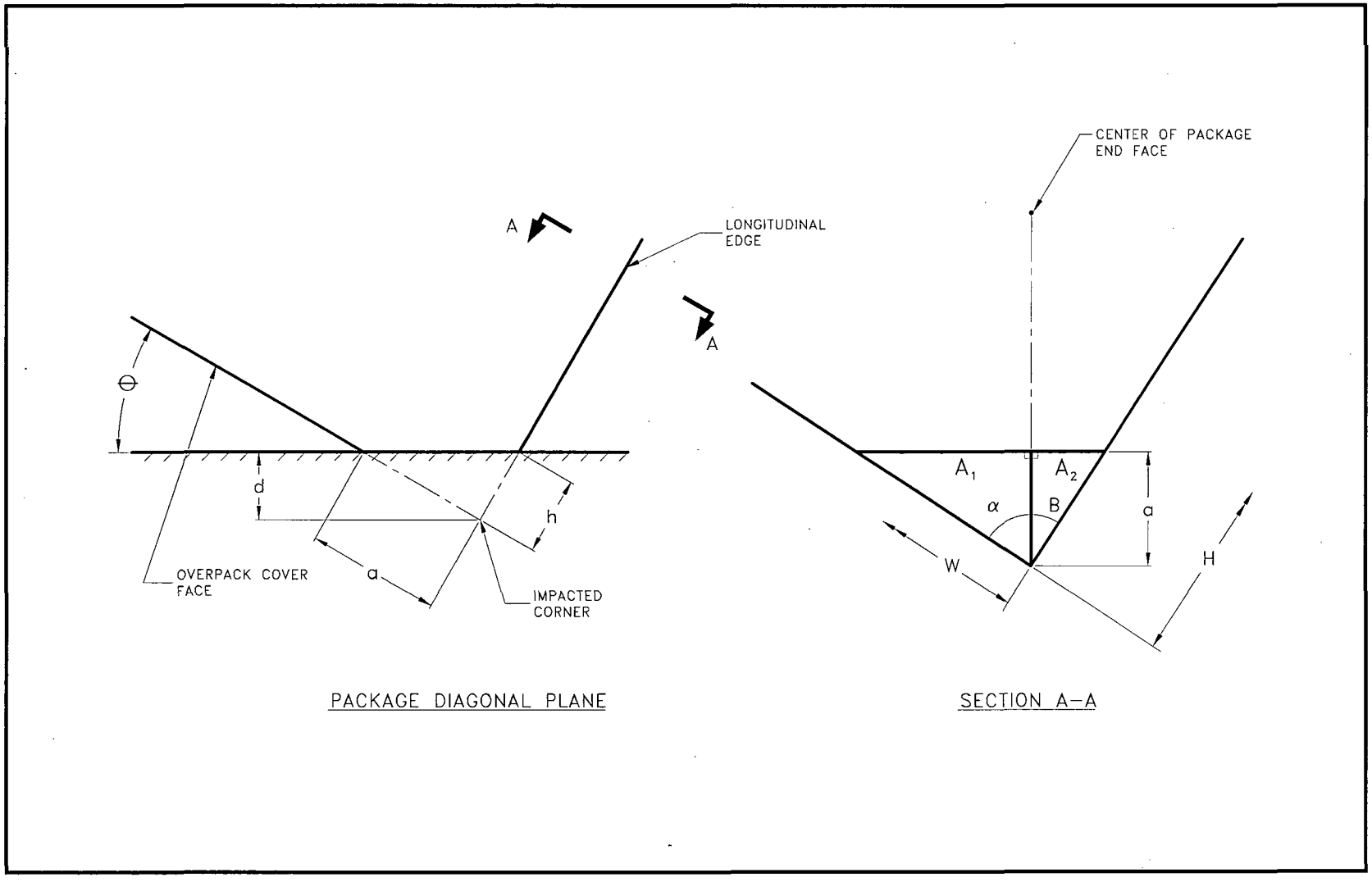

Figure 2.7-2 – CG-Over-Corner Impact Crush Area Relationships

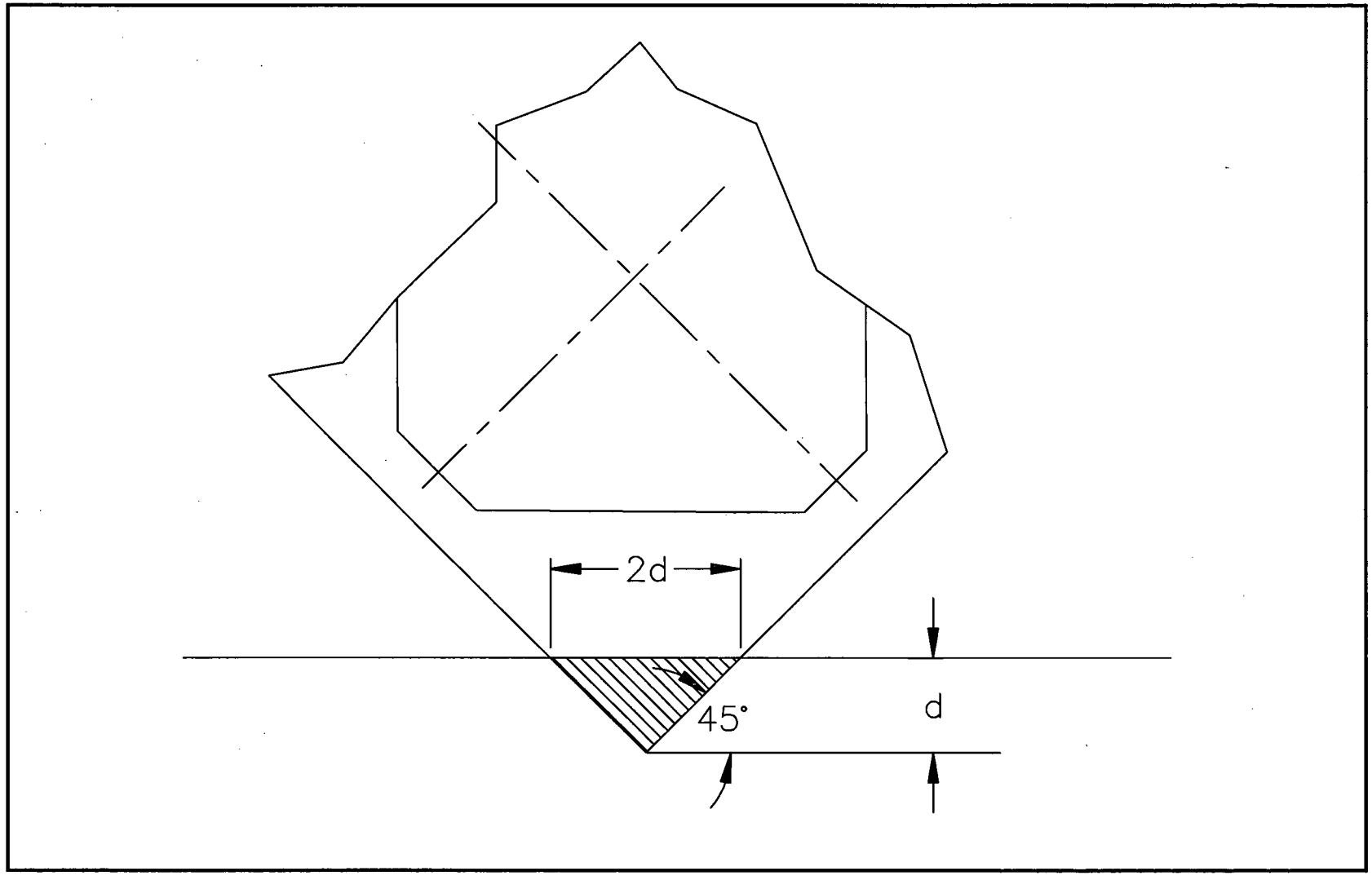

Figure 2.7-3 – Side-Edge Impact Crush Area Relationships

2.7.2 Crush

Subpart F of 10 CFR 71 requires performing a dynamic crush test in accordance with the requirements of 10 CFR §71.73(c)(2). Since the TRUPACT–III package weight exceeds 500 kg, the dynamic crush test is not required.

2.7.3 Puncture

Subpart F of 10 CFR 71 requires performing a puncture test in accordance with the requirements of 10 CFR §71.73(c)(3). The ability of the TRUPACT–III package to adequately withstand the specified puncture drop is demonstrated by testing of a full-scale CTU. A total of four puncture tests were performed on CTU-1 and two were performed on CTU-2. Each puncture drop was over a minimum distance of one meter between the top of the puncture bar and the target point on the CTU. The mild steel puncture bar had a nominal diameter of 150 mm and an edge radius not exceeding 6 mm. The puncture bar assembly was welded securely to the drop pad.

2.7.3.1 Technical Basis for the Puncture Drop Tests

In order to determine the worst-case puncture orientation, consideration of a number of possible orientations was made. Primary focus was on the ability of the TRUPACT–III package to withstand the puncture drop event without compromise to leaktight containment, and on the ability of the thermally-relevant structures located in the region of the closure lid containment O-ring seal to resist damage that could compromise their ability to adequately limit the temperature of the seal in the HAC thermal event. The criteria used to evaluate each puncture drop were based on the following considerations:

- Rupture of containment boundary
- Excessive deformation in the containment sealing area, particularly in combination with free drop damage
- Separation of the overpack cover from the package
- Excessive compression, damage, or exposure of the polyurethane foam or calcium silicate insulation.

Shielding and criticality are not of concern as discussed in Section 2.7.1.1, *Technical Basis for the Free Drop Tests*. A brief summary of the test unit configuration and test conditions is given in Section 2.7.1.2, *Certification Test Unit and Test Conditions*.

The following puncture drops (through the package CG unless stated otherwise) were considered in the worst-case evaluation:

A. Puncture on the side drop damage.

B. Puncture on the overpack cover.

C. Puncture on the overpack cover center.

D. Puncture on the closed end center.

E. Puncture on the overpack cover joint (front side). (non-CG)

F. Puncture on the overpack cover joint (top or bottom). (non-CG)

G. Puncture on the c.g.-over-corner drop damage.

H. Puncture on the side-edge drop damage. (non-CG)

I. Puncture on the region outside the puncture-resistant structure (non-CG)

Each puncture orientation is evaluated to determine whether it represents bounding damage to the containment boundary or to the containment sealing area that could affect thermal performance. The result of all of these evaluations is summarized in Table 2.7-2, and illustrated in Figure 2.7-5 and Figure 2.7-6. Note: in the following small figures, a number in parentheses (e.g., *LP1*), indicates that the particular test has been performed as summarized in Table 2.7-2.

A. Puncture on the Side. In this orientation, the bar axis is aimed through the c.g. of the package, and is oriented at 70° to the package surface (i.e., the package is oriented 20° from horizontal). The puncture took place on the side of the package which experienced the flat side free drop impact. The angle was chosen based on the results of a series of engineering puncture tests at different orientations using the half-scale test article as described in Section 2.12.1.7.3.2, *Puncture Drop Tests P105 through P405*. Other engineering tests performed in this orientation are described in Section 2.12.1.7.1.5, *Puncture Drop Test No. F5* and Section 2.12.1.7.1.8, *Puncture Drop Test No. F9*.

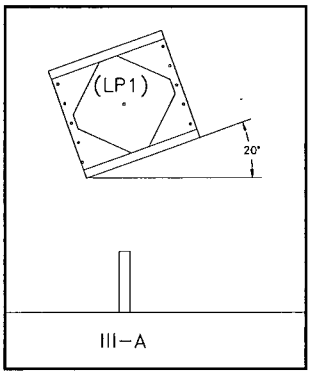

B. Puncture on the Overpack Cover. In this orientation, the bar axis was aimed through the c.g. of the package, at an angle which is oblique as possible considering the geometry of the overpack cover octagonal recess. The impact point was on the recessed octagonal surface. This puncture challenged the puncture-resistant plate near its edge. The impact point was also near the closure bolts and elastomeric containment seal. A similar puncture test was performed on the ends of the half-scale engineering test article as described in Section 2.12.1.7.2.5, *Puncture Drop Test No. P1* and Section 2.12.1.7.2.8, *Puncture Drop Test No. P4*. Based on the results of those tests, the puncture-resistant plates on both ends have been increased in thickness to 15 mm. The effectiveness of this measure was confirmed in another engineering test described in Section 2.12.1.7.3.3, *Puncture Drop Test No. P505*.

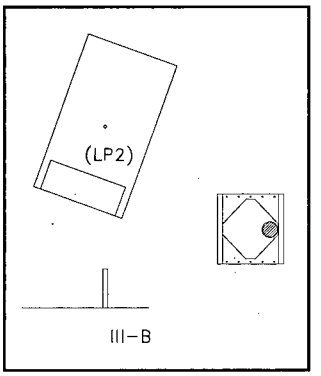

C. Puncture on the Overpack Cover Center. In this orientation, the puncture bar impacts the center of the overpack cover through the package c.g. Since the bar axis is not oblique to the surface, this test is not considered as severe as the oblique impact described in Section 2.7.3.1(B), *Puncture on the Overpack Cover*. Furthermore, an engineering test in this orientation was performed as described in Section 2.12.1.7.1.3, *Puncture Drop Test No. F3*. In that case, the overpack cover did not have a puncture-resistant plate, and the bar penetrated through the thickness of the octagonal region and left a depression in the lid outer sheet. However, the inner (containment boundary) sheet of the lid showed only insignificant deformation, and the test unit was leaktight. Due to the addition of the puncture-resistant plate to the overpack cover, and to the somewhat lighter

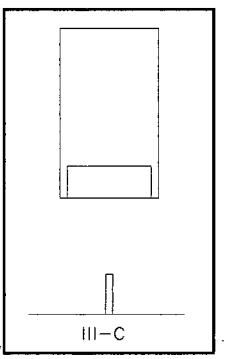

weight of the TRUPACT–III package compared to the full-scale equivalent weight of the engineering test unit, the margin of safety demonstrated in prior testing will be increased, and this puncture drop does not need to be performed.

D. Puncture on the Closed end Center. This orientation is similar to the one discussed in Section 2.7.3.1(C), *Puncture on the Overpack Cover Center*, except that the location is the center of the closed end octagonal area instead of the overpack cover. For the same reasons given in that section, this puncture drop does not need to be performed.

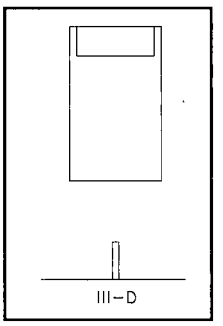

E. Puncture on the Overpack Cover Joint (Front Side). The purpose of this puncture is to damage the thermal protection of the lid elastomeric containment seal by compromising the integrity of the cheek structure. It is at an angle away from the package, in an attempt to tear the cheek away from the package, exposing the edge of the lid. Although the bar axis is not through the c.g., the damage is done before the package can rotate very far. The angle between the bar and package is not critical. The impact point is essentially on the ISO corner fitting, since this structure is a fairly rigid region and will help to distribute the load to the cantilever root of the cheek. An engineering test in this orientation was performed as described in Section 2.12.1.7.2.5, *Puncture Drop Test No. P2*. Essentially no damage resulted from this test. This demonstrated the effective resistance of the TRUPACT–III package to this mode of failure, and this puncture drop does not need to be performed.

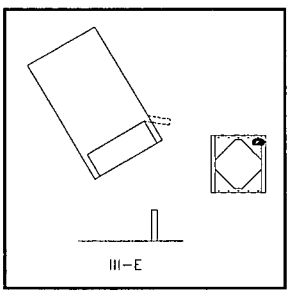

F. Puncture on the Overpack Cover Joint (Top/Bottom). The purpose of this puncture is to damage the thermal protection of the lid containment seal by opening up the joint between the overpack cover and body along the top or bottom of the package. This is an oblique impact on the overpack cover joint, aimed toward the package end so as to penetrate as deeply as possible. The bar axis is aimed away from the c.g., since damage is likely to be greater if the bar force is towards the nearby package end. If the bar were aimed toward the package c.g., the structure is more resistant to puncture due to the presence of the puncture-resistant plate, and any damage that occurred would tend to be further from the lid sealing area. The angle between the bar and package is not critical. An engineering test in this orientation was performed as described in Section 2.12.1.7.2.6, *Puncture Drop Test No. P3*. The impact point was in the region of slapdown secondary free drop damage. The resulting combined damage was not bounding compared to the combination of c.g.-over-corner free drop and puncture damage. For this reason, this puncture drop does not need to be performed.

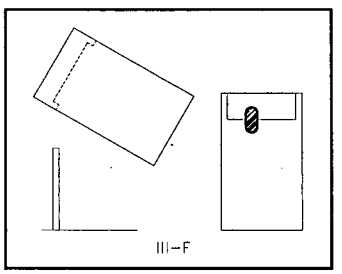

G. Puncture on the C.G.-over-Corner Drop Damage. The damage from the c.g.-over-corner free drop resulted in the greatest local crush distance, as described in Section 2.7.1.4.1, *Vertical, Lid Down Free Drop Results*. Therefore, the addition of puncture damage to the free drop damage may be bounding. This puncture drop was performed on CTU-1 using the same orientation as in the free drop test. It was also performed on CTU-2 to maximize the damage following free drop LD91.

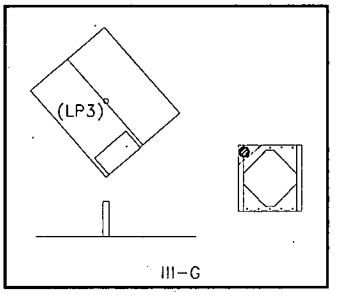

H. Puncture on the Side-Edge Drop Damage. The side-edge drop damage will result in deformation in the vicinity of the thermal shield (see Section 2.7.1.1.2(B), *Side-Edge Free Drop*). Puncture on this damage might interfere with the function of the thermal shield. The puncture bar should attack the package in a manner to cause the greatest compromise of the thermal shield. A puncture bar alignment through the package c.g. would be too steep (~45°) for maximum damage to occur. If the bar impacted the package at a lesser angle, more damage would likely occur even though it was not through the c.g. This puncture was performed with the package axis oriented at 30° to the horizontal for the worst case ripping effect on the damaged area opposite the thermal shield.

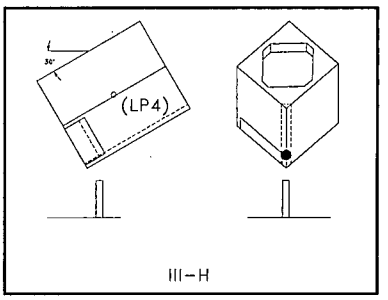

I. Puncture on the Region Outside the Puncture-Resistant Structure. As seen in Detail AX on sheet 20 of the drawings in Appendix 1.3.1, *Packaging General Arrangement Drawings*, there is a small region, 96 mm long, between the end of the puncture-resistant structures in the overpack sides and the inside end of the containment (inner shell of the CSA). Since this region lacks the puncture-resistant structures, it should be tested to ensure containment boundary integrity. Aiming the puncture bar through the package c.g. is not worst-case for two reasons. First, the angle between the bar and the package would be too small to allow it to rip into the outer skin. In other words, the bar axis and the package axis would differ by only 35°, which would likely cause the bar to glance off of the side and not penetrate the outer skin. Second (assuming that the bar did penetrate the outer skin), for a test through the package c.g., because of the small size of the subject region, the bar would strike either the strong corner-diagonal plate of the CSA (10-mm plate) or the strong end plate of the puncture-resistant region (8-mm plate). However, an angle of the package to the ground of 40° allows the bar to miss these structures, and aim at the weakest part of this region, as shown in Figure 2.7-4. It is also in the range of orientations where ripping into the outer skin is likely. This puncture was performed on the bottom side of the package between the rails, since the two vertical sides and the top side have significant reinforcements on the inner containment walls (i.e., the guide bars, see Figure 1.1-5).

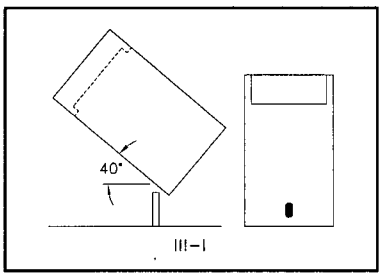

Summarizing the above discussions, the puncture drop tests performed on CTU-1 were:

- On Side Free Drop Damage (Section 2.7.3.1(A))
- On Overpack Cover (Section 2.7.3.1(B))

- On CG-Over-Corner Free Drop Damage (Section 2.7.3.1(G))
- On Side-Edge Free Drop Damage (Section 2.7.3.1(H))

The puncture drop tests performed on CTU-2 were:

- On CG-Over-Corner Free Drop Damage (Section 2.7.3.1(G))
- On the Region Outside the Puncture-Resistant Structure (Section 2.7.3.1 (I))

This information is summarized in greater detail in Table 2.7-2 and depicted in Figure 2.7-5 and Figure 2.7-6. To facilitate rigging CTU-1, the order of tests was LP3, LP4, LP1, and LP2.

2.7.3.2 Temperature of Puncture Drops

Since the puncture resistance of the TRUPACT–III is not significantly affected by temperature, all puncture drop tests were performed at ambient temperatures. The primary means of puncture resistance is afforded by the use of puncture-resistant plates, which are embedded in the overpack materials all over the package. There are three types of puncture-resistant plate. (1) On the longitudinal faces of the package, the plates are made of 10-mm thick Alloy UNS S31803 stainless steel, with a 60-mm thick layer of balsa wood on the outside. The inside layer is 0.10 kg/dm^3 polyurethane foam which is 109 mm thick on the top and bottom sides and 114 mm thick on the vertical sides. (2) On the recessed regions of the ends (overpack cover and closed end), the stainless steel plates are 15-mm thick. The outer layer is 60-mm thick balsa wood, and the inner layer is 120-mm thick, 0.10 kg/dm^3 polyurethane foam. (3) On the thicker, non-recessed regions of the ends, the sheets are fabricated of 6 mm thick Alloy UNS S31803 stainless steel, sandwiched between a 140-mm thick layer of 0.16 kg/dm^3 polyurethane foam on the outside and a massive block of 0.48 kg/dm^3 polyurethane foam on the other side. The edges of the puncture-resistant plates are essentially free to deform, since they are attached locally only by rivets or short tack welds. The material has been tested for ductility at cold temperatures according to ASTM E604[7]. Test specimens were as thick as or thicker than the puncture-resistant plates, and fabricated from fully certified material. Five specimens of the steel were tested at a temperature of -29 °C, and the results demonstrated 100% shear (i.e., ductile behavior) on each of the broken surfaces. Therefore, the behavior of the material at the regulatory cold temperature is ductile in nature. Since the puncture behavior is primarily dependent on a material that is ductile at both the cold and ambient temperatures, the extent and type of puncture damage will be essentially the same at ambient temperature as it would be at cold temperature.

2.7.3.3 Summary of Results from Puncture Drop Tests

The results of each of the puncture tests evaluated are described below indicating the reference number as listed in Table 2.7-2. Under each heading, the results of the puncture test are described. For puncture drop tests on CTU-1, detailed descriptions, results, and photographs are given in Appendix 2.12.3, *Certification Tests on CTU-1*. For puncture drop tests on CTU-2, see Appendix 2.12.6, *Certification Tests on CTU-2*. No puncture test caused significant weld tears or exposed significant amounts of foam.

[7] ASTM E604-83, *Standard Test Method for Dynamic Tear Testing of Metallic Materials.*

2.7.3.3.1 Puncture on Side Results (CTU-1, Ref. No. LP1)

The ambient temperature for this test was 22 °C. The puncture bar penetrated both the outer skin and the puncture-resistant plate, and left a dent of approximately 51 mm deep in the CSA outer structural sheet. There was no cutting or cracking of the CSA outer structural sheet, demonstrated by placing the CSA annular region under a vacuum. There was no deformation of the inner CSA containment sheet. The opening in the overpack was 254 mm long and 178 mm wide.

2.7.3.3.2 Puncture on Overpack Cover Results (CTU-1, Ref. No. LP2)

The ambient temperature for this test was 17 °C. The puncture bar struck the overpack cover approximately 292 mm from the left edge of the octagonal recess. The bar penetrated the outer sheet, and left a dent in the puncture-resistant plate approximately 145 mm deep. However, the puncture-resistant plate was not penetrated nor cracked. Removal of the overpack cover showed the impact to have been aligned between two V-stiffeners in the closure lid. A dent of approximately 5 mm deep was left in the outer sheet of the closure lid at the puncture location. There was no deformation of the inner closure lid containment sheet.

2.7.3.3.3 Puncture on CG-Over-Corner Results (CTU-1, Ref. No. LP3)

The ambient temperature for this test was 17 °C. The puncture bar struck at essentially the center of the prior c.g.-over-corner free drop (LD4) damage and created a further deformation of approximately 102 mm deep and 178 mm in diameter. The effect of the impact was to further locally compress the deformed materials in the damaged zone. Small amounts of foam were visible from the free drop test damage, and the puncture test did not significantly alter this. After cutting away the damaged material, a minimum distance of 51 mm was measured between the deformed steel resulting from the puncture drop and the nearest part of the calcium silicate protection box (i.e., thermal shield). This distance was filled with compressed, 0.48 kg/dm^3 foam.

2.7.3.3.4 Puncture on Side-Edge Results (CTU-1, Ref. No. LP4)

The ambient temperature for this test was 16 °C. The puncture bar struck on the prior damage from free drop test LD5, with the center of the bar placed approximately 584 mm from the cover end of the package, with the package inclined 30° from the horizontal. The bar penetrated the outer skin and struck the top corner of the thermal shield. This structure, made from 16 mm-thick plate material, is very rigid. Later disassembly showed relatively minor weld cracks in this region and only approximately 3 mm of deformation of the thermal shield, local to the impact. There was no damage to the calcium silicate insulating board, which maintained full integrity without crumbling or breaking.

No puncture drop test was able to significantly deform the closure lid sealing area, nor was any test able to impart significant damage to the thermally-relevant overpack structures protecting the containment sealing area. For thermal analysis, the worst-case damage from puncture was combined with the worst-case damage from free drop, as discussed in Section 3.5.2.6, *Description of Thermal Model for HAC Conditions.* The results of the puncture tests demonstrate that the TRUPACT–III can withstand the HAC puncture drop event without significant damage.

2.7.3.3.5 Puncture on CG-Over-Corner Results (CTU-2, Ref. No. LP91)

The ambient temperature for this test was 15 °C and the package surface temperature was 19 °C. The puncture bar struck on the overpack cover portion of the prior c.g.-over-corner free drop (LD91) damage. The depth of puncture, measured to the center of the damage hole in an axial direction from the undeformed surface of the overpack cover, was 146 mm. The damage loosened the entire lower quadrant of the overpack cover outer sheet and a significant portion of the low density (0.16 kg/dm^3) foam fell out. The bar corner partially sheared into the 6-mm thick puncture resistant plate located between the low density and high density (0.48 kg/dm^3) foam by an amount of 38 mm. However, little of the high density foam was exposed and essentially none was lost.

2.7.3.3.6 Puncture on Region Outside Puncture-Resistant Structure (CTU-2, Ref. No. LP-92)

The ambient temperature for this test was 12 °C, and the package surface temperature was 15 °C. The puncture bar struck as shown in Figure 2.7-6. The bar penetrated the outer skin and impacted the CSA outer structural sheet, creating a crack in the weld between the structural sheet and the rear diagonal corner stiffener of the CSA, and in some of the adjacent plug welds which connect the outer structural sheet to the V-stiffener nearest the impact. However, there was no evidence of any dent or bulge in the CSA inner (containment) sheet at the puncture site. In addition, the containment boundary was leaktight after all testing was completed.

Table 2.7-2 – Summary of Puncture Drops Performed on the TRUPACT–III

Test Description	Discussion Paragraph	Test Ref. No.	Orientation	Purpose
On Side Free Drop Damage (CTU-1)	Section 2.7.3.1(A)	LP1	Bar axis 70° to surface, thru c.g.	Test ability of puncture-resistant design to resist penetration at worst-case oblique angle.
On Overpack Cover (CTU-1)	Section 2.7.3.1(B)	LP2	Bar axis 65° to surface, thru c.g., impact in octagonal recess	Test ability of puncture-resistant design to resist penetration on package end.
On C.G.-over-Corner Free Drop Damage (CTU-1)	Section 2.7.3.1(G)	LP3	Bar axis thru c.g., centered on free drop damage	Quantifies possible maximum accumulation of free drop and puncture damage.
On Side-Edge Free Drop Damage (CTU-1)	Section 2.7.3.1(H)	LP4	Bar axis 60° to edge, not thru c.g., centered on thermal shield/seal area	Quantifies possible maximum accumulation of free drop and puncture damage.
On C.G.-over-Corner Free Drop Damage (CTU-2)	Section 2.7.3.1(G)	LP91	Bar axis thru c.g., centered on free drop damage	Quantifies possible maximum accumulation of free drop and puncture damage following free drop LD91.
On Region Outside Puncture-Resistant Structure (CTU-2)	Section 2.7.3.1(I)	LP92	Package 40° to horizontal, bar not thru c.g., contact approx. 476 mm from closed end	Test ability of puncture-resistant design to resist penetration in subject region.

Note: For convenience in rigging the tests on CTU-1, the order of testing was LP3, LP4, LP1, and LP2.

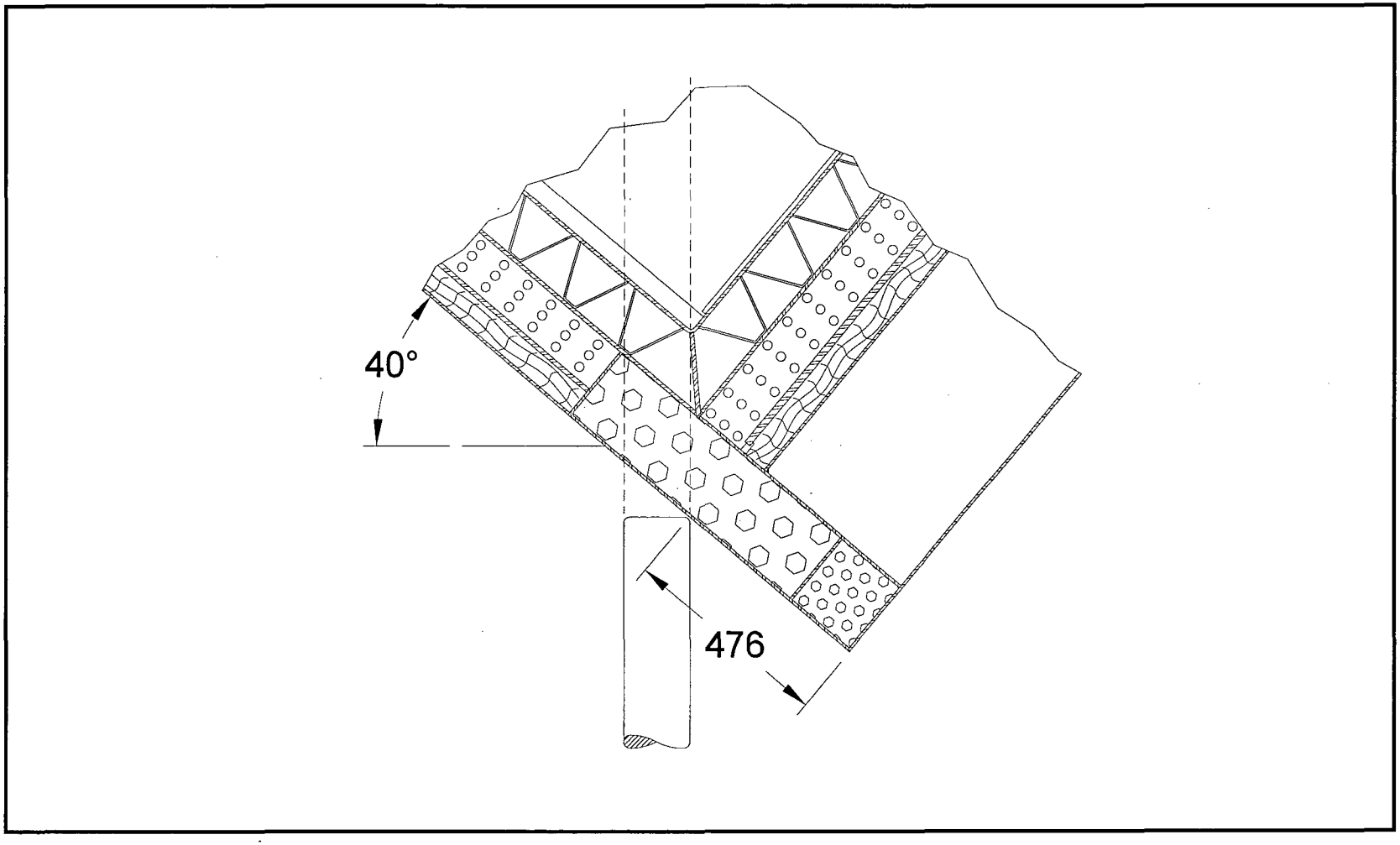

Figure 2.7-4 – Puncture On Region Outside Puncture Resistant Structure

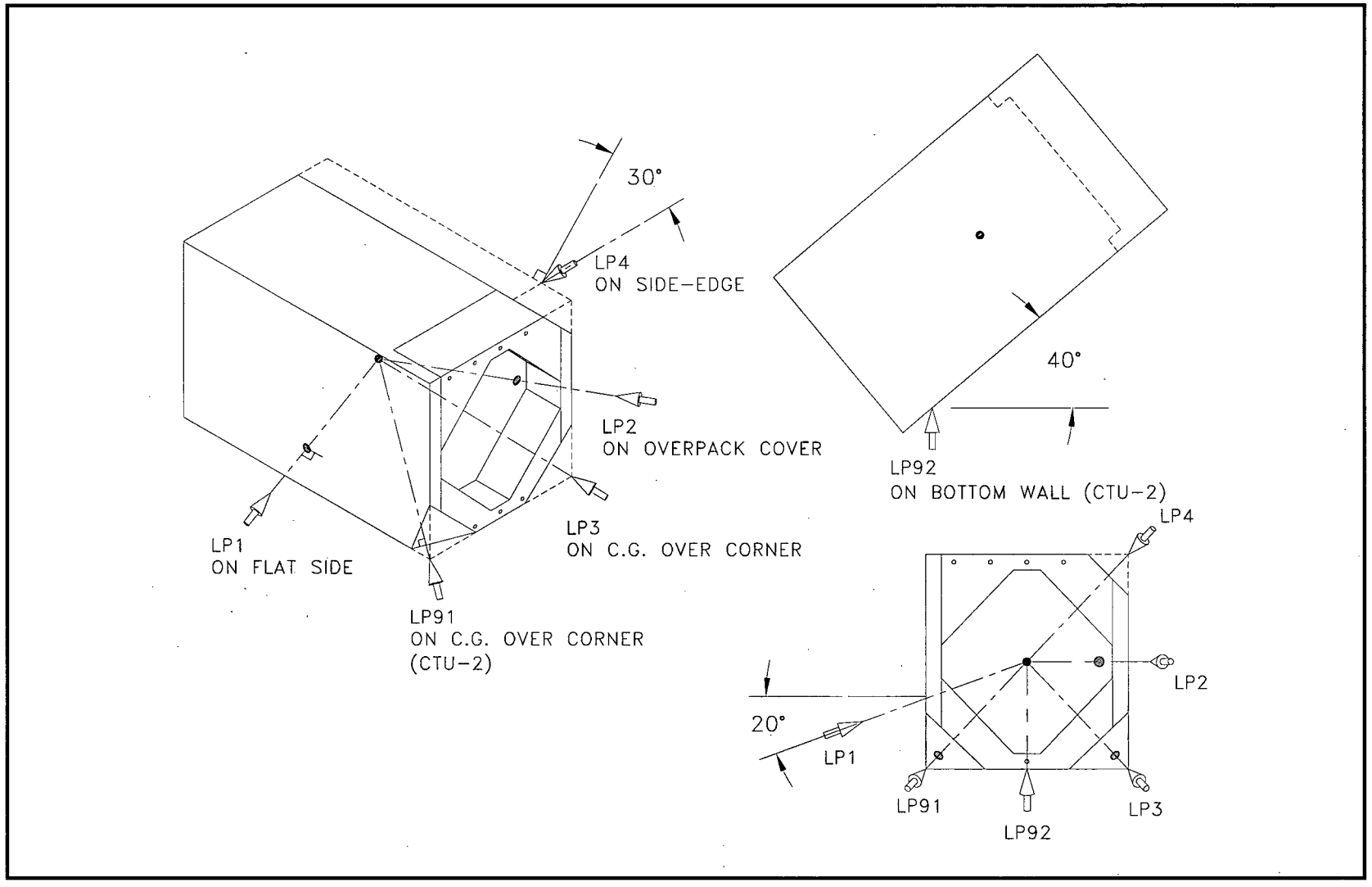

Figure 2.7-5 –TRUPACT–III Package Puncture Drop Orientations

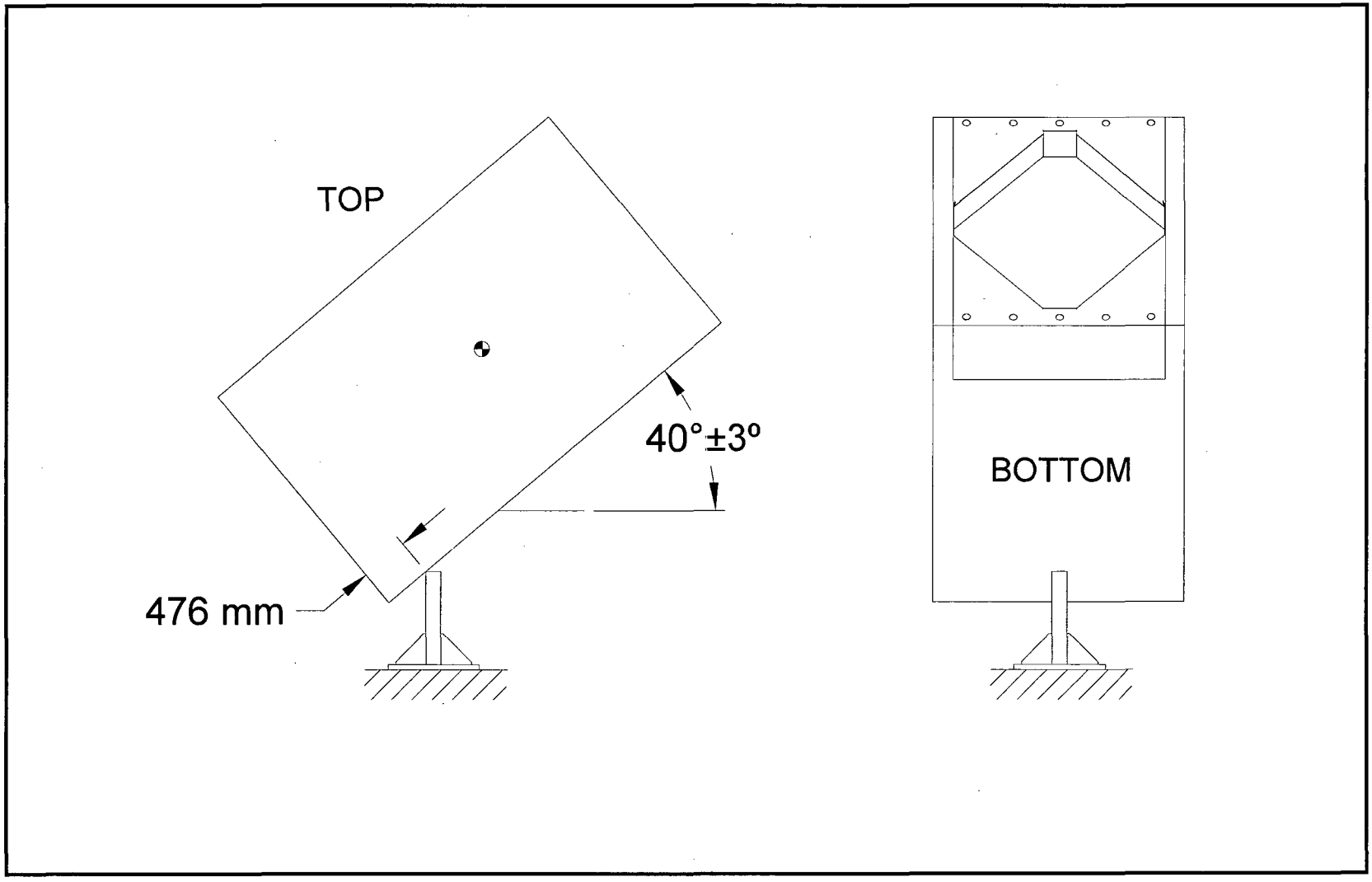

Figure 2.7-6 –TRUPACT–III Package Puncture Drop Orientation LP92

This page intentionally left blank.

2.7.4 Thermal

The TRUPACT–III is designed to withstand the HAC 30 minute fire specified in 10 CFR §71.73(c)(4). The thermal evaluation is presented in Section 3.4, *Thermal Evaluation under Hypothetical Accident Conditions*.

2.7.4.1 Summary of Pressures and Temperatures

As determined in Section 3.3.2, *Maximum Normal Operating Pressure*, the maximum normal operating pressure (MNOP) in the TRUPACT–III, including the effects of heat-up of ambient pressure air, generation of water vapor, and payload gas generation, is 172 kPa gauge. As discussed in Section 3.4.3, *Maximum Temperatures and Pressure*, the change in pressure due to the HAC thermal event is 77.3 kPa. This value conservatively considers the combination of the worst-case damage scenario and the bounding payload. From Table 3.4-1, the peak temperature of the CSA structural sheet is 689 °C, which is reached at the end of the 30-minute fire, and falls rapidly thereafter. This temperature is limited to a small region local to the modeled puncture damage. Although it exceeds the stated limit of 316 °C of the UNS S31803 material, it will not affect the ability of the package to maintain containment nor significantly inhibit post-accident recovery operations as discussed in Section 3.4.3.1, *Maximum HAC Temperatures*. The CSA containment sheet reaches a peak temperature of 222 °C, and the closure lid bolt peak temperature is 187 °C.

2.7.4.2 Differential Thermal Expansion

Differential thermal expansion is not of concern for the TRUPACT–III package. The package has a single containment, thus interference between two containment vessels is not possible. It has no shielding components such as lead or neutron shielding, and therefore no interference between package structures and shielding materials is possible. The maximum temperature for the CSA outer sheet stated in Section 2.7.4.1, *Summary of Pressures and Temperatures*, is for an area local to the puncture damage, and which is very small in relation to the CSA as a whole. Since the CSA outer sheet and containment sheets are connected with a large number of V-stiffeners which conduct heat, their overall temperatures do not differ significantly (except local to the puncture damage), and since they are made of the same material, differential thermal expansion between the CSA outer and containment sheets may also be neglected.

The only structurally significant components not made of UNS S31803 stainless steel are the lid closure bolts, which are made of ASTM A320, L43-material. Since the bolt is in intimate contact with the closure lid, the lid and bolt temperatures are essentially equal. The difference in thermal expansion coefficient between the two materials is small, as seen from Section 2.2.1, *Material Properties and Specifications*. At a temperature of 204 °C (greater than the peak closure bolt temperature), the difference is less than 7%. Since the closure lid is made of the material having the greater coefficient, an increase in temperature of the closure lid and bolt components leads to an increase in bolt clamping load, although due to the proximity of thermal expansion coefficients, the change is negligible. Therefore, differential thermal expansion of the closure bolts is not of concern.

2.7.4.3 Stress Calculations

Stresses in the TRUPACT–III package CSA are calculated for NCT in Section 2.6.1.3, *Stress Calculations*. Since those calculations included the MNOP of 172 kPa gauge along with the reduced external pressure of 25 kPa absolute, the stress computed corresponded to a net differential pressure of (172 + 101.3 – 25) = 248.3 kPa. Under HAC, the reduced external pressure is not required, and considering the HAC thermal event maximum pressure increase of 77.3 kPa, the HAC net differential pressure is only (172 + 77.3) = 249.3 kPa. The NCT calculated stresses may therefore be increased by the ratio 249.3/248.3 = 1.004 for HAC. From Section 2.6.1.3, *Stress Calculations*, the maximum membrane stress at any location is 153 MPa and the maximum membrane-plus-bending stress is 222 MPa. The equivalent stresses for HAC are:

Membrane:	153 × 1.004 =	154 MPa
Membrane-plus-bending:	222 × 1.004 =	223 MPa

2.7.4.4 Comparison with Allowable Stresses

As discussed in Section 3.4.3.1, *Maximum HAC Temperatures*, a small region of the CSA structural (outer) sheet will experience a maximum temperature whereby some reduction in ductility of the material may occur, although the time at temperature is not sufficient for the full embrittlement effect to occur. A reduction in ductility of the CSA structural sheet is not of concern for two reasons:

- The containment boundary components, having a maximum temperature of 222 °C, do not exceed the continuous-use temperature limit given by ASME Code Case N-635-1 (i.e., the highest temperature in the material property table of 316 °C). Therefore no reduction of ductility of the containment boundary components will occur.
- The fire test is the last hypothetical accident condition which is applicable per 10 CFR 71. As such, the only subsequent structural loads occurring for the package will arise from accident recovery operations. Therefore, even if reduction in ductility does occur over a small portion of the CSA structural sheet, no safety impact will result since sufficient ductility will remain to allow recovery operations. Of note, the average CSA structural sheet temperature equals 75 °C.

From Table 2.2-1 at a temperature of 316 °C, S_m = 185 MPa, and S_u = 556 MPa. From Table 2.1-1, the membrane stress allowable is the lesser of $2.4S_m$ or $0.7S_u$, which in this case equals 389 MPa. The membrane-plus-bending allowable is the lesser of $3.6\ S_m$ or S_u, which in this case is 556 MPa. The margin of safety on CSA membrane stress is:

$$MS = \frac{389}{154} - 1.0 = +1.53$$

The margin of safety on CSA membrane-plus-bending stress is:

$$MS = \frac{556}{223} - 1.0 = +1.49$$

Therefore, stresses in the TRUPACT–III package in the HAC thermal event are acceptable.

Per Regulatory Guide 7.6, paragraph C.7, the extreme range of stress must be considered. Of all the various allowable stresses corresponding to the different conditions evaluated (including fabrication stresses and normal conditions of transport), the largest allowable stress is equal to the material ultimate strength S_u. It is therefore conservative to assume that S_u bounds all stresses actually developed in the structure. For Alloy UNS S31803 stainless steel, S_u = 621 MPa at 38 °C. The maximum possible stress intensity range is twice this value, or 1,242 MPa. Applying a factor of four to account for possible stress concentrations at structural discontinuities gives a total stress range of 4,968 MPa. The alternating component is one-half of this value, or 2,484 MPa. To account for temperature effects, this value of alternating stress is factored by the ratio of modulus of elasticity. The ratio is formed between the modulus of elasticity at 38 °C and the design temperature of 71 °C. The adjusted stress is:

$$S_{alt} = 2{,}484\frac{E_{38}}{E_{71}} = 2{,}515 \text{ MPa}$$

where E_{38} = 194,000 MPa and E_{71} = 191,600 MPa. Per Table I-9.1M of the ASME Code (conservatively using the lower curve, for UTS of 793 - 896 MPa), the allowable value for S_{alt} at 10 cycles is 2,896 MPa. The margin of safety is:

$$MS = \frac{2{,}896}{2{,}515} - 1.0 = +0.15$$

Considering the significant conservatism used in the underlying assumptions (e.g., use of allowable stress rather than smaller actual stresses, assuming worst-case stresses are fully reversing, use of the maximum factor of stress concentration, use of the lower fatigue curve), it is apparent that the actual margin of safety is larger than 0.15. Thus, the requirement of paragraph C.7 of Regulatory Guide 7.6 is met.

2.7.5 Immersion – Fissile Material

Subpart F of 10 CFR 71 requires performing an immersion test for fissile material packages in accordance with the requirements of 10 CFR 71.73(c)(5). The criticality evaluation presented in Chapter 6.0, *Criticality Evaluation*, assumes optimum hydrogenous moderation of the contents, thereby conservatively addressing the effects and consequences of water in-leakage.

2.7.6 Immersion – All Packages

Subpart F of 10 CFR 71 requires performing an immersion test for all packages in accordance with the requirements of 10 CFR 71.73(c)(6). This condition is evaluated by analysis of the effects of a 150 kPa gauge pressure applied to the outside of the CSA.

The stress results are bounded by the analysis presented in Section 2.6.1.3, *Stress Calculations*, in which an internal gauge pressure of 172 kPa is used. Therefore, the immersion case is governed by allowable buckling loads. The buckling analysis for the TRUPACT–III package is presented in Section 2.12.4, *HAC Immersion Buckling Evaluation*. In that analysis, an external gauge pressure of 150 kPa is applied to the package, conservatively assuming an internal pressure of zero gauge. As shown, the stress in the most critical sidewall due to a combination

of normal pressure loading and wall edge loads is 88.7 MPa. The allowable inelastic buckling load is 391 MPa. The factor of safety against buckling is

$$FS = \frac{(\sigma_{cr})_x}{\sigma} = \frac{391}{88.7} = 4.41$$

This is considerably in excess of the minimum factor of safety of 1.34 for HAC per ASME Code Case N-284-1, corresponding to ASME Code, Service Level D conditions. Therefore, the immersion load of 150 kPa gauge is not of concern.

2.7.7 Deep Water Immersion Test (for Type B Packages Containing More than 10^5 A_2)

Subpart E of 10 CFR71 requires performing a deep water immersion test in accordance with 10 CFR §71.61. Since the TRUPACT–III does not transport payloads with an activity of greater than 10^5 A_2, this requirement does not apply.

2.7.8 Summary of Damage

From the discussions presented in Section 2.7.1 through 2.7.7, it is shown that the hypothetical accident sequence does not result in any significant structural damage to the TRUPACT–III package, and that the criteria established for hypothetical accident conditions in Section 2.1.2, *Design Criteria*, are satisfied. Full-scale physical model testing, including free drop and puncture tests on two certification test units, have shown that:

- The package can sustain a worst case free drop and puncture while remaining leaktight using the leak rate criterion of 1×10^{-8} Pa-m^3/s, air, per ANSI N14.5. Post-test leakage rate testing demonstrated that the containment metallic boundary, closure lid O-ring seal, and vent port insert O-ring seal remained leaktight after the conclusion of all certification testing on CTU-2. On CTU-1, the containment metallic boundary and the vent port insert O-ring seal remained leaktight, but the closure lid O-ring seal did not, due to the presence of debris in the sealing nip. The results from the testing of CTU-1 are further discussed in Section 2.7.8.1, *Debris Contamination of the Containment Seal on CTU-1.* The debris shield, which was fully implemented in CTU-2, was not present in CTU-1. The performance of the debris shield in preventing contamination of the containment O-ring seal was successfully demonstrated in the CTU-2 tests.
- Closure bolts retained an average of 56% of the initial tightening torque on CTU-1 after four HAC free drops and four puncture drops, and 79% of the initial tightening torque on CTU-2 after one HAC free drop and two puncture drops. The performance of the closure bolts is discussed in Section 2.7.8.2, *Closure Bolts*.
- The containment boundary was unaffected by any puncture test. The outer structural sheets of the CSA were subject to insignificant deformations or weld cracks local to the puncture bar impact, but no deformation of the inner containment components of the CSA was observed to occur from any puncture test on CTU-1 or CTU-2.
- Distortion or buckling of the CSA does not occur (see Section 2.7.1.4.1, *Vertical, Lid Down Free Drop Results*).

- The overpack cover is securely retained on both CTU-1 and CTU-2. At the conclusion of all testing, the overpack cover was still securely fastened to the body.
- Criticality assumptions regarding package reconfiguration are supported.
- Thermal fire event analysis assumptions regarding the integrity of thermal insulation and exposure of polyurethane foam are supported.

In addition, calculations have shown that the stress criteria of Table 2.1-1 are satisfied for the thermal and immersion events (see Section 2.7.4.4, *Comparison With Allowable Stresses* and Section 2.7.6, *Immersion – All Packages*, respectively).

Therefore, the TRUPACT–III package satisfies all of the requirements of 10 CFR §71.73.

2.7.8.1 Debris Contamination of the Containment Seal on CTU-1

As discussed in Section 2.12.5.2, *Contamination of the Containment O-ring Seal During Certification Testing*, the initial helium leakage rate test performed on the closure lid containment O-ring seal of CTU-1 at the conclusion of the certification test was not successful due to contamination of the sealing nip. The contamination was found to be in the form of small shards and flakes of aluminum, which were generated by the numerous collisions of the aluminum round bars which made up the CTU simulated payload. As a result of free drop impact, a transient gap can open between the CSA body and closure lid flanges. In certification testing, the debris from the simulated payload was transported across the containment seal with the aid of the internal air pressure, equal to MNOP. Even though the flanges returned to contact after only a few milliseconds, the seal was not leaktight per the criterion of 1×10^{-8} Pa-m^3/s, air, per ANSI N14.5. Since small amounts of grit or dirt could be present in the payload cavity in normal operation, a debris shield is utilized to ensure maintenance of a leaktight containment seal under all free drops and puncture drops. The debris shield shown in the drawings of Appendix 1.3.1, *Packaging General Arrangement Drawings*, is effective in preventing containment seal contamination, as demonstrated by the tests performed on CTU-2. A discussion of how the debris contaminated the CTU-1 containment seal, the design considerations for the debris shield, and an analytical evaluation of the effectiveness of the shield, are presented in Section 2.12.5, *Closure Lid Debris Shield.*

2.7.8.2 Closure Bolts

During the post-test disassembly of CTU-2, all of the closure bolts were found to be in good condition, having an average residual loosening torque of 79% of the initial tightening torque. The loosening torque is generally expected to be on the order of 75% of the tightening torque, even if no external loads are applied to the joint. Therefore, an average residual torque of 79% after application of HAC test loads is in the expected range. None of the bolts showed any bending deformation, nor was there evidence of any bolt heads being contacted by the overpack cover recess cups. Many of the closure bolt washers did show evidence of contact with the overpack cover recess cups, (evident also in the corresponding cups). However, evidence of contact of a washer with a cup did not correlate to lower residual loosening torque for the corresponding bolt. Details of the CTU-2 post-test results are given in Section 2.12.6.8, *Leakage Rate Tests and Post-Test Measurements.*

During post-test disassembly of CTU-1, it was discovered that some of the closure bolts, particularly on the right flange, had a residual torque which was significantly below the average for all bolts. The bolts having below-average residual torque were found to be bent. There was strong correlation between the amount of bending and the lowness of the residual torque. The greatest bending and lowest residual torque occurred close to the center of the right side of the lid. Moving towards each end of the right side (i.e., the top right corner and the lower right corner), bolt bending approached the as-fabricated average runout, and the residual torque approached the non-bent average value. Each of the affected bolts was bent in two opposite directions, with the axes of the threaded portion and of the bolt head nearly parallel, but with an offset. These bolts showed evidence of having been struck laterally on the bolt head, and the location of the strike aligned with the direction of bending. It was noted that the direction of bending, relative to the CTU, generally aligned with the 11:00 o'clock azimuth. The right side of the lid moved upward along the same orientation, and the guide pin on the right side was sheared by approximately 4.3 mm in the same direction. More details regarding the CTU-1 post-test findings is provided in Section 2.12.3.8.2.1, *Body Flange and Closure Lid Observations*, and Section 2.12.3.8.2.2, *Closure Lid Bolt Removal Torque and Related Observations*. It is apparent that the bolt bending was caused by the side impact on the bolt heads from the overpack cover recess cups, that struck the heads during a lateral translation of the overpack cover, which in some cases also struck the edge of the washer. Contact may have occurred in more than one free drop, but most likely the primary case was free drop LD4, the CG-over-corner orientation, based on the direction of bending. Because of the number of tests performed on CTU-1 (four HAC free drops and four puncture drops), the condition of the bolts was likely caused by, or at least exacerbated by, overtesting.

Two helium leakage rate tests were performed on CTU-1 to determine whether the non-leaktight condition of the closure lid O-ring seal was due to the reduced clamping load of the bolts on the right side, or due to the debris on the seal. For the first test, the seal surfaces were wiped clean of debris (without removing them from the lid), and the lid was reinstalled with all 44 closure bolts tightened to the lowest residual tightening torque of all bolts, equal to 149 N-m (see Table 2.12.3-4). This was very conservative since it represented only one-sixth of the average measured residual tightening torque of all 44 bolts of 898 N-m. Upon repeating the standard helium leakage rate test for the CTU, the testing criterion of a leakage rate less than 1×10^{-8} Pa-m^3/s, air, per ANSI N14.5, was achieved. For the second test, the lid was removed and reinstalled with only the four corner bolts installed and tightened to 149 N-m. This configuration represented a hypothetical case of the loss of preload on all four sides of the lid. The standard helium leakage rate test for the closure lid seal was repeated, and was again successful to the same criterion. These two tests demonstrated that only a negligible clamping force is required to obtain a leaktight seal between the lid and body of the TRUPACT–III, and that a significant preload reduction due to closure bolt damage can be sustained without affecting the leaktight condition of the closure O-ring seal as long as the seal is not contaminated by debris. With the implementation of the debris shield that was successfully demonstrated in CTU-2, the TRUPACT-III package will remain leaktight in the presence of any damage to the closure bolts that could credibly occur.

2.8 Accident Conditions for Air Transport of Plutonium

This section does not apply, since air transport is not used with the TRUPACT–III package.

This page intentionally left blank.

2.9 Accident Conditions for Fissile Material Packages for Air Transport

This section does not apply, since air transport is not used with the TRUPACT–III package.

This page intentionally left blank.

2.10 Special Form

This section does not apply, since special form is not claimed for the TRUPACT–III package.

This page intentionally left blank.

2.11 Fuel Rods

This section does not apply, since fuel rods are not included as an approved payload configuration for the TRUPACT–III package.

This page intentionally left blank.

2.12 Appendices

2.12.1 Engineering Tests

2.12.2 Elastomer O-ring Seal Performance Tests

2.12.3 Certification Tests on CTU-1

2.12.4 HAC Immersion Buckling Evaluation

2.12.5 Closure Lid Debris Shield

2.12.6 Certification Tests on CTU-2

2.12.7 Closure Lid, Bolt, and Washer Interaction

This page intentionally left blank.

2.12.1 Engineering Tests

This appendix documents the results of engineering free drop and puncture tests that have been performed in support of the TRUPACT–III certification. The results of these tests are used to guide the choice of test orientations and conditions in the full-scale certification test program, and to support calculations documented in Section 2.7.1.5, *Crush Deformation Extrapolations.* The certification test results are documented in Appendix 2.12.3, *Certification Tests on CTU-1* and in Appendix 2.12.6, *Certification Tests on CTU-2.*

2.12.1.1 Introduction

A large number of free drop and puncture tests were performed on the engineering test unit (ETU), which was fabricated as prototypical, in half-scale, to the TN-Gemini packaging. The TRUPACT–III packaging is a close derivative of the TN-Gemini, and for this reason, the test results recorded in this appendix are applicable to the TRUPACT–III. Differences between the ETU and the TRUPACT–III are detailed in Section 2.12.1.3, *Test Unit Configuration.* All of these tests were performed on the same half-scale test unit. Some refurbishment of the test unit occurred during the course of testing as described below.

A total of 23 engineering tests were performed: two NCT, 0.3-m free drops, eight HAC, 9-m free drops, and 13 puncture drops. Free drop tests were performed on a flat, essentially unyielding surface from a height of either 0.3 m (NCT) or 9 m (HAC). Puncture tests were performed using the puncture bar described in 10 CFR 71.73(c)(3), in half-scale, dropped from a height of 1 m. Free drop tests were performed at ambient and cold (-29 °C) temperatures. Most free drops were instrumented with accelerometers. Details concerning test parameters are given below.

The engineering tests comprised primarily three separate test series: The first, performed in support of the French certification of the TN-Gemini, took place in France in 1994. After refurbishment of the overpack structures and the closure lid, the second series took place in the U.S. in 2003. Further testing occurred in the U.S. in 2005. Each of these test series is described and documented in the following sections.

The engineering test results demonstrate the robust nature of the TN-Gemini and TRUPACT–III packaging designs. It is noteworthy that the ETU containment structural assembly (CSA) body structure experienced all 23 tests without refurbishment, only two different closure lids were used, and the external overpack structures were refurbished only once (a small region on the closed end was refurbished twice). With the exception of a single puncture test in 1994 (see below), the test unit was leaktight (a leak rate not exceeding 1×10^{-8} Pacals–cubic meters per second (Pa–m^3/s), air, as defined in ANSI N14.5) after each test.

2.12.1.2 Test Facilities

The test facilities utilized in France and the U.S. are described below.

2.12.1.2.1 Sandia National Laboratories (U.S.)

Most engineering free drop tests not performed in France were performed at Sandia National Laboratories' Coyote Canyon Aerial Cable Facility in Albuquerque, New Mexico. The drop pad

is designed to accommodate test packages weighing up to 90,000 kg. The embedded steel plate target has a varying thickness of approximately 100 to 200 mm. The pad therefore constituted an essentially unyielding surface for the ETU, which weighed approximately 3,775 kg.

2.12.1.2.2 Engineered Products Department (U.S.)

All puncture tests not performed in France were performed at Washington Group International's (WGI's) Engineered Products Department (EPD) in Carlsbad, New Mexico. In addition, one free drop test was performed there. The drop pad is designed to accommodate test packages weighing up to 12,600 kg. The steel plate target has a thickness of 44 mm, embedded in a reinforced concrete pad.

In accordance with the requirements of 10 CFR §71.73(c)(3), half-scale puncture bars were fabricated from a solid, 75 mm diameter mild steel with three different lengths: 750 mm, 1,200 mm, and 1,800 mm. Each puncture bar was welded with gussets perpendicularly to a 25-mm thick, mild steel, 610-mm square plate. The top edge of each puncture bar was finished to a 3-mm radius maximum. Each puncture bar assembly was securely welded to the impact surface.

2.12.1.2.3 CEA/CESTA (France)

The first series of free drop and puncture testing of the engineering test unit was performed at the Centre d'Etudes Scientifiques et Techniques d'Aquitaine du Commissariat à l'Energie Atomique (CEA/CESTA) in France. The drop pad is designed to accommodate test packages weighing up to 13,800 kg. The steel target consists of a 100-mm thick steel plate anchored in a reinforced concrete pad.

Half-scale puncture bars were fabricated from a solid, 75-mm diameter mild steel of varying length. Each puncture bar was welded perpendicularly to a 20-mm thick, mild steel, 300-mm square plate. The top edge of each puncture bar was finished to a 3-mm radius maximum. Each puncture bar assembly was securely welded to the impact surface.

2.12.1.3 Test Unit Configuration

2.12.1.3.1 U.S. Testing

The ETU was an essentially prototypic representation of the TN-Gemini package, in half-scale. The ETU differed from the TRUPACT–III in several details, however, most differences were either conservative (i.e., tending to lead to greater impact or damage) or not significant (i.e., the ETU test response would be similar to that of the TRUPACT–III.) Any ETU test results that might not be representative of the response of the TRUPACT–III were not used in certification test planning. A discussion of test article scaling is given in Section 2.12.1.4, *Scale Model Testing.*

All plate thicknesses, weld sizes, closure features, and structural dimensions were scaled by a factor of one-half. Over-reinforcement of weld beads was precluded during fabrication. The relatively large size of the ETU facilitated prototypic fabrication. The following list details the differences between the ETU and the full-scale TRUPACT–III.

1. Package length: The ETU full-scale equivalent length was 6,058 mm, whereas the TRUPACT-III length is 4,288 mm. This difference might affect drop performance in some orientations. However, this difference had no effect on data actually utilized from the ETU test results.

2. Package weight: The ETU full-scale equivalent weight was 30,000 kg, whereas the weight of the TRUPACT–III is 25,000 kg. This difference would affect free drop and puncture performance, but generally the differences would be conservative (i.e., the ETU results would in general be worse due to the greater weight).
3. Energy-absorbing materials: The phenolic foam, redwood, and most balsa wood utilized in the ETU are replaced by four different densities of polyurethane foam in the TRUPACT–III (some balsa is retained). The polyurethane foam densities used are engineered to provide similar or better performance (i.e., lower impacts and acceptable maximum deformations) compared to the ETU. Therefore, this substitution is conservative.
4. Debris shield: The ETU did not have a debris shield or guide bars. This had no effect on data utilized from the ETU test results.
5. Overpack seam welds: The configurations of some seam welds on the TRUPACT–III are of a more robust configuration than that utilized on the ETU. This difference had no effect on data utilized from the ETU test results.
6. Puncture-resistant plate design difference: The TRUPACT–III includes a 15-mm puncture-resistant plate in the octagonal recess on both ends, but the ETU (during the 2003 test series) had no puncture-resistant plate in the overpack cover, and a 10-mm thick puncture-resistant plate in the closed end. This difference had no effect on data utilized from the ETU 2003 test results. During the 2005 test series, the octagonal recess at the closed end of the ETU was refurbished to be fully prototypic to the TRUPACT–III design. The puncture test subsequently performed on this structure was therefore directly applicable to the TRUPACT–III design.
7. No thread inserts: The ETU utilized no thread inserts. However, the TRUPACT–III thread inserts are optional, and since the parent material is weaker than the thread inserts, the ETU conservatively represented the minimum pull-out strength possible in a TRUPACT–III.
8. Threaded boss: The thread bosses for the closure bolts of the TRUPACT–III are made from Alloy UNS S31803 material, while the ETU material was Type 304L. Since Alloy UNS S31803 is stronger than Type 304L, this substitution is conservative. In addition, the ETU thread bosses were connected only to the front flange face, where the TRUPACT–III bosses connect to front and rear flange faces. Since the ETU had a weaker, less rigid design, this difference is conservative.
9. Body flange: The body flange on the ETU was made by bending a plate into a U-shape, whereas the TRUPACT–III flange has a welded box structure with thicker inner and outer sheets, as shown in Figure 2.12.1-1. This difference is conservative.
10. CSA Rear Corner Containment Weld Joint: The corner weld joint on the closed end containment sheets was a two-sided fillet weld on the ETU, whereas the weld joint for the TRUPACT–III is a complete joint penetration (CJP) weld with fillet reinforcement. This difference had no effect on data utilized from the ETU test results.
11. Body vents and relief valves: The plastic plugs and pressure-relief valves located in the outer sheets are not included on the ETU. Since these plugs and valves are very small relative to the puncture bar, they would have no effect on structural behavior of the ETU.
12. ISO corner fittings: The ISO corner fittings used in the ETU were not exact replicas, but were fabricated to have equivalent rigidity to the full scale ISO corner fitting.

13. Payload dunnage: No rails, pallets, or energy absorbing dunnage were included in the half-scale test unit. Absence of these structures was conservative, since their beneficial capacity to absorb impact energy was not present. Their weight, however, was included in the simulated payload bundles, which are shown in Figure 2.12.1-2.
14. Special test ports: The ETU had special test ports on one side which were used for helium leakage rate testing during the test series. These ports were located outside any region of damage, and had no effect on data utilized from the ETU test results.

As noted previously, the ETU was manufactured by refurbishing the test unit originally tested in France in 1994. However, only the CSA body (the body weldment consisting of the inner containment boundary sheets, the structural outer sheets, the V-stiffeners, the body O-ring seal flange, and threaded holes) was original. All of the other components (the closure lid, closure lid bolts, O-ring seals, overpack, overpack cover bolts, phenolic foam, wood, calcium silicate insulating board, puncture-resistant plates, and external sheets) were newly fabricated.

Each payload bundle, which consisted of square-ended, 50 mm diameter aluminum bars, weighed approximately 29½ kg. For the 2003 engineering test series, the ETU was loaded with enough payload bundles to ensure that the total gross weight was at least equal to the equivalent half-scale weight of the TN-Gemini. The gross weight of the ETU was 3,776 kg, or 0.7% more than the maximum gross weight (in half-scale) of the TN-Gemini package.

For the 2005 engineering test series, the ETU from the 2003 test series was utilized. As noted previously, the octagonal recess on the closed end was refurbished to be prototypic to the TRUPACT–III. No other alterations were made. The same payload bars were loaded inside the ETU until a gross weight of 3,163 kg was achieved, or approximately 1% more than the maximum gross weight (in half scale) of the TRUPACT–III.

2.12.1.3.2 French Testing

The ETU utilized for the French tests was essentially the same ETU discussed in Section 2.12.1.3.1, *U.S. Testing*. The purpose of this section is to describe the configuration of the ETU for engineering tests conducted in France.

The first group of tests was performed in April, 1994, and included one NCT, 0.3-m free drop, three HAC, 9 m free drops, and three puncture drops. After each test, both the containment O-ring seal and the containment boundary were individually leaktight. The testing was halted when the last puncture test ruptured the containment boundary. The ETU was then refitted with a revised sidewall overpack design as described below. Testing was resumed in July, 1994, which repeated the same puncture test that had previously caused failure (with a successful outcome), and followed by one, 9-m free drop.

The following list itemizes differences between the ETU utilized in the French tests and the TRUPACT–III, which are in addition to the differences noted in Section 2.12.1.3.1, *U.S. Testing*.

1. Containment seal: The containment O-ring seals used were made of EPDM rubber. In the TRUPACT–III, the O-ring seals are made of butyl rubber. In addition, the width of the dovetail groove opening in the closure lid was slightly smaller than that specified for the TRUPACT–III. This difference had no effect on data utilized from the tests.

2. Puncture-resistant plates: The original configuration of the ETU had a somewhat different sidewall overpack design relative to puncture resistance. As shown in Figure 2.12.1-3, the sidewall overpack construction along the long sides (including lower and upper sides) and in the octagonal recess in the closed end was originally a layer of phenolic foam retained by a single stainless steel outer sheet. After this design proved inadequate to resist puncture, a puncture-resistant plate design was adopted. The single layer of phenolic foam was replaced by a sandwich of phenolic foam, a 5-mm thick (10-mm in full-scale) stainless steel puncture-resistant plate, and low-density balsa wood. Additionally, the outer sheet thickness was reduced to one-half of its former thickness over the same wall regions. Since the added plates were riveted in place in only a few locations, there was no significant change in any impact load paths. Since the only test which could be affected by this change was the puncture test that had failed, this change had no effect on any prior free drop and puncture tests, all of which are therefore applicable to the TRUPACT–III.
3. Closure lid bolts: The material used for the closure lid bolts was Class 8.8, which has somewhat lower yield and ultimate strengths, and lower elongation than the ASTM A320, L43 material specified for the TRUPACT–III. Since all of the important material properties were lower, this substitution was conservative.
4. Closure lid bolt length: The closure lid bolt length was shorter than the scaled specified length (98 mm vs. 102.5 mm). This difference resulted in slightly less thread engagement, which is conservative.

As with the U.S. testing, the simulated payload consisted of a large number of square-ended, round aluminum bars, varying in diameter between 50 mm and 65 mm. The bars were placed within simulated drums made of sheet metal. The ETU was loaded with enough payload bundles to ensure that the total gross weight was at least equal to the equivalent half-scale weight of the TN-Gemini. Prior to the puncture-resistant plate redesign, the gross weight of the ETU was 3,700 kg, or only 1.3% less than the maximum gross weight (in half scale) of the TN-Gemini package. Due to the added material present after implementation of the redesign, the gross weight of the ETU was 3,860 kg, or 2.9% more than the maximum gross weight of the TN-Gemini package.

2.12.1.4 Scale Model Testing

The engineering tests of the half-scale ETU were planned and executed according to the recommendations of Mok, *et al.*[1] Following the terminology of the reference, the ETU scale model used is of Type A-4, where length is the only independent scaling factor. Several important dependent parameters are discussed below.

When using a scale model to test a package design, it is important to control the essential parameters of the problem. One such parameter is fabrication. To be representative of the full-scale package, the methods and effects of fabrication must be properly scaled. To ensure proper scaling of fabrication for the ETU, a modest scaling factor of 1/2 was chosen. Since the full-scale package is very large, a half-scale model is sufficiently large to be readily fabricated prototypically.

[1] Mok, Gerald C., Carlson, Roger W., Lu, Stephen C., and Fischer, Larry E., *Guidelines for Conducting Impact Tests on Shipping Packages for Radioactive Material*, UCRL-ID-121673, Lawrence Livermore National Laboratory, September 1995.

Model Type A-4 is a general purpose scale model that has been used successfully in the past. With this model, all dimensions are scaled using the same value. Material properties, including impact limiting materials, as well as drop height and impact orientation, are identical to the full-scale package. As a result of this scaling, the model weight is 1/8 of the full-scale package. The duration of impact is 1/2, impact force is 1/4, and acceleration is twice that of the full-scale package. Resulting ETU deformations are 1/2, and material stress and strain is identical to that of the full-scale package, which is particularly relevant to regulatory compliance demonstrations. Scaling factors for other model parameters is given in Table 2.12.1-1.

Despite its general applicability, model Type A-4 suffers from some limitations in use. For the engineering tests performed, each of the stated limitations is avoided or accounted for as discussed below.

- The model should not be used in cases where impact loads are small compared to gravity. In the case of the ETU, test impact levels range up to 654g (vertical end drop.) The lowest test impact, that for the 0.3-m, NCT free drop, was 69g. These impacts are all large compared to gravity, and this issue is not of concern.
- The model should not be used in cases where strain rate-sensitive materials are used. In the case of the ETU, the primary strain rate-sensitive material is the crushable wood used in the impact limiting overpack structures. However, since the strain rate scales as S_L^{-1} per Table 2.12.1-1, the strain rate in the model wood is higher than the full-scale package, which results in a greater strain rate effect and conservatively higher impact loads applied to the CSA. For the stainless steel materials used in the CSA, the effect of a scale factor of 1/2 is not important. Therefore, strain rate sensitivity is not of concern.
- The model should not be used for materials having a coarse microstructure, such as concrete or honeycomb. In the case of the ETU, no materials having a coarse microstructure are scaled. The wood impact limiting materials are not scaled in microstructure, and therefore this issue is not of concern.
- The model should not be used to demonstrate the leak tightness of bolted closure joints. In the case of the ETU, the leakage rate test results of the scale model are not utilized to demonstrate the leak tightness of the closure joint in full-scale. However, while not conclusive, it is nonetheless significant that the closure joint of the half-scale ETU was leaktight after each test.
- The model should not be used to demonstrate structural and material failure modes such as brittle fracture and certain modes of buckling. In the case of the ETU, results relative to brittle fracture or buckling are not utilized. However, it is significant that, even though the initial out-of-flat of the ETU CSA sidewalls was conservatively larger than the maximum out-of-flat allowed by the general arrangement drawings, no evidence of bucking was present after the engineering tests.

Based on the foregoing discussion, the use of model Type A-4 is appropriate for the ETU scale model testing. The specific results of greatest importance are the rigid body impact acceleration and resulting deformations of the CSA. According to the scaling laws, the acceleration of the full-scale package will be one-half of the acceleration of the ETU, and the resulting deformations will be twice as large.

Table 2.12.1-1 – Scaling Parameters

Parameter	Value	Parameter	Value
Length	S_L	Acceleration	S_L^{-1}
Time	S_L	Deformation	S_L
Weight	S_L^3	Force	S_L^2
Drop height	1	Stress	1
Impact angle	1	Strain	1
Material properties	1	Strain rate	S_L^{-1}

Note: Contents of table are adapted from Mok, *et al*; S_L is the primary scale factor, equal to 1/2 for the ETU.

2.12.1.5 Test Conditions and Measurement

2.12.1.5.1 Accelerometers

Accelerometers were utilized to record each free drop impact in the U.S. 2003 engineering test series. A total of 24 single axis accelerometers were used: 12 placed parallel to the package longitudinal axis, and 12 placed perpendicular to the package longitudinal axis. The accelerometers were attached to solid stainless steel blocks that were fillet welded to the outer sheet on the body at the locations shown in Figure 2.12.1-4. The accelerometer type used in the tests was piezoresistive. Data was recorded, conditioned, and reduced by the Sandia Mobile Instrumentation Data Acquisition System (MIDAS). A Fast Fourier Transform (FFT) of the raw data was performed to determine the appropriate cutoff, or filtering frequency. The accelerometer data was filtered using a six-pole Butterworth filter with the cutoff set no lower than 300 Hz. No accelerometers were used for the one free drop performed in the 2005 engineering test series, nor were any used for any U.S. puncture drop tests.

In the test series conducted in France, accelerometers were utilized to record each free drop and puncture drop impact. A minimum of two single axis accelerometers were used for each drop test. The accelerometers were screwed into aluminum blocks that were bonded to the outer sheet on the body at various locations, and aligned with the axis of the drop test. Each accelerometer used in the tests had a minimum capacity of 5,000g. Data was recorded, conditioned, and reduced by a data acquisition system. The appropriate cutoff or filtering frequency was then determined by examining the spectral response. The cutoff frequency was set to encompass the initial peaks and correspond to the overall structure mode. Depending on the drop orientation, the accelerometer data was filtered using a cutoff frequency of either 150 Hz or 300 Hz.

2.12.1.5.2 Thermocouples

Maximum impact occurs at the minimum initial temperature condition of -29 °C, as defined in 10 CFR §71.73(b). For the U.S. 2003 engineering free drop tests, Type K thermocouples were installed and numbered in each end of the package to measure the temperatures of the critical impact absorbing material (wood). The thermocouple locations that were utilized for the free drop tests are shown in Figure 2.12.1-5. The thermocouples were utilized to monitor both the balsa and

redwood temperatures. Since only the balsa undergoes crush in end drops, the balsa temperature was of primary importance for these orientations. Consequently, for the end drops, only the balsa wood temperature on the impacting end was considered critical. For the slapdown free drop, only the wood temperatures on the impacting side were considered critical. No effort was made to ensure that temperatures in non-critical areas were below -29 °C. The data was monitored by Sandia's MIDAS data acquisition system during the chilling period, and continued after the ETU was removed from the insulated box. Monitoring ceased when the thermocouples were removed just prior to the actual drops. Temperature of the wood at the moment of impact was extrapolated from the data collected just prior to removal of the thermocouples. In the near-horizontal, slapdown free drop, the thermocouples were not removed, and data was collected up to and during impact. Temperature monitoring was not utilized in the French testing or in the U.S. 2005 testing.

2.12.1.5.3 Internal Pressure

Since internal pressure has the effect of increasing the stress on the containment boundary, in the U.S. 2003 test series, the ETU was pressurized (at ambient temperature) to an internal pressure of 172 kPa, equal to the design pressure. Since resistance to puncture is not significantly affected by internal pressure, the ETU was not pressurized for the puncture tests. Since the pressure is only an initial condition, monitoring the pressure was not performed. The U.S. 2005 testing and the French testing was performed with ambient internal pressure. The effect of internal pressure is not important for puncture drops.

2.12.1.6 Engineering Tests Performed

As stated previously, the engineering tests occurred in three separate series:

- Testing in France in 1994: One, 0.3-m free drop, four, 9-m free drops, and four, 1-m puncture drops. These tests are summarized in Table 2.12.1-2 and Figure 2.12.1-6, and discussed in Section 2.12.1.7.1, *French Engineering Test Results.*
- Testing in the U.S. in 2003: One, 0.3-m free drop, three, 9-m free drops, and four, 1-m puncture drops. These tests are summarized in Table 2.12.1-3 and Figure 2.12.1-7, and discussed in Section 2.12.1.7.2, *U.S. 2003 Engineering Test Results.*
- Testing in the U.S. in 2005: One, 9-m free drop and five, 1-m puncture drops. These tests are summarized in Table 2.12.1-4 and Figure 2.12.1-8, and discussed in Section 2.12.1.7.3, *U.S. 2005 Engineering Test Results.*

2.12.1.7 Engineering Test Results

The results of the engineering tests are described in chronological test order.

2.12.1.7.1 French Engineering Test Results

After installation of the simulated payload into the ETU payload cavity, helium leakage rate tests were performed on the main O-ring seal, the sampling/vent port plug O-ring seal, and the structural containment metallic boundary. Helium leakage rate tests of the main O-ring seal and the metallic boundary were also performed following each free drop and puncture drop test. The sampling/vent port plug O-ring seal was given a final test at the end since it was inaccessible during the test series.

All free drop and puncture drop testing was performed in accordance with IAEA Safety Series No. 6, §622 and §627, utilizing a test procedure prepared for the French certification testing program.

Orientation designations of the package utilized in the French tests are an alpha-numeric designator. The alpha characters are as follows: "A" designates an "edge", "F" designates a "face", and "C" designates a corner. The numeric character designates the sequence, so that test F2 follows test A1, etc. The only exception is test A6, which was performed last in the series.

2.12.1.7.1.1 Free Drop Test No. A1 (NCT, CG-over-Cheek Edge)

Free Drop Test No. A1 was a NCT edge drop from a height of 0.3-m, impacting the edge on the body cheek. As shown in Figure 2.12.1-6, the ETU was oriented at an angle of 68° from horizontal relative to the impact surface (essentially CG-over-edge), with the closure lid end down. The pre-test orientation is shown in Figure 2.12.1-10. The following list summarizes the test parameters:

- longitudinal axis 68°, closure lid end down
- free drop height 0.32 m
- conducted test on 4/25/94

The impact resulted in a slight bulge of the side wall (approx. 7 – 10 mm). The accelerometer signal was filtered using a cutoff frequency of 150 Hz, with a peak accelerometer reading of 56g.

2.12.1.7.1.2 Free Drop Test No. F2 (HAC, Vertical, Closed End Down)

Free Drop Test No. F2 was a HAC flat end drop from a height of 9-m, impacting the closed end. As shown in Figure 2.12.1-6, the ETU was oriented at an angle of 90° from horizontal relative to the impact surface, with the closed end down. The following list summarizes the test parameters:

- longitudinal axis 90°, closed end down
- free drop height 9.05 m
- conducted test on 4/26/94

The impact resulted in small bulges on the side walls. The side bulges ranged from 19 to 32 mm, with the bulge length approximately 92.5 mm long. The principal damage to the body was the failure of three outer edge weld joints in the octagonal recess (largest split approximately 5 mm wide × 400 mm long), and a failure of the short edge weld joint over its width. The post-test damage is shown in Figure 2.12.1-11. The accelerometer signals were filtered using a cutoff frequency of 300 Hz. The peak readings of the two accelerometers were 382g and 333g (average 358g).

2.12.1.7.1.3 Puncture Drop Test No. F3 (Puncture on Overpack Cover Center)

Puncture Drop Test No. F3 impacts the center of the overpack cover/closure lid. As shown in Figure 2.12.1-6, the ETU was oriented at an angle of 90° from horizontal relative to the impact surface, with the closed end down and the CG over the bar. The following list summarizes the test parameters:

- longitudinal axis 90°, closure lid end down
- free drop height 1.18 m
- conducted test on 4/28/94

The puncture bar impacted the ETU very close to the center of the overpack cover. The puncture bar penetrated through to the inner sheet of the recess in the overpack cover. The resulting deformation in the closure lid structural sheet was approximately 21 mm deep. No penetration of the closure lid structural sheet occurred. The orientation is shown in Figure 2.12.1-12, and the damage is shown in Figure 2.12.1-13. The accelerometer signals were filtered using a cutoff frequency of 150 Hz. The peak readings of the two accelerometers were 31g and 32g.

2.12.1.7.1.4 Free Drop Test No. A4 (HAC, CG-over-Overpack Cover Edge)

Free Drop Test No. A4 was a HAC edge drop from a height of 9-m, impacting the closure lid end short edge. As shown in Figure 2.12.1-6, the ETU was oriented at an angle of 66° from horizontal relative to the impact surface (essentially CG-over-edge), with the closure lid end down. The following list summarizes the test parameters:

- longitudinal axis 66°, closure lid end down
- free drop height 9.15 m
- conducted test on 4/29/94

The impact resulted in a flat contact area of approximately 267 mm wide on the cheeks and overpack cover. The resultant side bulge in the center of the overpack cover was approximately 85 mm wide × 170 mm long. The principal damage to the overpack cover was the failure of an outer edge weld joint in the octagonal recess in the impact zone. The width of the resultant opening was a maximum of 30 mm. The orientation is shown in Figure 2.12.1-14 and the post-test damage is shown in Figures 2.12.1-15 through 2.12.1-16. The accelerometer signal was filtered using a cutoff frequency of 150 Hz, with the peak reading of the accelerometer of 196g.

2.12.1.7.1.5 Puncture Drop Test No. F5 (Puncture on Side)

Puncture Drop Test No. F5 impacted the center of the side wall at an oblique angle of 30°. Shown in Figure 2.12.1-6, the ETU longitudinal axis was horizontal and rotated at an angle of 30° relative to the impact surface, with the CG over the bar. The following list summarizes the test parameters:

- longitudinal axis 0°
- rotational axis 30°
- free drop height 1.20 m
- conducted test on 5/02/94

The puncture bar impacted the ETU side wall and penetrated all the way through the CSA containment sheet, which resulted in a breach of the containment boundary. The orientation is shown in Figure 2.12.1-17 and the damage is shown in Figures 2.12.1-18 through 2.12.1-20. Since this test was a failure, the accelerometer data is not meaningful.

As a result of this puncture drop test, the design of the side wall was modified to the current specified configuration. After performing two further tests on the closure lid end (test nos. C7 and C8), the sidewalls of the ETU were refurbished to the new design, as shown in Figure 2.12.1-3, for the final two tests.

2.12.1.7.1.6 Free Drop Test No. C7 (HAC, CG-over-Corner, Lid Down)

Free Drop Test No. C7 was a HAC corner drop from a height of 9-m, impacting the closure lid end lower right corner. As shown in Figure 2.12.1-6, the ETU diagonal edge was oriented at an angle of 59° from horizontal relative to the impact surface (essentially CG-over-corner), with the closure lid end down. The following list summarizes the test parameters:

- longitudinal axis 59° and 43°, closure lid end down
- free drop height 9.20 m
- conducted test on 5/04/94

The impact resulted in deforming the corner to a flat measuring approximately 210 mm deep along the package side × 530 mm wide × 500 mm high. Some cracking of the welds around the ISO corner fitting occurred, but were very minor. No wood or foam was exposed in the deformed area. The orientation is shown in Figure 2.12.1-21 and the damage is shown in Figures 2.12.1-22 through 2.12.1-23. The accelerometer signal was filtered using a cutoff frequency of 150 Hz, with a peak reading of 122g.

2.12.1.7.1.7 Puncture Drop Test No. C8 (Puncture on Overpack Cover/Body Gap)

Puncture Drop Test No. C8 impacts the gap between the overpack cover and the body cheek, on the lower left corner. As shown in Figure 2.12.1-6, the ETU diagonal edge was oriented at an angle of 59° from horizontal relative to the impact surface, with the closure lid end down and the CG over the bar. The impact point was in an undamaged area. The following list summarizes the test parameters:

- longitudinal axis as 59°, closure lid end down
- free drop height 1.35 m
- conducted test on 5/05/94

The puncture bar impacted the edge of the overpack cover and next to the body cheek. The puncture bar penetrated the outer sheet of the overpack cover to an approximate depth of 100 mm. The gap between the body "cheek" and the overpack cover increased to approximately 100 mm wide × 90 mm long. The orientation is shown in Figure 2.12.1-24 and the damage is shown in Figure 2.12.1-25. The accelerometer signal was filtered using a cutoff frequency of 150 Hz, with a peak reading of 14g.

2.12.1.7.1.8 Puncture Drop Test No. F9 (Puncture on Side)

Puncture Drop Test No. F9 impacts the center of the side wall at an oblique angle of 30° (repeat of Puncture Drop Test F5). As shown in Figure 2.12.1-6, the ETU longitudinal axis was horizontal and rotated at an angle of 30° relative to the impact surface, with the CG over the bar. The following list summarizes the test parameters:

- longitudinal axis 0°
- rotational axis 30°
- free drop height 1.12 m
- conducted test on 7/04/94

The puncture bar impacted the ETU side wall directly opposite from the one attacked in F5. The puncture bar penetrated to the puncture resistant plate, but did not perforate it. No penetration and no deformation of the CSA structural sheet occurred. The maximum depth of the puncture bar was approximately 90 mm. The orientation is shown in Figure 2.12.1-26 and the damage is shown in Figure 2.12.1-27. The accelerometer signal was filtered using a cutoff frequency of 150 Hz, with a peak reading of 12g.

2.12.1.7.1.9 Free Drop Test No. A6 (HAC on Side-Edge)

Free Drop Test No. A6 was a HAC edge drop from a height of 9-m, impacting the long side edge (essentially CG-over-edge). See Figure 2.12.1-6. The ETU was oriented at a small angle of 5° from horizontal relative to the impact surface, with the closed end lower. The following list summarizes the test parameters:

- longitudinal axis 5°, closed end lower
- rotational axis 46°, long side edge down
- free drop height 9.15 m
- conducted test on 7/04/94

The impact resulted in a flat along the entire length of the edge, which ranged from 120 mm to 175 mm in width. The orientation is shown in Figure 2.12.1-28 and the damage is shown in Figures 2.12.1-29 through 2.12.1-30. The accelerometer signals were filtered using a cutoff frequency of 150 Hz. The peak readings of the three accelerometers were 122g, 220g, and 227g. Discarding the low reading, the average of the two higher readings is 224g.

2.12.1.7.1.10 Post-Test Disassembly

Post-test disassembly of the ETU was performed in two stages. The initial disassembly was performed following Puncture Drop Test No. C8 in May 1994. Following the refurbishment with the puncture-resistant design, reassembly, and performing Puncture Drop Test No. F9 and Free Drop Test No. A6, the final disassembly was performed in July 1994. Prior to removing the closure lid in the final disassembly, helium leakage rate tests of the containment main O-ring seal and the metallic boundary were performed on 7/5/94. Helium leakage rate testing of the sampling/vent port O-ring seal was performed on 7/6/94. A view of the simulated payload after testing is shown in Figure 2.12.1-31, and the payload cavity in Figure 2.12.1-32.

During the removal of the closure lid, the residual tightness of the closure bolts was checked. Ten of the forty-four bolts exhibited slightly less tightening torque than the nominal installation torque of 200 N-m. However, the decrease was less than one-quarter turn. A view of the damage to the closure lid from puncture test F3 is shown in Figure 2.12.1-33.

Following removal of the loose simulated payload, the inner surfaces of the CSA containment sheets were examined and revealed no measurable deformations. Four dents from the aluminum rods used for simulated payload were noted in the CSA containment sheets. The depth of these dents ranged from 6 mm to 9 mm.

Demonstration of containment boundary leak tightness of the ETU was accomplished by utilizing the test ports located on the side of ETU (main O-ring seal and metallic boundary) and

the sampling/vent port plug (O-ring seal). The interior cavity was evacuated sufficiently to operate a mass spectrometer leak detector (MSLD). The cavity on the outside of the main and sampling/vent port O-ring seals were evacuated and subsequently backfilled with helium gas. For the CSA metallic structure, the annulus between the CSA containment and the structural sheets was evacuated and subsequently backfilled with helium gas. Results of the successful mass spectrometer helium leakage rate testing are summarized below:

Sealing Component	Leakage Rate
Main O-ring Seal	1.6×10^{-8} Pa-m^3/s, helium
Sampling/Vent Port Plug O-ring Seal	1.6×10^{-9} Pa-m^3/s, helium
CSA Metallic Structure	1.6×10^{-8} Pa-m^3/s, helium

When accounting for the conversion between air leakage (per ANIS N14.5) and helium leakage, a 2.2 factor applies for standard temperatures and pressures. Thus, a reported helium leakage rate of 1.6×10^{-8} Pa-m^3/s, helium, is equivalently 7.3×10^{-9} Pa-m^3/s, air, a level below the "leaktight" criterion of 1×10^{-8} Pa-m^3/s, air, per ANSI N14.5.

In conclusion, based on visual inspection and on leakage rate testing, there was no evidence of buckling of the CSA containment sheets, gross distortion of the O-ring sealing flanges that would cause a sealing failure, or rupture of the containment boundary for the final puncture-resistant plate design.

2.12.1.7.2 U.S. 2003 Engineering Test Results

Prior to performing any free or puncture drop tests, extensive pre-test measurements of the ETU were made. They were compared to post-test measurements as discussed in Section 2.12.1.7.2.10, *ETU Measurements*. A pressure test using an internal pressure of 1.5 times MNOP was performed, and then the simulated payload was installed into the cavity. Helium leakage rate tests were then performed on the main O-ring seal and the sampling/vent port plug O-ring seal. The structural containment boundary leakage rate test was performed as a part of ETU acceptance testing. All free drop and puncture drop measurements and testing were performed in accordance with a written test plan. The alpha-numeric test designator includes the letters "FD" for free drops and "P" for punctures, followed by a sequence number. The order of testing was FD1 to FD4, followed by P1 to P4.

In the three vertical drops, acceleration readings increased with increasing distance from the ground. That is, the vertical accelerations nearest the ground were least, the accelerations farthest from the ground were greatest, and the accelerations at the package axial middle were in between. For example in free drop FD3, the average acceleration of the four accelerometers located farthest from the ground was about 23% greater than the average of the four nearest the ground. Since this phenomenon was likely a result of a global elastic response of the package in an axial mode, the accelerometers nearest the ground therefore represented the best approximation to the rigid-body acceleration of the package upon impact. All of the accelerometer summaries presented herein are for the accelerometers nearest the ground.

2.12.1.7.2.1 Free Drop Test No. FD1 (HAC Vertical, Closed End Down)

Free Drop Test No. FD1 was a HAC flat end drop from a height of 9-m, impacting the closed end (package vertical). As shown in Figure 2.12.1-7, the ETU was oriented at an angle of 90°

from horizontal relative to the impact surface, with the closed end down. The following list summarizes the test parameters:

- verified internal pressure as 172 kPa, +25/-0 kPa
- package temperature was accepted at -21 °C
- verified longitudinal axis as 90° ± 5°, closed end down
- verified free drop height as 9-m, +75/-0 mm
- measured ambient temperature as 19 °C at time of test
- conducted test at 9:16 a.m. on 9/16/03

Although the ETU was suspended in the correct orientation (90° ± 5°), the ETU impacted at an angle between 83° – 85°. This impact angle was apparently caused by a very slight delay in cutting one of the four cables. The impact surface (judged by rust transfer from the pad) covered approximately 2/3 of the closed end face of the ETU. Viewed from the end, the lower left corner impacted first, and deformed approximately 67 mm. The diagonally opposite corner crushed approximately 1.5 mm. The vertical left and bottom weld seams between the side and end sheets split open, although the openings were nearly filled with deformed steel material from the outer sheets. Some weld seams also split around the edge of the octagonal recess, with a maximum gap opening of approximately 6 mm. Openings also occurred around the ISO fitting on the initially impacted corner. The post-test damage is shown in Figures 2.12.1-34 through 2.12.1-35.

The accelerometer signals were filtered using a cutoff frequency of 300 Hz. The peak readings of the four accelerometers nearest to the impact surface are as follows:

Accelerometer	A3	A4	A9	A10	Avg.
Peak Value (g)	229	219	185	236	217

After the test, the overpack cover was removed and the closure lid bolts retightened. Out of the forty-four closure lid bolts, only one bolt turned slightly when retightened to 200 N-m torque. The overpack cover was replaced and its ten bolts were retightened to 200 N-m torque.

2.12.1.7.2.2 Free Drop Test No. FD2 (NCT Vertical, Lid End Down)

Free Drop Test No. FD2 was a NCT flat end drop from a height of 0.3-m, impacting the closure lid end (package vertical). As shown in Figure 2.12.1-7, the ETU was oriented at an angle of 90° from horizontal relative to the impact surface with the closure lid end down. The following list summarizes the test parameters:

- verified internal pressure as 172 kPa, +25/-0 kPa
- measured package temperature as -37 °C
- verified longitudinal axis as 90° ± 5°, closure lid end down
- verified free drop height as 0.3-m, +25/-0 mm
- measured ambient temperature as 16 °C at time of test
- conducted test at 8:36 a.m. on 9/17/03

There was almost no visible damage from the impact. No weld seams failed. As shown in Figure 2.12.1-36, the only deformation was a small bulge on one side. The maximum

deformation of the closure lid end was approximately 6 mm near the upper right corner, as viewed in the normally transported horizontal orientation.

The accelerometer signals were filtered using a cutoff frequency of 300 Hz. The peak readings of the four accelerometers nearest to the impact surface are as follows:

Accelerometer	A1	A6	A7	A12	Avg.
Peak Value (g)	78	51	82	64	69

2.12.1.7.2.3 Free Drop Test No. FD3 (HAC Vertical, Lid End Down)

Free Drop Test No. FD3 was a HAC flat end drop from a height of 9-m, impacting the closure lid end (package vertical). As shown in Figure 2.12.1-7, the ETU was oriented at an angle of 90° from horizontal relative to the impact surface with the closure lid end down. The following list summarizes the test parameters:

- verified internal pressure as 172 kPa, +25/-0 kPa
- measured package temperature as -28 °C
- verified longitudinal axis as 90° ± 5°, closure lid end down
- verified free drop height as 9-m, +75/-0 mm
- measured ambient temperature as 12 °C at time of test
- conducted test at 8:47 a.m. on 9/18/03

A review of the video recording of the drop demonstrated that the impact was essentially perfectly flat on the closure lid end. Post-test photographs are shown in Figures 2.12.1-37 through 2.12.1-38. There were no significant weld seam splits as a result of this free drop. The maximum crush distance of the ETU closure lid end was an additional 17 mm (measured from the post-Free Drop Test No. FD2 position).

The accelerometer signals were filtered using a cutoff frequency of 400 Hz, rather than 300 Hz, based on consideration of the FFT of the data. The peak readings of the four accelerometers nearest to the impact surface are as follows:

Accelerometer	A1	A6	A7	A12	Avg.
Peak Value (g)	781	641	671	521	654

2.12.1.7.2.4 Free Drop Test No. FD4 (HAC Slapdown, Lid End Secondary)

Free Drop Test No. FD4 was a HAC free drop from a height of 9-m, impacting 25° from horizontal with primary impact on the closed end and secondary impact on the closure lid end, as shown in Figure 2.12.1-7. The top short edge on the closed end was the primary impact point. The following list summarizes the test parameters:

- verified internal pressure as 172 kPa, +25/-0 kPa
- measured balsa temperature as -34 °C, and redwood temperature as -31 °C
- verified longitudinal axis as 30° ± 5°, top edge of closed end down
- verified free drop height as 9-m, +75/-0 mm

- measured ambient temperature as 13 °C at time of test
- conducted test at 9:47 a.m. on 9/19/03

Primary Impact: The principal damage to the closed end was the relatively wide split of weld joints in the octagonal recess near the impacted edge, as shown in Figure 2.12.1-39. Although affected by prior damage from Free Drop No. FD1, it was concluded that the damaged weld joints would occur even in the absence of damage accumulation.

The accelerometer signals were filtered using a cutoff frequency of 300 Hz. The peak readings of the eight accelerometers at the primary impact end (closed end) are as follows:

Direction	Perpendicular to Axis				Parallel to Axis			
Accelerometer	A15	A16	A21	A22	A3	A4	A9	A10
Peak Value (g)	200	193	221	368	26	No Data	550	-98

The high reading shown for A9 was not consistent with the readings of other accelerometers (for example, A3), and was therefore considered to be a test anomaly.

Secondary Impact: The secondary impact occurred at an inclination of approximately 2° – 4° to the horizontal. The maximum crush distance at the outside edge of the overpack cover was approximately 25 mm, and the length of the impact zone, measured from the overpack cover end, was approximately 483 mm. A gap of up to 35 mm developed between the overpack cover and the side cheeks, but this gap was not open all the way to the root of the cheek. As shown in Figure 2.12.1-40, the gap was blocked by buckled sheet material from the inside face of the cheek. Some weld seams on the overpack cover split (approximately 10 mm wide), while many of the split weld seams remained essentially closed after impact. An overall view of the impact damage and a close-up view of the ISO fitting damage are shown in Figures 2.12.1-41 and 2.12.1-42, respectively.

The peak readings of the eight accelerometers at the center and at the secondary impact end (closure lid) during secondary impact are as follows:

Position	Direction	Perpendicular to Axis				Parallel to Axis			
Center	Accelerometer	A14	A17	A20	A23	A2	A5	A8	A11
	Peak Value (g)	No Data	350	286	No Data	-131	222	-208	186
End	Accelerometer	A13	A18	A19	A24	A1	A6	A7	A12
	Peak Value (g)	631	671	657	640	-103	202	-168	175

Note: The average acceleration at the package end, perpendicular to the package axis, was equal to (631 + 671 + 657 + 640)/4 = 650g.

2.12.1.7.2.5 Puncture Drop Test No. P1 (Puncture on Overpack Cover Near Bolts)

Puncture Drop Test No. P1 impacted the recess on the overpack cover. As shown in Figure 2.12.1-7, the ETU was oriented at an angle of 71° from horizontal relative to the impact surface, with the closure lid end down. The following list summarizes the test parameters:

- verified 750 mm long puncture bar welded to pad

- verified longitudinal axis as 71° ± 5°, closure lid end down
- verified free drop height as 1-m, +25/-0 mm
- measured ambient temperature as 27 °C at time of test
- conducted test at 9:00 a.m. on 9/23/03

Due to the characteristics of the rigging, the ETU translated slightly to the side on release so that the puncture bar impact occurred approximately 200 mm from the recess edge. The puncture bar penetrated the overpack cover end and created a 216 mm long tear on the closure lid outer structural sheet. The CSA containment boundary sheet was not damaged. Post-test photographs are shown in Figures 2.12.1-43 through 2.12.1-45.

2.12.1.7.2.6 Puncture Drop Test No. P2 (Puncture on Overpack Cover Joint)

Puncture Drop Test No. P2 impacted the lower corner joint between the side cheek and the overpack cover. As shown in Figure 2.12.1-7, the ETU was oriented at a compound angle of 120° and 45° from horizontal relative to the impact surface, with the closure lid end down. The following list summarizes the test parameters:

- verified 1,200 mm long puncture bar welded to pad
- verified longitudinal axis as 120° & 45° ± 5°, closure lid end down
- verified free drop height as 1-m, +25/-0 mm
- measured ambient temperature as 32 °C at time of test
- conducted test at 11:20 a.m. on 9/23/03

The puncture bar impacted on the gap between the overpack cover and the cheek, approximately 232 mm from the bottom edge of the lower right cheek structure (viewed as normally transported from the overpack cover end). The bar struck as desired, and did essentially no damage to the ETU structure, as shown in Figure 2.12.1-46.

2.12.1.7.2.7 Puncture Drop Test No. P3 (Puncture on Slapdown Damage)

Puncture Drop Test No. P3 impacted the joint between the body and the overpack cover. As shown in Figure 2.12.1-7, the ETU was oriented at an angle of 30° from horizontal relative to the impact surface, with the closed end down. The following list summarizes the test parameters:

- verified 1,800 mm long puncture bar welded to pad
- verified longitudinal axis as 30° ± 5°, closed end down
- verified free drop height as 1-m, +25/-0 mm
- measured ambient temperature as 34 °C at time of test
- conducted test at 3:05 p.m. on 9/23/03

The puncture bar impacted the upper overpack cover joint, in the same area as the secondary slapdown impact damage from Free Drop No. FD4. The impact point was about halfway between overpack cover bolt Nos. 3 and 4. The resulting deformation covered approximately 46

mm on the body, and 83 mm on the overpack cover, with a maximum depth of 36 mm. The puncture drop damage is shown in Figures 2.12.1-47 through 2.12.1-49.

2.12.1.7.2.8 Puncture Drop Test No. P4 (Puncture on Closed End)

Puncture Drop Test No. P4 impacted the recess on the closed end, adjacent to the wall of the recess. As shown in Figure 2.12.1-7, the ETU was oriented at an angle of 71° from horizontal relative to the impact surface, with the closed end down. The following list summarizes the test parameters:

- verified 750 mm long puncture bar welded to pad
- verified longitudinal axis as 71° ± 5°, closed end down
- verified free drop height as 1-m, +25/-0 mm
- measured ambient temperature as 21 °C at time of test
- conducted test at 7:57 a.m. on 9/30/03

The puncture bar impacted the ETU approximately 152 mm from the octagonal recess edge. The puncture bar penetrated through to the outer structural sheet of the CSA. The deformation in the CSA structural sheet was approximately 29 mm deep, and a section approximately 1/3 of the bar circumference (~80 mm) sheared completely through the sheet. The damage is shown in Figures 2.12.1-50 through 2.12.1-52.

2.12.1.7.2.9 ETU Post-Test Disassembly

Post-test disassembly of the ETU was performed in two stages. The initial disassembly was performed following Puncture Drop test No. P3 on 9/24/03. Following removal of the overpack cover and inspection of the damage to the exterior of the closure lid, a helium leakage rate test of the containment O-ring seals was performed. Following detailed inspection and measurement of the O-ring sealing flange on the closure lid and body, the ETU was reassembled for Puncture Drop Test No. P4. Final helium leakage rate testing of the metallic boundary was performed on 10/1/03.

Demonstration of containment boundary leak tightness of the ETU was accomplished by utilizing the test ports located on the side of ETU (main O-ring seal and metallic boundary) and the sampling/vent port plug (O-ring seal). The interior cavity was evacuated sufficiently to operate a mass spectrometer leak detector (MSLD). The cavities on the outside of the main and sampling/vent port O-ring seals were evacuated and subsequently backfilled with helium gas. For the CSA metallic structure, the annulus between the CSA containment and the structural sheets was evacuated and subsequently backfilled with helium gas. Results of the successful mass spectrometer helium leakage rate testing are summarized below:

Sealing Component	Leakage Rate
Main O-ring Seal	$<1.0 \times 10^{-9}$ Pa-m^3/s, helium
Sampling/Vent Port Plug O-ring Seal	$<1.0 \times 10^{-9}$ Pa-m^3/s, helium
CSA Metallic Structure	$<1.0 \times 10^{-9}$ Pa-m^3/s, helium

When accounting for the conversion between air leakage (per ANIS N14.5) and helium leakage, a 2.2 factor applies for standard temperatures and pressures. Thus, a reported helium leakage

rate of 1.0×10^{-9} Pa-m^3/s, helium, is equivalently 4.6×10^{-10} Pa-m^3/s, air, a level well below the "leaktight" criterion of 1×10^{-8} Pa-m^3/s, air, per ANSI N14.5. Views of the disassembled ETU are shown in Figures 2.12.1-53 through 2.12.1-56.

2.12.1.7.2.10 ETU Measurements

Extensive measurements of the ETU were made both before and after testing. Measurements of the payload cavity dimensions, closure bolt residual torque, closure lid lateral position, closure lid global flatness, and the local flatness of the body and closure lid sealing flanges were made. The following is a summary of the results.

- The length, width, height, and diagonals of the payload cavity were measured. The length, width, and diagonal measurements remained essentially unchanged. The only measurable change was in the height of the cavity at the open end, which decreased by approximately 2 mm. This was probably due to the forces resulting from the slapdown secondary impact. Some waviness in the containment sheets, parallel to the v-stiffeners, was noted before testing, most likely due to welding distortion. The depth of several "waves" were measured before and after testing, and no significant change in their depth or shape was noted.
- Closure bolt residual torque was measured prior to removing the closure lid. The average residual torque of all 44 bolts was 145 N-m, and the minimum value was 83 N-m. Since the applied torque was 200 N-m, the average represents a residual torque of 72%, and the minimum, 41%, of the originally applied value.
- The position of the closure lid was measured in order to characterize its behavior in the slapdown drop, where large lateral forces were generated. Post test measurements showed that the lid moved 2 mm toward the normally transported bottom of the package. Since the slapdown drop occurred on the top of the package, the lid moved away from the ground under the forces generated by the overpack cover structures in the secondary impact event. The direction of motion is parallel to the sealing flange face, and therefore had no consequences to the containment seal leakage rate. The amount of movement, 2 mm, was much less than the 7 mm clearance between the closure bolts and lid holes, and no visual evidence of contact between the lid shear lip and the body opening was present.
- Lid global flatness was checked to see if the forces from the payload (primarily from free drop FD3 or from puncture drop P1) could cause permanent deformation of the lid structure. The result showed that essentially no permanent deformation of the inside sheet of the closure lid occurred as a consequence of the testing.
- The body and closure lid flanges were measured before and after testing to determine if the test loads caused any permanent deformation of the flanges, and specifically, if any significant permanent reduction in the compression of the containment O-ring seal occurred. This was done using a multi-axis machine tool holding a dial indicator. Two rows of 13 points each were measured on each of the four sides of both the body and the lid flanges for a total of 208 individual measurements each time. The inner row of points was located 12 mm from the inner edge of the flange, and the outer row was located 10 mm from the outer edge. Points 1 – 4, 6, 8, 10, and 11 – 13 were located halfway between two bolts, and points 5, 7, and 9 were located at bolt locations near the center of the flange length. Thus, the density of measurement points increased near the center of each side. Refer to Figure 2.12.1-9. Each

point on the body was nominally coincident with a point on the lid. The position of the flange face in a direction axial to the ETU was measured relative to a common, arbitrary datum plane. From the raw measurements of the body and lid, gaps were calculated for all of the measurement locations around the flange. Each gap value represents the distance between the body and lid flange faces at the outside edge of the flange for the assembled, post-test configuration. Since the flange measurements were made with the lid removed, the calculations omit the effect of the closure bolt residual tightness, and are therefore very conservative. Note that the gap value is not necessarily equal to a change due to testing, but the total present after testing, which includes the effect of any pre-testing gaps. The flange gaps are given in Table 2.12.1-5. The maximum gap is 0.89 mm, located in the top flange at position 2. For comparison, a post-test feeler gauge measurement of the same location showed a gap of only 0.28 mm, demonstrating the conservatism of this calculation method.

Since all of the gaps between the body and the lid were located on the outside edge of the flange face, the movement at the containment O-ring seal, which is located near the inside edge of the flange, is much less. The seal is located 12.5 mm from the inside edge of the flange, and the total width of the top flange is 70.5 mm. Using linear interpolation, the maximum movement at the containment O-ring seal is:

$$M_{max} = \left(\frac{12.5}{70.5}\right) 0.89 = 0.16 \text{ mm}$$

In full scale, the maximum movement would be twice this amount, or 0.32 mm. This is a very small movement compared to the compression of the elastomer seal of nominally 3 mm.

In conclusion, there was very little accumulated damage to the CSA structure resulting from the four free drops and four puncture drops. There was no evidence of buckling of the CSA containment sheets, gross distortion of the O-ring sealing flanges that would cause a sealing failure, or rupture of the containment boundary.

2.12.1.7.3 U.S. 2005 Engineering Test Results

The U.S. 2005 testing was performed at EPD in Carlsbad, NM, in September, 2005. The objectives of this test were:

1. To determine the effectiveness of the 15-mm thick (equivalent full-scale) puncture-resistant plate on the bottom end and in the overpack cover. Results were evaluated by general observations and measurements.
2. To determine the worst-case puncture attack angle for the side panels. Results were evaluated by comparison of the dent depth in the CSA outer sheet as described below.
3. To ensure that the package can withstand the 30 ft, horizontal side drop. Results were evaluated by general observation of the puncture damage.

Prior to testing, the internal width and height at mid-length of the CSA were measured for comparison with post-test measurements. After installation of the closure lid, a hard vacuum was placed between the two O-ring seals to ensure proper installation. Since the vent/test port had not been disturbed since the prior test series, it was not retested. No thermocouples or accelerometers were used. No internal pressure was used, and all tests occurred at ambient

temperature. Prior damage and weathering may have had an effect on the free drop results, and possibly on two of the five puncture tests. However, since the free drop was considered an order-of-magnitude test, the ETU pre-condition was not disqualifying. The effect of ETU condition on the punctures is discussed below. The free drop test is designated "FD05". The puncture tests are designated "P*x*05" where x = 1 through 5.

2.12.1.7.3.1 Free Drop Test FD05 (Flat Side)

In this test, the ETU was dropped flat on the (normally) vertical side opposite the special test ports. The test was planned as an order-of-magnitude test of the large impact forces that can be expected on the certification test of the same orientation. Although the actual impact magnitude was not recorded, the results demonstrate that the TRUPACT–III can withstand this impact without deformation of the CSA or damage to the closure flange and containment sealing area. Post-test measurements showed no change to the CSA-internal height and width measurements and only a very small (approximately 2-mm full scale) lateral slip of the closure lid. The closure bolts had essentially undiminished removal torque, and the containment seal was capable of a hard vacuum (application of a hard vacuum was utilized in lieu of a helium leak test.) Due to the large size of the impact area of the ETU, the impact deformation was too small for meaningful measurements.

2.12.1.7.3.2 Puncture Drop Tests P105 through P405 (Oblique on Sides)

In this series of puncture tests, the sides of the ETU, which were not damaged from prior testing, were used. In all cases, the line of puncture was through the center of gravity. The tests differed only in the oblique angle between the package surface and the puncture bar axis. The ETU axis was horizontal, and rotated by different amounts about that axis to achieve the desired orientations.

The results are shown in Table 2.12.1-6. In most cases, the puncture bar impact caused a shear fracture in the puncture-resistant plate. In no case did a shear fracture occur in the outer sheet of the CSA.

To fully support the conclusions drawn from the engineering puncture tests, the results in Table 2.12.1-6 are augmented by the results from puncture test P4 (see Section 2.12.1.7.2.8, *Puncture Drop Test No. P4*) that occurred during the U.S. 2003 test series. In that test, the puncture drop energy was approximately only 7% greater than in the U.S. 2005 puncture test series, and the impacted structure was identical, and therefore it may be included along with the other puncture tests documented here. Of note, a small fracture did occur in the CSA outer sheet in that test as shown in Figure 2.12.1-52.

As shown in the table, the puncture test severity, measured as the dent depth of the CSA outer sheet, increases with decreasing oblique angle, until a maxima is reached in the range of 20° to 25°. Of note, inspection of the puncture damage after test P305 showed that the outer layer of balsa wood contained moisture due to weathering during storage of the ETU. Since it was unclear what effect that might have on the results, the test at 25° was repeated (as test P405) in a different location. In that case, the impact occurred on a patch made in the CSA outer sheet subsequent to the test F5 in France, causing a small fracture in the patch material. The depth of the dent shown in the table for test P405 on the patch may not be representative of the response of prototypical CSA structure. Figures of the puncture damage for puncture tests P105 through P405 are shown in Figures 2.12.1-57 through 2.12.1-60.

2.12.1.7.3.3 Puncture Drop Test P505 (On Closed End)

The purpose of this test was to confirm the performance of the 15-mm puncture-resistant plates in the overpack cover and closed end octagonal recess areas. The angle of impact was as oblique as possible given the need to enter the recessed area with the puncture bar. The ETU axis was inclined 71° from the horizontal. The orientation of the closed end wall was equal to 90 – 71 = 19° from horizontal. The results showed that the puncture-resistant plate dented, but did not experience any shear fracturing. The puncture damage is shown in Figure 2.12.1-61.

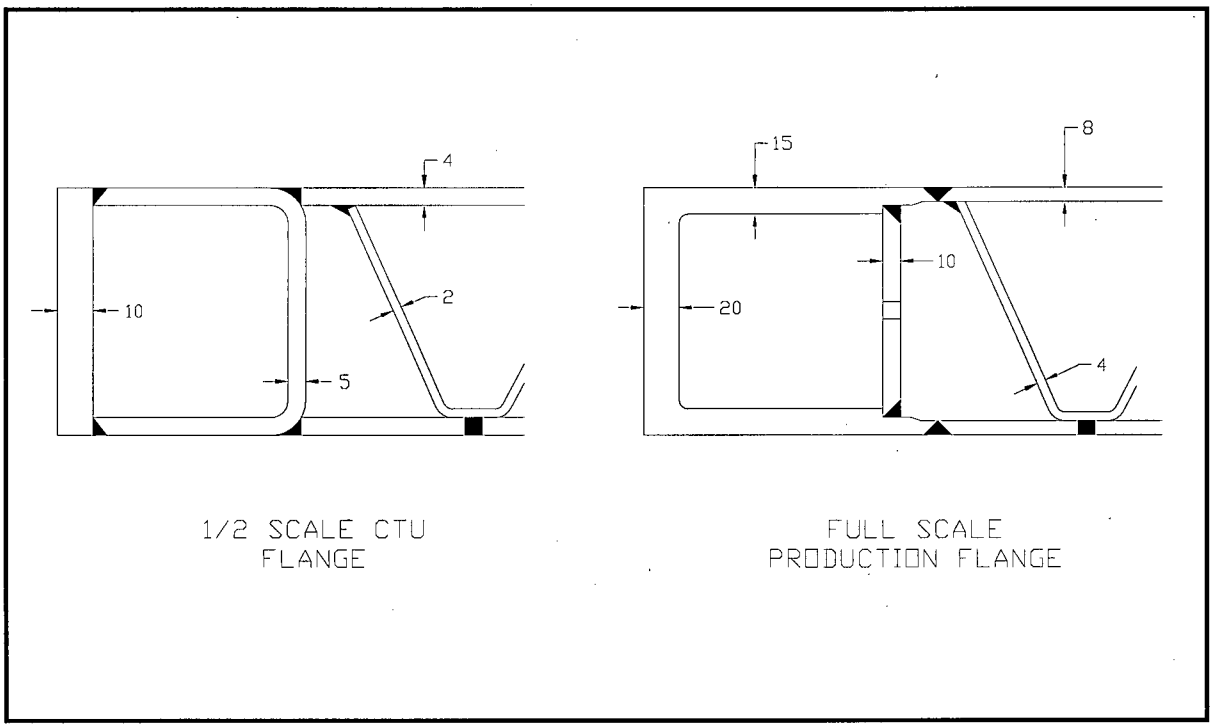

Figure 2.12.1-1 – ETU and TRUPACT–III Body Flange Construction Comparison

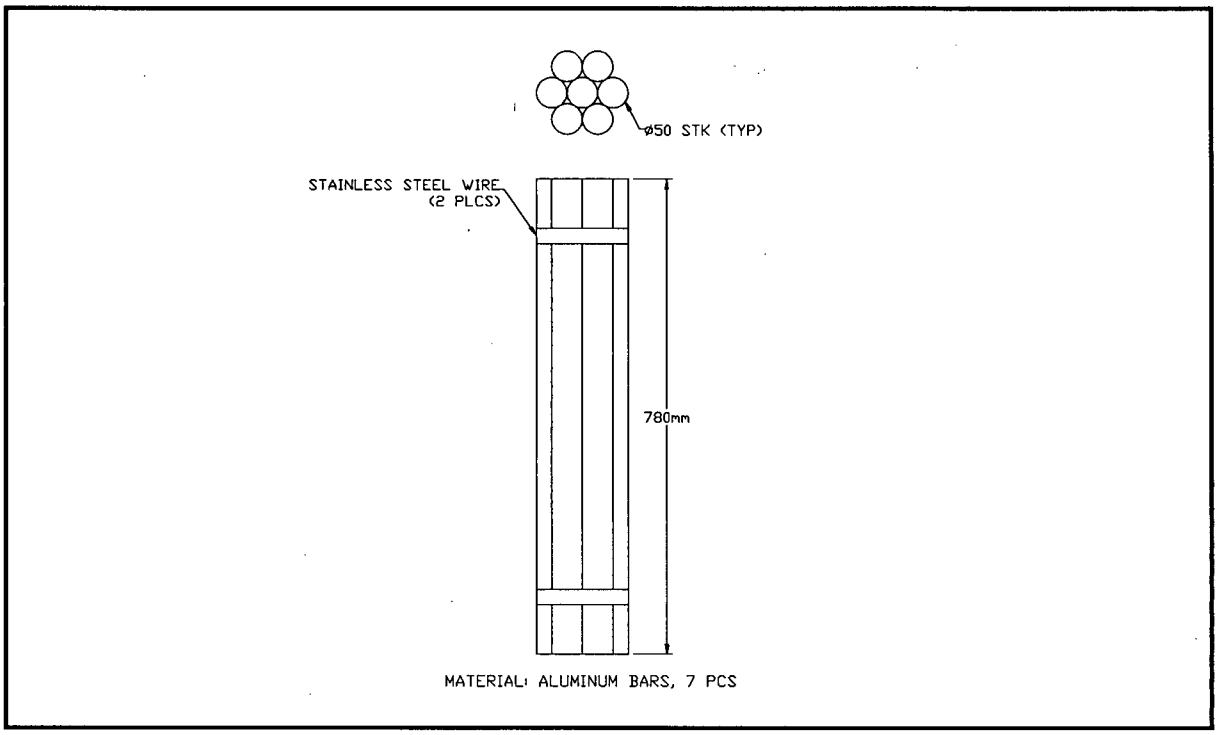

Figure 2.12.1-2 – ETU Simulated Payload Bundle – U.S. 2003 Testing

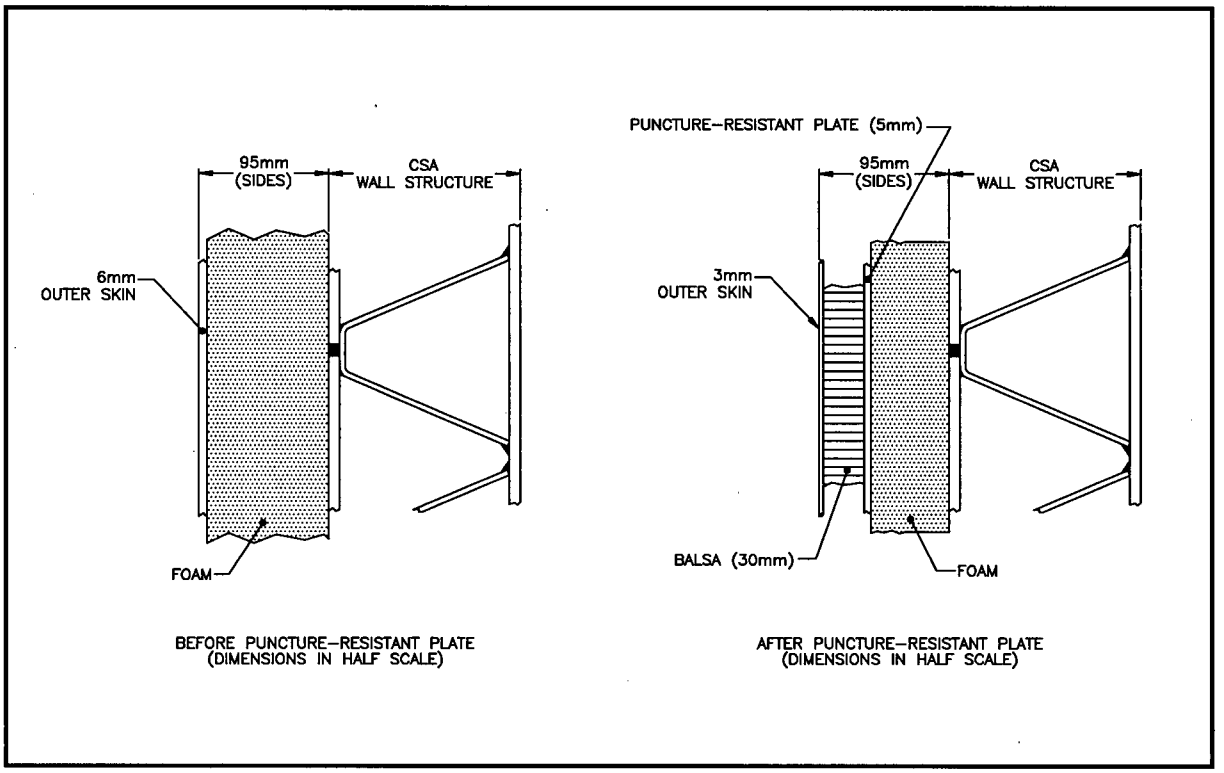

Figure 2.12.1-3 – Comparison of ETU Sidewall Designs in French Testing

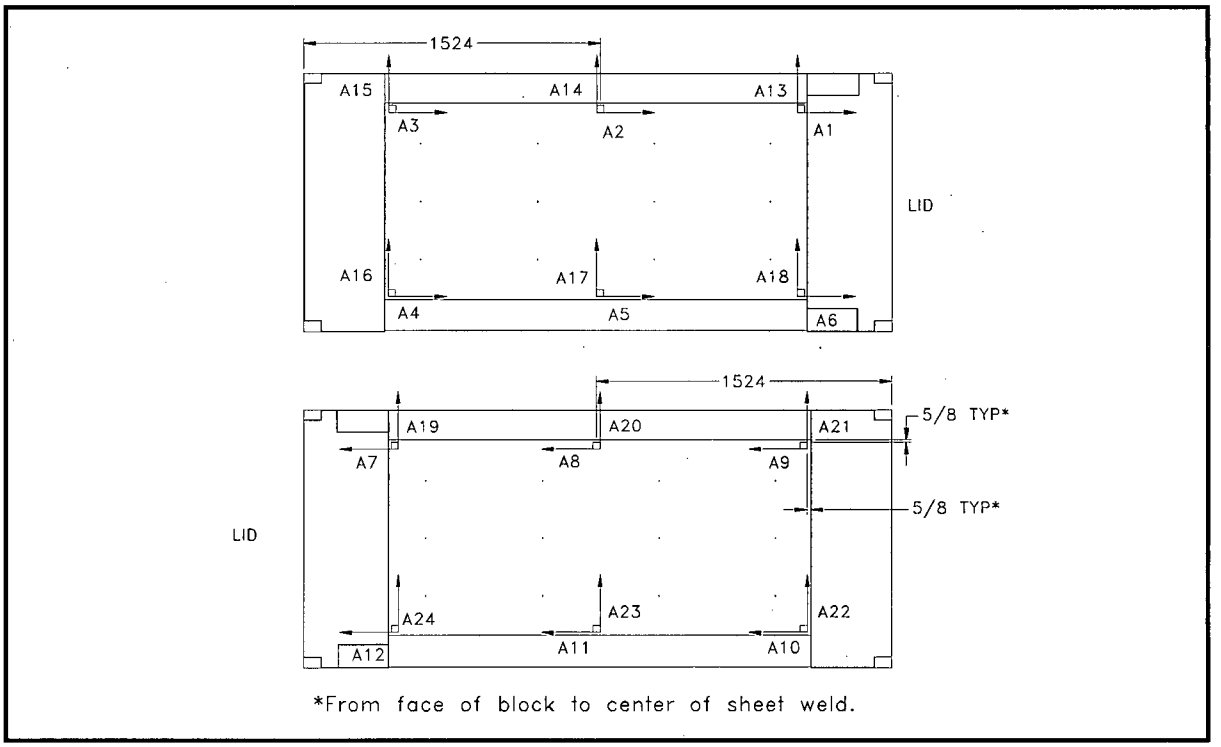

Figure 2.12.1-4 – Accelerometer Locations – U.S. 2003 Testing

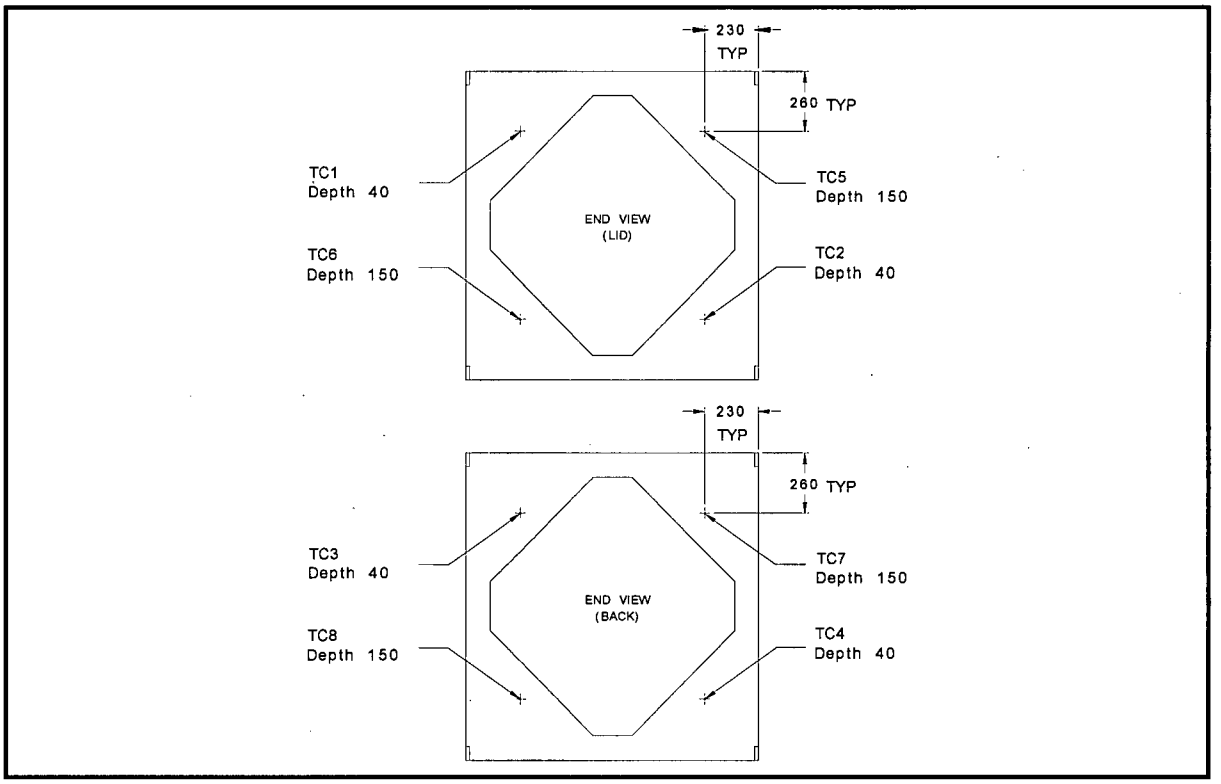

Figure 2.12.1-5 – Thermocouple Locations and Depths – U.S. 2003 Testing

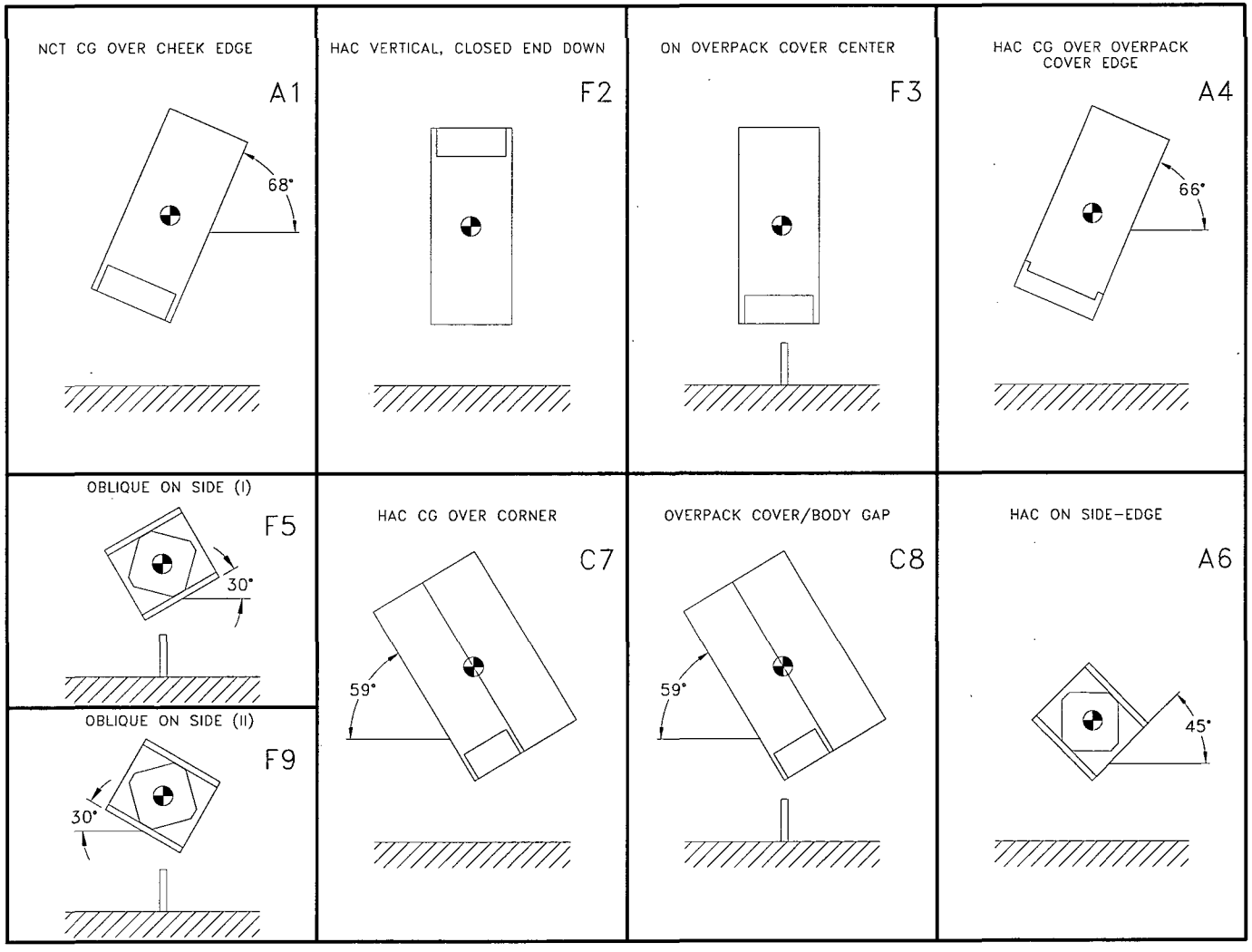

Figure 2.12.1-6 – Schematic of French Engineering Tests

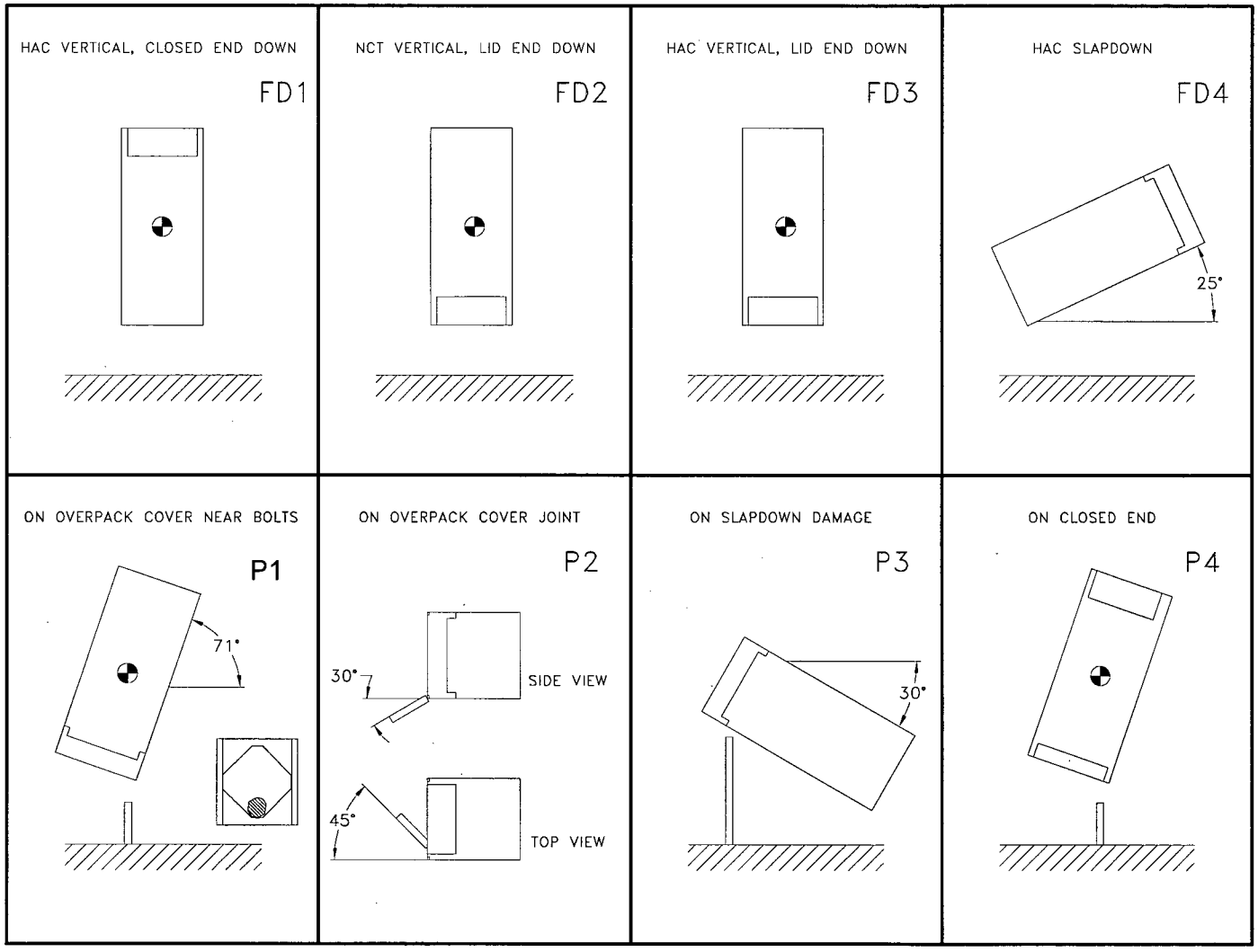

Figure 2.12.1-7 – Schematic of U.S. 2003 Engineering Tests

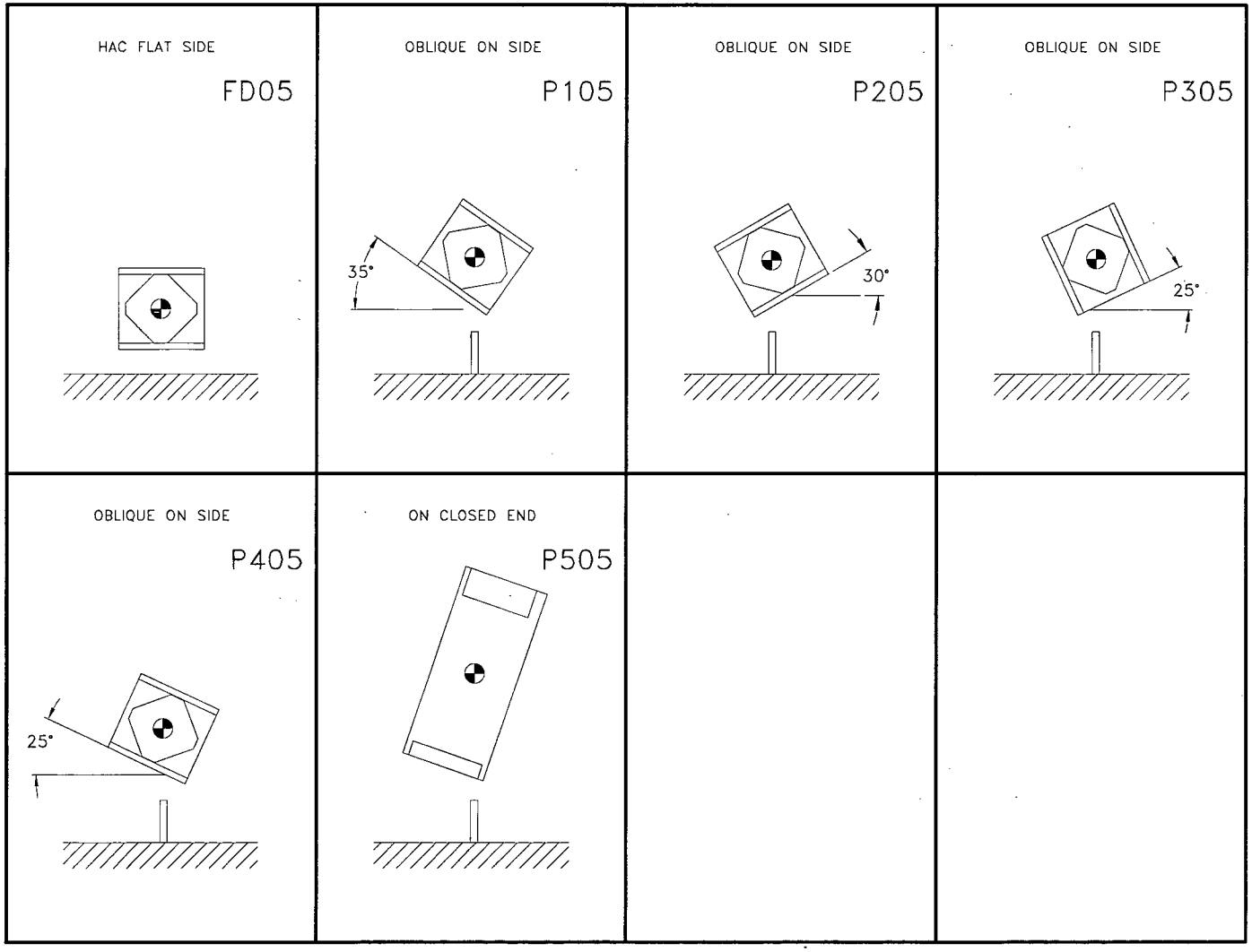

Figure 2.12.1-8 – Schematic of U.S. 2005 Engineering Tests

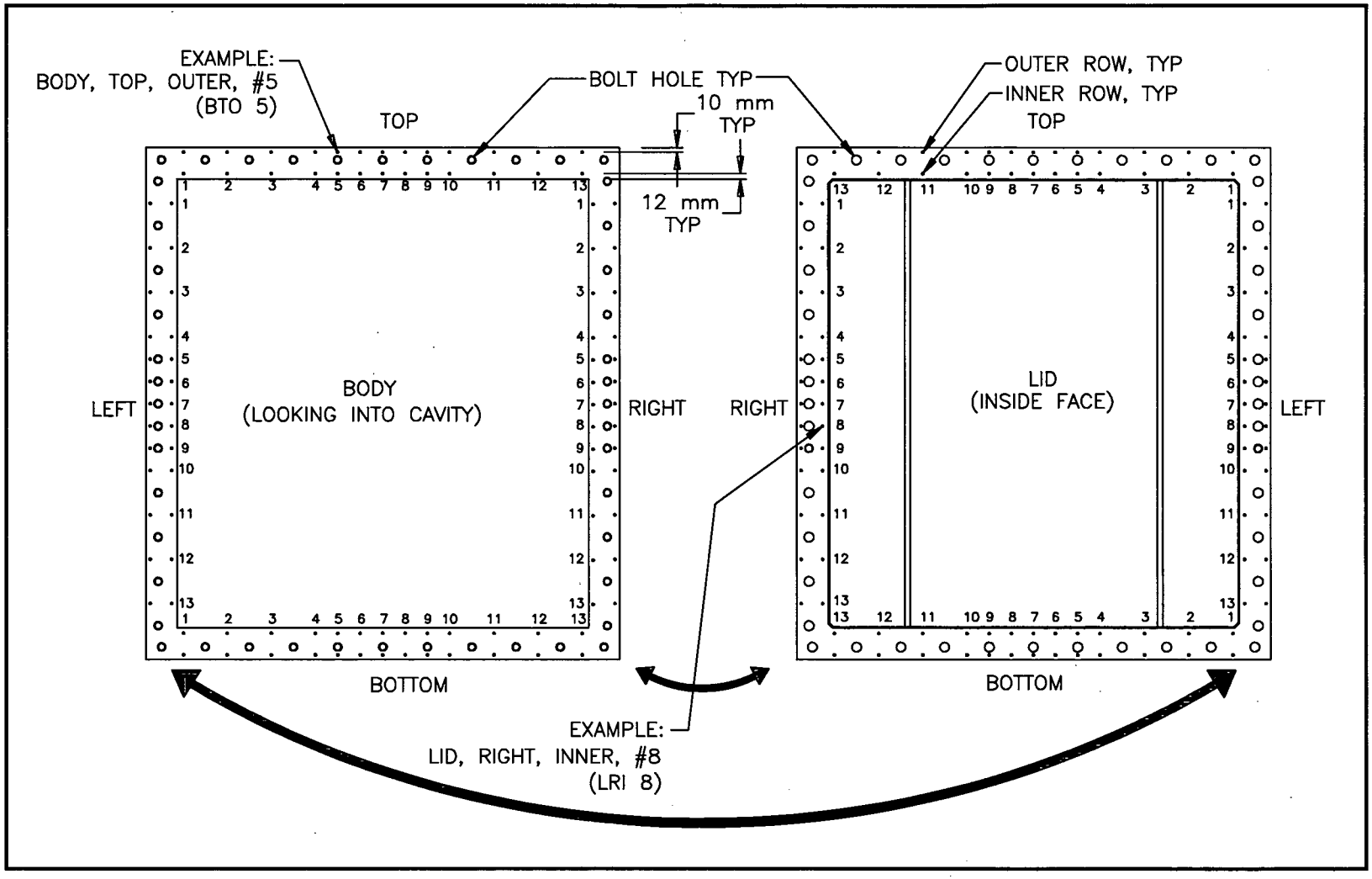

Figure 2.12.1-9 – Body and Lid Flange Measurement Locations

Table 2.12.1-2 – Summary of French Engineering Tests①

Test No.	Test Description	Orientation②	Test Temperature	Observations and Results
A1	NCT CG-over-cheek edge	68°	All tests performed at ambient temperatures.	~7 - ~10 mm bulge on side walls
F2	HAC vertical, closed end down	90°		Ave ~25 mm bulge on side walls, failure of three weld joints in octagon recess
F3	Puncture drop on cover center	90°		~21 mm dent in closure lid structural sheet
A4	HAC CG-over-cover edge	66°		~267 mm wide flat, max ~30 mm wide split in failed weld joint in octagon recess
F5	Puncture drop on side (30° oblique impact)	0°		Penetration through CSA containment sheet.
C7	HAC CG-over-corner, lid end	Fig. 2.12.1-6		~210 mm deep × ~530 mm wide × ~500 mm high flat
C8	Puncture on overpack cover/body gap	Fig. 2.12.1-6		~100 mm wide × ~100 mm deep gap
F9	Puncture drop on side (30° oblique impact)	0°		~90 mm penetration to CSA structural sheet
A6	HAC on side-edge	5°		~120 mm to ~175 mm wide flat along edge

Notes:

① Tested 4/25/94 – 7/4/94.

② Orientation is longitudinal axis of the package relative to the horizontal impact surface.

Table 2.12.1-3 – Summary of U.S. 2003 Engineering Tests①

Test No.	Test Description	Orientation②	Test Temperature③	Observations and Results
FD1	HAC vertical, closed end down	90°	-21 °C	~32 mm max crush (lower corner), creating a ~64 mm bulge. Some weld joints failed in octagon recess (maximum opening ~6 mm wide × ~686 mm long).
FD2	NCT vertical, lid end down	90°	-37 °C	~16 mm high × ~254 mm long bulge, no weld joint failures.
FD3	HAC vertical, lid end down	90°	-28 °C	~17 mm maximum crush, ~25 mm bulge of inner horizontal sheet in octagon, (2) small weld cracks (maximum width ~6 mm).
FD4	HAC slapdown, lid end secondary	25°	-34/-31 °C	~57 mm × ~152 mm flat (primary end), ~25 mm × ~483 mm flat (secondary end)
P1	Puncture drop on cover near bolts	71°	Ambient	Penetration to closure lid structural sheet, creating a ~216 mm long tear.
P2	Puncture drop on overpack cover joint	Fig. 2.12.1-7	Ambient	~19 mm wide scuff mark on cheek surface.
P3	Puncture drop on slapdown damage	30°	Ambient	~36 mm deep dent, ~46 mm on body, & ~83 mm on overpack cover (no penetration).
P4	Puncture drop on closed end	71°	Ambient	Penetration to CSA structural sheet, creating a dent ~29 mm deep, ~80 mm long tear. Dent depth on CSA structural sheet 29 mm

Notes:

① Tested 9/15/03 – 9/30/03.

② Orientation is longitudinal axis of the package relative to the horizontal impact surface.

③ Temperatures listed for wood. Ambient temperatures ranged between 21 °C and 34 °C for the puncture tests.

Table 2.12.1-4 – Summary of U.S. 2005 Engineering Tests①

Test No.	Test Description	Orientation②	Test Temperature	Observations and Results
FD05	HAC Flat Side Drop	0°	All tests performed at ambient temperatures.	Little external deformation; no permanent deformation of CSA, good retention of closure bolt torque, seals held hard vacuum
P105	Oblique Puncture on Side	35°		Least damaging of the P105 – P405 series
P205	Oblique Puncture on Side	30 °		Shear fracture of PRP③, moderate damage
P305	Oblique Puncture on Side	25°		Shear fracture of PRP, deepest CSA dent
P405	Oblique Puncture on Side	25°		Approximately the same as P305
P505	Oblique Puncture on Closed End	71°		No shear fracture of PRP, moderate dent only

Notes:

① Tested 9/2005.

② Orientation is longitudinal axis of the package relative to the horizontal impact surface.

③ Puncture-resistant plate (PRP).

This page intentionally left blank.

Table 2.12.1-5 – Lid-to-Body Gaps at Outside Edge of Flange (mm)

Position	Left Flange	Top Flange	Right Flange	Bottom Flange
1	0.30	0.81	0.46	0.25
2	0.30	0.89	0.43	0.36
3	0.23	0.84	0.30	0.33
4	0.18	0.79	0.33	0.25
5	0.18	0.79	0.25	0.28
6	0.08	0.86	0.28	0.18
7	0.00	0.84	0.33	0.08
8	0.08	0.66	0.38	0.10
9	0.18	0.84	0.38	0.23
10	0.18	0.84	0.38	0.36
11	0.15	0.79	0.30	0.48
12	0.23	0.84	0.25	0.56
13	0.36	0.86	0.15	0.48

Table 2.12.1-6 – U.S. 2005 Engineering Puncture Test Results

Test No.	Angle, degrees①	CSA Dent Depth, mm
P105	35	②
P205	30	14
P305	25 #1	29
P405	25 #2	24
U.S. 2003, P4	19	29

Notes:

① Angle defined as between ETU impact surface and the ground as shown in Figure 2.12.1-8. For U.S. 2003 P4 test, 71° orientation of ETU axis to ground is equivalent to 19° orientation of closed end surface to ground.

② Since the puncture-resistant plate did not shear, the dent depth is assumed negligible.

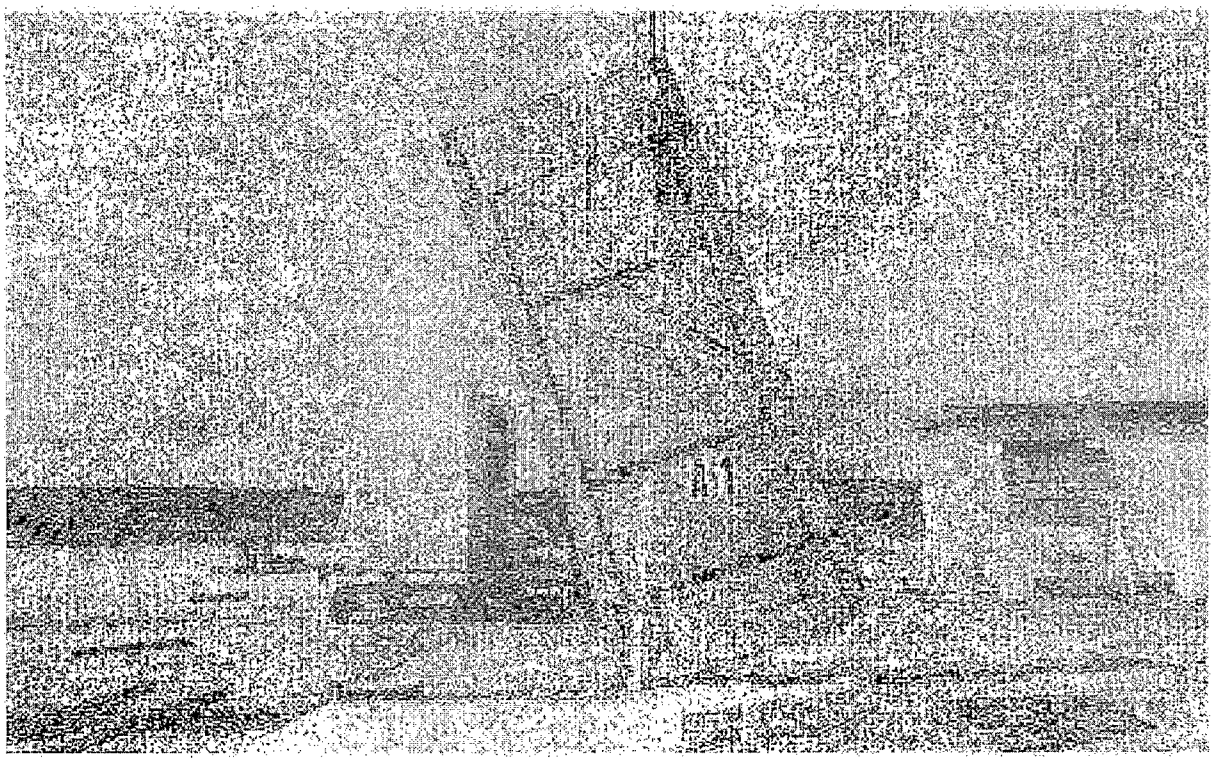

Figure 2.12.1-10 – Free Drop Test A1: Pre-Test View of CTU Orientation

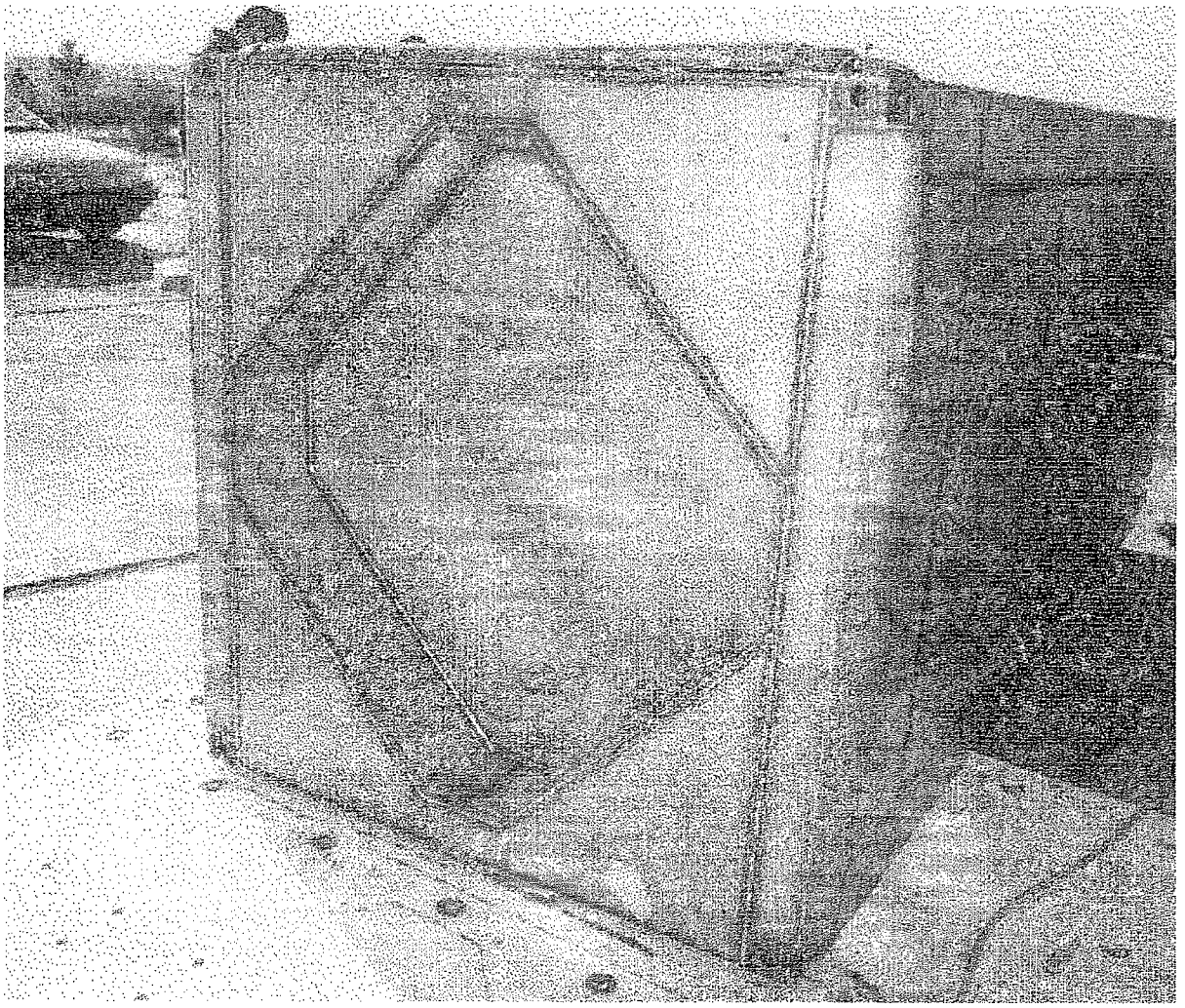

Figure 2.12.1-11 – Free Drop Test F2: Overall View of Closed End Damage

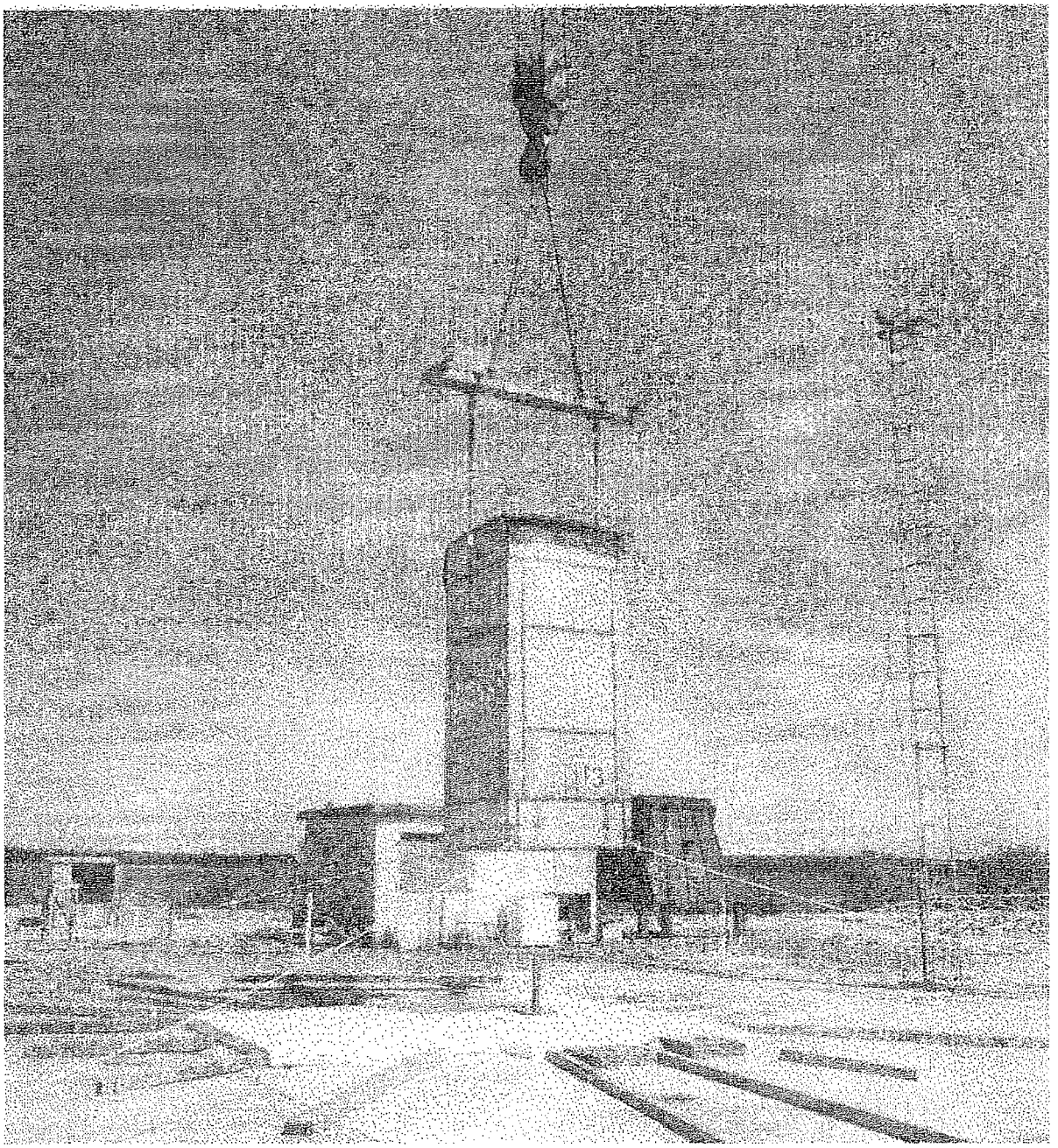

Figure 2.12.1-12 – Puncture Drop Test F3: Pre-Test View of CTU Orientation

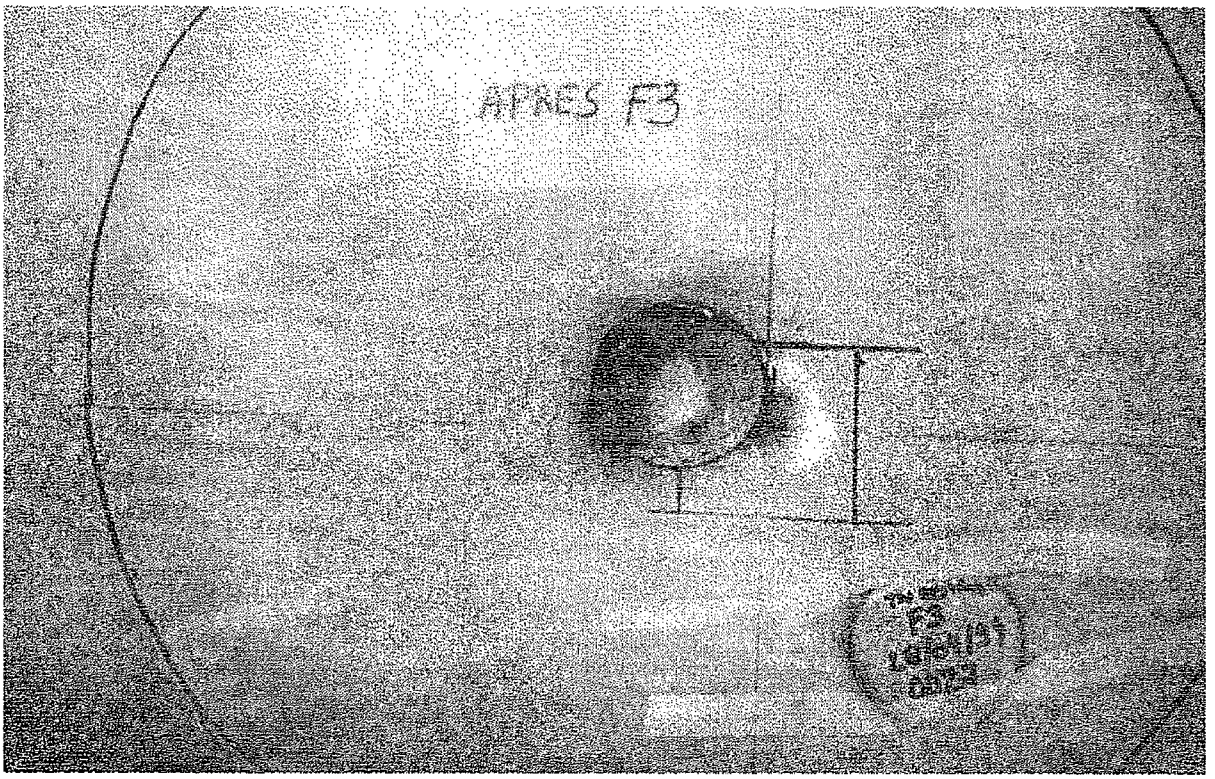

Figure 2.12.1-13 – Puncture Drop Test F3: Close-up View of Damage, ~120 mm Deep

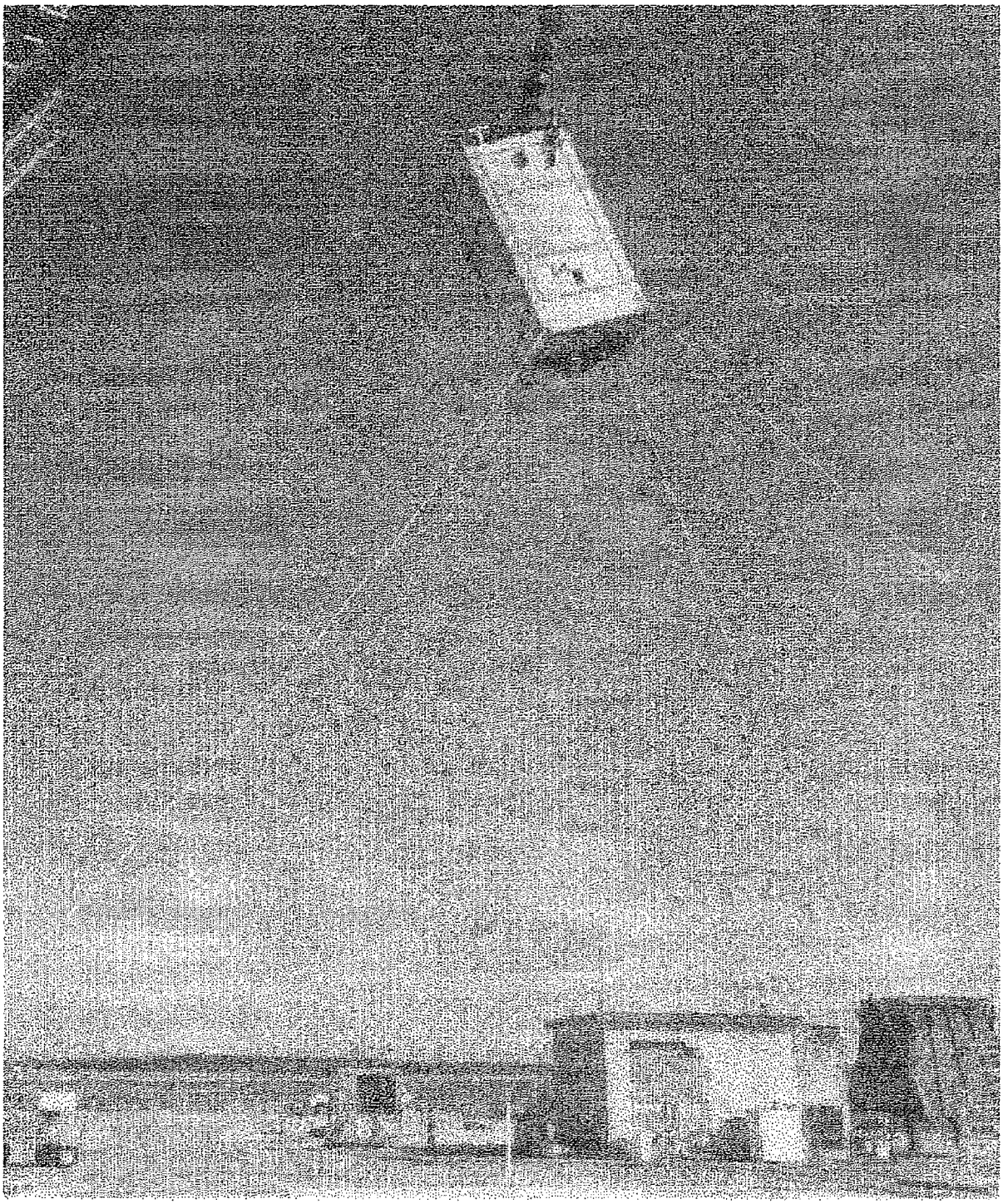

Figure 2.12.1-14 – Free Drop Test A4: Pre-Test View of CTU Orientation

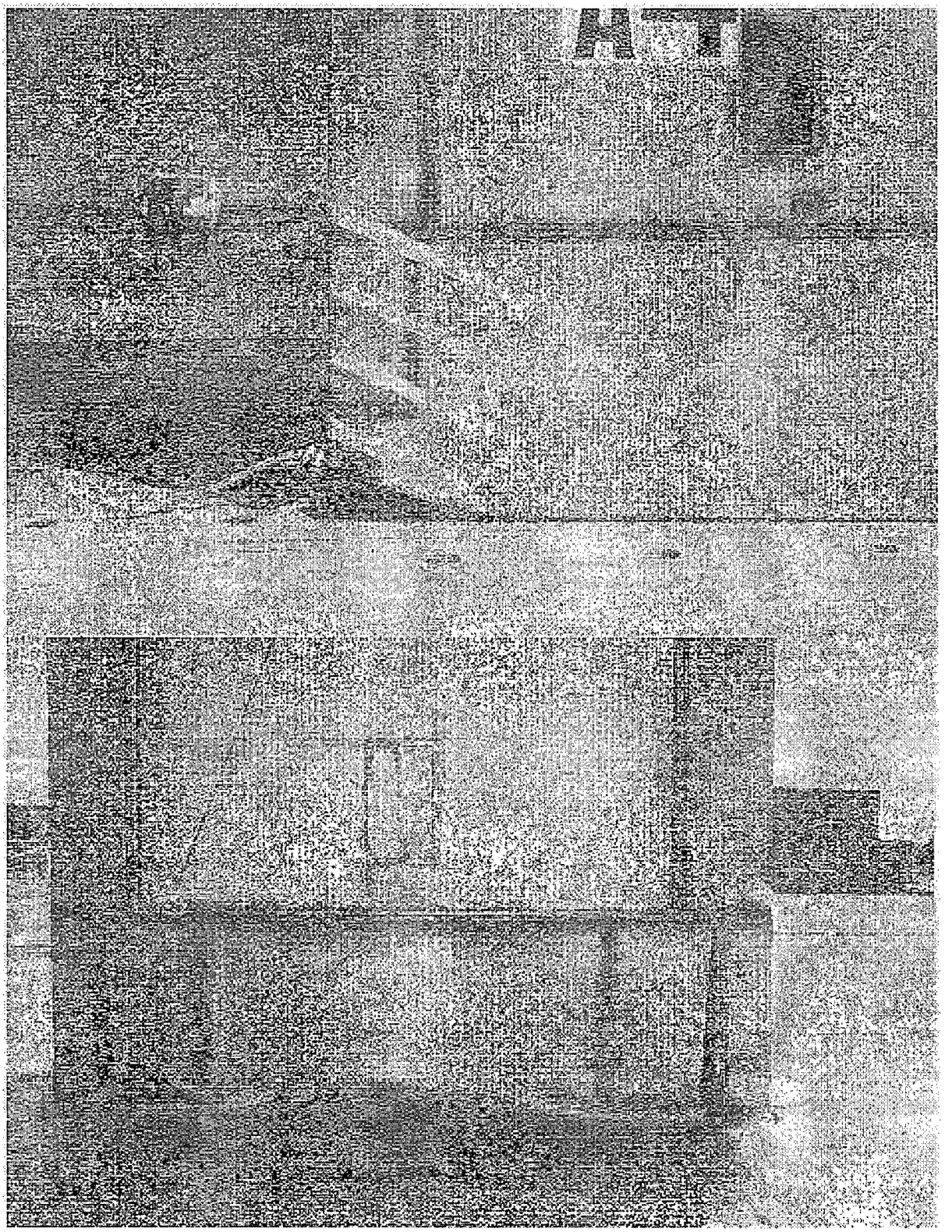

Figure 2.12.1-15 – Free Drop Test A4: Close-up Views of Edge Damage

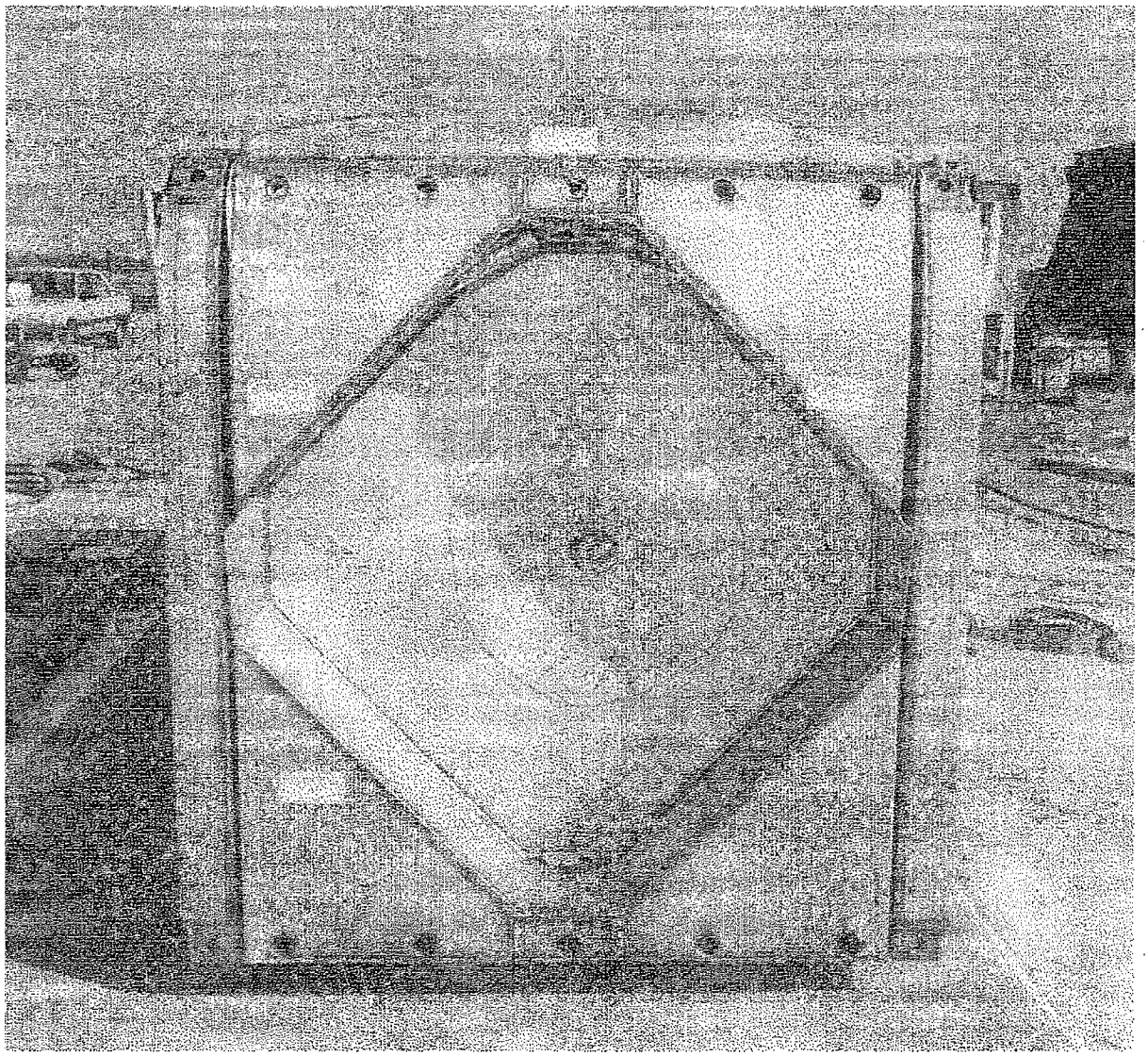

Figure 2.12.1-16 – Free Drop Test A4: Overall View of Overpack Cover Damage

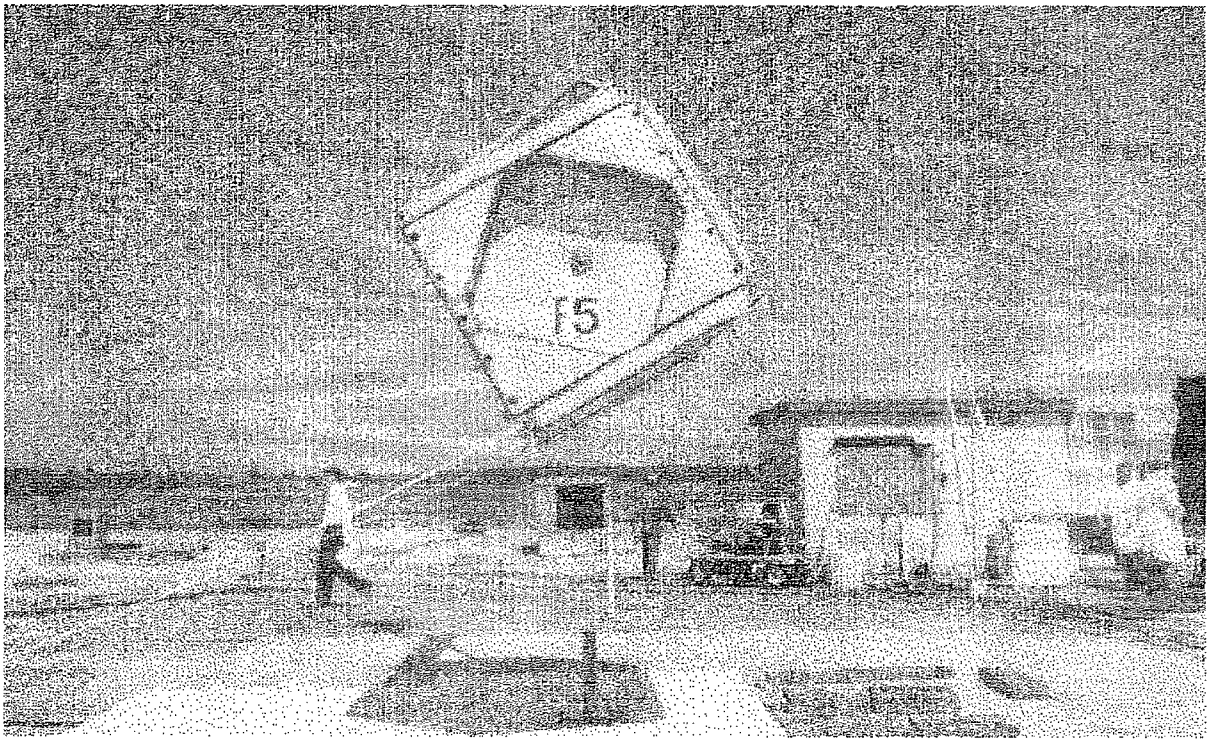

Figure 2.12.1-17 – Puncture Drop Test F5: Pre-Test View of CTU Orientation

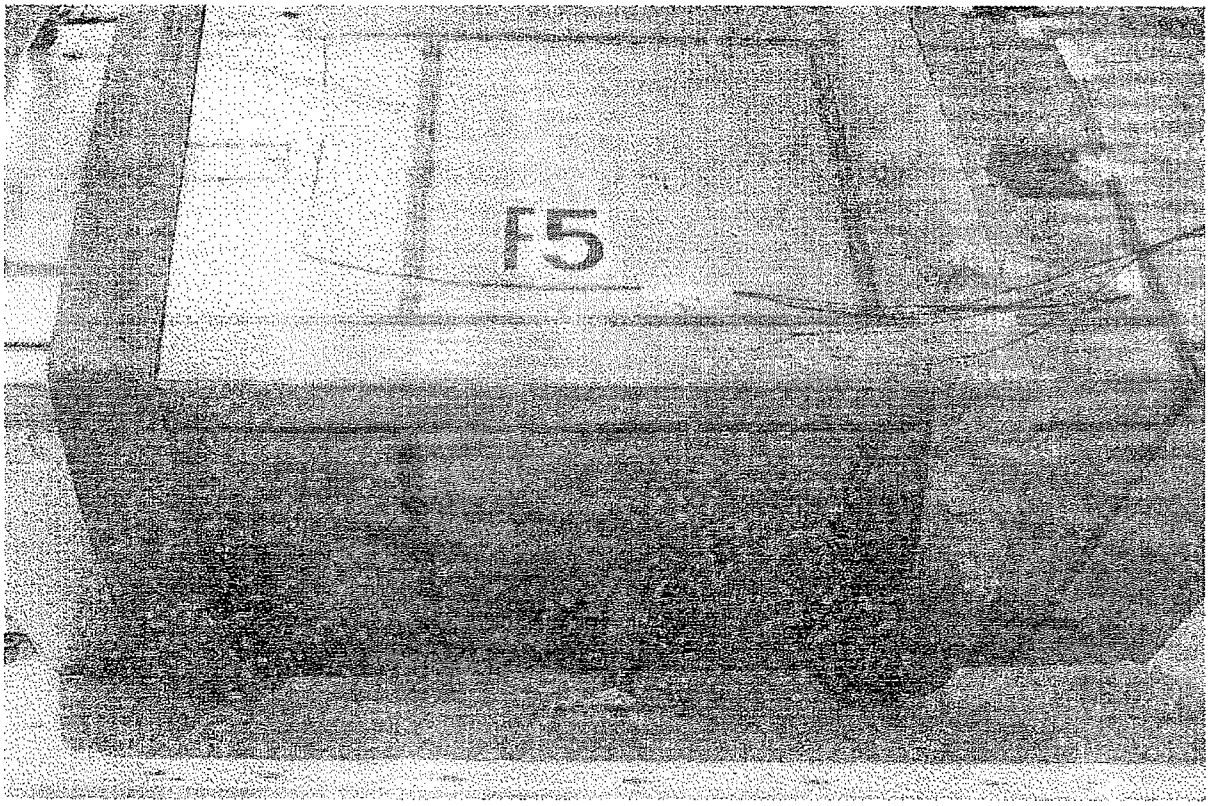

Figure 2.12.1-18 – Puncture Drop Test F5: View Immediately Following Impact

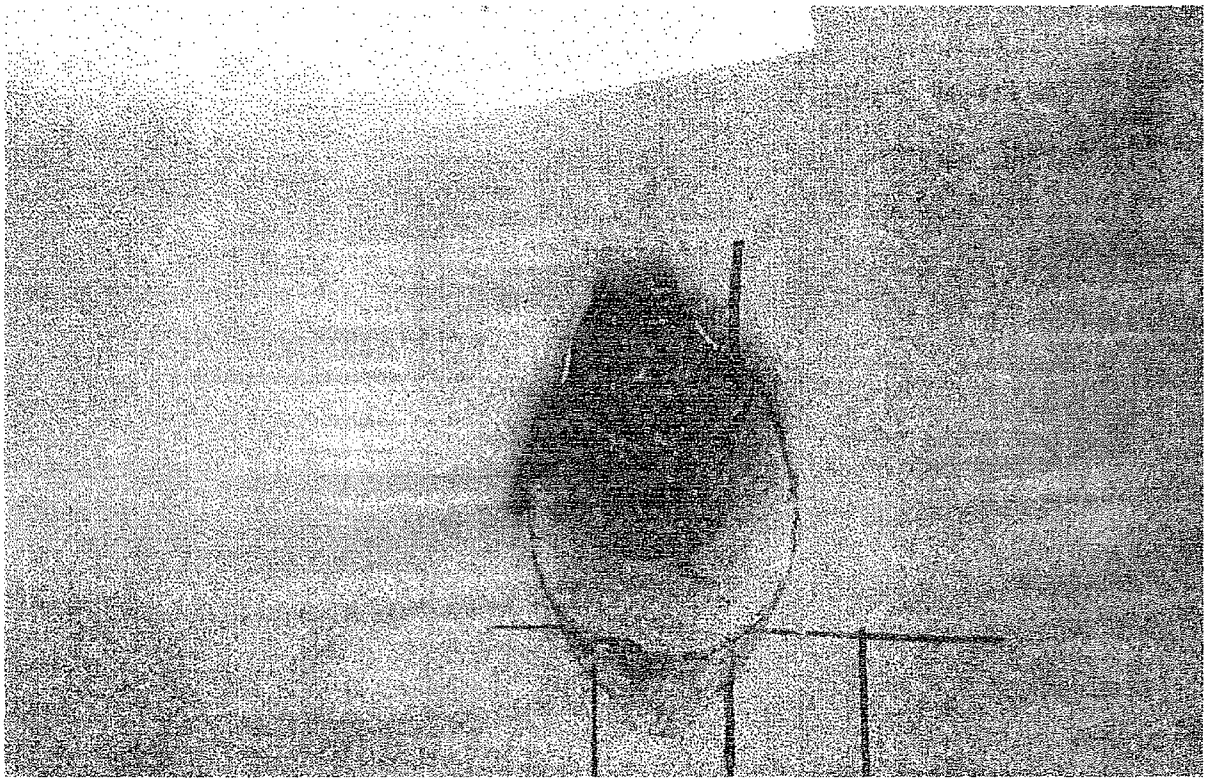

Figure 2.12.1-19 – Puncture Drop Test F5: Close-up View of Damage

Figure 2.12.1-20 – Puncture Drop Test F5: View of Internal Damage (with Welded Patch)

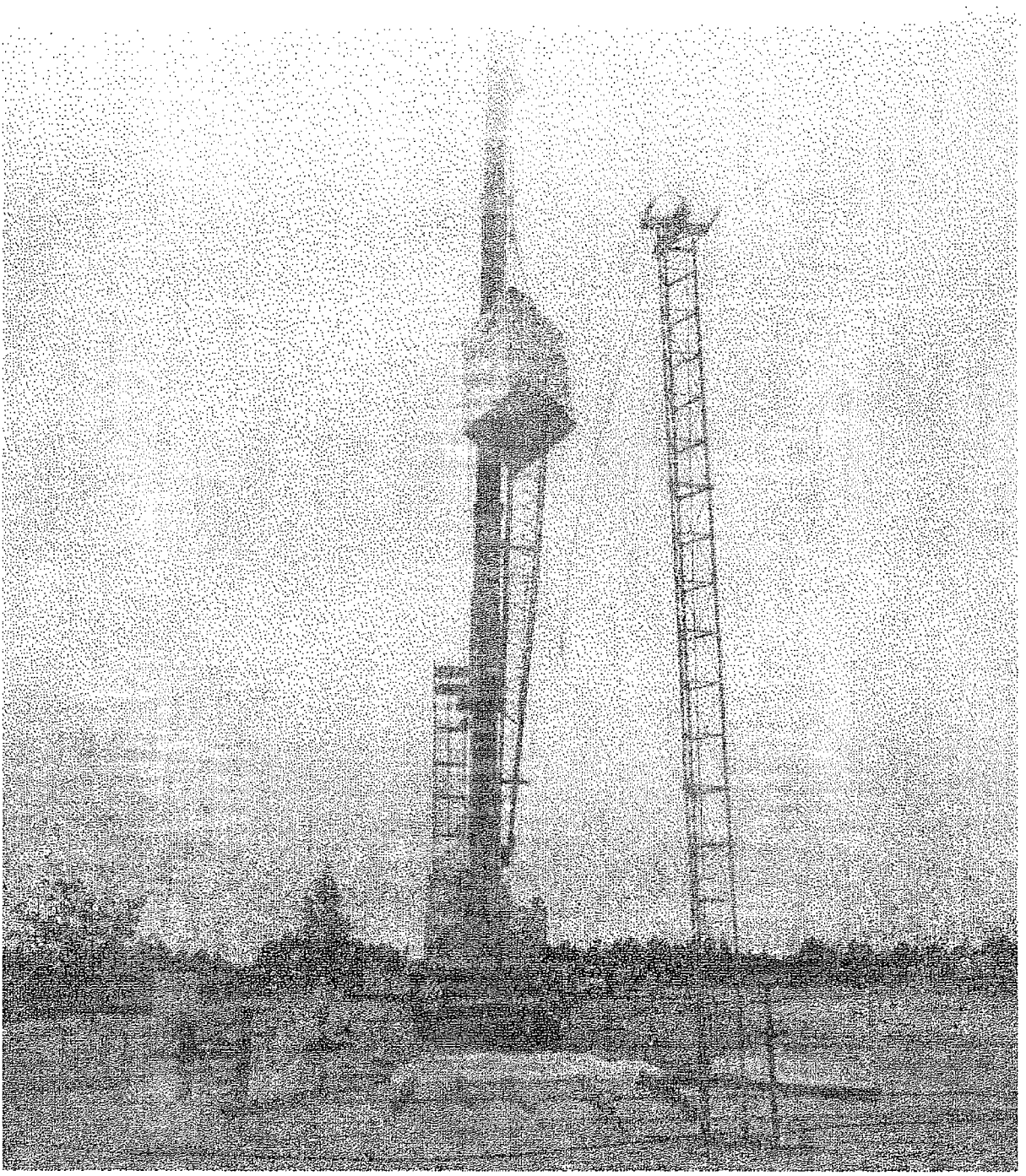

Figure 2.12.1-21 – Free Drop Test C7: Pre-Test View of CTU Orientation

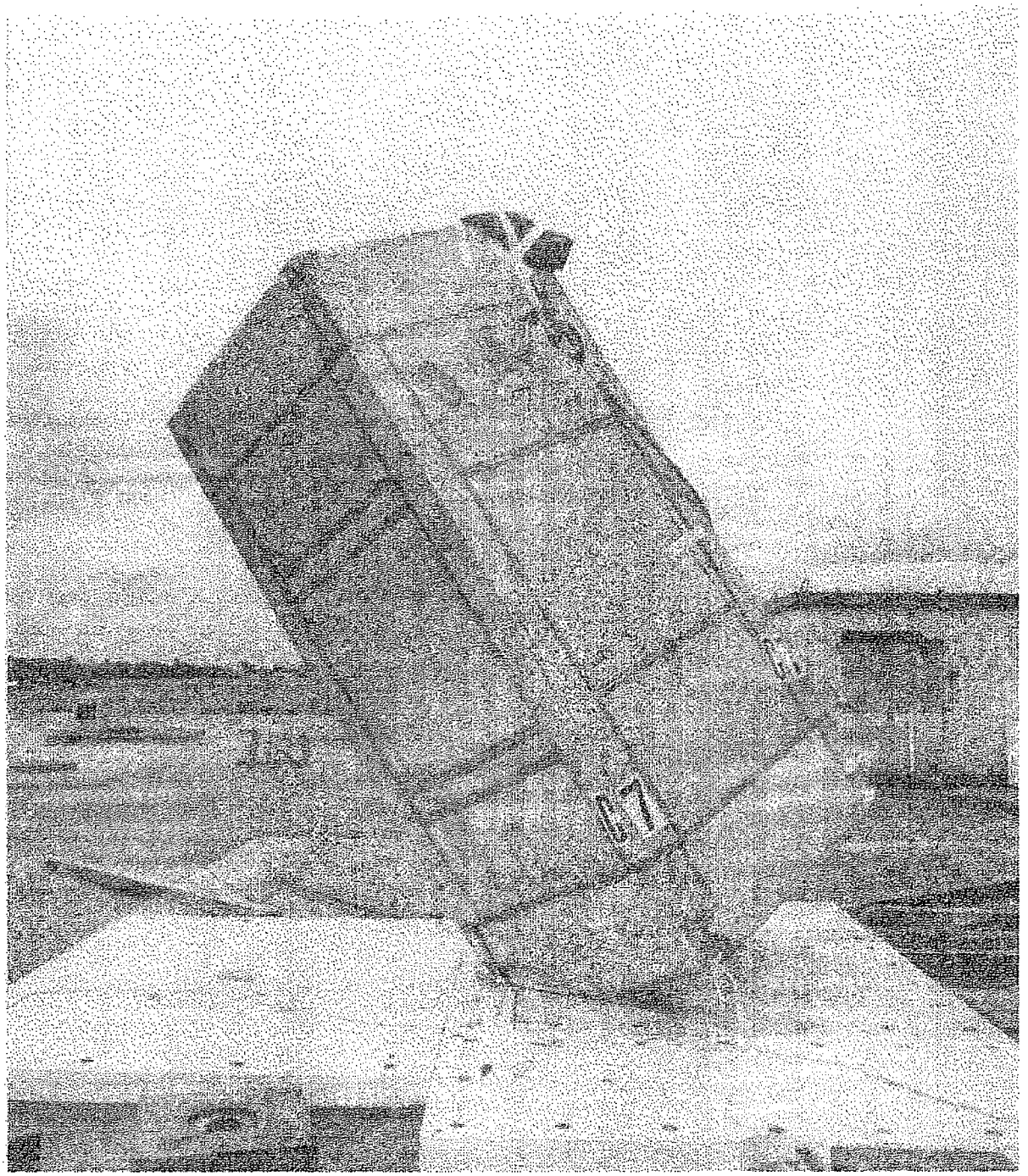

Figure 2.12.1-22 – Free Drop Test C7: View Immediately Following Impact

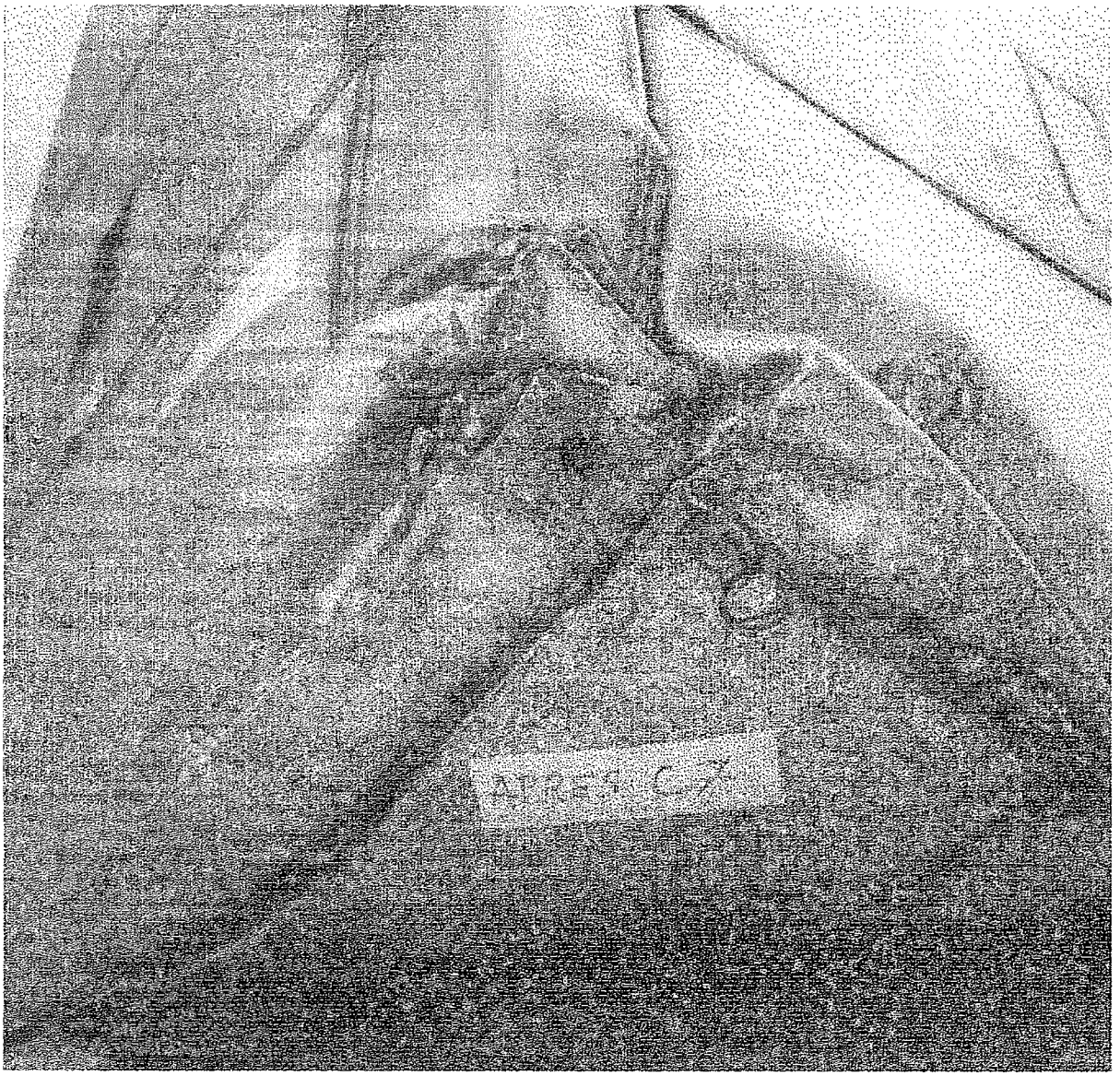

Figure 2.12.1-23 – Free Drop Test C7: Close-up View of Overpack Cover/Cheek Damage

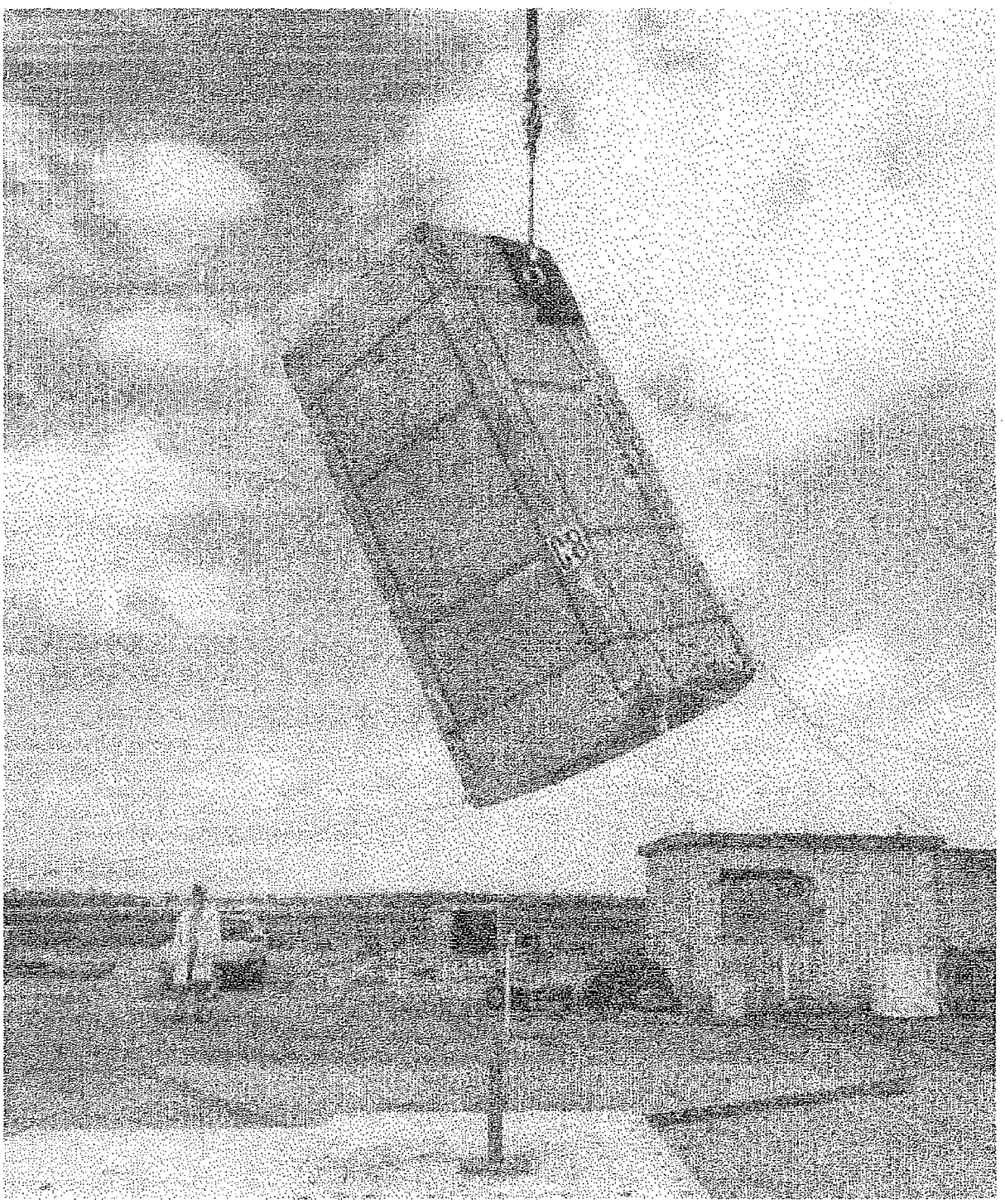

Figure 2.12.1-24 – Puncture Drop Test C8: Pre-Test View of CTU Orientation

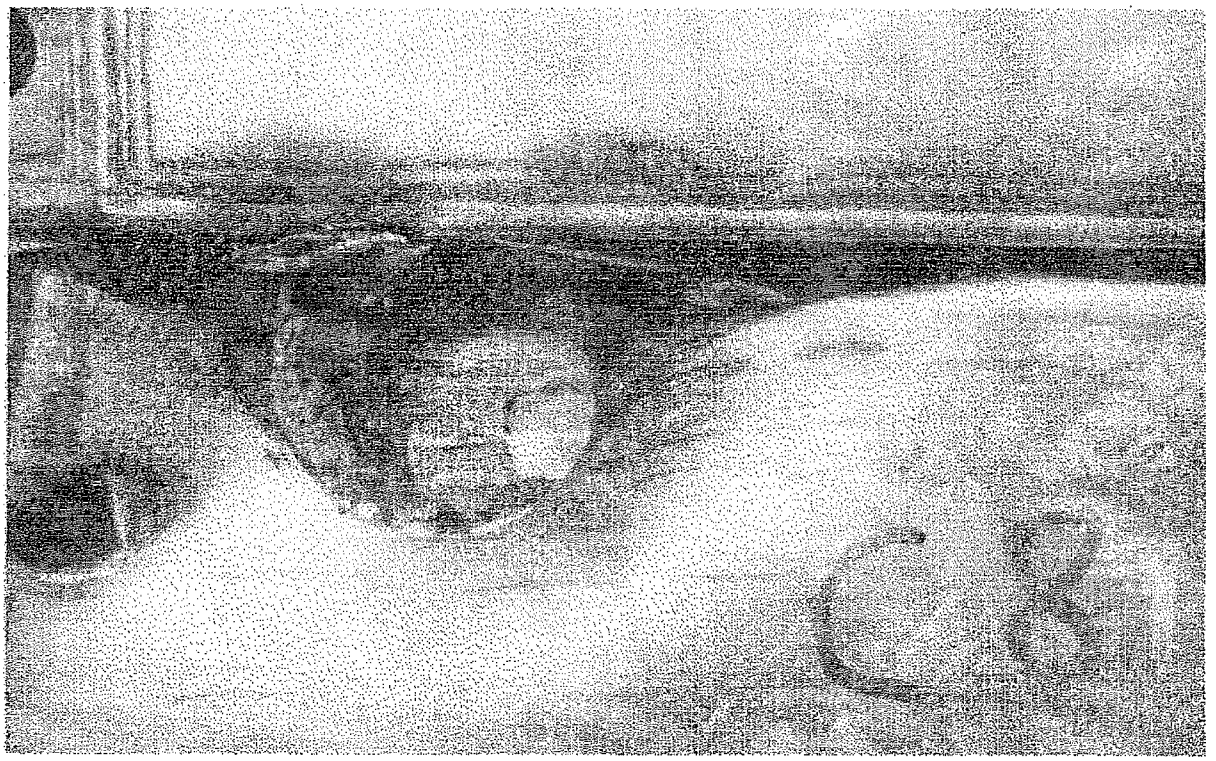

Figure 2.12.1-25 – Puncture Drop Test C8: Close-up of Overpack Cover/Cheek Damage

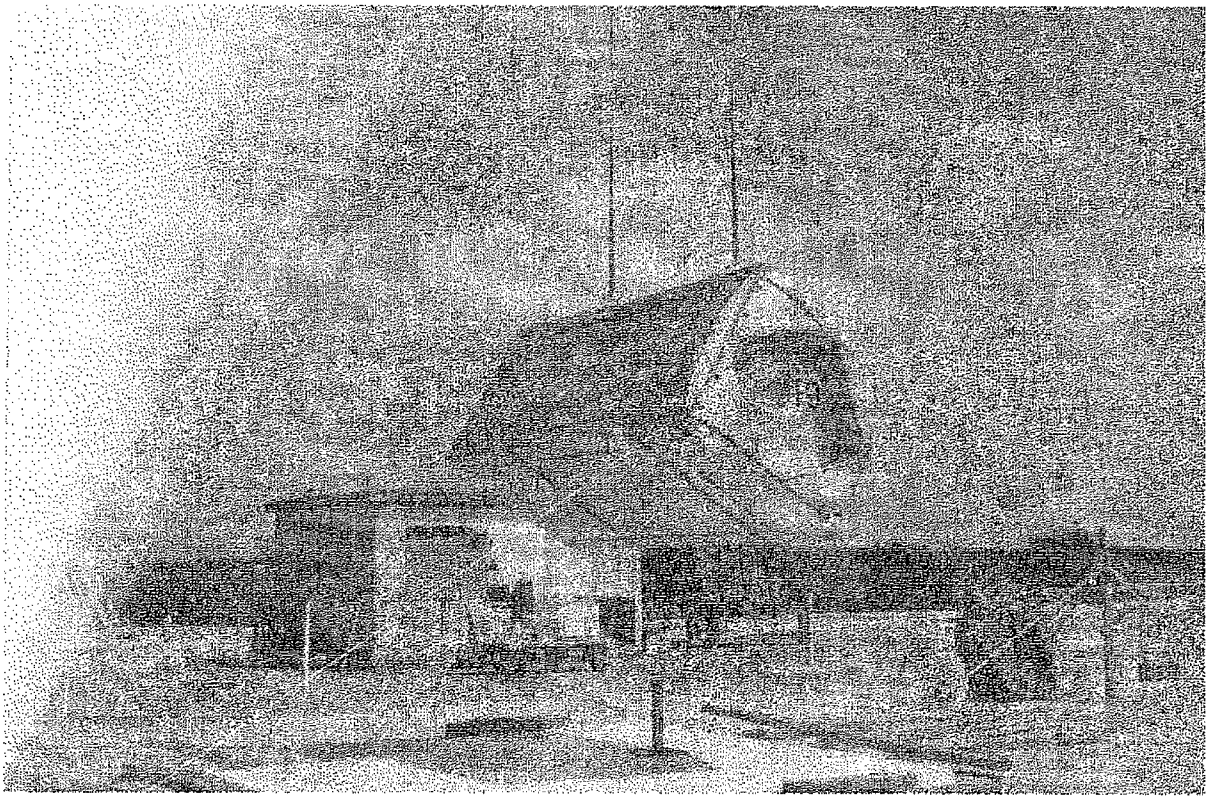

Figure 2.12.1-26 – Puncture Drop Test F9: Pre-Test View of CTU Orientation

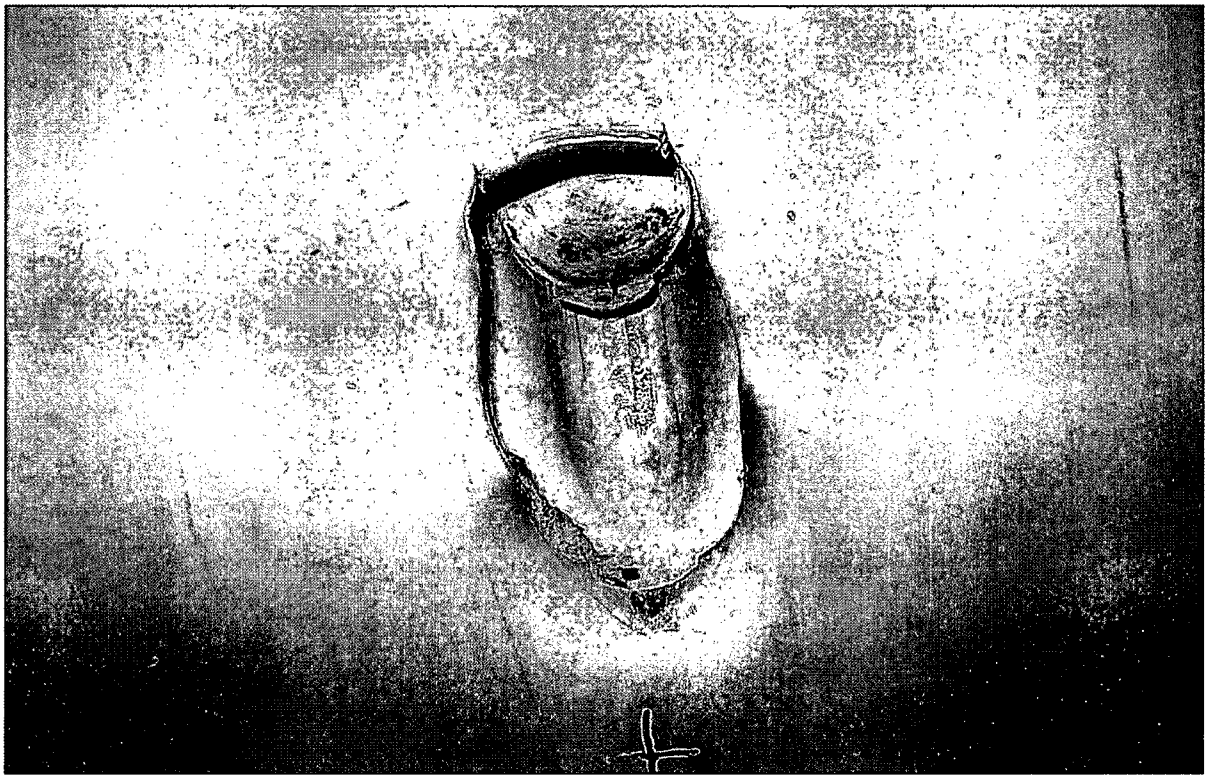

Figure 2.12.1-27 – Puncture Drop Test F9: Close-up View of Damage

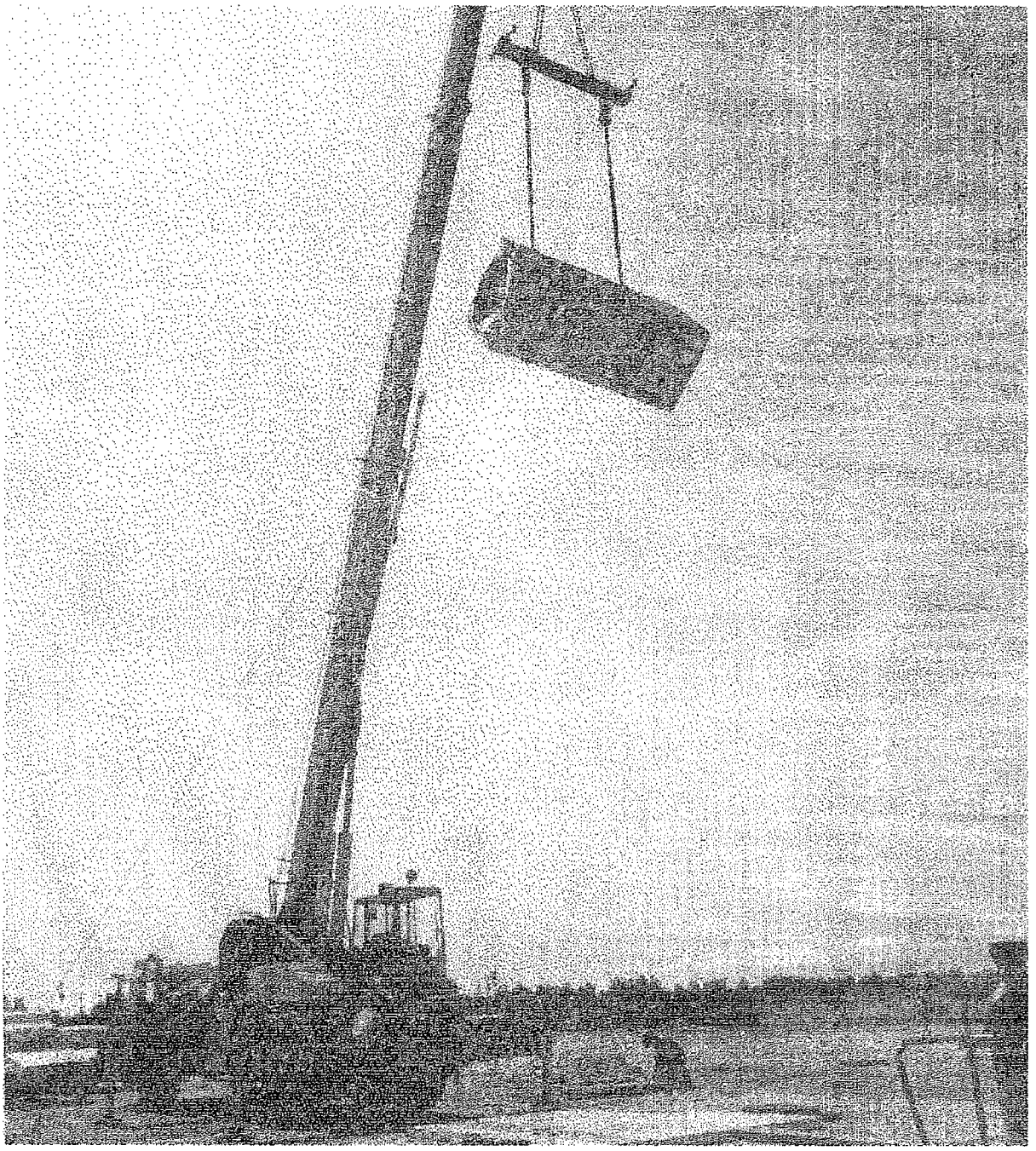

Figure 2.12.1-28 – Free Drop Test A6: Pre-Test View of CTU Orientation

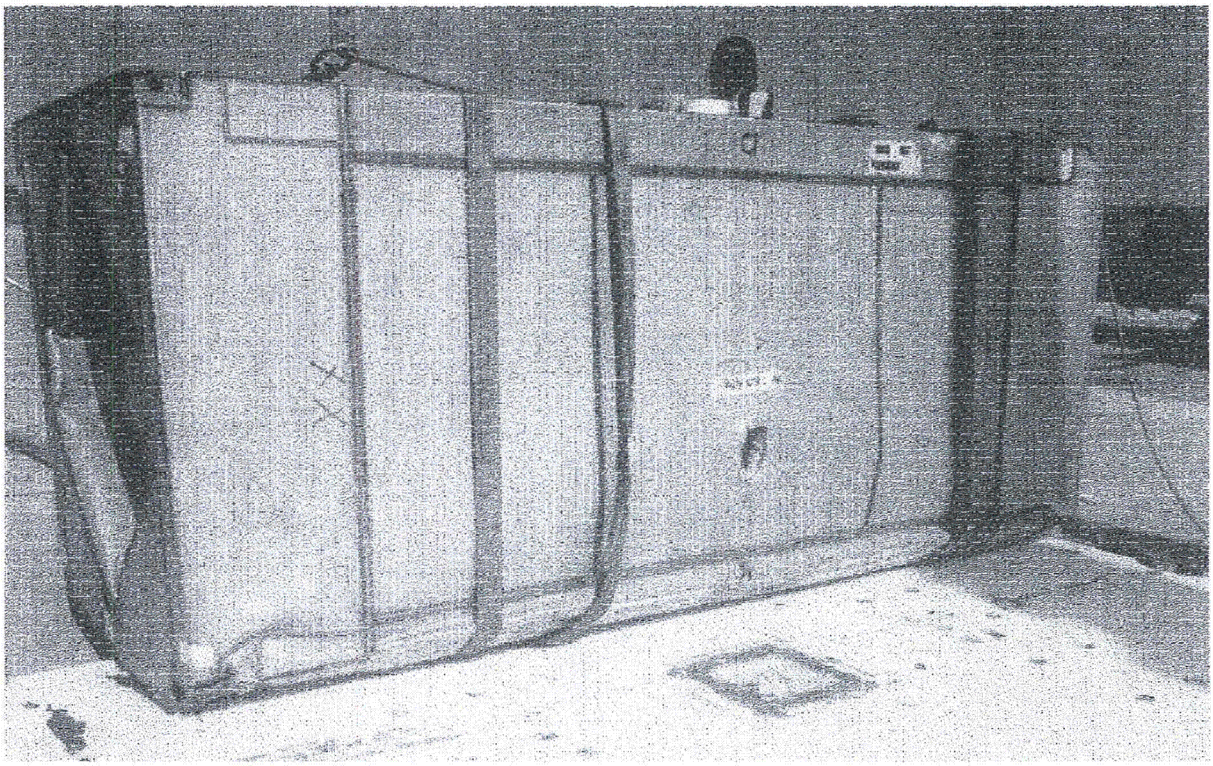

Figure 2.12.1-29 – Free Drop Test A6: Overall View of Damage Following Impact

Figure 2.12.1-30 – Free Drop Test A6: Overall View of Long-Edge Damage

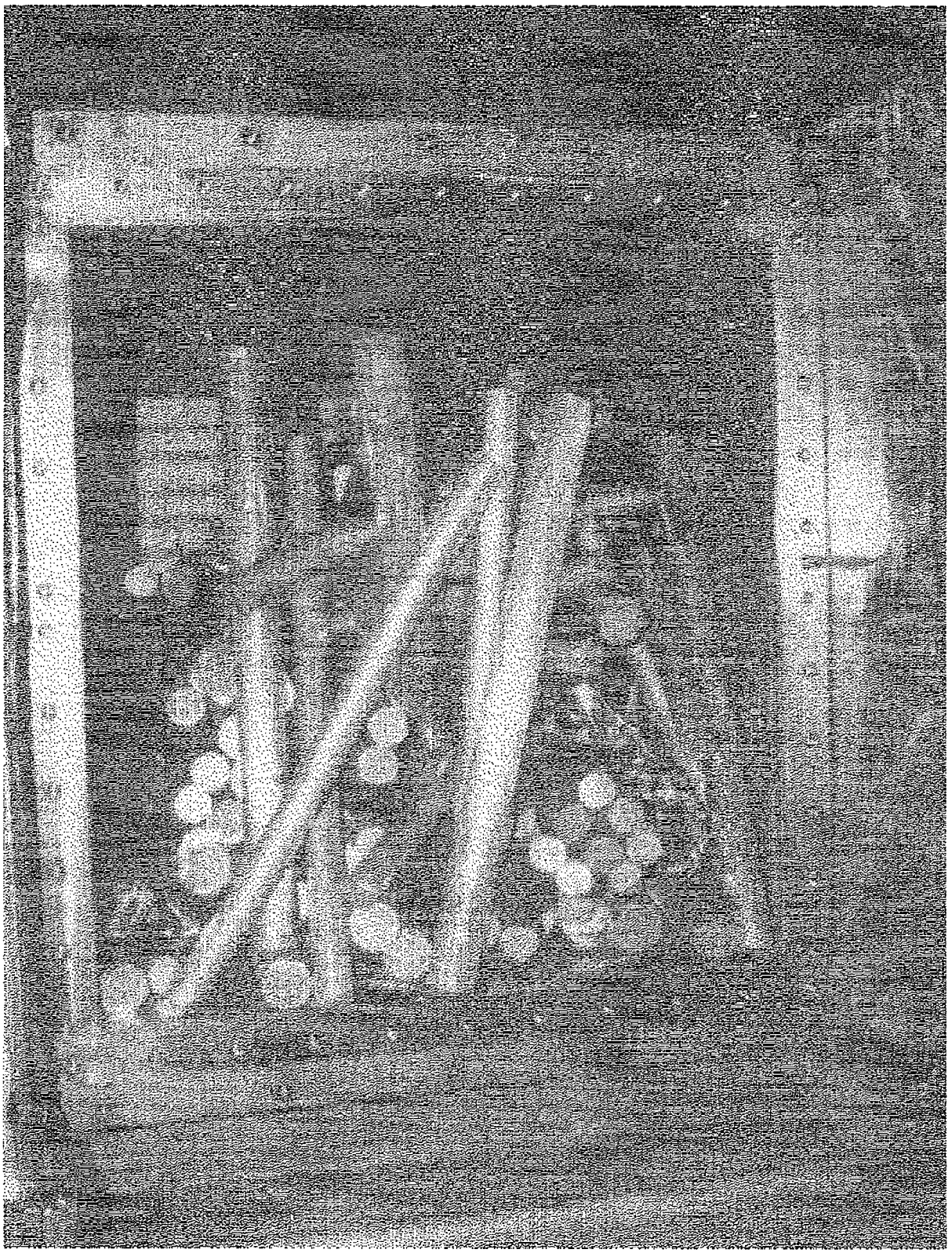

Figure 2.12.1-31 – Post-Test Disassembly: View of Loose Simulated Payload in Cavity

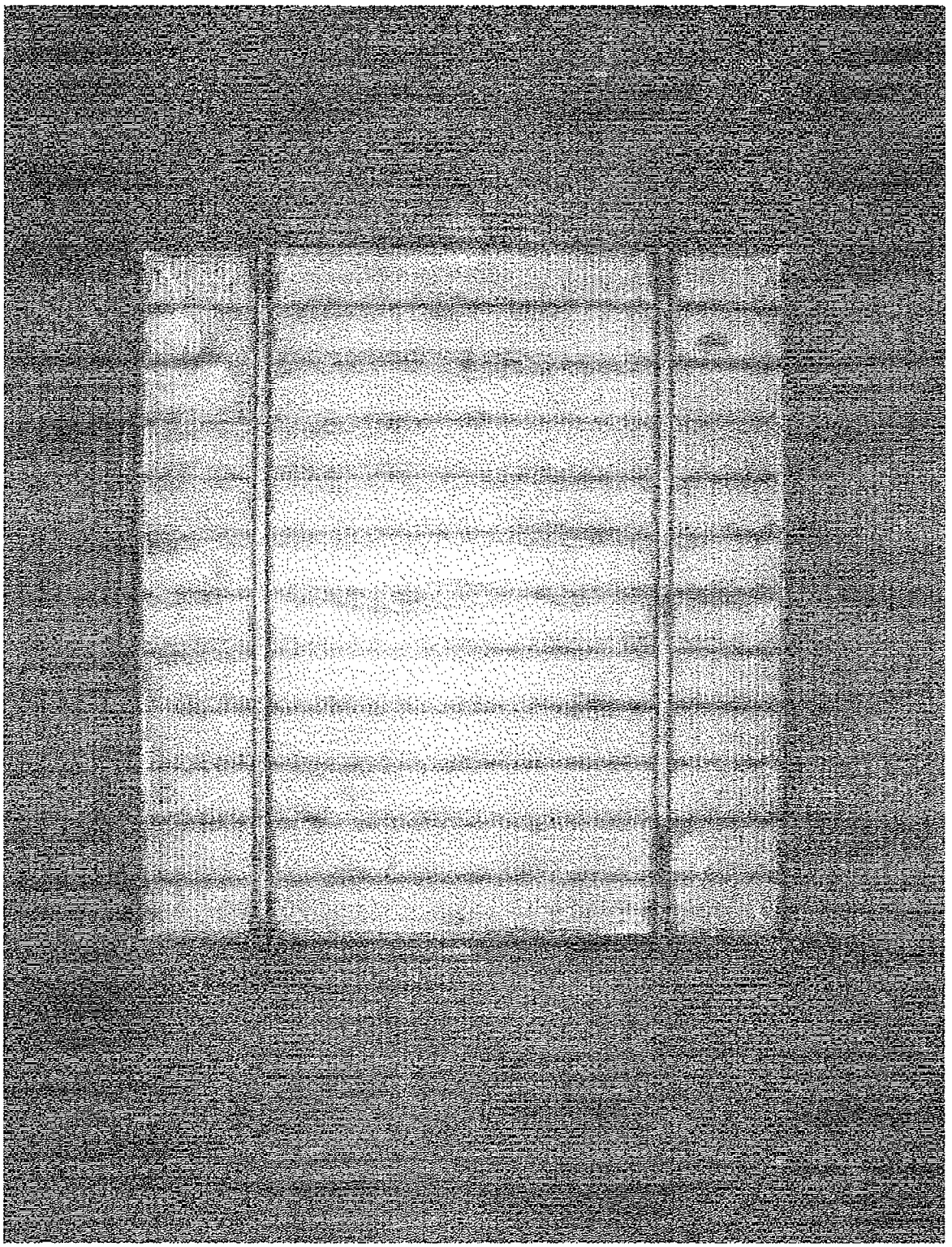

Figure 2.12.1-32 – Post-Test Disassembly: View of Cavity with Simulated Payload Removed

Figure 2.12.1-33 – Post-Test Disassembly: Close-up View of Closure Lid Puncture Damage

Figure 2.12.1-34 – Free Drop Test FD1: Close-up View of Weld Joint Damage

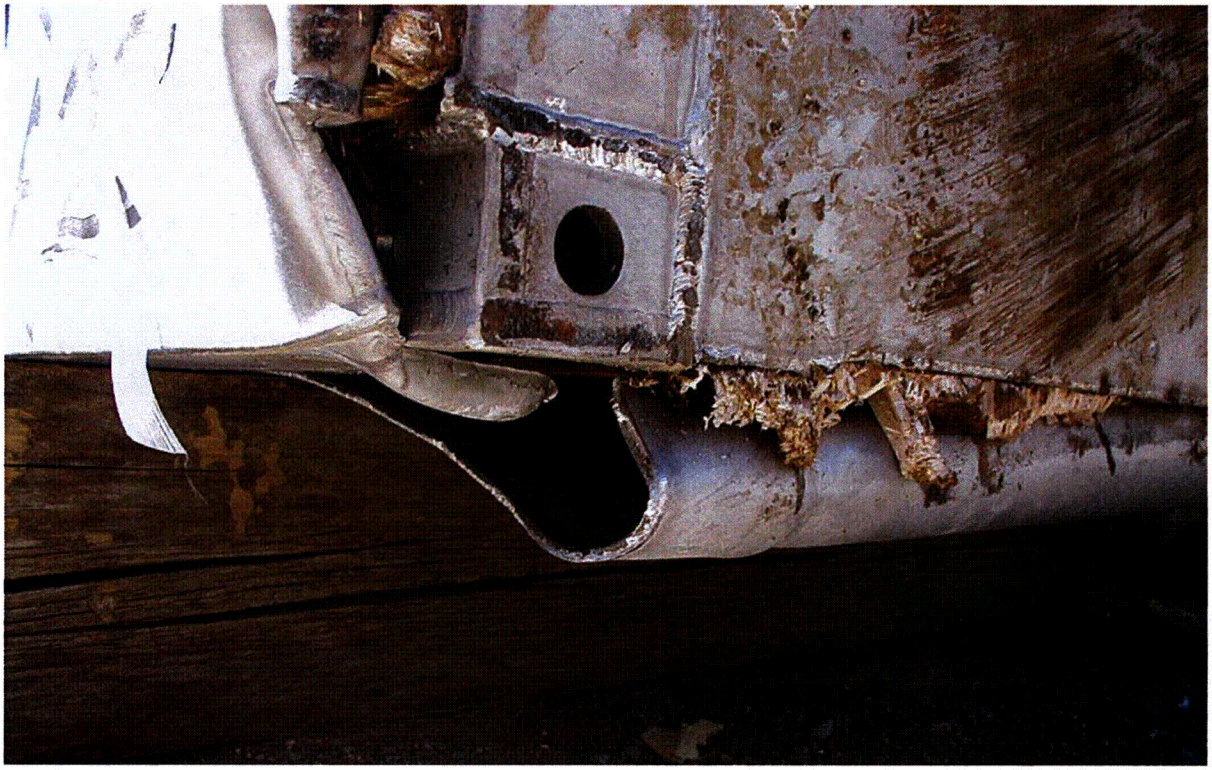

Figure 2.12.1-35 – Free Drop Test FD1: Close-up View of ISO Fitting Damage

Figure 2.12.1-36 – Free Drop Test FD2: View of Overpack Cover Edge Damage

Figure 2.12.1-37 – Free Drop Test FD3: Overall View of Overpack Cover Damage

Figure 2.12.1-38 – Free Drop Test FD3: Close-up View of ISO Fitting Damage

Figure 2.12.1-39 – Free Drop Test FD4: Overall View of Primary Impact Damage

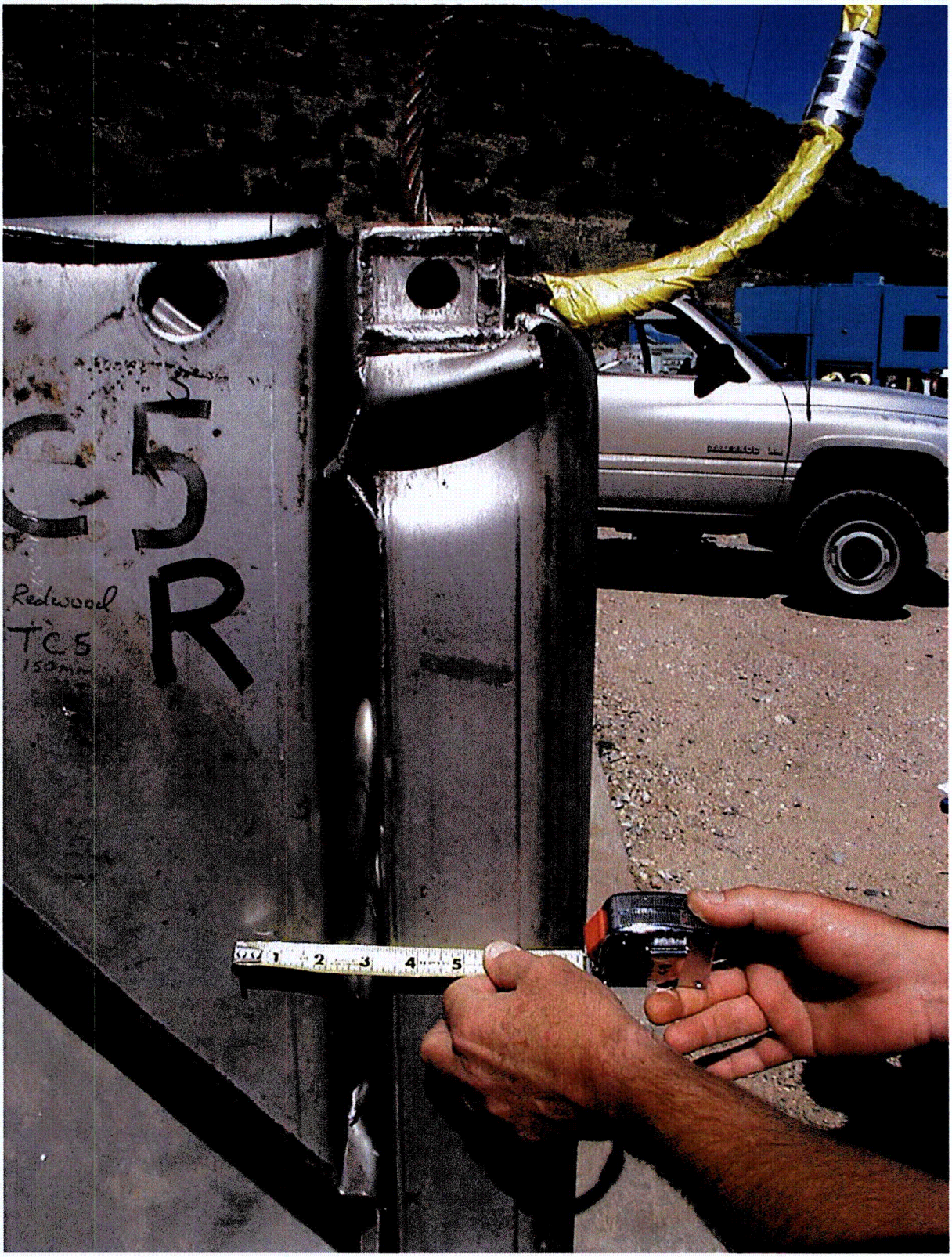

Figure 2.12.1-40 – Free Drop Test FD4: Close-up View of Secondary Impact Damage

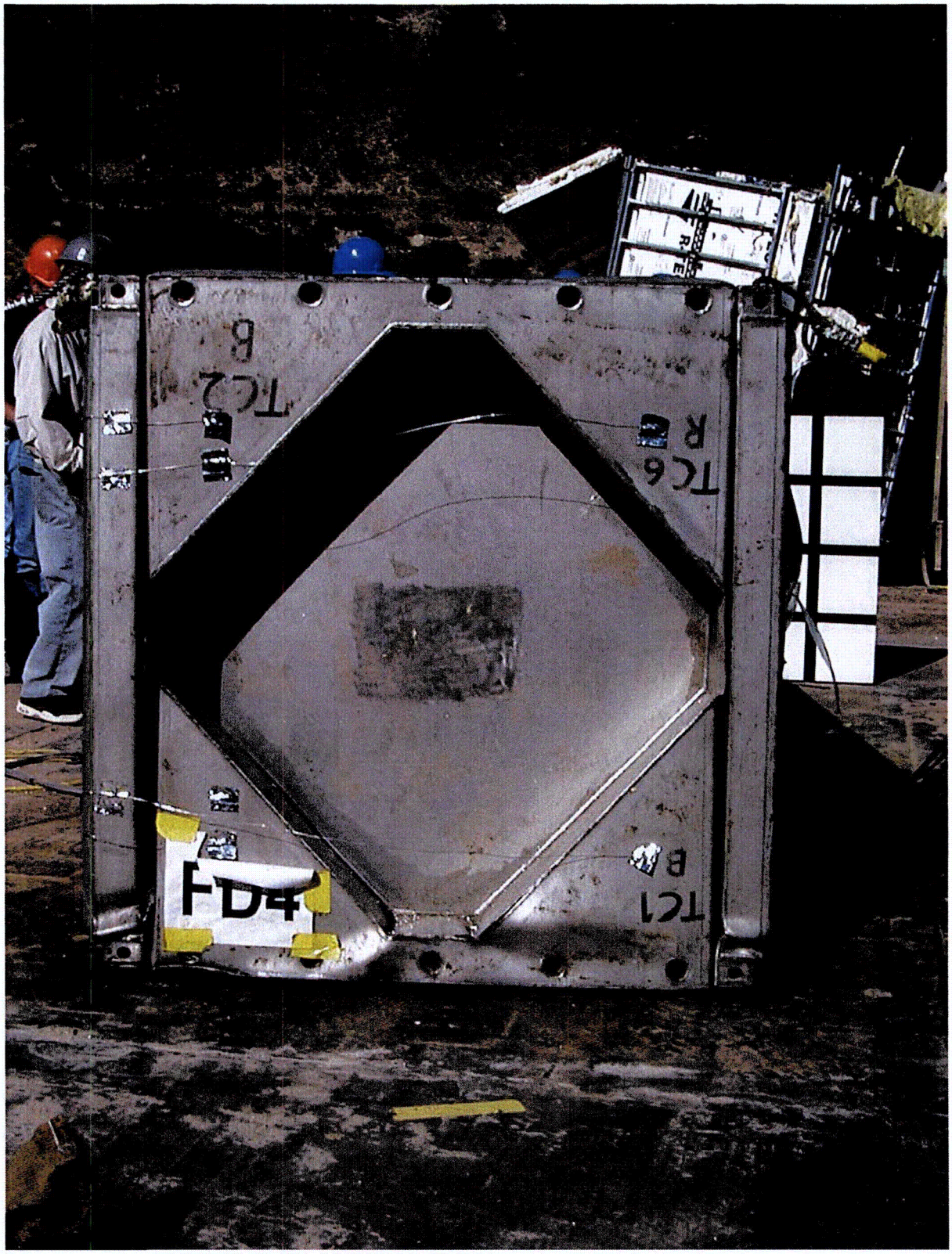

Figure 2.12.1-41 – Free Drop Test FD4: Overall View of Secondary Impact Damage

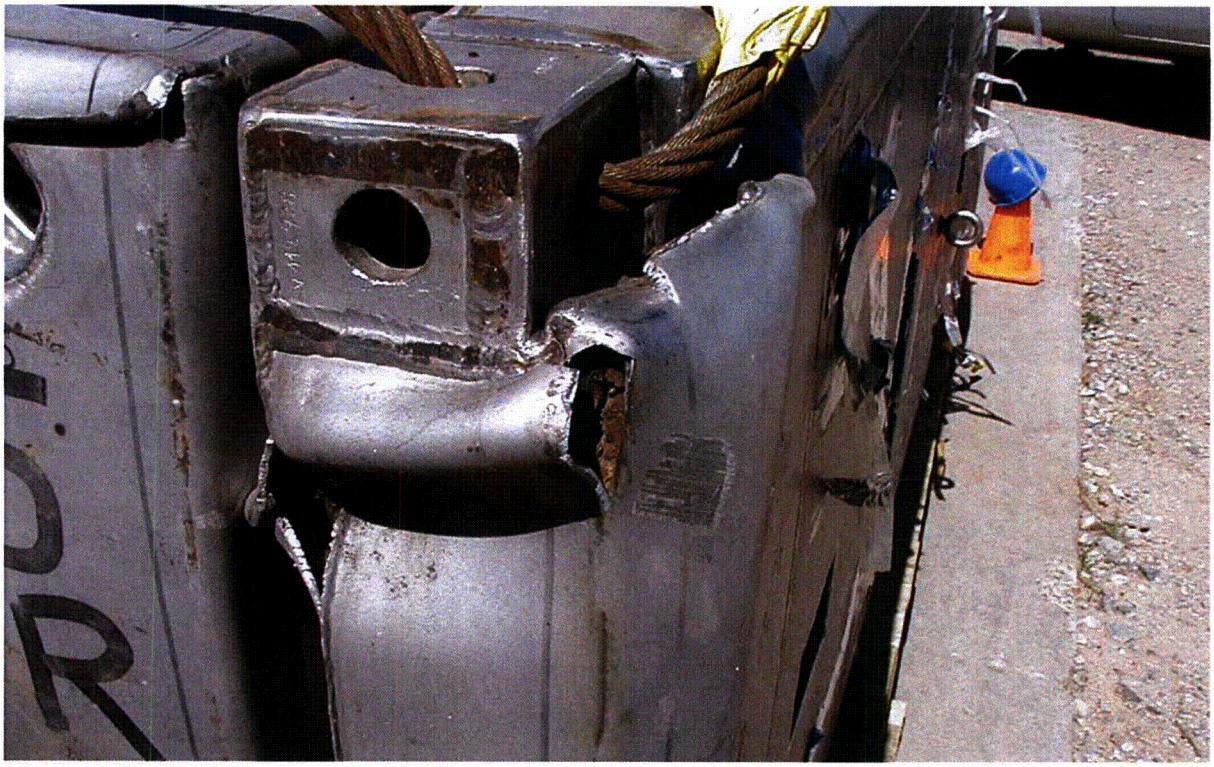

Figure 2.12.1-42 – Free Drop Test 4: View of ISO Fitting Damage, Secondary Impact

Figure 2.12.1-43 – Puncture Drop Test P1: Overall View Immediately After Impact

Figure 2.12.1-44 – Puncture Drop Test P1: Close-up View of Overpack Cover Damage

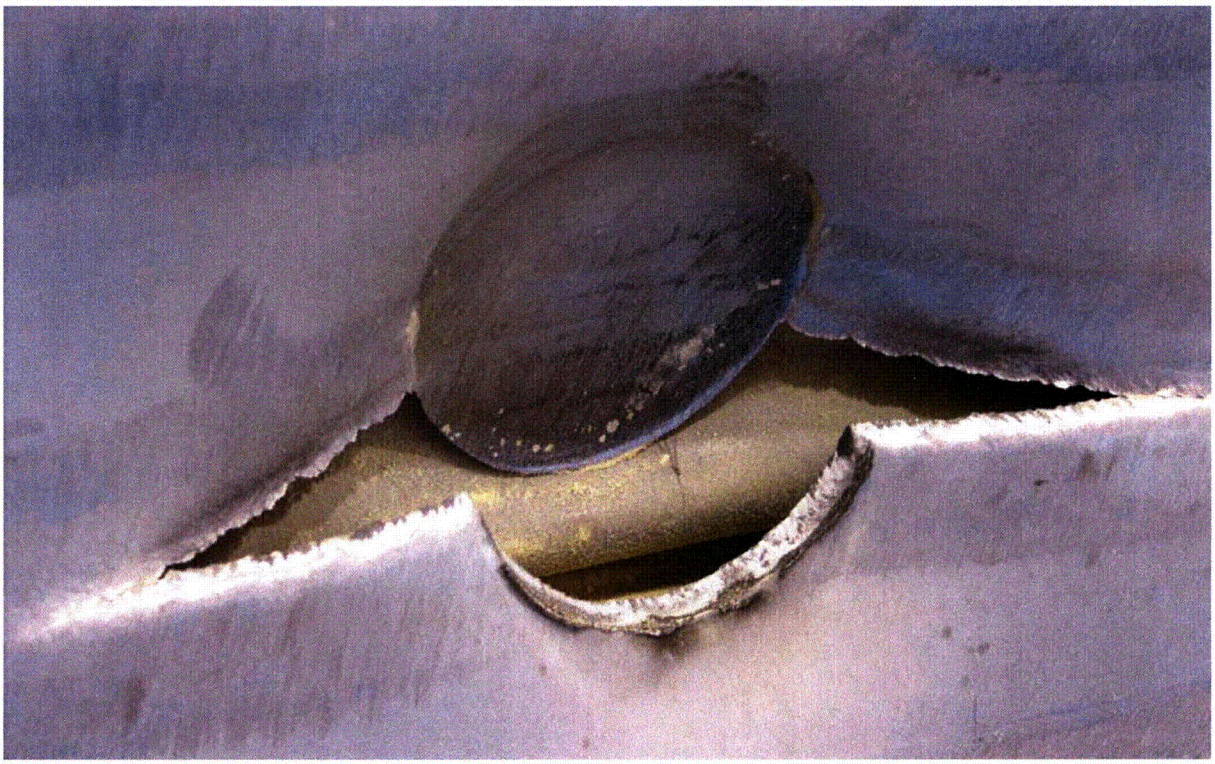

Figure 2.12.1-45 – Puncture Drop Test P1: Close-up View of Closure Lid Damage

Figure 2.12.1-46 – Puncture Drop Test P2: Overall View of Cheek Damage

Figure 2.12.1-47 – Puncture Drop Test P3: Overall View Immediately After Impact

Figure 2.12.1-48 – Puncture Drop Test P3: Overall View of Damage to Overpack Cover-Body Joint

Figure 2.12.1-49 – Puncture Drop Test P3: Close-up of Damage to Overpack Cover-Body Joint

Figure 2.12.1-50 – Puncture Drop Test P4: Overall View of Damage to Closed End

Figure 2.12.1-51 – Puncture Drop Test P4: View of Damage to CSA Structural Sheet

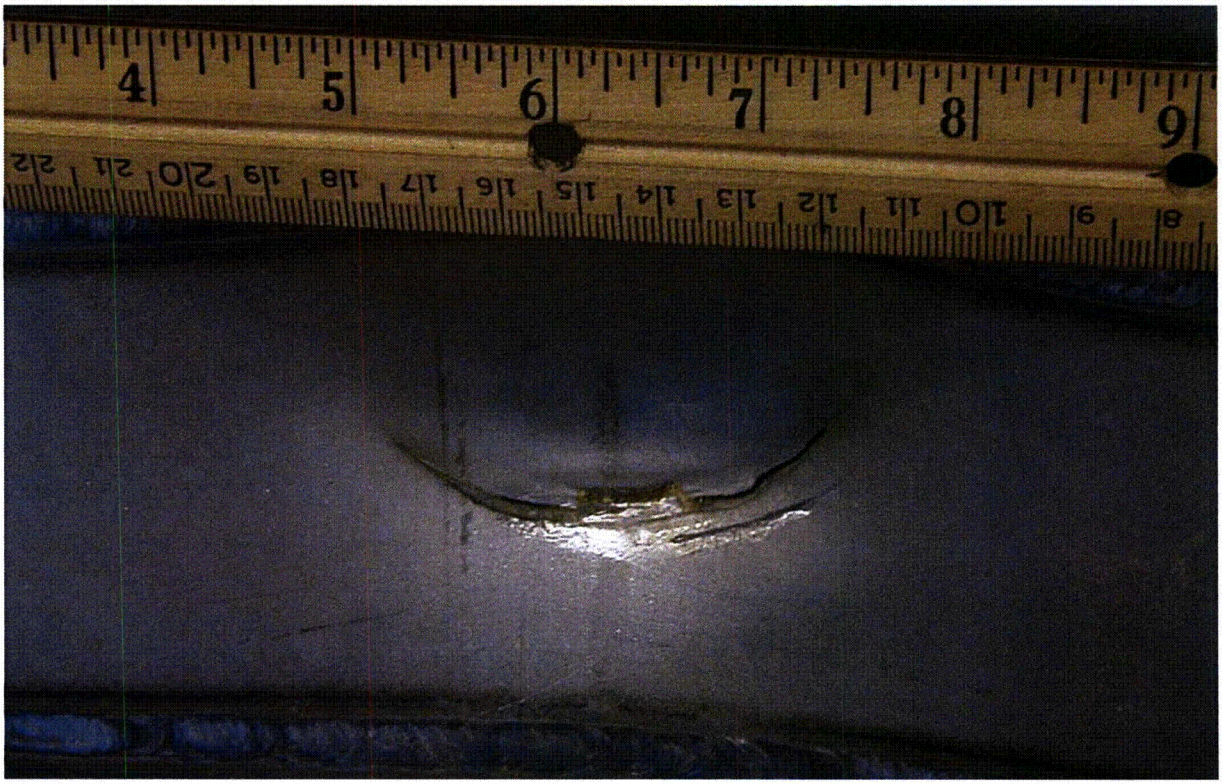

Figure 2.12.1-52 – Puncture Drop Test P4: Close-up of CSA Structural Sheet Damage

Figure 2.12.1-53 – Post-Test Disassembly: View of Loose Simulated Payload in Cavity

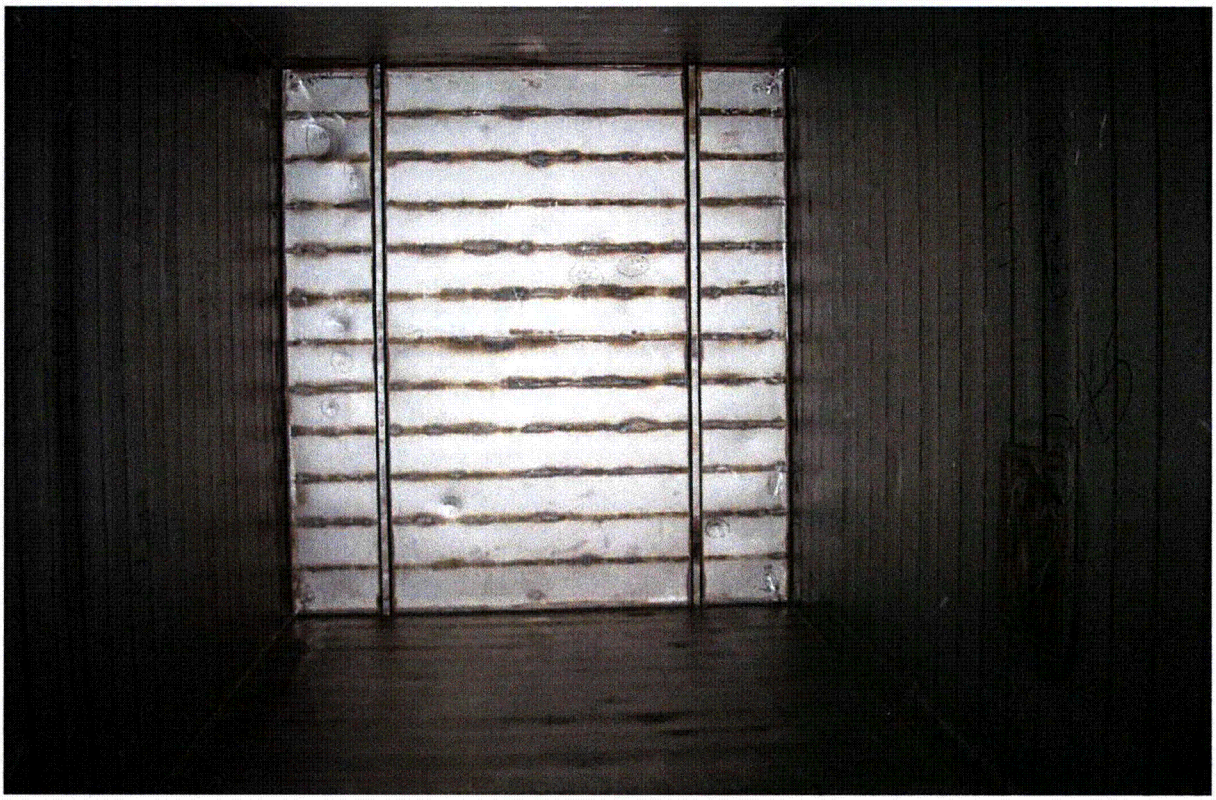

Figure 2.12.1-54 – Post-Test Disassembly: View of Cavity with Payload Removed

Figure 2.12.1-55 – Post-Test Disassembly: Overall View of Closure Lid, Inner Surface

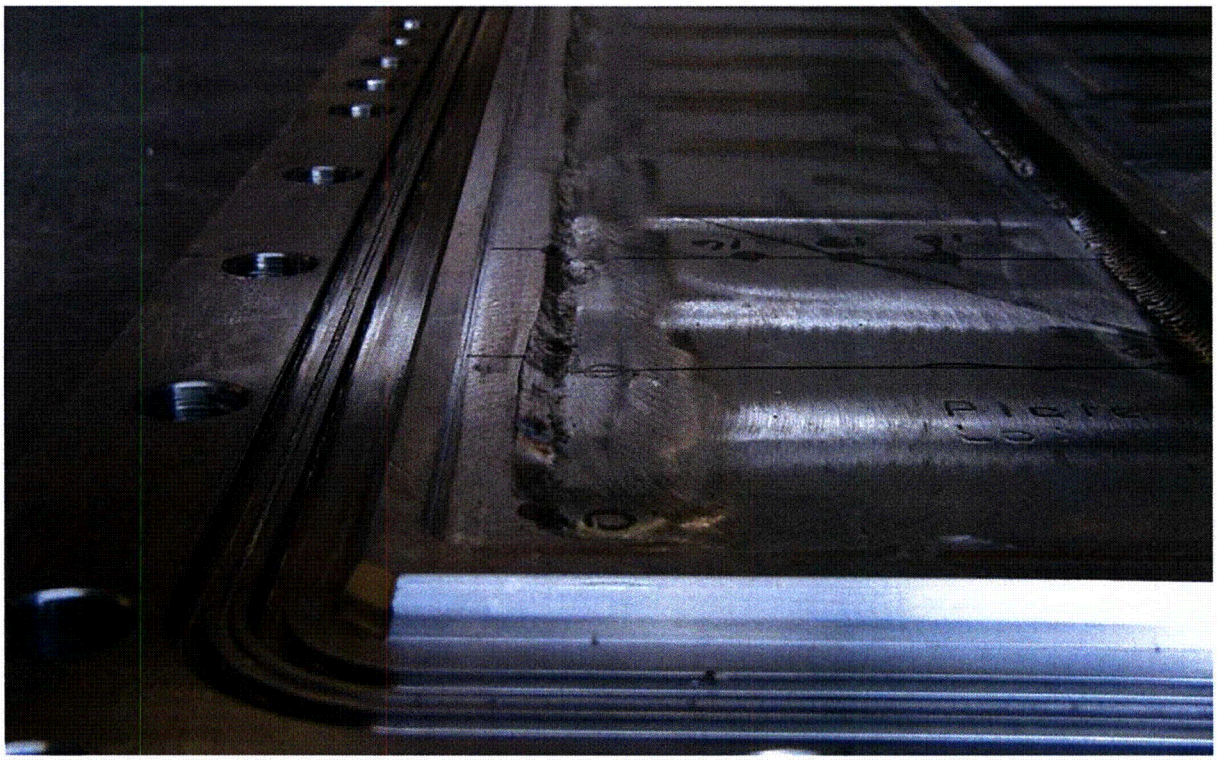

Figure 2.12.1-56 – Post-Test Disassembly: Close-up View Closure Lid O-ring Seal Grooves

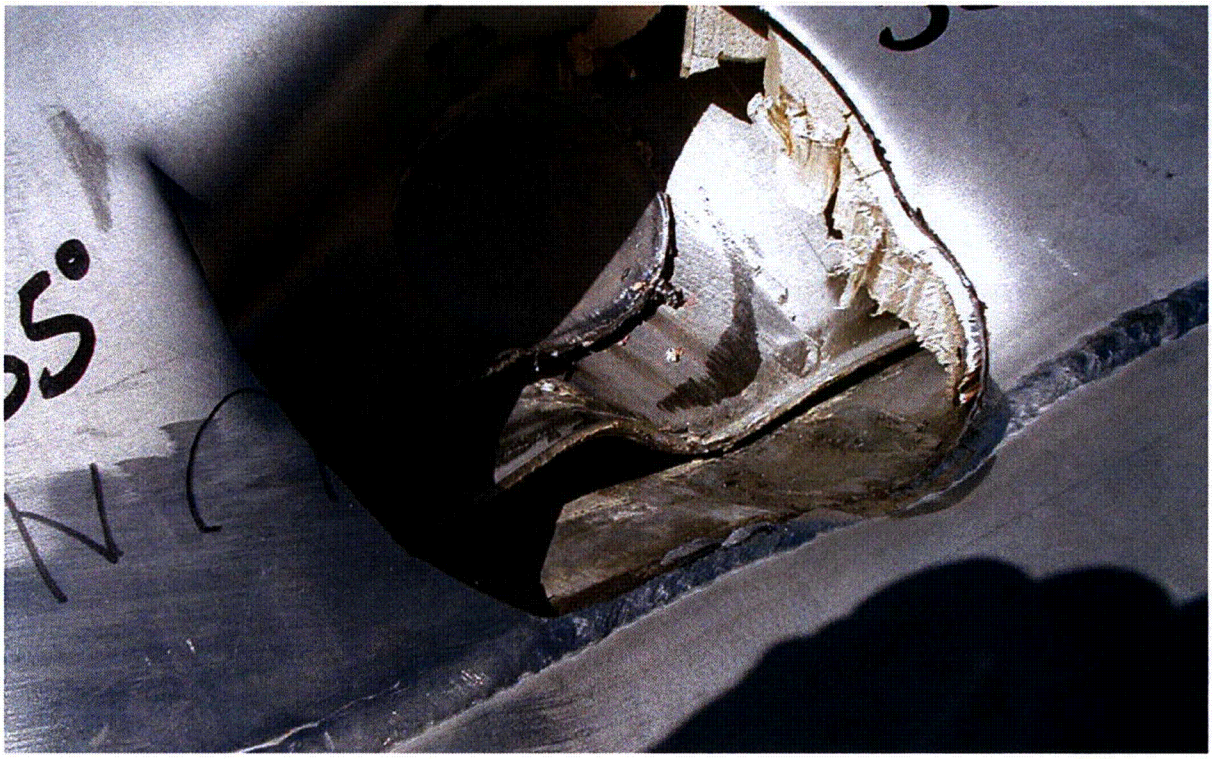

Figure 2.12.1-57 – Puncture Drop Test P105 at 35°

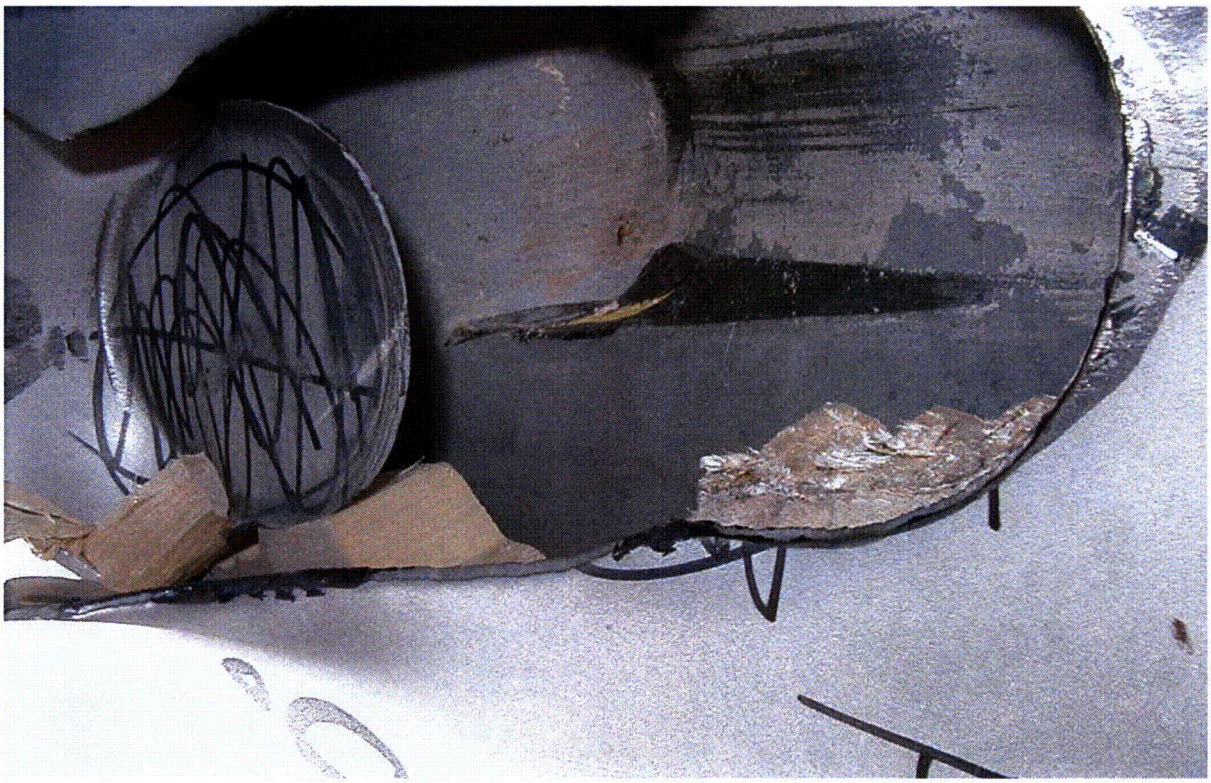

Figure 2.12.1-58 – Puncture Drop Test P205 at 30°

Figure 2.12.1-59 – Puncture Drop Test P305 at 25º

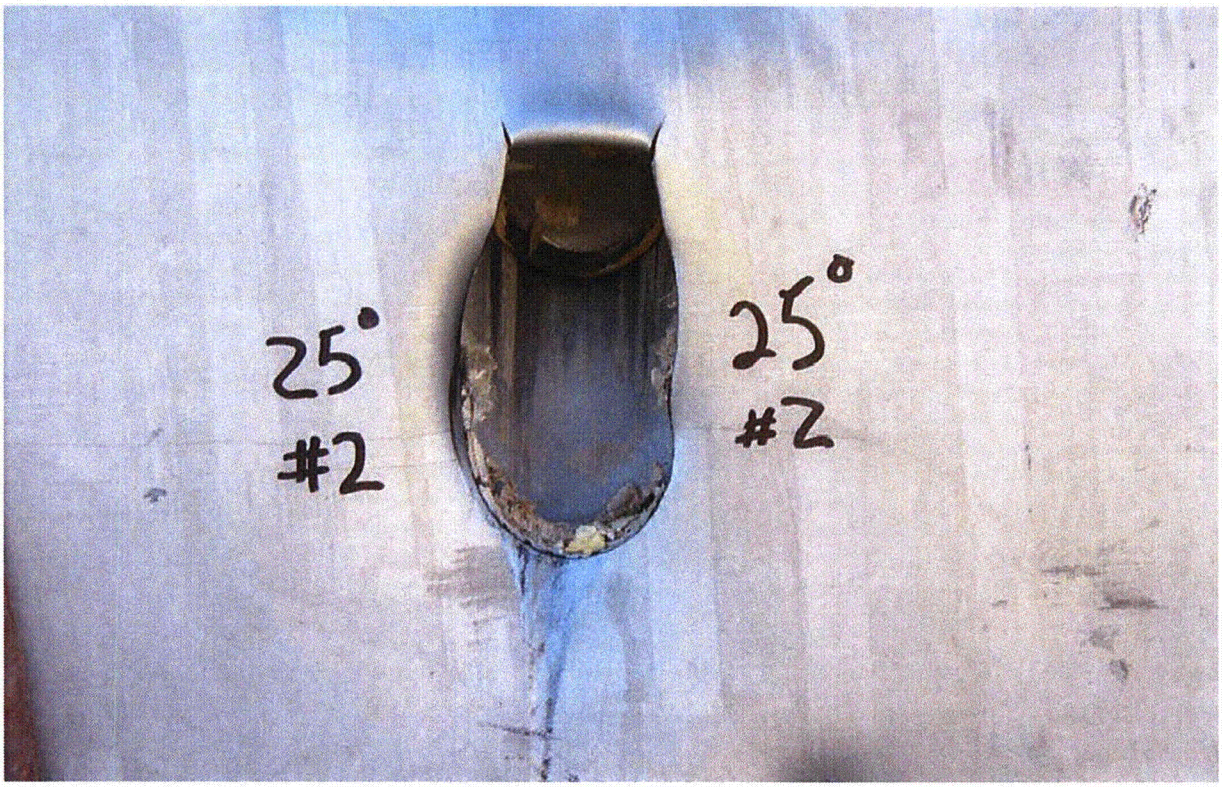

Figure 2.12.1-60 – Puncture Drop Test P405 at 25º

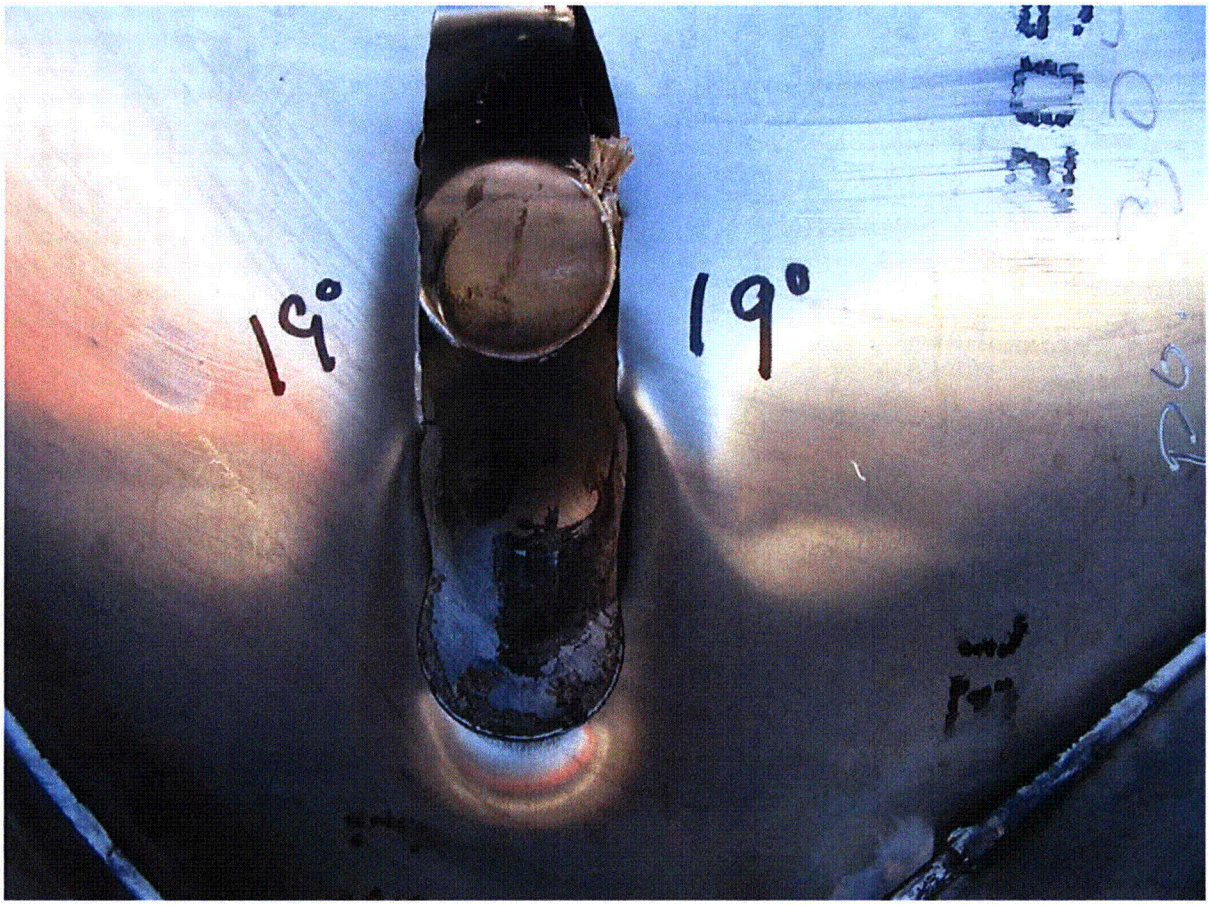

Figure 2.12.1-61 – Puncture Drop Test P505 at 19° (ETU longitudinal axis 71°)